KIT SCIENTIFIC REPORTS 7629

1st Workshop Proceedings of the Collaborative Project „Crystalline Rock Retention Processes“ (7th EC FP CP CROCK)

Thomas Rabung, Jorge Molinero,
David Garcia, Vanessa Montoya (eds.)

KIT Scientific Publishing

Thomas Rabung, Jorge Molinero, David Garcia, Vanessa Montoya (eds.)

1st Workshop Proceedings of the Collaborative Project „Crystalline Rock Retention Processes“ (7th EC FP CP CROCK)

Karlsruhe Institute of Technology
KIT SCIENTIFIC REPORTS 7629

1st Workshop Proceedings of the Collaborative Project „Crystalline Rock Retention Processes“ (7th EC FP CP CROCK)

Thomas Rabung
Jorge Molinero
David Garcia
Vanessa Montoya
(eds.)

KIT Scientific Publishing

Report-Nr. KIT-SR 7629

The report is printed without colours. The report with the original colours in different photos, tables, figures and logos, can be downloaded from the KIT Scientific Publishing homepage.

Karlsruher Institut für Technologie (KIT)
Institut für Nukleare Entsorgung

Amphos 21 Consulting S.L.
Passeig de Garcia i Faria, 49-51, 1º-1ª
E08019 Barcelona
SPAIN

Impressum

Karlsruher Institut für Technologie (KIT)
KIT Scientific Publishing
Straße am Forum 2
D-76131 Karlsruhe
www.ksp.kit.edu

KIT – Universität des Landes Baden-Württemberg und
nationales Forschungszentrum in der Helmholtz-Gemeinschaft

KIT Scientific Publishing 2012
Print on Demand

ISSN 1869-9669
ISBN 978-3-86644-925-1

FOREWORD

The present document is the proceedings of the 1st Workshop of the EURATOM FP7 Collaborative Project CROCK (Crystalline Rock Retention Processes). The electronic version of these proceedings is also available in the webpage of the project (www.crockproject.eu). The Workshop was hosted by SKB and held in Stockholm (Sweden) 22nd – 24th May 2012. The project started January 2011 and has two and a half years duration. It has 10 beneficiaries including 5 research organizations, 2 universities and 3 Small and Medium Enterprises (SME's).

The proceedings serve several purposes. The key purpose is to document and make available to a broad scientific community the outcome of the CROCK project. For this purpose, a considerable part of the project activity reporting is done through the proceedings, together with the outcome of a large number of scientific-technical contributions and Topical Sessions on different topics, which could be important for the development of the project. In the 1st CP CROCK Workshop this topic focused on Reactive Transport Modelling. Additional purposes of the proceedings are to ensure ongoing documentation of the project outcome, promote systematic scientific-technical development throughout the project, and to allow thorough review of the project progress.

All Scientific and Technical papers submitted for the proceedings have been reviewed by the EUG (End-User-Group). The EUG is a group specifically set up within the project in order to represent the interests of the end users to the project and its desired outcome. To this aim, the composition of the EUG includes organizations representing national waste management (SKB, POSIVA, RAWRA) and national regulators (SSM, STUK).

Finally, we want to thank all those who submitted Scientific and Technical contributions for review and, especially, the Workpackage leaders who provided the summary of the different workpackages for publication in these proceedings. We also want to give a special thanks to the reviewers, whose effort and hard work reflect their commitment and dedication to the project.

TABLE OF CONTENTS

THE PROJECT

The EURATOM 7th EC Framework Program Collaborative Project Crystalline ROCK retention processes (CROCK) started in January 2011 and extends over 2 and a half years. The key driver for initiation the CP CROCK, identified by national Waste Management Organizations, is the undesired high uncertainty and the associated conservatism with respect to the radionuclide transport in the crystalline host-rock far-field around geological disposal of high-level radioactive wastes. In response to this, the CROCK project has been established with the overall objective to develop a methodology for decreasing the uncertainty in the long-term prediction of the radionuclide migration in the crystalline rock repository far-field and to show how the outcome of the project can be used in the Safety Assessment and in the forthcoming site investigations programs. From a more scientific point of view, the CROCK project is increasing the process understanding in the transport simulations used to support Performance Assessment (PA) exercises with the purpose of increasing confidence in the safety of nuclear waste disposal.

The project is implemented by a consortium of 10 beneficiaries consisting on 5 large European Research Institutions, 2 Universities and 3 small and medium enterprises from six different countries with dedicated crystalline host-rock disposal programs and particular competence in this field. The Coordination Team is based on two organizations, namely the Coordinator (KIT) and the Coordination Secretariat (AMPHOS). National Waste Management organizations and Regulators also participate in the project contributing with co-funding to beneficiaries, infrastructures, knowledge and information. The scientific-technical work program of the project is structured along six RTD (Research and Technological Development) workpackages (WP1-6). Workpackage 1 started at the very beginning of the project providing new drill core fracture samples and characterizing the experimental materials. Workpackage 2 focuses on radionuclide transport and sorption studies. Workpackage 3 deals with matrix diffusion and natural chemical homologue analysis. The general objective of workpackage 4 is to conceptualize and model radionuclide transport processes on systems at different scales. In workpackage 5 is described how the outcome of the other WPs can contribute to decrease the uncertainty in PA related with transport treatment. Workpackage 6 is a cornerstone of the project, since its first objective is to establish a state-of-the-art of the current knowledge on retention processes in crystalline rocks, then to continuously collect the results obtained in the other workpackages, and finally to deliver a report summarizing the major advances which will have been accomplished at the end of the project. There is also one workpackage on knowledge management, dissemination and training (WP7). The last workpackage is on administrative and financial project management (WP8).

The present proceedings document the outcome of the 1st Project Workshop and give an overview of the outcome of the 1st project year.

THE FIRST WORKSHOP

The 1st Project Workshop was held in Stockholm (Sweden) 22nd – 24th May 2012. The Workshop was hosted by SKB. There were 33 attendees at the workshop, representing beneficiaries, the End-User Group, and project external organizations. The workshop was organized in three days of oral presentations on results obtained within the project, a poster session, and a topical session on reactive transport modelling.

Objectives

The Workshop combines different activities and meetings with the following objectives:

- Informing about the scientific progress. For this purpose, plenary sessions and the poster session are used for communicating results from the different technical workpackages.
- Informing about the administrative status.
- Informing/agreeing upon forthcoming reporting.
- Discussing various topics of interest for the consortium.
- Agreeing upon the forthcoming work program.

Emphasis was on scientific-technical topics with administrative issues kept to the minimum necessary.

RTD sessions

The workshop included plenary sessions where the results from the different workpackages were presented. Next to an overview of the achievements within the respective WP, scientific highlights were presented. The following presentations were given within the project.

WP1 session:

- Th. Schäfer, E. Stage, S. Büchner, F. Huber, H. Drake and S. Holgersson. Characterization of new crystalline material for investigations within CP CROCK.
- Miguel García-Gutiérrez, Manuel Mingarro, Tiziana Missana. Block-scale experiment at CIEMAT.
- V.G. Petrov, I.E. Vlasova, N.V. Kuzmenkova, V.A. Petrov, V.V. Poluektov, A. Grivot, S.N. Kalmykov. Characterisation of rock samples from areas of the proposed Russian HLW and SNF repository (Nizhnekansky massive) and first sorption studies
- S. Holgersson. Characterisation of rock samples from Äspö using gas adsorption

WP2 session:

- E. Stage, F. Huber, S. Heck and Th. Schäfer. Sorption/desorption studies of ^{137}Cs(I), ^{152}Eu(III), ^{233}U(VI) and ^{99}Tc(VII) onto new CROCK derived Äspö diorite.
- V. Havlová, K. Videnska, J. Vejsadú and P. Sajdl. NRI experimental work overview.
- T. Missana, M. García-Gutiérrez. Comparison of the cesium adsorption on different crystalline rocks.
- K. Schmeide, S. Gürtler, K. Müller, R. Steudtner, C. Joseph, F. Bok and V. Brendler Sorption of U(VI) and Np(V) onto diorite from Äspö HRL.

WP3 session

- J. Crawford and M. Lögfren. Diffusive retention processes. Estimation of in-situ formation factors by electrical resistivity measurements.

- J. Molinero and P. Trinchero. On the relevance of matrix diffusion for the hydrogeochemical stability of the Deep Geological Repository.

WP4 session

- J. Crawford, Processes based sorption modelling.
- M. Olin, E. Puhakka, A. Itälä, , M. Tanhua-Tyrkkö, V.-M. Pulkkanen. Multiscale modelling of sorption and retardationF. Papanicolaou, S. Antoniou, I Paschalidis. Uranium chemistry in Phosphogypsum under oxic and anoxic Conditions.
- J. Molinero, C. Domènech and D. García. Cs sorption onto crystalline rock. From mechanistic sorption models to Kd.

WP5 session

- À. Piqué, L.M. de Vries, P. Trinchero, L. Duro and J. Molinero. Radionuclide retention in fractured media: coping with uncertainty in PA studies.
- J. Crawford. Application to the safety case. Deployment of process-based models in safety assessment.
- M. Olin, V.-M. Pulkkanen, H. Nordman, A. Poteri. How to predict Kd values outside experimental studied conditions and to estimate related uncertainty?

WP6 session

- A. Idiart, M. Pekala and M. Grivé. State of the art.

Poster presentations

The following posters were presented during the 1st Workshop:

- K. Schmeide, S. Gürtler, K. Müller, R. Steudtner, C. Joseph, F. Bok, and V. Brendler, Sorption of U(VI) and Np(V) onto diorite from Äspö HRL
- T. Missana, and M García-Gutiérrez, Analysis of the cesium sorption behavior on biotites of different origin
- U. Alonso, T. Missana, A. Patelli, V. Rigato, D. Ceccato, Uranium retention under anoxic conditions on Äspö diorite: First micro-scale analyses

- D. García and C. Domènech. Cs sorption onto crystalline rock. From mechanistic sorption models to Kd.
- E. Puhakka and M. Olin, Molecular modelling approach for the formation of water molecular layer onto biotite surfaces.
- A. Itälä, M. Tanhua-Tyrkkö, E. Puukko and M. Olin, Kd-values and surface complexation modelling for biotite.

Topical session

The Topical Sessions aim at covering the key areas of knowledge along with the project. The Topical Session of the 1st CP CROCK Workshop focuses on Reactive Transport Modelling.

Presentations within this topic were:

- P. Trinchero, G. Roman-Ross and J. Molinero, New Approaches for Efficient Reactive Transport Modelling
- M. Olin, V.-M. Pulkkanen, K. Kajanto, How to evaluate uncertainties in rock fracture transport modelling?
- M. Löfgren and M. Sidborn, Amounts and distribution of fracture minerals, available for reaction in crystalline rocks
- L.M. de Vries, A. Nardi, J. Molinero and P. Trinchero, High Performance Reactive Transport Modelling (I): DT-PF Pilot Project
- S. Joyce, High Performance Reactive Transport Modelling (II): Reactive Transport in ConnectFlow
- A. Nardi, L.M. de Vries, A. Idiart, P. Trinchero and J. Molinero, High Performance Reactive Transport Modelling (III): The COMSOL Phreeqc Approach
- J. Crawford, Some numerical issues related to modelling of reactive transport with matrix diffusion
- A. Idiart and J. Molinero, Scoping analysis of PhreeqC capabilities for colloidal-facilitated radionuclide transport modelling.

Structure of the proceedings

The proceedings are divided into the following sections:

- WP activity overviews, with summaries of the Research, Technology and

Development Components

- Individual Scientific and Technical Contributions, containing reviewed scientific and technical manuscripts

All the Scientific-technical contributions submitted were reviewed by the EUG members (End-User Group).

SUMMARY OF WP ACTIVITIES

WORKPACKAGE 1
EXPERIMENTAL MATERIAL AND CHARACTERIZATION

Thomas Rabung[1*]

[1]Institute of Nuclear Waste Disposal, Karlsruhe Institute of Technology, Hermann-von-Helmholtz-Platz 1, 76344 Eggenstein-Leopoldshafen

* Corresponding author: thomas.rabung@kit.edu

Introduction

The main objective of WP1 is to organize new drill-core samples from Äspö URL, sampled and handled under anoxic conditions. If required, also samples from previous studies should be accessible. Previous investigations are based on crystalline rock material that has been drilled under the use of oxidizing surface water and/or where the drill cores have subsequently been treated, handled, transported and stored in contact with air. Especially the sorption processes for redox-sensitive radionuclides can strongly be affected due to this sample treatment, but also the inventory of sorbing minerals and mineral components might be affected significantly.
The new experimental material has to be characterized for its chemical/mineralogical composition, including structure and properties of accessible fluid systems (porosity, hydraulic conductivity etc.). In addition, BET surface area should be determined for different size fractions of crushed material and a special focus should lie on the natural chemical homologue behaviour. The new Äspö samples have to be provided to the different partners as required (drill-cores, disks and crushed material).

Note that originally the duration of WP1 was set to 18 months and was extended to 24 months to give some partners the opportunity to finish their work.

Description of the work performed

KIT-INE

KIT-INE was responsible for organizing the new drill-core samples from Äspö. Therefore, a first planning meeting for the CP-CROCK drilling campaign was organized by Henrik Drake (Isochron) as consultant for SKB and held at Äspö in March 2011 together with participants from KIT and CTH. The drilling campaign was done in the first week of May 2011 with the same group including MIRO, a local drilling company (Figure 1). Two boreholes were drilled, one from tunnel surface parallel to water conducting feature, the other from a niche parallel to tunnel surface in a distance of approx. 7 m slightly dipping (~5°) perpendicular to structural features. In total, 71 bore-cores have been collected. In addition to bore-cores also natural groundwater was

collected as well as samples from the drilling water. A special attention was drawn on a widely exclusion of oxygen during sampling, storage and transportation. Details on that procedure can be found in the S&T contribution within the Workshop Proceedings: *Characterization of new crystalline material for investigations within CP CROCK* by Thorsten Schäfer et al. (2012) and in Stage et al. (2012a, b). It also contains a detailed characterization of the different water and solid samples.
Äspö diorite samples (discs, crushed material and cores) were prepared in an argon glove box (equipped with a diamond saw) for the partners CIEMAT, NRI-REZ, HZDR and KIT-INE as requested and shipped to the partners in autoclaves under argon atmosphere. Chemical and mineralogical characterization of the Äspö samples was mainly performed on the Crushed Material (CM) and included also BET surface area determination of different size fractions, XRF and SEM-EDX measurements. Determination of the iron content was done with a special focus on Fe(II) concentration, as the Fe(II) content should have an important impact on sorption of redox-sensitive elements studied in WP2. Furthermore, the measured Fe(II) concentrations point to the fact that due to the sampling and preparation procedure at least a part of the ferrous iron pool in the rock material could be preserved. Results were also compared with material from older studies (Huber et al., 2011).

Within the next reporting period the detailed hydraulic characterization of fractured systems which will be used in subsequent migration studies will be done.

Figure 1: *Sampling in Äspö URL*

CIEMAT

The objective of **CIEMAT** was to document the progress of results obtained in the block-scale diffusion experiment started at CIEMAT in 2007 simulating a high level radioactive waste repository in granite (including compacted bentonite) after 5 years of experiment.
Within the first reporting period of CROCK the evolution of the activity of Cs, Cl and HTO in the tracer reservoir (within the bentonite) has been analyzed and modeled. The evolution of the activity of the conservative tracers Cl and HTO has been periodically measured in 11 different boreholes placed in granite at different distances from the source (García-Gutiérrez et al., 2012).

For the second reporting period the collection of diffusion data for conservative tracers (HTO and Cl) as a function of time and space (3D) will be continued and characteristic data of granite from different sites will be compared.

HZDR

HZDR has prepared various grain size fractions of the Äspö diorite material for the sorption studies and characterized the material.
From the provided grain size fractions of KIT of 0.5 – 1 mm and 1 – 2 mm as well as from provided bore cores additional grain size fractions were prepared by crushing and sieving: the grain size fractions 0.063 – 0.2 mm and < 0.063 mm (required for spectroscopic studies) were prepared as well as additional material of the grain size fraction 1 – 2 mm. The grain size fractions were characterized by determining Kr-BET surface areas. Furthermore, the mineralogical composition of the diorite was investigated.

For the forthcoming reporting period the distribution of biofilm components and of uranium on fracture surfaces from Äspö samples will be mapped by spectroscopic methods.

CTH

CTH was also involved in the sampling of new Äspö bore-cores within the sampling campaign in May 2011. Additional objectives for WP1 are sample preparation and characterization of drill-core samples as well as of crushed and sieved material.
Within the first reporting period the drill core samples for CTH have been sawed in sections of 3 cm, using a water-cooled low-speed saw. The work was made in an inert gas atmosphere glove-box. Problems with finding an appropriate saw and its installation in a glove-box were encountered. As a consequence, some delay in performing the subsequent sample characterization occurred. Up to now some selected drill-core sections have been crushed and sieved into four different size fractions for later characterization with a) Kr-BET gas adsorption measurements for specific surface area and with b) N_2-BJH gas adsorption/desorption for specific pore volume (André et al., 2009; Dubois et al., 2011). Some Kr-BET gas adsorption measurements for specific surface area have already been started. More detailed information on the work performed by CTH can be found in the S&T contribution of Stellan Holgersson (2012)

in the First CROCK Workshop Proceedings: *Characterisation of rock samples from Äspö using gas adsorption.*

For the next reporting period crushing and sieving of the drill-core material will be finalized as well as gas adsorption measurements.

MSU

The objective of **MSU** in WP1 is to provide and characterize sample material from disposal sites in Russia, including rock samples from the proposed international repository of spent nuclear fuel in Niznekansk rock massive.
Core materials from two of the supposed areas (area Kamenny, drilling depth down to 700 m, and area Itatsky, drilling depth down to 500 m) have been studied in terms of petrographic and mineralogical characterization; definition of filtration, elastic, petro-physical and strength properties; estimation of hydrothermal-metasomatic transformation of rocks. It was established that the most part of the core material from the area Kamenny is presented by granites and leucogranites, while the core material from the area Itatsky is mostly diorites and quartz diorites. More details are given by Petrov et al. (2012) in the S&T contribution included in the First Annual Workshop Proceedings: *Characterization of rock samples from areas of the proposed HLW and SNF repository in Russia (Nizhnekansky massive) and first sorption studies.*

As the work could be finished as scheduled, no additional work is planned for the next reporting period.

References

André, M., Malmström, M.E. and Neretnieks, I. (2009). Specific surface area measurements on intact drillcores and evaluation of extrapolation methods for rock matrix surfaces. Journal of Contaminant Hydrology 110, 1-8.

Dubois, I.E., Holgersson, S., Allard, S. and Malmström, M.E. (2011). Dependency of BET surface area on particle size for some granitic minerals. Proc. Radiochim. Acta 1, 75-82.

García-Gutiérrez, M., Mingarro, M., Missana, T. (2012). Block-scale experiment at CIEMAT - 1st CROCK Workshop (May 22-24, 2012, Stockholm, Sweden), Oral communication.

Holgersson, S. (2012). Characterization of rock samples from Äspö using gas adsorption - 1st CROCK Workshop (May 22-24, 2012, Stockholm, Sweden), Paper & Oral communication.

Huber, F., Kunze, P., Geckeis, H., Schäfer, T. (2011). Sorption reversibility kinetics in the ternary system radionuclide–bentonite colloids/nanoparticles–granite fracture filling material. Applied Geochemistry, 26(12): 2226-2237.

Petrov, V.G., Vlasova, I.E., Kuzmenkova, N.V., Petrov, V.A., Poluektov, V.V., Grivot, A., Kalmykov, S.N. (2012) Characterization of rock samples from areas of the proposed HLW and SNF repository in Russia (Nizhnekansky massive) and first sorption studies - 1st CROCK Workshop (May 22-24, 2012, Stockholm, Sweden), Paper & Oral communication.

Schäfer, Th., Stage, E., Büchner, S., Huber, F., Drake, H. (2012). Characterization of new crystalline material for investigation within CP CROCK - 1st CROCK Workshop (May 22-24, 2012, Stockholm, Sweden), Paper & Oral communication.

Stage, E. (2012a). Experimentelle Untersuchungen zur Cs, Eu und U Sorptionskinetik an Äspö-Granodiorit, Freie Universität Berlin, Berlin, 77 pp.

Stage, E., Huber, F., Heck, S., Schäfer, Th. (2012b). Soprtion/desorption of ^{137}Cs(I), ^{152}Eu(III) and ^{233}U(VI) onto new CROCK derived Äspö diorite – A batch type study - 1st CROCK Workshop (May 22-24, 2012, Stockholm, Sweden), Paper.

WORKPACKAGE 2
RADIONUCLIDE TRANSPORT AND SORPTION STUDIES

Tiziana Missana[1*]

[1]CIEMAT (ES), Avenida Complutense 40, 28040 Madrid

*Corresponding author e-mail: tiziana.missana@ciemat.es

Introduction

The large discrepancies, found when analysing retention data from different sources, or the lack of reproducibility on the determination of transport parameters in crystalline rocks are often not explicable in a straightforward way. Thus, to improve the performance assessment of geologic disposals of high-level radioactive waste in crystalline rocks is necessary to reduce the uncertainties related to radionuclide retention processes.
These uncertainties can be related to conceptual aspects, as the kinetic of these processes, the dependence of transport parameters on the hydrodynamic conditions of the system, the heterogeneity of the medium, up-scaling factors as well as other not well-understood mechanisms. The poor understanding of processes may lead to biased data interpretation and therefore poor modelling and predictive capability of the radionuclide behaviour at a long-term.
Problems related to experimental determinations might be also present. First of all, experimental data are sometimes gathered under conditions, which are not fully representative of the scenario of interest or, sometimes, using samples not correctly characterized or handled. Other factors can represent source of uncertainty and have to be taken into account and evaluated: for example, the origin of samples, their mineralogical composition or accessible surface area. Very important elements are groundwater chemistry and rock/water interactions.
Factors as sampling, crushing or cutting and storing of the solids, or the conservation of the natural groundwater can significantly affect the outcome of the experiments as well. In particular, the oxidation of the solid or aqueous phase may be decisive on parameter determination for redox sensitive elements.
The main objective of the work performed in Work Package 2 (WP2, Radionuclide Transport and Sorption Studies) is to provide methodologies to lower the degree of uncertainty on the determination of retention parameters in crystalline rocks and consequently on the prediction of radionuclide migration in the host rock at a long-term.
In this work package, radionuclide transport and sorption studies have been planned for determining radionuclide transport properties in crystalline rock systems, over different

spatial scales, thus experiments are conducted with small to large block-scale samples. Granite from different sites will be used and experiments are being carried out using different techniques (from batch to column experiments) and different type of analyses, at a macro and micro scale. Results obtained with the same material (Äspö diorite) but in different laboratories will be compared, trying to identify possible sources of uncertainties in the experimental determinations.

In parallel, an improvement of the knowledge on retention mechanisms is foreseen. Their kinetic and irreversibility as well as their relation to different relevant minerals will be analyzed. This will allow developing sorption models for a more reliable description of retention in heterogeneous rocks.
The studies will be focused on these radionuclides: an ion-exchangeable dominated (Cs), a strongly sorbing surface complexation dominated (Eu), redox sensitive elements (U, Tc, Se) and conservative non-sorbing tracers (HTO, Cl), as agreed by all the partners at the CROCK kick-off meeting.
Data generated within WP2 will feed models developed in WP4 (Conceptualization and Modeling) and WP5 (Application to the Safety Case).

The following organizations are participate to WP 2: **KIT-INE** and **HZDR** (Germany); **CIEMAT** (Spain); **CTH** (Sweden); **NRI-Rez** (Czech Republic); **MSU** (Russia).

Description of the work performed

KIT-INE

KIT-INE focused on the study of sorption and desorption of ^{137}Cs(I), ^{152}Eu(III) and ^{233}U(VI) onto the Äspö diorite obtained from new samplings performed within the frame of the CROCK Project.
A summary of these results was presented at the first CROCK Workshop as an oral contribution (Stage et al., 2012). Additionally, they studied the sorption behaviour of Tc (VII) and the results are summarized in an S+T contribution (Totskiy et al., 2012).
One of the objectives of their work was to compare sorption data obtained with well-preserved rock samples, with those obtained with oxidized samples. Previous to sorption experiments, the solid phases were characterized by different techniques. The aqueous phase used for sorption experiments was the synthetic Äspö groundwater, which composition was provided by Heck and Schäfer (2011) at the beginning of the project.
Desorption studies were carried out with both the synthetic Äspö water and with natural groundwater coming from the Grimsel Test Site (GTS, Switzerland).
Adsorption of Cs and Eu onto Äspö diorite was rapid and almost quantitative; the adsorption of U was lower but presented a slower kinetic, with a maximum of ~ 50% sorption after 9 weeks contact times. The distribution coefficients of Cs, Eu and U and their time-evolution were not significantly different when obtained on the well-preserved or oxidized samples. This was expected in the case of Cs and Eu because they are non-redox sensitive elements. In the case of U, the Eh measurements in the aqueous solution indicated that U should not have been reduced in the solution. However, XPS measurements on an unaltered Äspö diorite fragment in presence of U(VI) revealed 50% U(IV) on the diorite surface after 28 days of contact time, indicating that both sorption and reduction act as retention/retardation process in parallel.

Instead, in the case of Tc, large differences on distribution coefficients obtained with oxidized and non-oxidized samples were observed, indicating the importance of working with well-preserved samples. Sorption studies of Tc(VII), on new crystalline rock materials from Äspö Hard Rock Laboratory (Sweden), performed to estimate potential mobility under natural conditions revealed, under low concentrations ($1 \cdot 10^{-8}$ to $1 \cdot 10^{-9}$M) of Tc(VII) added, almost full retention by un-oxidized granite after 1 month contact time, whereas considerably lower retention in the case of elevated concentration ($1 \cdot 10^{-5}$M) or oxidized diorite material is found.
Desorption experiments did not show evidences for irreversible sorption; less of 10 % of tracer was desorbed for Cs and Eu, this value being independent on time, whereas desorption of U was increasing with time. Desorption depended on the chemistry of the fresh water (Äspö or Grimsel) and its redox potential, but it did not depend on the solid used (oxidized or not-oxidized). For Tc, desorption was almost negligible and independent of contact time.

HZDR

HZDR objective is to perform batch sorption experiments to determine the sorption capacity of granite and fracture infill materials, respect to neptunium, uranium and selenium. The results obtained for U(VI) and Np(V) sorption onto Äspo diorite are summarized in the S+T contribution at the first CROCK workshop (Schmeide et al., 2012). Additional results are presented in Gürtler (2012).
HZDR analysed the influence of several parameters (solid to liquid ratio, grain size, temperature) on actinides sorption. These investigations were complemented by fluorescence spectroscopy and vibrational spectroscopy.
The speciation of U(VI) and Np(V) in the synthetic Äspö groundwater (Heck and Schäfer, 2011) was dominated by $Ca_2UO_2(CO_3)_3(aq)$ or NpO_2^+, respectively. For U, the speciation was very sensitive to the groundwater composition, thus possible ions leached out from the solid, particularly calcium and carbonate, may significantly affect speciation and consequently its sorption behavior. On the other hand, the speciation of Np(V) is less sensitive to the water composition. This was seen performing studies at different solid to liquid ratios and with different aqueous phases.
Adsorption of both actinides in Äspö diorite was comparable and decreased with the temperature. U adsorption decreased with decreasing surface area, whereas for Np the correlation with the surface area was not clear.
In situ time-resolved attenuated total reflection Fourier-transform infrared (ATR FT-IR) spectroscopy was applied to analyze the surface species formed upon sorption experiments onto Äspö diorite and compared with those previously observed in SiO_2 and illite. For U, the identified surface specie was $UO_2(CO_3)_3^{4-}$ whereas for Np the surface specie was NpO_2^+, i.e. the possible formation of Np(IV) surface specie was evidenced.

CIEMAT

CIEMAT aim is to determine diffusion and sorption parameters on granite a different scales by means of the combination of different techniques (radio-analytical, μPIXE, RBS autoradiography, SEM-EDAX), with the objective of identifying the main source of uncertainties; matrix diffusion processes are being studied in a large block scale (30 x 30 cm). The block scale diffusion experiment started in 2007 and simulates a high level

radioactive waste repository in granite: it includes a central compacted bentonite in which the radionuclide (Cs, Cl and HTO) reservoir is placed. The evolution of the activity of Cs, Cl and HTO in the tracer reservoir was analysed and modelled. The evolution of the activity of the conservative Cl and HTO has been periodically measured in 11 different boreholes placed in granite at different distances from the source during approximately 5 years now. This work was presented as an oral communication at the 1st Workshop of the Project (García-Gutiérrez et al., 2012).
An additional objective of CIEMAT is to analyse sorption onto granite and granite minerals of different origin (Spain, Switzerland, Sweden) to develop sorption models for different radionuclides, which would allow a more reliable description of retention in heterogeneous rocks. The understanding of the sorption behaviour of these radionuclides in the main minerals composing the rock can be very useful for the mechanistic understanding of retention processes in such a heterogeneous system. ^{137}Cs sorption in different minerals (biotite, muscovite, K-feldspar, quartz) is being analysed in detail in parallel to sorption onto granite. The results of these studies carried out so far with Cs have been published in S+T contributions to the 1st CROCK Workshop (Missana and García-Gutiérrez, 2012a, b) and to an international conference (Missana et al., 2012).
Adsorption in the different materials was studied under as similar as possible experimental conditions to reduce the experimental uncertainties and data were analysed as a whole with the aim of evidencing the possible differences in the sorption behaviour amongst the different rocks (mineral content, BET area, chemistry of the water, competitive ions in solution, radionuclide concentration, etc.).
In all the solids, Cs sorption showed a similar behaviour which could be satisfactorily fit according to a three-site ionic exchange simplified model.
Additionally, CIEMAT performed first micro-scale analyses on U retention onto Äspö diorite samples under anoxic conditions were and the results were published in a S+T contribution (Alonso et al., 2012b) and international congresses (Alonso et al, 2012a, c). Experiments were carried out maintaining anoxic conditions from the rock core extraction to the micro-scale analyses. Uranium distribution and the elemental concentration of ion in the substrate were analysed by the ion beam technique μPIXE. Results showed that U retention on Äspö diorite surface was heterogeneous. Quantitative distribution coefficients (K_a) on selected minerals were obtained by PIXE spectra analyses. Higher sorption values were generally observed on Fe-bearing minerals. These experiments were compared to those previously obtained with granite from the Grimsel Test Site (Switzerland) and El Berrocal (Spain).

CTH

CTH will study radionuclide diffusion and sorption by cell experiments. The drill cores will be transferred into an inert atmosphere glove-box and sawn into sections of about 2-5 cm. Some sections will be used for in-diffusion studies of radiotracer cocktails and other sections will be crushed and sieved for batch sorption experiments. Batch sorption experiments will be made both from the fracture surface and the undisturbed zone. Surface area normalized sorption coefficients (Ra) will be determined. All diffusion and batch sorption experiments will be made in inert atmosphere and at a precisely regulated low temperature, simulating the sampling site conditions. At present, CTH carried out the preparation of drill core sections for diffusion experiments and started HTO diffusion experiments.

NRI

NRI is studying sorption and diffusion processes in different rock materials (crushed or in disks) under both anoxic and oxic conditions to emphasize the potential O_2 effect on the determination of retention/transport parameters. Most of NRI's activities are focused on sorption experiments with the redox sensitive tracer, selenium, and on electro-migration measurements for the determination of diffusion parameters. The main results obtained by NRI are reported in Vecernik et al. (2012) and in Videnska et al. (2011, 2012).
The O_2 protected Äspö rock samples were safely removed to the anaerobic box where some of them were prepared for further analyses (grinding, cutting). Synthetic groundwater was prepared on the basis of the information given by Heck and Schäfer (2011).
Selenium speciation calculations were performed using Geochemist´s Workbench prior to the experiments in order to evaluate which phases might be present in the Äspo system. Afterwards, the first round of sorption experiments under oxic conditions with Se(IV) and Se(VI) at a concentration of 10^{-5} M were performed. It was found that the sorption of Se(VI) was almost negligible. Sorption of Se(IV) was detectable, however it was quite low (below 10 ml/g). The anaerobic sorption experiments with Äspö granodiorite were started also in the glove box, gaining the very first results.
Sorption experiments with Se(IV) and Se(VI) and Äspö granite disks were performed in order to determine Se distribution and its oxidation state on the rock surface. ICP-LA and ESCA respectively will be used for those analyses.
The other objective was to use the electro-migration method with for Äspö rock samples. The apparatus was successfully tested for samples 10 mm thick and also for samples of 30 mm thickness. The formation factor (F_f) and the effective diffusion coefficient (D_e) were measured in 3 samples, for iodine. The final aim is to use electro-migration cell for longer samples (up to 100 mm) to look on migration parameters dependency on the sample length. The cell for longer samples is under constructing and verification.

MSU

MSU will study sorption onto fracture samples collected from different nuclear waste disposal sites in Russia accompanied by various spectroscopic investigations with micro- to nano-resolution and bulk scale. Sorption onto different mineral grains within the fracture samples will be studied by radiographic techniques accompanied by various microscopic and mass-spectrometric measurements. Core materials from two areas (area Kamenny, drilling depth down to 700 m, and area Itatsky, drilling depth down to 500 m) have been studied in terms of petrographic and mineralogical characterization.
Preliminary sorption experiments were carried out onto granite disks under atmospheric conditions with ^{137}Cs and ^{233}U. One side of the disk was polished and reverse side was left rough to determine the roughness effect on sorption of radionuclides. First results show that sorption kinetic for Cs is quite slow and probably depends on diffusion and equilibrium were reached after 100 hours of experiments. U showed lower sorption that can be explained by relatively high concentration of U. This work has been reported in an S+T contribution to the first workshop (Petrov et al., 2012).

References

Alonso U., Missana T., Garcia-Gutierrez M., Patelli A., Rigato V., Ceccato D. (2012a). Ion beam analyses of radionuclide migration in heterogeneous rocks. Ion Beams'12: Multidisciplinary Applications of Nuclear Physics with Ion Beams. Legnaro, Italia, 6-8 June 2012, Oral Communication.

Alonso U., Missana T., Patelli A., Rigato V., Ceccato D. (2012b). Uranium retention under anoxic conditions on Äspö diorite: first micro-scale analyses- 1st CROCK Workshop (May 22-24, 2012, Stockholm, Sweden), Paper & Poster.

Alonso U., Missana T., Patelli A., Ceccato D., García-Gutiérrez M., Rigato V. (2012c). Micro-scale study of uranium retention on granite – Interface Against Pollution (IAP 2012) Conference, Nancy France 11 -14 June 2012. Poster.

García-Gutiérrez M., Mingarro M., Missana T. (2012). Block scale experiment at CIEMAT – 1st CROCK Workshop (May 22-24, 2012, Stockholm, Sweden) Oral Communication.

Gürtler, S. (2012). Sorption von U(VI) und Np(V) an Äspö-Granit unter anaeroben und aeroben Bedingungen (Sorption of U(VI) and Np(V) onto Äspö granite under anaerobic and aerobic conditions). Hochschule Fresenius, University of Applied Sciences, Zwickau, 2012 (Diploma Thesis).

Heck, S. and Schäfer T. (2011). Short Note: CP Crock groundwater sample characterization. Note distributed to all the project participants.

Missana T. and García-Gutiérrez M. (2012a). Analysis of the caesium sorption behaviour on biotites of different origin - 1st CROCK Workshop (May 22-24, 2012, Stockholm, Sweden) Paper & Poster.

Missana T. and García-Gutiérrez M. (2012b). Comparison of the caesium adsorption on different crystalline rocks – 1st CROCK Workshop (May 22-24, 2012, Stockholm, Sweden) Paper & Oral Communication.

Missana T., Garcia Gutierrez M., Alonso U. (2012). Adsorption processes in heterogeneous rock: top-down vs bottom-up modelling approach in modelling experimental data - Interface Against Pollution (IAP 2012) Conference, Nancy France 11 -14 June 2012. Poster.

Petrov V.G., Vlasova I.E., Kuzmenkova N.V., Petrov V.A., Poluektov V.V., Grivot A., Kalmykov S.N. (2012). Characterisation of rock samples from areas of the proposed Russian HLW and SNF repositories (Nizhnekansky massive) and first sorption studies - 1st CROCK Workshop (May 22-24, 2012, Stockholm, Sweden). Paper.

Schmeide, K., Gürtler, S., Müller, K., Steudtner, R., Joseph, C., Bok, F., Brendler, V. (2012). Sorption of U(VI) and Np(V) onto diorite from Äspö HRL – 1st CROCK Workshop (May 22-24, . 2012, Stockholm, Sweden). Paper & Oral Communication

Stage E., Huber F., Heck, S., Schäfer T. (2012). Sorption desorption of ^{127}Cs(I), ^{152}Eu(III) and ^{233}U(VI) onto new crock derived Äspö diorite - A batch type study – 1st CROCK Workshop (May 22-24, 2012, Stockholm, Sweden). Paper & Oral Communication;

Totskiy Y., Geckeis H., Schäfer T. (2012). Sorption of Tc(VII) on Äspö diorite - 1st CROCK Workshop (May 22-24, 2012, Stockholm, Sweden). Paper

Vecernik P., Havlova V., Lögfren M (2012). Determination of rock migration parameters (Ff, De): application of electromigration method on samples of different length - 1st CROCK Workshop (May 22-24, 2012, Stockholm, Sweden). Paper.

Videnska K. (2011). Study of Se(IV) and Se(VI) sorption processes in granitic environment. Seminar of the project Research on barriers of deep geological repository (CZ, 1H-PK/25), December 9, 2011, Rez.

Videnska K., Havlova V., Vecernic P., Vejsadu J., Sajdi P. (2012). Speciation of selenium sorbed species on Äspo granodiorite surface - 1st CROCK Workshop (May 22-24, 2012, Stockholm, Sweden). Paper.

WORKPACKAGE 3
REAL SYSTEM ANALYSIS

John Smellie[1*]

[1] Conterra AB (Sweden)

* Corresponding author: john.smellie@conterra.se

Introduction

Real systems analysis is used specifically for identification of matrix diffusion on real time and spatial scales. The matrix diffusion process is identified by real system analysis making use of findings from the past Swedish site selection programme.

WP3 overall objectives are twofold:

- to use WP3 data in order to obtain insight into matrix diffusion processes based on natural conservative tracers determined in real system samples selected from profiles extending from water conducting fracture surfaces out into the adjacent low transmissive rock matrix. Furthermore, using data generated from these natural chemical homologues, the effect of matrix diffusion on the far field behaviour of radionuclides in fractured crystalline rock in Sweden will be evaluated;
- to use WP3 data, (i.e. natural conservative tracers determined in real system samples from Sweden selected from profiles extending from water conducting fracture surfaces out into the adjacent low transmissive rock matrix), to produce estimates of the geometric formation factor for solute diffusion with corrections for surface conduction bias.

It is hoped that this calibration process can provide reliable effective parameters (e.g. effective diffusion coefficient, capacity ratio, retardation factors etc.) to be used in the framework of the benchmark exercise for WP5.

Description of the work performed

CONTERRA AB

All relevant background sources of analytical and field pore water data, together with interpretations, from the Swedish site characterisation programme with a focus on

matrix diffusion have been documented and distributed among the project beneficiaries (Smellie, 2011; 2012a; 2012b).

AMPHOS 21

The work performed to date has focussed on establishing relevant and reliable models to achieve the above-mentioned objectives. This has involved the implementation of alternative dual porosity formulations within a numerical framework for reactive transport modelling using multiple streamlines (FASTREACT). Numerical simulations have been carried out using synthetic realisations (i.e. to resemble streamlines) showing the capability of the approach to capture accurately the key features of a synthetic geological medium, including both fractures and matrix (Molinero and Trinchero, 2012).

KEMAKTA

Based on porewater conductivity data supplied within WP3, together with relevant borehole resistivity-log data from other sources, *in-situ* formation factors have been estimated. In addition, tentative numerical corrections for the bias introduced by surface conduction artefacts have also been addressed (Crawford, 2012a; 2012b).

This work, focussing on borehole KFM01A from the Forsmark repository site, Sweden, will be written in collaboration with Dr. Martin Löfgren (Niressa AB) and submitted for publication in due course.

References

Crawford, J. (2012a). Diffusive retention processes. Estimation of in-situ formation factors by electrical resistivity measurements - 1st CROCK Workshop (May 22-24, 2012, Stockholm, Sweden), Oral communication.

Crawford, J. (2012b). Decreasing uncertainty of radionuclide migration predictions in safety assessment modelling - 1st CROCK Workshop (May 22-24, 2012, Stockholm, Sweden), Paper.

Molinero, J. and Trinchero, P. (2012). On the relevance of matrix diffusion for the hydrogeochemical stability of the Deep Geological Repository - 1st CROCK Workshop (May 22-24, 2012, Stockholm, Sweden), Oral communication.

Smellie, J. (2011). Real system analysis. Deliverables D3.1 and D3.2 published in the CP CROCK web homepage.

Smellie, J. (2012a). Real system analysis: Update. Deliverables D3.1 and D3.2 published in the CP CROCK web homepage.

Smellie, J. (2012b). Real system analysis - 1st CROCK Workshop (May 22-24, 2012, Stockholm, Sweden), Paper.

WORKPACKAGE 4
CONCEPTUALIZATION AND MODELLING

James Crawford[1*]

[1] Kemakta konsult AB, Warfinges väg 33, S-112 93 Stockholm (SWE)

* Corresponding author: james@kemakta.se

Introduction

The challenge in PA is to be able to make predictions with sufficient physical realism that the main adsorptive retardation processes are accounted for in a fashion that neither leads to underestimation of risk, nor such broad ranges of predicted behaviour that highly over-conservative risk assessments are produced that can no longer be considered representative of the system under consideration. The work carried out by the various groups in this Work Package attempts to put process based modelling approaches front-and-centre, both to inform the selection of K_d values for use in simplified PA modelling approaches as well as to improve risk assessment by way of direct implementation of process based models in PA in such a way that does not lead to computational intractability.

The Work Package 4 (henceforth, WP4) component of the CROCK project has the relatively broad objective of developing process based models of radionuclide sorption on systems at different spatial scales with the intention of eventually deploying such models in performance assessments (PA). More specifically, the aims include: 1) the identification of key processes governing the overall retention processes in granitic rock systems; 2) development of models for process description including different radionuclides and over different spatial scales in support of reactive transport modelling performed in work package 5 (WP5), and; 3) identification of main sources of uncertainty in processes and parameters.

Given that PA transport modelling involves taking molecular- and micro-scale processes and extrapolating them to systems that may span many hundreds of metres, if not kilometres, much of this work therefore involves harmonising physical and chemical descriptions over the various spatial scales of mechanistic abstraction. This paper summarises the work carried out in the first year of the CROCK project by the various beneficiaries within WP4 where the overall aim is improvement of PA realism and achieving harmonisation over different scales of phenomenological description.

Description of the work performed

AMPHOS 21

The work carried out by AMPHOS during the first reporting period has focused primarily on reinterpretation of data from literature studies with particular emphasis on the sorption of Cs in crystalline rocks and fracture filling materials. The work was described in a poster by García and Domènech (2012) and as an oral presentation by the same authors at the first annual workshop. It is intended that the range of model substances will subsequently be expanded to include U and Eu. The overall aim is to develop an approach based on the use of Surface Complexation Modelling (SCM) to predict appropriate K_d values for a given geochemical system. In the present work, literature data for Cs sorption on magnetite have been examined. These data represent a range of conditions where the parameters of interest include contact water composition (i.e. differing pH and ionic strength), different spike concentrations of Cs, and different solid to liquid ratios. Magnetite was chosen as a study object since it is a relatively common accessory mineral in granitic rocks and is known to sorb a number of solutes that are considered relevant for PA studies. The data were reinterpreted in terms of a Diffuse Layer Model (DLM) description of sorption using parameters described in Granizo and Missana (2006). The model included a single binding site type and a description of pH dependent surface charge due to protonation-deprotonation reactions. The sorption of Cs is described using two separate inner-sphere chemisorption reactions with parameters fitted to macroscopic sorption data in the cited reference.

A central feature of diffuse layer sorption models is a correction for the effects of electrostatic charge on the mass action equations describing reactions of surface groups. This is necessary since the interaction of surface charge with that of ionic solutes gives rise to concentrations at the solid-liquid interface that differ from those which can be measured in the bulk solution. Since it is not possible to directly measure concentrations of reacting species at surfaces it is necessary to cast the mathematical description of sorption in terms of measurable quantities in the bulk solution. The electrostatic corrections attempt to provide a phenomenologically consistent mathematical framework to achieve this.

In general, the K_d for sorption of Cs as described in the literature references could be independently predicted to within about an order of magnitude using the DLM modelling approach conditioned on the Granizo and Missana (2006) data set. Furthermore, the results suggest that there is a good correlation between pH, ionic strength, and the electrostatic correction term associated with the sorption of Cs^+. This raises the possibility that it may be feasible to predict Cs sorption semi-empirically using the established parametric correlation without the need for detailed surface complexation modelling.

Kemakta Konsult AB

The work carried out by Kemakta Konsult focuses at the present time on reinterpretation of laboratory sorption data obtained during the SKB site investigations at the Forsmark and Laxemar sites in Sweden (SKB, 2008; 2009). The main drive of the work performed during the first reporting period as described in the S+T contribution

(Crawford, 2012) was to understand the dynamics of sorption inferred from the macroscopic measurement data in more detail (i.e. apparent K_d versus time curves). Thus far the data set for Cs, as well as Am and its chemical homologue Eu have been studied in most detail since these are the most detailed data sets. Interpretation of the sorptive uptake time dependency in this particular case is complicated by possible changes in the chemistry of the contact solutions during the course of the experiments. It is argued, however, that the time dependent sorption behaviour does not originate from bulk chemical changes in the contact solutions and rather is postulated to have a physical basis in diffusion kinetics. The diffusive disequilibrium is related to the use of coarsely crushed rock materials as it should take many weeks to months for sorbing solutes to access the surfaces within the internal microporosity of the crushed rock particles.

The apparent K_d values derived from the laboratory experiments scale similarly in proportion to particle size at both short and long contact times for the different crushed size fractions. This seems to imply that rock crushed to small sieve sizes has proportionally larger internal as well as external sorbing surface area. The time constant associated with solute uptake also appears to be very similar, if not identical, for different particle size fractions. In the work which is described in more detail in the S+T contribution, it is speculated that this might be consistent with a biporous description of diffusive uptake where a sparsely distributed secondary porosity dominates both the overall sorptivity of the rock and the kinetics of solute uptake. If the secondary porosity is sufficiently sparse and poorly interconnected with the primary porosity, this may explain the apparent proportional scaling of internal sorptive surface area. It is furthermore postulated that this might be related to the preferential sorption of solutes on the biotite accessory mineral and associated hydrous ferric oxide microprecipitates in the microporosity of the rock.

VTT

In the work performed by VTT an attempt is made to link the description of sorption processes over different spatial scales ranging from molecular- to laboratory- and finally the field-scale. The aim of this work is to provide a mechanistically based means of partially validating the much simplified models used in PA modelling using detailed mechanistic information gathered from lower hierarchies of detailed model abstraction. As described more fully in the S+T contribution by VTT (Olin et al., 2012), the work encompasses a three-stage approach corresponding to the different spatial scales referred to above. The first level involves density function calculations made to understand physical processes which give rise to the macroscopic surface reactive properties of sorbing minerals. This is a quantum mechanical modelling technique that seeks to simulate the electronic structure (and hence chemical reactivity) of the hydrated mineral interface and its relation to mineral crystal structure. In the first instance, the technique is applied to the understanding of the surface reactivity of biotite, a mineral that is thought to dominate the sorption properties of granitic rocks for a number of PA relevant radionuclides.

The molecular-scale modelling aims to inform choices underlying the formulation of Surface Complexation Models (SCM's) describing the macroscopic sorptivity of various solutes in association with biotite. Here, the SCM modelling work addresses the

sorption of Eu and Ni and builds upon previous modelling work carried out in the FP6 fundamental processes of radionuclide migration (FUNMIG) project (Olin et al. 2008). Using the information provided by SCM simulations, it is anticipated that mechanistically reasoned K_d values for groundwater compositions outside the range of experimental calibration can then be predicted for subsequent deployment in the simplified PA models at the highest level of abstraction.

The work underway also seeks to compare the predictions made by K_d based transport models with more complex simulations where the underlying surface complexation model is incorporated directly in a transport model for flow and solute migration in a fracture using the COMSOL Multiphysics program.

References

Crawford J. (2012). Decreasing uncertainty of radionuclide migration predictions in safety assessment modelling. 1st CROCK Workshop (May 22-24, 2012, Stockholm, Sweden), Paper.

Garcia D., Domènech C. (2012). Cs sorption onto crystalline rock. From mechanistic sorption models to K_d. 1st CROCK Workshop (May 22-24, 2012, Stockholm, Sweden), Oral communication & Poster.

Granizo N., Missana T. (2006). Mechanisms of cesium sorption onto magnetite, Radiochimica Acta, 94 (9-11), pp. 671-677. doi:10.1524/ract.2006.94.9.671

Olin M., Puhakka E., Itälä A., Tanhua-Tyrkkö M., Pulkkanen V-M., Nordman H., Kajanto K., Puukko E., Koskinen L. (2012). Radionuclide transport modelling by molecular chemistry, surface complexation and reactive transport modelling. 1st CROCK Workshop (May 22-24, 2012, Stockholm, Sweden), Paper.

Olin, M., Puukko, E., Puhakka, E., Hakanen, M., Lindberg, A. and Lehikoinen, J. (2008). Sorption on biotite. Final Annual Workshop Proceedings- 6th EC FP-FUNMIG IP, Forschungszentrum Karlsruhe Report. Forschungszentrum Karlsruhe GmbH, pp. 335-343. http://bibliothek.fzk.de/zb/berichte/FZKA7461.pdf

SKB (2008). Site description of Forsmark at completion of the site investigation phase. SDM-Site Forsmark. SKB Technical Report TR-08-05, Swedish Nuclear Fuel and Waste management Company, Stockholm, Sweden. http://skb.se/upload/publications/pdf/TR-08-05_part1of2.pdf

SKB (2009). Site description of Laxemar at completion of the site investigation phase. SDM-Site Laxemar. SKB Technical Report TR-09-0q, Swedish Nuclear Fuel and Waste management Company, Stockholm, Sweden. http://skb.se/upload/publications/pdf/TR-09-01_part1of2.pdf

WORKPACKAGE 5
APPLICATION TO THE SAFETY CASE

Jorge Molinero[1*]

[1]Amphos 21 Passeig de Garcia i Fària, 49-51, 1-1, 08019 Barcelona

* Corresponding author: jorge.molinero@amphos21.com

Introduction

The objective of WP5 is to gather that information produced in the other workpackages that can help to reduce the uncertainty associated to Performance Assessment (PA) applications. These data will be preprocessed and used as prior information in coupled reactive transport simulations focused on potential PA exercises. The simulations will account for the fate and transport of radionuclides through complex and extended networks of fractures (i.e. discrete fracture networks) and will consider a non-homogeneous composition of the fracture filling material in terms of sorption properties.
The results of the reactive transport simulations will provide effective Kd values that will be time and space dependent. Thus, "smart" and efficient procedures will be defined to feedback tailored Kd-based simulations of radionuclide transport with these computed values. A critical analysis of the results will be performed: the resulting effective parameters will be critically analyzed by comparing them with available compilations of relevant parameters for radionuclide transport.
Simple non-coupled radionuclide transport calculations using effective sorption parameters will be also used for comparative purposes. Implementing the effective Kd values obtained from previous coupled simulations will test the applicability of the simplified models. Finally, a strategy will be developed for the efficient application of the approach to a broader set of data with the aim of reducing the overall conservatism in the PA studies.

Description of the work performed

AMPHOS 21.

In the first half of the project, the beneficiary has been working on the development of a numerical tool MCPhreeqc (MCPhreeqc, 2011) that provides an extensible and flexible environment for the rational treatment of uncertainty (Figure 1). Furthermore, a modelling prototype has been defined for the calculation of "intelligent" Kd values. The prototype is based on the evidence that pH and redox conditions, which govern the Kd values of the considered radionuclides, are controlled by few minerals (e.g. calcite,

pyrite, FeS), which in turn can be often described under equilibrium assumption. Thus, the prototype consists of two companion numerical models: (a) the "classical" Kd-based numerical model and (b) a fully explicit reactive transport model where the (equilibrium) mineral reactions are described using the efficient procedure proposed by De Simoni et al. (2008). After each simulation step, new pH and redox conditions are inferred from the "supporting" model. This geochemical information and a companion data-base (i.e. pH and redox vs Kd), feedbacks the Kd-based model by providing new Kd-values in each node of the model domain.

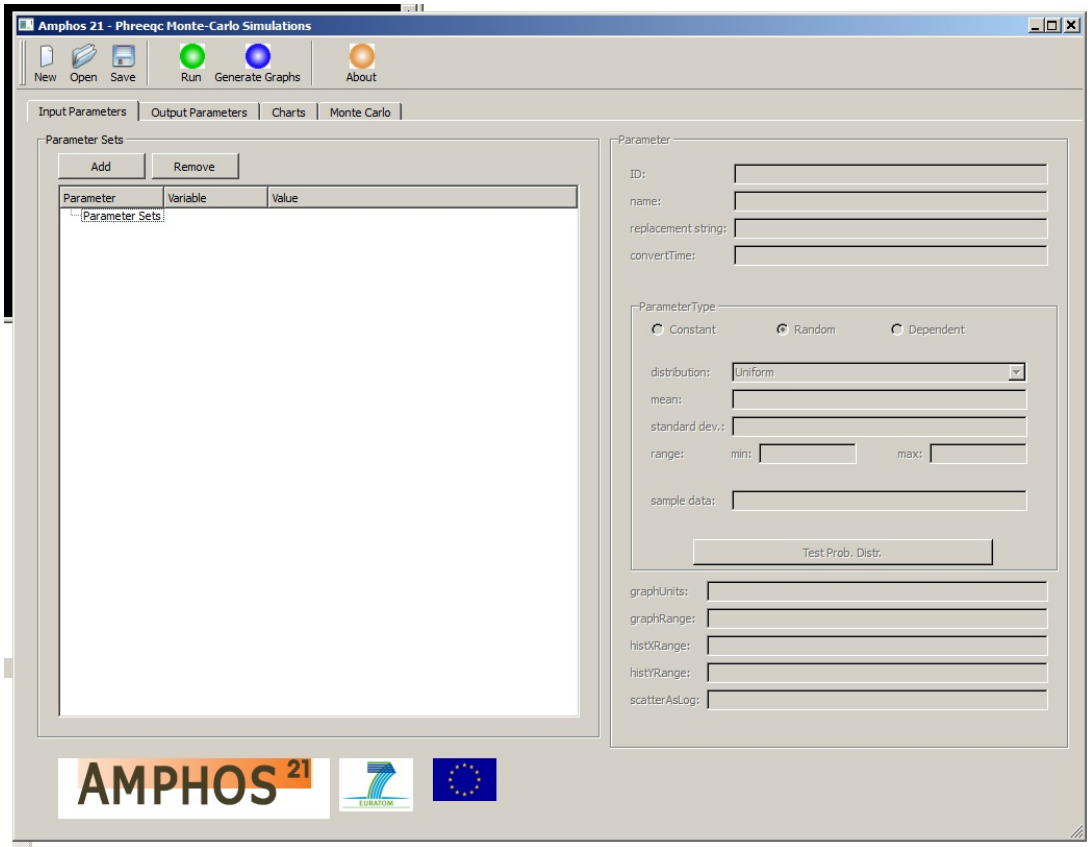

Figure 1 *Screenshot of the MCPhreeqc graphical user interface*

Additional work for WP5 has been presented at the 1st CP CROCK Workshop (Trinchero et al., 2012).

KEMAKTA

Sorption of Ra, Sr, and Cs has been simulated using a model of ion-exchange described in the literature for Swedish granitic rock. Using this model the Kd for sorption of each of these radionuclides was estimated for different groundwater mixing factions of the saline and fresh end-members. Using an analytical model describing transport of a non-reactive component, the mixing fraction of the different groundwater types could be determined as a function of space and time along a one-dimensional advective flowpath and in the adjacent rock matrix. Based on the spatially and temporally variable Kd value, the transport of the reactive solutes Ra, Sr, and Cs could be simulated using a simplified modelling approach implemented in Matlab. The breakthrough curves of the reactive solutes exhibited clearly non-linear features related to the alternating pulses of

saline and fresh groundwater that cannot be modeled using a constant Kd modelling approach. Full details of the work performed may be found in the Scientific and Technical contribution (Crawford, 2012a) and the oral communication (Crawford, 2012b) from the beneficiary as presented at the First Workshop of the CROCK project in Stockholm, Sweden held on May 22-24, 2012.

VTT

VTT has start applying typical PA flow and transport models to support the selection of the benchmark exercise. A number of sensitivity analyses on the Kd values computed in WP4 have been carried out in order to identify the governing retention zones at the PA scale. Additional information regarding VTT activities may be found in the Scientific and Technical contribution (Nordman, 2012), the poster Tanhua-Tyrkkö and Italä (2012) and the oral communication (Olin et al., 2012) from the beneficiary as presented at the First Workshop of the CROCK project in Stockholm, Sweden held on May 22-24, 2012.

References

Crawford, J. (2012a). Decreasing uncertainty of radionuclide migration predictions in safety assessment modeling - 1st CROCK Workshop (May 22-24, 2012, Stockholm, Sweden), Paper.

Crawford, J. (2012b). Application to the safety case. Deployment of process-based models in safety assessment - 1st CROCK Workshop (May 22-24, 2012, Stockholm, Sweden), Oral communication.

De Simoni, M., Carrera, J., Sanchez-Vila, X. y Guadagnini, A. A procedure for the solution of multicomponent reactive transport problems. Water Resources Research, 41(11):W11410, November 2005.

MCPhreeqc (2011). A tool for PHREEQC Monte-Carlo simulations. Amphos 21. http://www.Amphos21.com/software

Nordman, H. (2012). Snapshots of importance of geosphere parameters - 1st CROCK Workshop (May 22-24, 2012, Stockholm, Sweden), Paper.

Olin, M., Pulkkanen, V.M., Nordman, H., Poteri, A. (2012) How to predict Kd values outside experimental studied conditions and to estimate related uncertainty? - 1st CROCK Workshop (May 22-24, 2012, Stockholm, Sweden), Oral communication.

Parkhurst, D.L, Appelo, C.A.J, 1999. User's guide to PHREEQC (version 2) - A computer program for speciation, batch-reaction, one-dimensional transport and inverse geochemical calculations. U.S. Geological Survey Water Resources investigations report 99-4259.

Itälä, A., Tanhua-Tyrkkö, M., Puukko, E. and Olin, M. (2012) Kd-values and surface complexation modelling - 1st CROCK Workshop (May 22-24, 2012, Stockholm, Sweden), Poster.

Trinchero, P., de Vries, L.M, Piqué, À., Duro, L., Molinero, J. (2012). Radionuclide retention in fractured media: coping with uncertainty in PA studies - 1st CROCK Workshop (May 22-24, 2012, Stockholm, Sweden), Paper & Oral communication.

S + T CONTRIBUTIONS

List of contributions

CHARACTERIZATION OF ROCK SAMPLES FROM AREAS OF THE PROPOSED HLW AND SNF REPOSITORY IN RUSSIA (NIZHNEKANSKY MASSIVE) AND FIRST SORPTION STUDIES

V.G. Petrov[1*], I.E. Vlasova[1], N.V. Kuzmenkova[2], V.A. Petrov[3], V.V. Poluektov[3], A. Grivot[1], S.N. Kalmykov[1]

[1] Lomonosov Moscow State University, Chemistry Department, Moscow, Russia
[2] Vernadsky Institute of Geochemistry and Analytical Chemistry, Russian Academy of Science, Moscow, Russia
[3] Institute of Geology of Ore Deposits, Petrography, Mineralogy and Geochemistry, Russian Academy of Sciences (IGEM RAS), Moscow, Russia

* Corresponding author: vladimir.g.petrov@gmail.com

Abstracts

Granites from two areas of Nizhnekansky massive (Russia) have been studied in terms of mineralogical composition of different types of granites along with sorption and distribution of Cs on the different minerals surfaces. After 100 hours of sorption experiment 30-65% of Cs has been bound to granites. According to the autoradiography data the microdistribution of Cs on the granite surface as a result of sorption experiment was uneven; the most part of Cs have sorbed to the surface of the dark minerals (biotite, chlorite).

Introduction

Main provisions of the concept of high level wastes (HLW) and spent nuclear fuel (SNF) isolation into the deep crystalline rock formations are accepted in Russia. Some areas of the Nizhnekansky Granite Massive are supposed as the most perspective location for the future HLW and SNF disposal. Sorption properties of granites relatively to different radionuclides are of great importance for the prediction of radionuclides migration behavior within the granite body of the disposal. In this work sorption properties of granite samples towards Cs are studied.

Experimental

Core materials from two sites of the supposed areas (area **Kamenny**, drilling depth down to 700 m, and area **Itatsky**, drilling depth down to 500 m) have been studied in terms of petrographic and mineralogical characterization; definition of filtration, elastic, petro-physical and strength properties; estimation of hydrothermal-metasomatic transformation of rocks.

Two undisturbed slices from each area were collected (Figure 1) to perform sorption experiments onto their surface in order to reveal the mineral phases of granites which are responsible for the preliminary sorption of radionuclides. The following rocks were chosen for this experiment: spessartite and biotite quartz diorite from **Kamenny** area; quartz diorite – monzodiorite and biotite granite from **Itatsky** area. More detailed information is listed in Table 1.

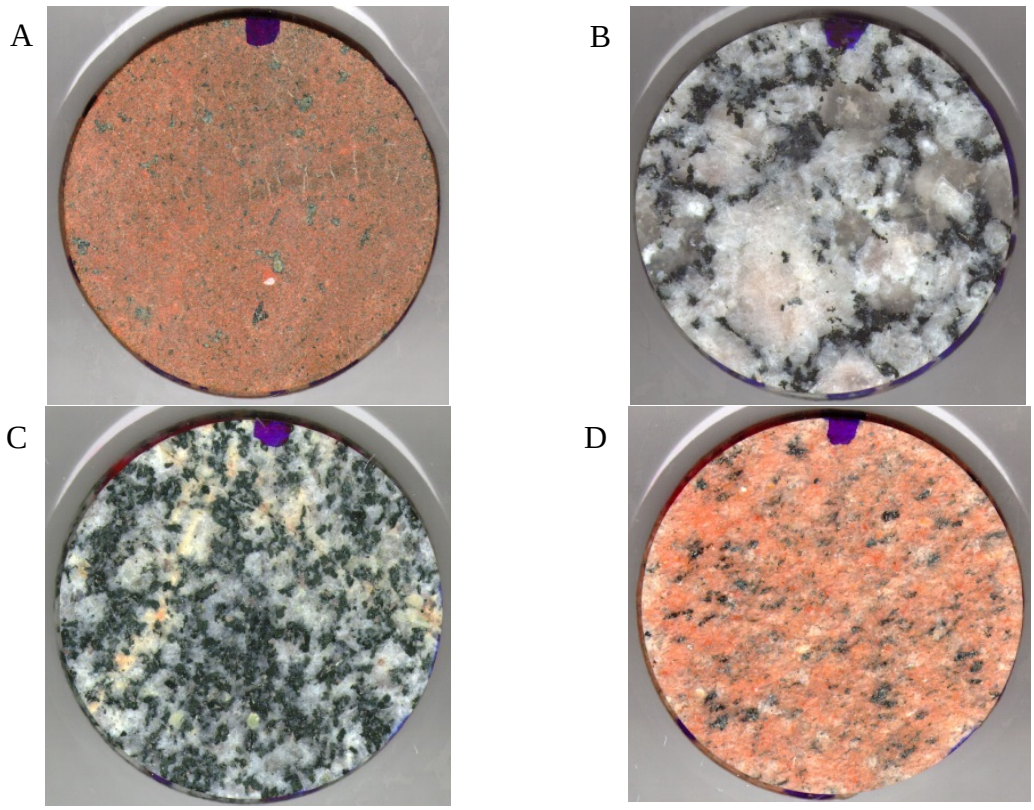

Figure 1: *Rock slices for sorption experiments from Kamenny (A, B) and Itatsky (C, D) areas.*

Sorption experiments were carried out under ambient atmospheric conditions in modeled groundwater: $Ca(HCO_3)_2$ – 187.5 mg/L, $NaHCO_3$ – 62.5 mg/L, pH = 6.7. Initial concentration of Cs-137 was $1 \cdot 10^{-9}$ mol/L. The rate of sorption was controlled by measuring aliquots by gamma-spectrometry. A quarter of each sliced disk was placed vertically in plastic vessel. One side of the disk was polished and reverse side was left rough to determine the roughness effect on sorption of radionuclides.
Autoradiography studies have been performed using Cyclone Plus Storage Phosphor System (PerkinElmer), including Cyclone Plus scanner, software and storage phosphor screens. The spatial resolution of autoradiography images is 42 µm.

Table 1: *Petrographic characterization of rock samples from Nizhnekansky massive*

Sample	Rock	Textural (Tex) and Structural (Str) characteristic	Mineralogical composition* (%), Intensity of hydrothermal-metasomatic transformations (IHMT)
		Kamenny area	
A	Spessartite metasomatically transformed	**Tex:** massive **Str:** aphyric, panidyomorphogranular, metasomatic; **evenly granular**, **grain size:** < 1 mm	**HB, Chl, CM** (35-40)**, Pl** (50-55), **Ab, Pfs, FS** (5-7), **Ap, Gr, NM (**3-5) ***IHMT-medium***
B	Biotite quartz	**Tex:** massive **Str:** gipidyomorphogranular; **unevenly granular**, **grain size:** 2-5 mm, >5 mm, 10-40 mm	**Bi, Chl (**10-15), **Q** (10-15), **Pfs** (5-10), **Pl** (65-70), **Gr, NM** (1-2) ***IHMT-0 (original rock)***
		Itatsky area	
C	Quartz diorite – monzodiorite	**Tex:** massive, weakly gneissic **Str:** gipidyomorphogranular, monzonitic; **evenly granular**, **grain size:** 1-2 mm**,** 2-5 mm	**Bi, HB** (25), **Q** (15), **Pfs** (5-10), **Pl** (45-50), **Gr, Zr, NM** (2-3) ***IHMT-0 (original rock)***
D	Biotite granite	**Tex:** massive, gneissic **Str:** granitoid, transitional to porphyritic; **unevenly granular**, **grain size:** 2-5mm	**Bi, Chl** (5-7), **Q** (30), **Pfs** (30-35), **Pl** (25-30), **NM (**1-2) ***IHMT-minimun***

* Ab – albite, Ap – apatite, Bi – biotite, Car – carbonate, Chl – chlorite, CM – clay minerals (kaolin, illite, montmorillonite, et al.), FS – metasomatic non-transparent feldspars, Gr – grothite, HB – hornblende, LLA – leucoxenelike aggregate, NM – non-transparent minerals (magnetite, leucoxene, hematite), Pfs – potash feldspar (microcline, orthoclase), Pl – plagioclase, Q – quartz, Ser – sericite, Zr – zircon.

Results and discussion

Characterization of granites

It was established that the most part of the core material from the area **Kamenny** is presented by *granites* and *leucogranites*, while the core material from the area **Itatsky** is mostly *diorites* and *quartz diorites*. The profiles of the both areas have several zones (of not more than 50 m in depth each) of high-intermediate temperature metamorphism of amphibolite-greenschist facies (gneisses, granite-gneisses, plagiogneisses). Low-temperature around-fractural hydrothermal metasomatism is wide spread in the both profiles: chloritization, argillization, sericitization. The density of the crystalline rocks varies from 2.61-2.63 g/cm^2 (granites and leucogranites) to 2.74-2.79 g/cm^2 (quartz diorites and tonalities). Effective porosity of granite rocks varies from 0.14% to 0.95% while in some rare cases it reaches 1.31% (hypergenic-transformed granites) and even 5.6% (lamprophires). The values of rocks permeability differ from $n \cdot 10^{-20}$ till $n \cdot 10^{-16}$ m^2. Maximal values of permeability were measured for leucogranites, quartz diorites and metasomatic spessartites. In the both areas there are significant intervals of

undisturbed slightly permeable rocks which are alternated by zones of increased fracturing and matrix permeability. The structure of permeable zones is based on the net of fractures filled with quartz, carbonates, chlorite, sulphides and clayey minerals (kaolin, illite, smectite) which have been formed as a result of low-temperature hydrothermal metasomatism. It was revealed three fractured zones in both profiles (**Kamenny** and **Itatsky**).

Cs sorption onto granite slices

First results show that sorption kinetic for Cs is quite slow and probably depends on diffusion (Figure 2).
For ***biotite quartz*** and ***quartz diorite*** rocks maximum of Cs sorption reaches about 70% after 300 hours. Absolute maximum of sorption (about 90%) corresponds to ***spessartite*** from area **Kamenny** and did not reach equilibrium after 1000 hours. Minimum conforms to ***biotite granite*** from the area **Itatsky.**

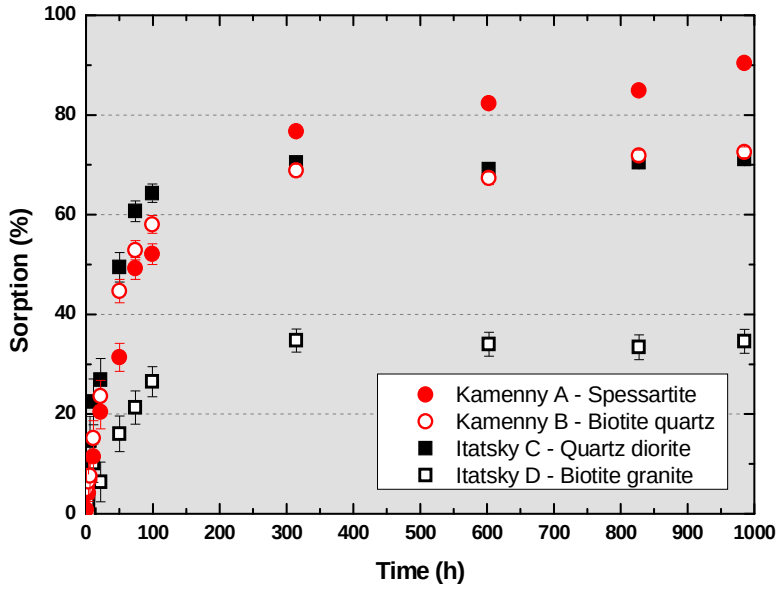

Figure 2: *Cs-137 sorption onto rock samples from Kamenny and Itatsky areas.*

Cs distribution among mineral surfaces of granites

After the sorption experiments were finished the microdistribution of Cs on the surface of granite slices was studied. It was observed that cesium sorbed unevenly. The most part of Cs was bound to dark minerals (Figure 3).
Optical microscopy and SEM-EDX studies proved that the dark minerals are ***biotite*** and ***chlorite***.
Roughness of all the samples was measured by profilometry, obtained data showed huge discrepancy. The calculated ratios of roughness average absolute values for unpolished and polished surfaces were 3.0 ± 1.9, 4.3 ± 0.9, 9.8 ± 2.8 and 9.0 ± 5.0 for samples Kamenny A,B and Itatsky C,D, respectively. Similar calculated ratios of Cs sorption were (unpolished/polished) 1.1 ± 0.3, 1.3 ± 0.4, 1.0 ± 0.3 and 6.0 ± 0.7 for the same samples. Thus there was no correlation between surface roughness and Cs sorption quantity observed. This result can be explained either by assuming the

differences in mineral abundance of polished and unpolished surfaces of slices or by excess of sorption sites on both types of surface.

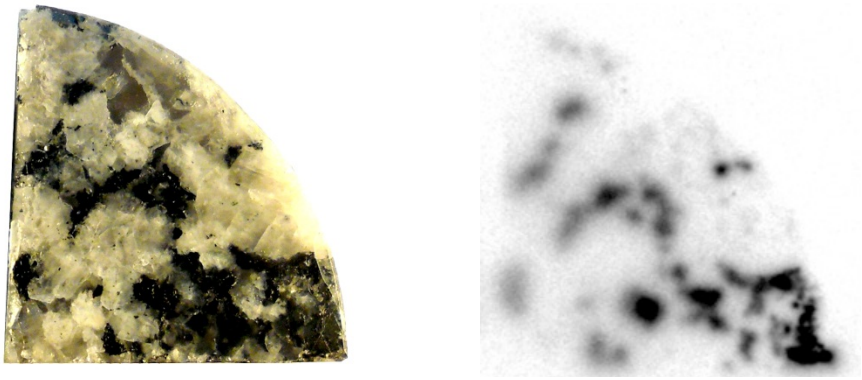

Figure 3: *An example of granite slice (Kamenny, 702 m) – on the left, and radiography image of Cs sorption on its surface – on the right.*

Conclusions and outlook

Mineralogical composition of crystalline rock material from two proposed sites of HLW and SNF repository in Russia (Nizhnekansky massive) was determined as well as density, porosity and permeability. First sorption studies showed slow kinetic of Cs sorption probably due to diffusion into bulk. Equilibrium was reached after two weeks of contact time. It was observed that cesium sorption controlled mostly by dark minerals (***biotite*** and ***chlorite***). No correlation between surface roughness and quantity of sorbed Cs was observed.
Future studies will be performed using four types of rocks collected from each area (Kamenny and Itatsky) for further sorption (U, Eu, Tc) experiments with granulated material of 2 mm in size (Figure 4).

Figure 4: *Rock samples to be granulated for sorption experiments from Kamenny (left) and Itatsky (right) areas.*

The types of collected rocks are as follows: granite-adamellite, leucogranite, diorite (tonalite), spessartite (Kamenny area) and diorites, quartz diorites (Itatsky area). The rocks were taken from the various depths, which was signed on the samples.

Further studies will include radionuclide sorption on the crashed samples including the kinetics, Kd measurements, radionuclides speciation and surface complexation modeling. Local distribution and preferential sorption of radionuclides onto different mineral grains within the sample will be studied for thin sections using radiography, SEM-EDX, SIMS, etc.

CHARACTERISATION OF ROCK SAMPLES FROM ÄSPÖ USING GAS ADSORPTION

Stellan Holgersson[1*]

[1] Department of Chemical and Biological Engineering, Division for Nuclear Chemistry, Chalmers University of Technology (SE)

*Corresponding author: stehol@chalmers.se

Abstract

Drill cores from the Äspö Laboratory have been obtained and characterised with a gas adsorption instrument for: 1) specific surface area, using Kr gas and interpreted with the Brunauer-Emmet-Teller (BET) model, and 2) specific pore volume (porosity), using N_2 gas and interpreted with the Barrett-Joyner-Halenda (BJH) model. Before the measurements each drill core were sawn into 3cm long samples, by the use of a low speed saw. Some of these samples were crushed and sieved into two fractions: 90-250µm and 500-1000µm. The results were interpreted with a model for the interdependency of specific surface area and porosity, by assuming a disturbed zone in the geological material. It is suggested that the origin of the disturbed zone can be the mechanical treatment of the rock particles or inherited porosity zones in the rock, or a combination of both.

Introduction

In the CROCK project, one task is to measure sorption R_d (m^3/kg) values for some selected radioactive tracers at different laboratories, using the same geological material. The material was sampled in the form of drill-cores at the Äspö laboratory, near Oskarshamn, Sweden (KIT-INE, 2011). Special care was taken to preserve the reducing conditions for the samples, both at sampling and the subsequent handling and measurements. The overall aim of this task is to try to reduce the experimental uncertainties in R_d values, in order to obtain more exact calculations of radiotracer migration in a performance assessment of a nuclear waste repository in granitic rock. A preliminary characterization of the geological material in the form of surface area and porosity is necessary in order to normalize the sorption data that will be obtained from batch sorption measurements of crushed and sieved material. The characterization is also necessary to normalize and interpret the sorption and diffusion data that will be obtained from diffusion experiments. The specific surface area have been identified as a key parameter for extrapolating the results from laboratory experiments to the field-scale (André *et al.*, 2009, Dubois *et al.*, 2011), in order to obtain surface area normalized R_a (m) values. Also, the available porosity may not be constant between different size fractions up to the intact rock. It is also an essential parameter in the interpretation of sorption R_d values obtained from diffusion experiments. The porosity

may therefore also be a key parameter to understand how sorption should be extrapolated from laboratory to field-scale. The interdependency of specific surface area and porosity for pure minerals have been the object of separate investigations (Brantley and Mellott, 2000, Dubois *et al*, 2012) and in this work, the rock is now investigated for similar interdependency.

Objective and scope

The first objective of this work is to prepare geological samples for subsequent batch sorption and diffusion experiments within the CROCK project. A number of drill cores were sampled at the Äspö laboratory (KIT-INE, 2011). Priority for Chalmers drill-core samples were cores sampled perpendicular to a fracture. Each drill-core was then sawn into smaller slices of 3cm length, starting from each side of the fracture. One half of the sliced core will be used in subsequent diffusion experiments later in the CROCK project, the other half will be crushed and used in batch sorption experiments. The scope of the investigation is limited to two drill cores. Another objective for this work is to obtain specific surface area for the 3cm long drill core samples of rock from Äspö, by measurments with gas adsorption. Also, specific surface area for samples of crushed and sieved rock is to be obtained. A third objective is to obtain the porosity for the crushed samples, by measurements with gas adsorption. Measurement of the porosity of an intact core slice with this method can be difficult or impossible due to the very low volumes involved (Dubois *et al*. 2012). Therefore, extrapolation methods of porosity from crushed samples, using a model of specific surface area and specific volume interdependency is to be used for later comparison with alternative porosity measurements, for example using HTO diffusion and gravimetric experiments, to be made later in this project.

Experimental

Sampling of drill cores

Altogether 18 samples of drill cores were obtained for Chalmers from the Äspö facility. The sampling took place during May 2011 in the tunnel gallery NASA2376A, located at a depth of approximately 300m below surface (KIT-INE, 2011). Two boreholes were drilled, KA2368A-01 and KA2370A-01, both directed perpendicular to the tunnel wall. The drill cores were of 42mm diameter and the rock type was found to be predominately Äspö diorite (ÄD), sometimes with minor components of Fine-grained granite (FGG) and Ävrö granite (ÄG) (KIT-INE 2011). The drill core samples obtained for Chalmers are described in Tables 1 and 2 below.

Table 1: *Description of drill core samples from first borehole (KIT-INE, 2011).*

Drill core from KA2368A-01		
label	**drilling length (m)**	**note**
1.11	4.77-4.90	fracture half
1.12	4.90-5.40	fracture half
1.20	8.13-8.26	sealed fracture, re-opened, complete
1.30	12.11-12.66	sealed fracture, re-opened, complete

Table 2: *Description of drill core samples from second borehole (KIT-INE, 2011).*

Drill core from KA2370A-01		
label	**drilling length (m)**	**note**
2.4	1.3-1.69	fracture half
2.5	1.69-1.93	fracture half
2.7	2.45-2.89	fracture half
2.10	3.81-4.35	fracture, complete
2.19	7.30-7.57	possible fracture half
2.20	7.57-7.91	two fracture halves, one complete, contains ÄG
2.23	8.47-8.91	two fracture halves, contains ÄG
2.24	8.91-9.24	fracture half, contains ÄG
2.26	9.54-9.81	fracture half
2.27	9.81-10.20	fracture half, contains ÄG
2.37	13.69-14.05	two fracture halves, one complete
2.38	14.05-14.60	two fracture halves, one complete

At the drilling site, the samples were put into aluminium-foil coated plastic bags, flushed with N_2 gas and sealed immediately after they were obtained from drilling. The samples were transported to Chalmers and put into an N_2 flushed glove-box (MBraun InLab, $[O_2(g)]$~1ppm, T~20°C) for storage.

Sample preparation

The samples were sawn into sections of 3cm length using a low speed saw (Buehler IsoMet 1000) set to 300-325rpm with a Ø=17.5cm diamond wafering blade (Buehler 20LC) cooled by water bath. The cutting was made inside the N_2 flushed glove-box and the cooling water degassed and stored in N_2 atmosphere. Some of these sections were used for obtaining crushed material with the following procedure, also made inside a glove-box. This was produced by smashing samples put into a clean towel with a hammer. The coarse pieces were then crushed further, using an agate mortar and pestle. Two fractions were collected with plastic and nylon mesh sieves (CISA): 90-250µm, and 500-1000µm. The fractions were washed with ethanol for removing finer particles.

Specific surface area measurements

Samples were measured with a gas adsorption instrument (ASAP 2020, Micromeritics) using Kr gas (99.998%, Air Liquide). Before measurements, samples were dried at the vacuum station of the instrument at room temperature for at least 25 hours (crushed samples) or several days (sections of drill cores). The samples for specific surface area were measured using a 10 point Kr sorption isotherm with p/p_0 from 0.05 to 0.2. The results were interpreted with the instrument software using the BET model (Brunauer *et al.* 1938). For samples of drill core sections a special made glass sample holder of 455mL measured free space (Figure 1) was used, with a glass insert. For crushed samples, standard 1/2-inch glass tubes of 16mL volume (Micromeritics p/n 240-61003-00) and filler rods (Micromeritics p/n 240-61016-00) were used.

Figure 1: *The specially made holder for gas adsorption measurements of 3cm drill-core sections.*

Porosity measurements

Crushed samples were measured with the same gas adsorption instrument (ASAP 2020, Micromeritics) that was used for the specific surface area measurements but using N_2 gas (99.999%, AGA/Linde). Before measurements, the samples were dried at the vacuum station of the instrument at room temperature for at least 25 hours. The samples for porosity were measured using N_2 adsorption up to saturation pressure p_0 and then desorption with, in total, 98 pressure points. The results were interpreted with the instrument software using the BJH model (Barrett *et al.* 1951). Sample holders were the same as for specific surface area measurements.

Results

For the moment, only two fractions have been measured and two 3 cm drill core pieces. All samples are taken from core 1.30 in Table 1. Results of the specific surface area and

specific volume measurements of crushed fractions of Äspö diorite are shown in Table 3, below. Errors μ are given as

$$\mu = \bar{x} \pm \frac{t_{\ 95\%} \cdot s}{\sqrt{3}} \quad (1)$$

Where *x*-bar is the mean value of three measurements, *s* is the standard deviation and $t_{95\%}$ is Student´s t value for 95% confidence level and two degrees of freedom (the t value is 4.3).

Table 3: *Results for three specific surface area and volume measurements of two crushed fractions of Äspö diorite.*

	90-250µm		**500-1000µm**	
	BET sp. area (m^2/g)	**BJH sp. volume (µL/g)**	**BET sp. area (m^2/g)**	**BJH sp. volume (µL/g)**
#1	0.252	0.926	0.103	0.354
#2	0.246	0.963	0.105	0.355
#3	0.262	0.939	0.129	0.355
average	0.253±0.020	0.943±0.047	0.112±0.036	0.355±0.001

The results of two measurements of specific surface area of drill-cores are shown in Table 4 below. The error is not calculated correspondingly for two measurements, one more measurement will be made later in order to have exactly the same error calculation as in equation 1.

Table 4: *Results for two measurements of specific surface area of 3cm long drill core pieces of Äspö diorite (core #1.30, Table 1).*

	BET sp. area (m^2/g)
#1	0.021
#2	0.026
average	0.024

Conclusions

The results are shown as a plot between specific volume and specific surface area in Figure 3, below. A model has been developed that assumes that the crushed particles consist of a non to low-porous core surrounded with a porous shell (Figure 2).

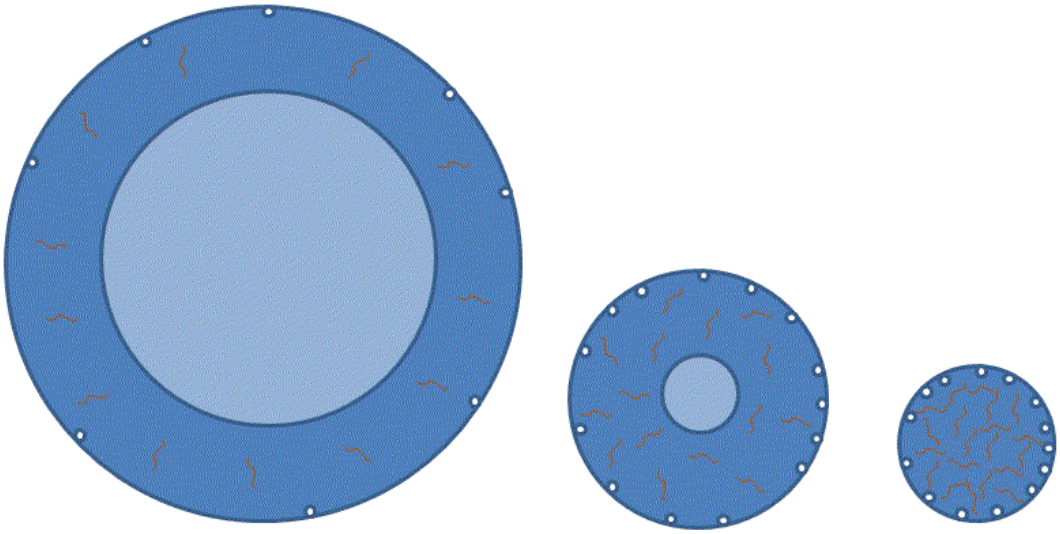

Figure 2: *Schematic representation of different particle sizes, comprising of a porous shell (dark) of fixed thickness and a low- or non-porous core (light). For small enough particles it can be assumed that there will be no core left.*

The porous shell is assumed to be of constant thickness for all particle sizes. The model equation is

$$A_{sp} = \frac{2V_{sp}}{r_{pore}} + \frac{F_p}{r_s \cdot \rho} - \frac{F_p}{r_s \cdot \rho} \cdot \sqrt[3]{\frac{V_{sp} \cdot \rho - \varepsilon_s}{\varepsilon_c - \varepsilon_s}} \qquad (2)$$

Where A_{sp} and V_{sp} are the experimentally determined specific surface area and pore volume, respectively. F_p is a form factor, here assumed to be 3, assuming an ideal sphere and no surface roughness. The fitting parameters are the pore radius r_{pore}, the shell thickness r_s, shell porosity ε_s and core porosity ε_c. The model equation 2 is valid for the case when a solid core is present and is based on hundreds of independent measurements of specific surface area and specific volume for granitic minerals (Dubois *et al*. 2012). Results from fitting the equation to the experimental data in Tables 3 and 4 are shown in Figure 3.

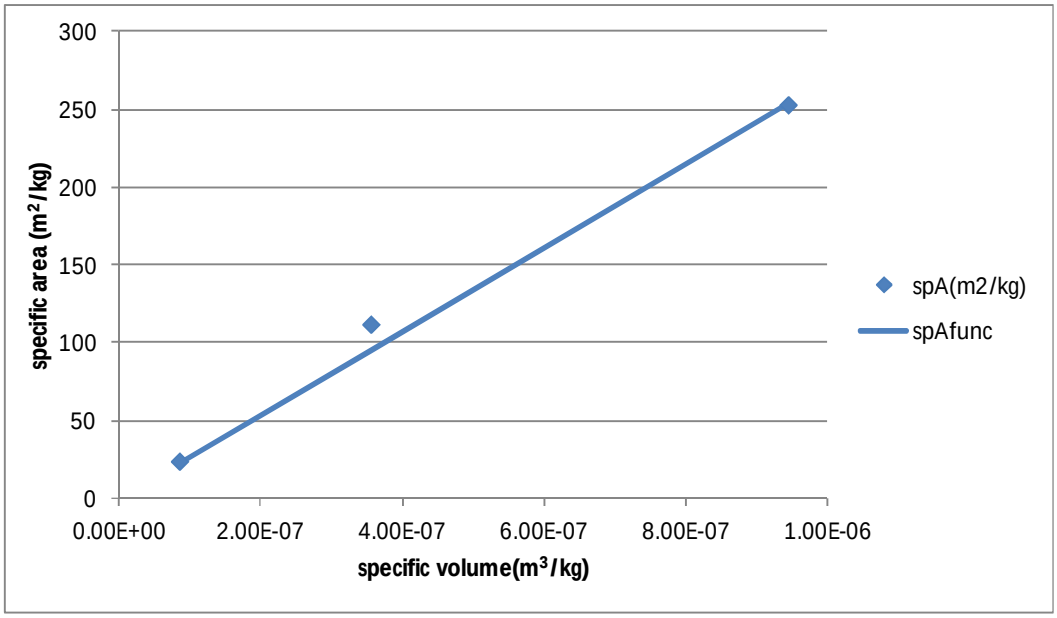

Figure 3: *Model for relationship between specific pore volume and specific surface area. Legend "spA" stands for specific area, either as measured mean values (diamonds) or calculated with equation 2 (line).*

In the figure, it should be noted that the specific volume for the 3cm drill core piece is an extrapolated value from the model. By assuming a density of 2700kg/m^3 and using the extrapolated value of 0.085µL/g from Figure 3, one obtains an average porosity of 0.02%. More experimental data are to be collected and a new fitting of the model equation will be made when at least one more size fraction have been measured for specific surface area and pore volume and also one more sample of the drill core sections have been measured for specific surface area. The uncertainty in the extrapolated porosity may then also be estimated. This extrapolated porosity should be compared with measurements of porosity with the HTO diffusion method, which will be the next step for this investigation on the properties of the Äspö rock.

Acknowledgements

Henrik Drake, Torsten Schäfer, Sebastian Büchner and the MiRo drilling team are gratefully acknowledged for help with sampling of the drill cores.
The research leading to these results has received funding from the European Union's European Atomic Energy Community's (EURATOM) Seventh Framework Programme FP7/2007-2011 under grant agreement n° 269658 (CROCK project) and SKB, the Swedish Nuclear Fuel and Waste Management Company.

References

André, M., Malmström, M.E. and Neretnieks, I. (2009). Specific surface area measurements on intact drillcores and evaluation of extrapolation methods for rock matrix surfaces. Journal of Contaminant Hydrology, 110, 1-8.

Barrett, E.P., Joyner, L.G. and Halenda, P.P. (1951). The determination of pore volume and area distributions in porous substances. I. Computations from nitrogen isotherms. J.Am. Chem. Soc., 73(1), 373-380.

Brantley, S.L. and Mellott, N.P. (2000). Surface area and porosity of primary silicate minerals. American Mineralogist, 85, 1767.

Brunauer, S., Emmet, P.H. and Teller, E. (1938). Adsorption of gases in multimolecular layers. J.Am. Chem. Soc., 60(2), 309-319.

Dubois, I.E., Holgersson, S., Allard, S. and Malmström, M.E. (2011). Dependency of BET surface area on particle size for some granitic minerals. Proc. Radiochim. Acta, 1, 75-82.

Dubois et al. (2012). Interdependency of specific surface area and specific volume for some granitic minerals (Manuscript to be submitted during 2012).

KIT-INE (2011). Provision of new fracture bearing drill core samples obtained, handled, transported and stored under anoxic conditions, including first documentation. Deliverable D-N°1-1, published in the EU CROCK Project homepage.

SORPTION/DESORPTION OF ^{137}Cs(I), ^{152}Eu(III) AND ^{233}U(VI) ONTO NEW CROCK DERIVED ÄSPÖ DIORITE – A BATCH TYPE STUDY

Eike Stage[1,2], Florian Huber[1*], Stephanie Heck[1] and Thorsten Schäfer[1,2]

[1] Karlsruhe Institute of Technology (KIT), Institute for Nuclear Waste Disposal (INE), P.O. Box 3640, 76021 Karlsruhe (DE)
[2] Institute of Geological Sciences, Department of Earth Sciences, Freie Universität Berlin, Berlin (DE)

* Corresponding author: florian.huber@kit.edu

Abstract

In the prevailing study we present batch type experiments on Cs, Eu and U sorption onto Äspö diorite (1-2 mm size fraction) under Ar atmosphere using a synthetic Äspö groundwater. Both, freshly non-oxidized and artificially oxidized Äspö diorite was applied in the experiments. Subsequently to the batch sorption experiments, desorption experiments have been conducted using either synthetic Äspö groundwater or natural Grimsel groundwater to mimic the influence of low mineralized glacial melt water intrusion on the Äspö system.

Introduction

Mafic (e.g. basalts) and/or felsic (e.g. granites) crystalline rocks are the only available host rock formations in Sweden and Finland for a nuclear waste disposal. Its major advantages are the low permeability and mechanical stability. Governing retardation/retention processes in crystalline rocks are sorption, matrix diffusion and reduction. To perform sound performance assessment calculations reliable information is needed e.g. radionuclide distribution coefficients (Kd) as input data. Numerous studies dating back at least 30 years have been carried out to examine the retention/retardation capacity of crystalline rocks comprising both in-situ and laboratory experiments. The major drawback of most laboratory experiments is the use of solid material which has been altered compared to in-situ conditions. This alteration is mainly due to an exposure of the solid material to oxygen (ambient atmosphere) during drilling, crushing/sieving and storing of the material prior to the experiments. In consequence, the transfer of results obtained in the laboratory to in-situ conditions is always coupled to high uncertainties. To reduce these uncertainties, it is mandatory not only to conduct the experiments under oxygen free conditions (Ar glove box) but also to use non oxidized, fresh solid material, regarding especially redox-sensitive radionuclides like U, Pu or Tc. Towards this goal, the prevailing study presents results of batch type sorption kinetic experiments under the application of unaltered (non-oxidized) solid material (Äspö diorite) for ^{137}Cs(I), ^{152}Eu(III) and ^{233}U(VI).

Materials and Methods

Solid phases

Äspö diorite obtained from the recent drilling campaign in May 2011 in the Äspö Hard Rock Laboratory (for more information the reader is referred to the S&T contribution by Schäfer et al. (2012b)) was used in the batch experiments. The cores (#1.32 and #1.33) were cut into discs with a circular diamond saw, subsequently crushed manually with a hammer and finally sieved into several sizes fractions (< 125µm, 125 – 250µm, 250 – 500µm, 500 – 1000µm and 1-2mm). The solid material preparation has been carried out under Ar atmosphere in a glovebox. In the batch experiments the 1-2 mm size fraction has been used exclusively. The solid material has been characterized by specific surface area analysis (BET N_2 gas adsorption), scanning electron microscopy (SEM), energy dispersive X-ray microanalysis (EDX), X-ray fluorescence analysis (XRF) and X-ray diffraction (XRD). In
Figure *1* SEM pictures of the Äspö diorite are depicted. It shows the rough morphology of the artificially cut grains and verifies the grain size obtained by the sieving procedure. The BET N_2 adsorption revealed a specific surface area of 0.14m^2/g. For a thorough characterization of the solid material obtained within the CROCK project the reader is referred to the S&T contribution by Schäfer et al.

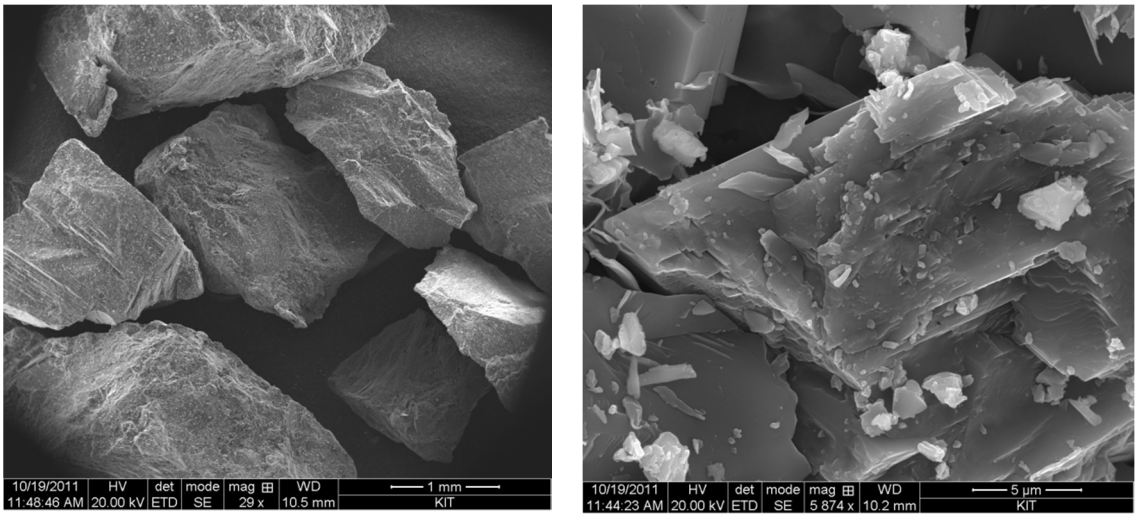

***Figure 1*:** *SEM pictures of the Äspö diorite 1-2 mm size fraction. Note the different scale bars.*

Synthetic Äspö groundwater

For application in the batch experiments, a synthetic Äspö groundwater was prepared on basis of an analysis of the natural Äspö groundwater (KA-3600-F-2) obtained during the sampling campaign of the drill cores in May 2011. Table 1 lists the chemical analysis of both waters. The synthetic groundwater mimics the natural Äspö water quite good in terms of major cation and anion composition, ionic strength and pH. To assure anoxic conditions in the batch type experiments the synthetic groundwater was purged with Ar for at least one hour to strip out, as far as possible, oxygen and dissolved

carbonate. Though, it has to be stated that traces of both O_2 and CO_2 may be left in the synthetic groundwater after purging with Ar. Thermodynamic simulations show an influence of CO_2 on the U speciation for dissolved carbonate concentration (> 1×10^{-6} M) yielding the species $(UO_2)_2CO_3(OH)_3^-$ as major species besides the second U hydrolysis species $UO_2(OH)_2$ at pH 8. It is well known that dissolved carbonate forms strong aqueous complexes with U weakening the sorption at higher pH values (pH > ~8) (Davis, 2001). In Table 1 the composition of the synthetic water after a contact time of 122h with the Äspö diorite is listed showing higher amounts of Al, Mn, Th and U due to dissolution processes of the solid phase. In the desorption experiments natural Grimsel groundwater (which was transported and stored in 50L barrels under Ar overpressure prior to the experiments) is used in parallel to the synthetic Äspö groundwater. Its composition is also listed in Table 1. The Grimsel groundwater represents a low mineralized (I = ~ 0.001 M), meteoric Na-Ca-HCO_3-type water with a higher pH value (9.7) compared to the Äspö groundwater.

Table 1: *Overview of the chemical compositions of the synthetic Äspö groundwater, natural Äspö groundwater and natural Grimsel groundwater, respectively.*

	Synth. Äspö GW	**Synth. Äspö GW after 122h contact time**	**Äspö GW (KA-3600-F-2)**	**Grimsel GW (MI-shear zone)**
pH	8.0	8.1	7.8	9.67
$Eh_{(SHE)}$	~ +0.18 V (lab.)	~ +0.18 V (lab.)	0.031 V (lab.)	~ -0.2 V (lab)
$[Mg^{2+}]$	103.64 ± 0.84 mg/L	104.6 mg/L	69.4 mg/L	12.6 µg/L
$[Ca^{2+}]$	1109.36 ± 94.46 mg/L	1134 mg/L	1135 mg/L	5.3 µg/L
$[K^+]$	19.346 ± 3.855 mg/L	21.56 mg/L	10.5 mg/L	
$[Li^+]$	2.526 ± 0.04 mg/L	2.50 mg/L	6.0 mg/L	
$[Fe^{2+.3+}]$	n.m.	n.m.	0.2 mg/L	< D.L.
$[Mn^-]$	2.32 ± 3.02µg/L	23.8 µg/L	0.338 mg/L	< D.L.
$[Sr^{2+}]$	19.678 ± 0.294 mg/L	20.14 mg/L	19.9 mg/L	182 µg/L
$[Cs^+]$	<D.L	< D.L		0.79 µg/L
$[La^{3+}]$	<D.L.	<D.L		< D.L.
[U]	0.05 ± 0.01 µg/L	1.70 µg/L	0.105 µg/L	0.028 µg/L
[Th]	0.024 ± 0.005 µg/L	0.07 µg/L	0.001 µg/L	0.00136 µg/L
$[Al^{3+}]$	182.75 ± 56.29 µg/L	439.6 µg/L	13.3 µg/L	42.9 µg/L
$[Na^+]$	1929.25 ± 28.58 mg/L	1905 mg/L	1894 mg/L	14.7 mg/L
$[Cl^-]$	4749.408 ± 145.046 mg/L	4895.10 mg/L	4999 mg/L	6.7 mg/L
[Si]	n.m.	n.m.	4.7 mg/L	5.6 mg/L
$[SO_4^{2-}]$	408.682 ± 4.967 mg/L	411.88 mg/L	394.4 mg/L	5.8 mg/L
$[F^-]$	1.974 ± 0.093 mg/L	1.98 mg/L	1.41 mg/L	6.3 mg/L
$[Br^-]$	21.17 ± 0.37 mg/L	20.96 mg/L	23.2 mg/L	
$[NO_3^-]$	< D.L	< D.L	< D.L	< D.L.
[DIC]	n.m.	n.m.	11.68	3.0 mg/L
[B]	306.54 ± 212.54 µg/L	146.1 µg/L	885 µg/L	

n.m. = not measured; < D.L. = lower as detection limit; lab. = measured in laboratory under Ar atmosphere (glovebox);

Experimental procedure

All experiments have been conducted in a glove box under Ar atmosphere (~1 ppm O_2) at room temperature (~ 21°C). The chemicals used were of ultra pure or supra pure grade, respectively. The pH measurements were done using a semi micro Ross electrode (81-03, Orion Co.) calibrate with at least 4 pH buffers in conjunction with a digital pH meter (720A, Orion Co.). For all redox potential measurements a standard platinum combination electrode (Metrohm Co.) was applied. The sieved solid material was washed several times with the synthetic groundwater to remove fines. For comparative studies, part of the fresh Äspö diorite crushed material was artificially oxidized by handling of the material for one week under ambient atmosphere and washing it several times with bi-distilled water (Milli-Q) prior to the experiments. Afterwards the solid material was weighted into Zinsser vials (20 ml, HDPE) (2g solid material) and equilibrated with synthetic groundwater (8 ml) for 5 days exchanging the solution at least four times. After the equilibration step, the contact water was removed completely from the Zinsser vials and again filled with 8 ml synthetic groundwater spiked with radionuclides. Several batch series have been prepared in this study (Table 2 gives further details):

- Series#1: Sorption experiments
  - Series#1.1 non-oxidized Äspö diorite
  - Series#1.2 oxidized Äspö diorite
- Series#2: Desorption experiments (using non-oxidized material only)
  - Series#2.1: synthetic Äspö GW
  - Series#2.2: natural Grimsel GW

Table 2: *Overview of all batch series prepared in the prevailing study.*

Series name	Radio-nuclides	V/m [ml/g]	Sample interval [days]	Concentration [mol/l]	Ground-water
Series#1.1: ÄnCs	Cs-137	4/1	1h, 1, 4, 7, 14 ,35, 49, 63	9.98×10^{-10}	Synth. Äspö
Series#1.1: ÄnEu	Eu-152	4/1	1h, 1, 4, 7, 14 ,35, 49, 63	2.75×10^{-9}	Synth. Äspö
Series#1.1: ÄnU	U-233	4/1	1h, 1, 4, 7, 14 ,35, 49, 63	1.04×10^{-7}	Synth. Äspö
Series#1.2: ÄnoCs	Cs-137	4/1	1h, 1, 4, 7, 14 ,35, 49, 63	9.98×10^{-10}	Synth. Äspö
Series#1.2: ÄnoEu	Eu-152	4/1	1h, 1, 4, 7, 14 ,35, 49, 63	2.75×10^{-9}	Synth. Äspö
Series#1.2: ÄnoU	U-233	4/1	1h, 1, 4, 7, 14 ,35, 49, 63	1.04×10^{-7}	Synth. Äspö
Series#2.1: ÄnCs Äspö GW	Cs-137	4/1	1h, 1, 4, 8, 27		Synth. Äspö
Series#2.2: ÄnCs GGW		4/1	1h, 1, 4, 8, 27		Grimsel GW
Series#2.1: ÄnEu Äspö GW	Eu-152	4/1	1h, 1, 4, 8, 27		Synth. Äspö
Series#2.2: ÄnEu GGW		4/1	1h, 1, 4, 8, 27		Grimsel GW
Series#2.1: ÄnU Äspö GW	U-233	4/1	1h, 1, 4, 8, 27		Synth. Äspö
Series#2.2: ÄnU GGW		4/1	1h, 1, 4, 8, 27		Grimsel GW

Selected samples have been ultra-centrifuged (Beckmann XL-90, rotor type 90Ti) to examine possible eigencolloid formation in case of Eu and U or colloid associated radionuclides. For this, an aliquot of the sample hast been centrifuged for 1h at 90,000 rpm (centrifugal force ~ 500,000 g). This procedure has been proven to effectively remove Th(IV) eigencolloids from solution (Altmaier et al., 2004) as well as bentonite colloids (e.g. (Huber et al., 2011)).

Thermodynamic modelling

To gain knowledge about the aqueous speciation thermodynamic simulations for the conditions of the batch experiments have been conducted using the Hydra/Medusa code (Puigdomenech, 2004) under application of NEA constants (Guillaumont et al., 2003) only. It has to stated that the influence of the Äspö material in terms of radionuclide sorption or sorptive reduction effects on the aqueous speciation have not been included in the calculations. Also, due to the stripping of the synthetic groundwater with Ar for 1h dissolved carbonate is excluded in the simulations.

Results and Discussion

Sorption experiments

Series#1.1 (Non oxidized Äspö diorite)

The sorption kinetics for Cs, Eu and U obtained in the batch studies in presence of non-oxidized diorite are depicted in
Figure *2*. Cs and Eu show fast kinetics with > 80 % sorption after 1 day contact time. The Eu data show little scatter due to analytical uncertainties near the detection limit. Sorption equilibriums are reached after ~ 7 d for Cs and Eu. The high sorption affinity of Cs and Eu can be reasonably explained by the aqueous speciation. Caesium is stable as the positively charged Cs^+ species at pH 8 (Baes and Mesmer, 1976). The calculated speciation for Eu is displayed in
Figure ***3***b showing positively charged Eu species ($Eu(OH)_2^+$ and $EuSO_4^+$) at the conditions of the Äspö groundwater. Thus, it seems reasonable to assume a strong electrostatic interaction of both radionuclides with the negatively charged Äspö diorite at pH 8 (Huber et al., 2012).
U only shows a lesser pronounced sorption behaviour with ~40% sorption after 1 d contact time (Figure 2c). The last data point after 9 weeks contact time still shows a slight increase in sorption indicating that sorption equilibrium might not be fully reached and/or the sorption kinetics became very slowly. The sorption behaviour may again be explained via the solution speciation shown in
Figure ***3***a. At pH 8, U is present as the neutral charged $UO_2(OH)_2(aq)$ and the negatively charged $UO_2(OH)_3^-$ (or $(UO_2)_2CO_3(OH)_3^-$ in case of 1×10^{-6} M dissolved CO_2 present) indicating a much lesser electrostatic interaction with the negatively charged mineral surfaces of the Äspö diorite. Moreover, in contrast to the non-redox sensitive elements Cs and Eu, reduction may also be responsible for the removal of U from solution. Based on the macroscopic data presented no differentiation between sorption and reduction is possible. To circumvent this lack of information, surface sensitive spectroscopy like X-ray photoelectron spectroscopy (XPS) has been applied.

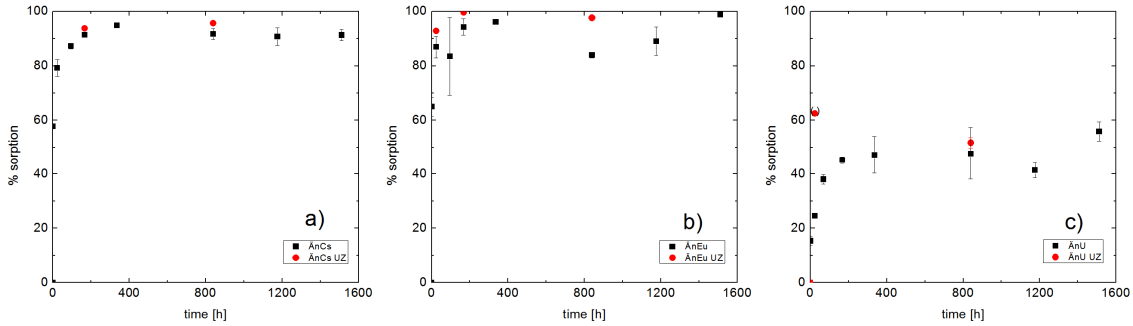

Figure 2: *Results of the batch experiments with the non-oxidized Äspö diorite (1-2mm). a) Cs b) Eu and c) U.*

For this, a fragment of the non-oxidized Äspö diorite (~0.5x~0.5x~1cm) was brought into contact for 28 d with the synthetic Äspö groundwater containing 3×10^{-5} mol/l U. After the desired contact time, the sample was transferred to the XPS (Physical Electronics Inc. (PHI) Model 5600ci) using an O-ring sealed vacuum transfer vessel (PHI model 04-110). The XPS results are shown in
Figure ***4***. To estimate the amounts of the U valence states of U reacted Äspö diorite, U $4f_{7/2}$ spectra are curve fitted by Gaussian-Lorentzian sum functions with same Gaussian fractions and full width at half maximum (FWHM). The fitting results yield ~ 50% tetravalent U on the diorite surface. Although one should keep in mind the high uncertainties coupled to redox potential measurements ((Grenthe et al., 1992; Lindberg and Runnells, 1984), experimentally determined redox potentials in this study (Eh_{SHE} = ~ + 183 mV; after 27d contact time to the ÄD material under Ar atmosphere in the glove box) do not indicate a U reduction from a thermodynamic point of view. Therefore, we hypothesize a sorptive reduction process with an initial sorption of a U(VI) species and a subsequent reduction to U(IV) e.g. by structural Fe^{2+} in biotite or magnetite.

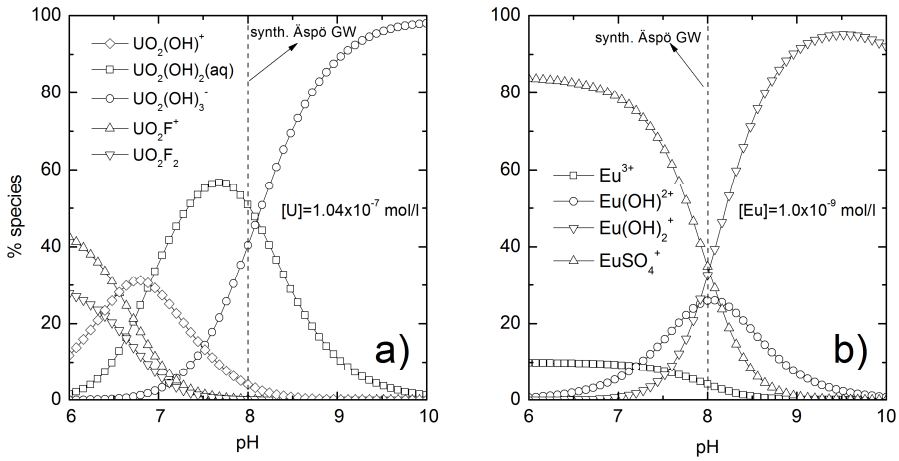

Figure 3: *Pre-dominance plots for U species (a) and Eu species (b) for the chemical conditions of the batch experiments (in absence of dissolved carbonate).*

Additionally inserted in
Figure *2* are data for ultra-centrifuged samples (red points). These data points are in close agreement to non-ultra-centrifuged samples. That is, (i) no colloidal phases like

e.g. eigencolloids in case of Eu have been formed and remain stable in solution and/or (ii) possible radionuclide associated Al-, Si- and/or Fe-colloids are not present or stable in solution. Concerning the relatively high ionic strength of the synthetic Äspö groundwater (I = 0.2 mol/l), a low colloid stability is expected corroborating the interpretation given above (Schäfer et al., 2012a).

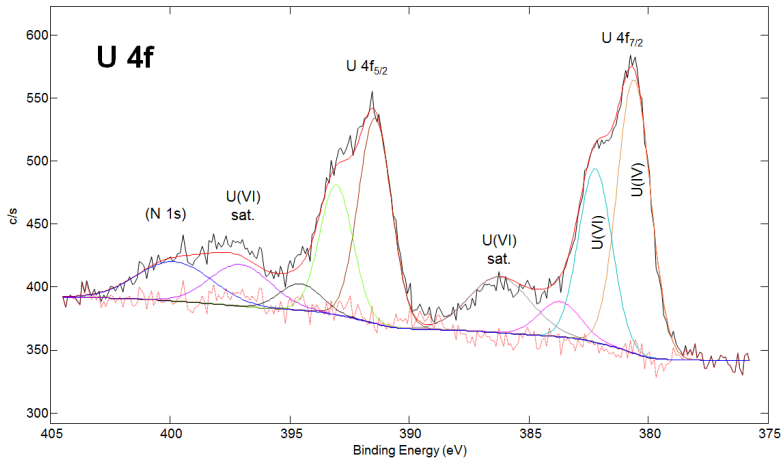

Figure 4: *U4f XPS spectra of the non-oxidized Äspö diorite fragment showing both U(IV) and U(VI) associated to the surface.*

Series#1.2 (Oxidized Äspö diorite)

For comparison to the non-oxidized Äspö diorite experiments, a batch series with the identical geochemical conditions has been prepared using artificially oxidized Äspö diorite (
Figure ***5***). Similar results as in Series#1.1 have been obtained. That is, Cs and Eu show fast sorption kinetics and almost quantitative (> 90%) sorption while U again shows a much lesser pronounced sorption behaviour (max. ~ 55%). The sorption kinetics is similar to the ones in Series#1.1. As it was the case in Series#1.1, selected samples have been ultra-centrifuged (red points). Again, no indications for the formation/presence or stability of colloidal phases were observed. In case of U, the data show no sorption equilibrium after 8 weeks contact time in line with the results in Series#1.1. No XPS measurements have been conducted with the oxidized diorite so far to examine a possible reduction of U. XPS measurements using the oxidized diorite will be conducted in the future to elaborate on this issue.

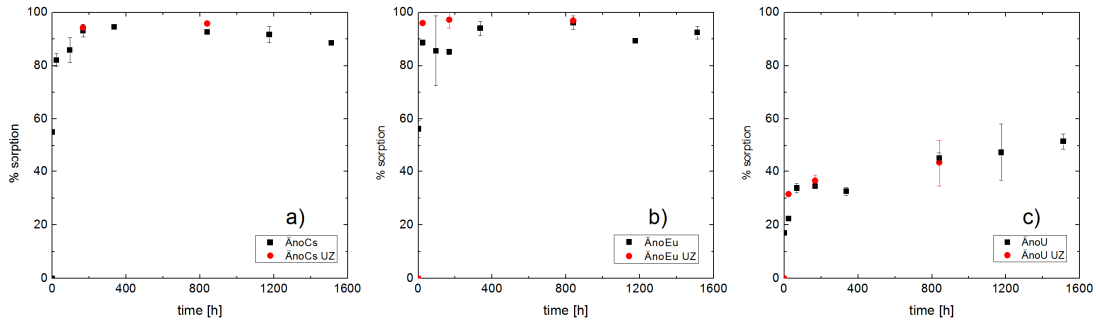

Figure 5: *Results of the batch experiments with the oxidized Äspö diorite (1-2mm). a) Cs b) Eu and c) U.*

Comparison of the Cs results to literature data

A thorough experimental study focused on granitic Äspö material characterization, sorption/desorption and diffusion behaviour of several radiotracers (restricted to mono- and divalent cations; among them $^{137}Cs^{+}$) was presented by (Byegård et al., 1998). The batch type sorption experiments conducted by (Byegård et al., 1998) are similar in terms of mineralogy and size fraction of the Äspö diorite applied (1-2mm, BET: 0.038m^2/g), solid-to-liquid ratio (12.5g/l) and Cs^{+} concentrations (1×10^{-6} mol/l). However, oxidized Äspö diorite has been used in the batch experiments. In
Figure *6* results of this study and by (Byegård et al., 1998) are plotted as surface normalized Kd values, respectively. In general, the data show similar sorption kinetics starting at a log Kd value of ~ -1.25 and rise up to ~ -0.5 after ~400h contact time. Regarding longer contact times, the values obtained by (Byegård et al., 1998) show higher Kd values (~-0.25) compared to this study (~ -0.75). Moreover, it seems that the data by (Byegård et al., 1998) are still increasing with a slow kinetic. (Byegård et al., 1998) focussed on weakly sorbing tracers, data on Eu and U are not presented.

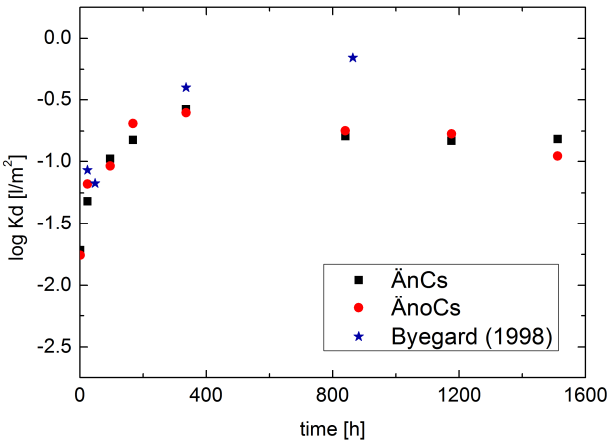

Figure 6: *Surface normalized log Kd values for Cs obtained in this study and by (Byegård et al., 1998).*

Series#2: Desorption experiments

Subsequent to the sorption experiments, the sorption samples from the Series #1.1 have been used to examine the desorption behaviour of Cs, Eu and U both for synthetic Äspö groundwater (Series#2.1) and natural Grimsel groundwater conditions (Series#2.2), respectively. All desorption experiments have been carried out in the same Ar glove box as the sorption experiments.
Figure ***7*** shows the results obtained of the desorption experiments. Regarding Cs, the desorption equilibrium is reached very fast showing maximum desorption values of ~ 5% within 24h up to 27d. No influence of the groundwater chemistry is observable. Similar results are obtained for Eu where again, a fast desorption of ~ 5 % is visible after 24h. The last data points after 27d show a desorption of ~ 10% in case of the ÄnEu sample series, whereas all other samples remain below 5% desorption. It is therefore likely that this may represent an analytical artefact. That is, both in case of Cs and Eu, the amount of desorption is in the expected equilibrium range considering the almost quantitatively sorption. U desorption results differ from Cs and Eu in many respects. First, desorption equilibrium is not reached within the experimental duration of 27d. The maximum percentage of desorption is ~ 20% and thus below the expected desorption equilibrium concentration of ~ 25% (considering full sorption reversibility; K_d-approach). Thus, U shows much slower desorption kinetics compared to Cs and Eu.

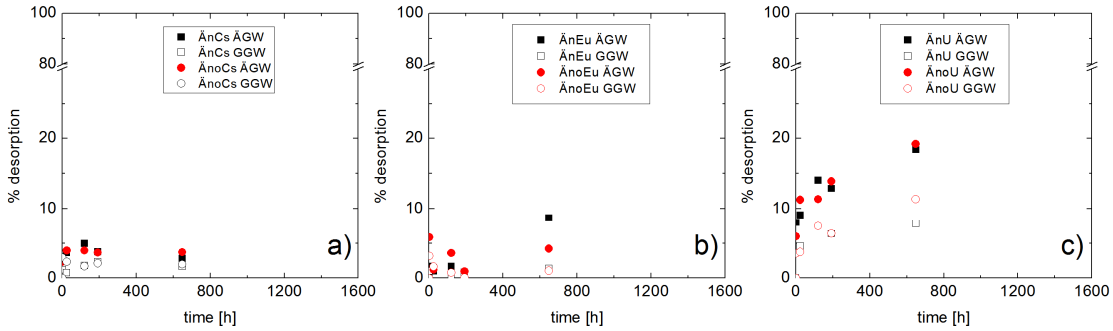

Figure 7: *Results of the desorption experiments using both synthetic Äspö groundwater (ÄGW) and natural Grimsel groundwater (GGW). a) Cs, b) Eu and c) U.*

Moreover, a clear difference in the desorption behaviour is visible as function of the type of groundwater applied. The samples with Äspö groundwater show higher (~10 %-units) desorption values as the samples in contact to the natural Grimsel groundwater. The reason for this difference may be referred to the completely different redox potentials of both groundwaters. While the synthetic Äspö groundwater possesses mildly oxidizing redox potentials of Eh_{SHE} = ~ +180 mV (after 27 days contact time to the solid material), mildly reducing conditions are measured for the Grimsel groundwater (Eh_{SHE} = ~ -185mV; after 27 days contact time to the solid material). Unfortunately, no dissolved Fe(II) was measured in the experiments prevailing which could give some indications about the redox state of the groundwaters independently of the Eh measurements. It has to be stated that it is well known that Eh measurements may be coupled to quite high uncertainties especially in natural systems with low Fe(II)/Fe(III) concentrations (Grenthe et al., 1992; Lindberg and Runnells, 1984). The redox potentials in case of the Grimsel groundwater are located near the borderline

between U(VI) and U(IV) while the redox potentials in the Äspö groundwater are clearly oxidizing (
Figure ***8***). As a preliminary working hypothesis we propose the following explanations: (i) it may be possible that hexavalent U sorbed on the diorite is reduced to tetravalent U remaining immobilised at the mineral surfaces and/or (ii) a reduction of desorbed hexavalent U in solution to sparingly soluble U(IV) and a subsequent precipitation of a U(IV) phase could also be a potential explanation for the restricted desorption behaviour observed in case of the Grimsel groundwater. On the basis of the macroscopic data prevailing no differentiation between both processes is possible.

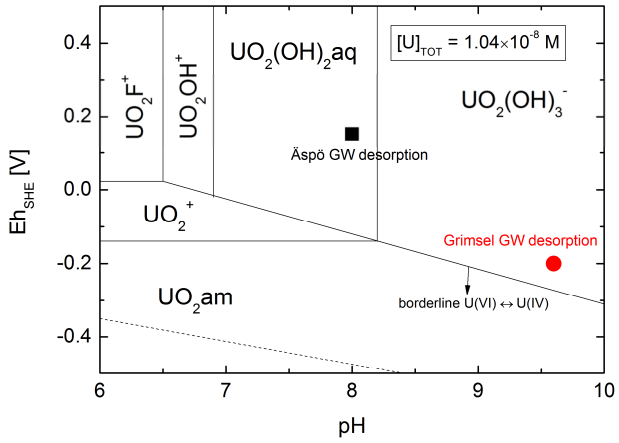

Figure 8: *Calculated predominance diagram of the desorption experiments. Indicated are the pH-Eh$_{SHE}$ conditions for the Äspö (square) and Grimsel (dot) groundwater, respectively.*

Conclusions and Future work

Concerning the influence of oxidization of the Äspö diorite on the sorption behavior, no differences have been observed for both Cs and Eu under the experimental conditions chosen. Both radionuclides show a strong sorption (> 90%), fast kinetics and thus reached sorption equilibriums within a few days. In contrast, U shows a lesser pronounced sorption behavior with a maximum of ~ 50% sorption after 9 weeks contact time. Moreover, XPS measurements on an unaltered Äspö diorite fragment in presence of U(VI) revealed 50% U(IV) on the diorite surface after 28d contact time proving that both sorption and reduction act as retention/retardation process in parallel. Additional XPS measurements will be conducted under the application of oxidized diorite. Desorption experiments using synthetic Äspö GW and Grimsel GW showed fast equilibrium conditions in case of Cs and Eu while U desorption takes considerable longer. A clear difference in the desorption behavior is visible for both types of groundwater applied. That is, U desorption is weaker under Grimsel conditions which is here referred to the considerably more reducing conditions of the Grimsel GW causing U reduction/immobilization. A comparison of Cs^+ sorption results to a similar study by (Byegård et al., 1998) showed similar sorption kinetics and K_d values providing confidence in the results. A thorough comparison of Eu (Am) and U sorption kinetics and K_d values obtained in this study to literature data will be conducted in the next project phase.

Acknowledgement

We gratefully acknowledge the help of the INE workshop team, namely V. Krepper and E. Schmidt, in the preparation of the solid material. The research leading to these results has received funding from the European Union's European Atomic Energy Community's (EURATOM) Seventh Framework Programme FP7/2007-2011 under grant agreement n° 269658 (CROCK project).

References

Altmaier, M., Neck, V. and Fanghanel, T. (2004). Solubility and colloid formation of Th(IV) in concentrated NaCl and MgCl2 solution. Radiochimica Acta, 92(9-11): 537-543.

Baes, C.F. and Mesmer, R.E. (1976). The hydrolysis of cations In: R.E.j.a. Mesmer (Editor). Wiley, New York :.

Byegård, J., Johansson, H., Skålberg, M. and Tullborg, E.L. (1998). The interaction of sorbing and non-sorbing tracers with different Äspö rock types. Sorption and diffusion experiments in the laboratory scale. SKB Technical report TR-98-18. SKB Technical report TR-98-18, Svensk Kärnbränslehantering AB, Stockholm, Sweden.

Davis, J.A. (2001). Surface complexation modeling of uranium(VI) adsorption on natural mineral assemblages. 6708, US Nuclear Regulatory Commission, Washington, D.C.

Grenthe, I., Stumm, W., Laaksuharju, M., Nilsson, A.C. and Wikberg, P. (1992). Redox potentials and redox reactions in deep groundwater systems. Chemical Geology, 98(1-2): 131-150.

Guillaumont, R., Fanghänel, Th., Fuger, J., Grenthe, I., Neck, V., Palmer, D.A., Rand, M. (2003). Update on the chemical thermodynamics of uranium, neptunium, plutonium, americium and technetium. Elsevir B.V., Amsterdam, The Netherlands.

Huber, F., Enzmann, F., Wenka, A. Bouby, M., Dentz, M., Schäfer, Th. (2012). Natural micro-scale heterogeneity induced solute and nanoparticle retardation in fractured crystalline rock. Journal of Contaminant Hydrology, 133(0): 40-52.

Huber, F., Kunze, P., Geckeis, H. and Schäfer, T. (2011). Sorption reversibility kinetics in the ternary system radionuclide-bentonite colloids/nanoparticles-granite fracture filling material. Applied Geochemistry, 26(12): 2226-2237.

Lindberg, R.D. and Runnells, D.D. (1984). Groundwater redox reactions: An analysis of equilibrium state applied to Eh measurements and geochemical modeling. Science, 225: 925 - 927.

Puigdomenech, I. (2004). HYDRA and MEDUSA chemical equilibrium software.Software and documentation. http://web.telia.com/~u15651596/.

Schäfer, Th., Huber, F., Seher, H., Missana, T., Alonso, U., Kumke, M., Eidner, S., Enzmann, F. (2012a). Nanoparticles and their influence on radionuclide mobility in deep geological formations. Applied Geochemistry, 27(2): 390-403.

Schäfer, Th., Stage, E., Büchner, S., Huber, F., Drake, H. (2012b). Characterization of new crystalline material for investigation within CP CROCK - 1st CROCK Workshop (May 22-24, 2012, Stockholm, Sweden), Paper.

CHARACTERIZATION OF NEW CRYSTALLINE MATERIAL FOR INVESTIGATIONS WITHIN CP CROCK

Thorsten Schäfer[1,2*], Eike Stage[1,2], Sebastian Büchner[1], Florian Huber[1], Henrik Drake[3]

[1] Institute of Nuclear Waste Disposal, Karlsruhe Institute of Technology (DE)
[2] Department of Earth Sciences, Freie Universität Berlin (DE)
[3] Environmental Science, Geochemistry Research Group, Linnaeus University (SE)

* Corresponding author: thorsten.schaefer@kit.edu

Abstract

This S&T contribution in hand gives an overview of the activities of the first project period concerning drilling of new core samples under anoxic conditions, the preparation of samples for the partners CIEMAT, HZDR, NRI-REZ and KIT-INE and the current status of material characterization.

Introduction

The provision of samples for the experimental program is a key step in CP-CROCK as already stated in the proposal. Previous investigations are based on crystalline rock material that has been drilled under the use of oxidizing surface water and/or where the drill cores have subsequently been treated, handled, transported and stored in contact with air. In general, the chemical sorption processes are affected by redox reactions of the radionuclides, but also the inventory of sorbing minerals and mineral components is affected. The physical retention by residence in flow stagnant regions relative to the fractures is probably less affected, changes in the texture, pore and micro-pore structure is not expected to change significantly. Redox processes are investigated in the CP *"Redox phenomena controlling systems"* (ReCosy). In that project, however, there was no access to crystalline rock far-field fracture samples that have been obtained, handled and stored in absence of air.
Having these unaltered materials now available the impact of oxidation of samples is also considered as the usage of inadvertently oxidized samples in most laboratory studies, as well as quantification of oxidized water intrusion under specific scenarios overall leading to a data uncertainty reduction. Another focus will be on determining the reactivity for sorption relevant processes on surfaces on the heterogeneous nano- to micro-resolution scale.

Field activities (drilling & water sampling)

In the first week of May 2011 a drilling campaign for new drill-cores was performed in the Äspö Hard Rock Laboratory (HRL) Niche NASA2376A over one week. To preserve the in situ redox conditions as much as possible (and also technical feasible) it was decided to work with the double tube technique and use a drilling fluid (natural anoxic Äspö groundwater) permanently stripped with N_2 in a reservoir. As drilling strategy it was decided to orient the first borehole from the tunnel surface parallel to a water conducting feature (named borehole KA2368A-01) and perform a second borehole drilling from a niche parallel to the tunnel surface in a distance of approx. 7m slightly dipping (~5°) perpendicular to structural features (named borehole KA2370A-01). In general, the sampling procedure of bore cores consisted of the following steps, (a) after the end of drilling a core section with anoxic drilling fluid (drill core length: ~1m, core diameter: 5.1 cm) the core was transferred to a wooden sampling box under tunnel atmosphere, (b) after a short visual inspection (max. 5 min) the core was placed in a transparent LD-PE bag and this bag three times evacuated (~-0.4bar) and purged with nitrogen gas before welding. Finally, the same procedure was applied with an Al bag for second confinement to prevent oxidation during transport. Details on the sampling and short characterization of the cores can be found in the project deliverable 1.1. and Annexes. In short, three types of rock material were drilled, *Äspö diorite (ÄD* and as enclaves/xenoliths), *fine grained granite (FGG)* and *Ävrö granite (ÄG)*. In addition, ground water samples were taken from the drilling fluid tank (water originating from borehole KA2598, bubbled with nitrogen gas, Figure 1) before the start of the 1st borehole KA2368A-01 and at the end of the drilling campaign (Figure 1). In addition, the natural outflow of the fracture after setting a single packer in borehole KA2368A-01 and groundwater taken from borehole KA3600-F-2 were sampled. In Table 1 the sample number and details on the sampling procedure are given. No on-site analyses were performed.

Figure 1: *(left) drilling fluid tank before sampling of sample CROCK-1 (see Table 1), (right) Example of a core sealed in LD—PE bag and second confinement by Al bag.*

Table 1: *Details on ground water sampling procedure*

Sample number:	CROCK-1	CROCK-2	CROCK-3	KA3600-F-2
Type:	Gas mouse	50mL PE & gas mouse	50mL PE & gashouse	50l Teflon coated Al-barrel
Description:	Water from drilling fluid tank (taken from borehole KA2598) before the start of the drilling borehole **KA2368A-01**.	Set single packer in borehole **KA2368A-01** at 9:00h, natural groundwater outflow observed.	Water from drilling fluid tank after the end of the drilling campaign finishing borehole **KA2370A-01**.	Water from borehole KA3600-F-2 SKB chemistry file 2009-09: 5060 mg/L Chloride, 0.196 mg/L Fe(II), 0.212 mg/L Fe(tot), pH: 7.35, cond.: 1500 mS/cm)
Date:	02.05.2011	04.05.2011	05.05.2011	02.-03.05.2011
Flow rate:	Tank sampling	~10mL/min	Tank sampling	2L/min

Sample Preparation & Characterization

Ground water

The off-site analytical results of the different ground waters taken are listed in Table 2. Concerning the measured redox potential time dependent measurements in an argon glove box showed clearly a tendency to decrease even after 24 h measurement time and the values given in Table 2 are definitely upper limits.
Based on the chemical analysis of the natural outflow water of borehole KA2368A-01 the sampled water from borehole KA3600-F-2 has very comparable composition, whereas the drilling fluid used throughout the campaign taken from borehole KA2598 has significantly higher salt content documented by an ionic strength of 0.32M compared to 0.155-0.177M. Currently approximately 50L of groundwater from borehole KA3600 –F-2 are available at INE. Based on the chemical composition given in Table 2 for the CROCK-2/KA3600-F-2 samples a synthetic groundwater was proposed (see below) and used for the studies of KIT-INE (see S&T contributions Stage et al. (2012) and Totskiy et al. (2012)).

Salts used:

1.0E-5 mol/L Na-Borax Merck (pro analysis) 1.06308.0500/Charge A193908 036
8.2E-2 mol/L NaCl Merck (pro analysis) 1.06404.1000/Charge K40666004 005
4.1E-3 mol/l $MgSO_4$ Merck (pro analysis) 1.05886.0500/Charge A295686 114
7.4E-5 mol/L LiF Merck (pro analysis) 1.05690.0100/Charge B0059190 709
2.7E-4 mol/L KBr Merck (Uvasol) 1.04907.0100/Charge B816807 110
1.9E-4 mol/L $NaHCO_3$ Merck (pro analysis) 1.06329.0500/Charge K28996729 114
2.8E-2 mol/L $CaCl_2$ Merck (pro analysis) 1.02382.0500/Charge A0211082 115
2.3E-4 mol/l $SrCl_2$ Merck (pro analysis) 1.07865.1000/A674965 707

Table 2: Geochemical parameters and anion (ion chromatography), cation (ICP-MS) analysis of waters sampled.

Sample number:	CROCK-1	CROCK-2	CROCK-3	KA3600-F-2
pH:	8.03	7.98-8.04	7.95-8.00	7.81
Elec. Cond. [mS/cm]:	21.00	11.75-11.96	19.45-20.4	13.31
Eh(SHE) [mV]:*	140	62-153	46-101	31
Flow rate:	Tank sampling	~10mL/min	Tank sampling	2L/min
	*measured with redox electrode M3.			
Anions [mg/L]:				
F^-	1.42	1.35-1.51	1.35-1.53	1.41
Cl^-	8499	4370-4371	8437-8457	4999
Br^-	53.3	19.1-19.3	52.1-53.0	23.2
B	0.765	0.84-1.16	0.575-0.593	0.885
SO_4^{2-}	461.9	296.2-302.4	463.7-465.5	394.4
Inorganic Carbon:	5.62 ± 0.03	5.10 ± 0.64	3.85 ± 0.02	11.68 ± 0.03
DOC	5.84 ± 0.09	4.40 ± 2.67	4.20 ± 0.54	3.48 ± 0.15
Cations [mg/L]				
Na	1972	1622-1700	1936 – 2954	1894±18
K	9.3	13.6-48.6	9.7-36.9	10.5±0.1
Li	9.9	2.6-3.5	8.8-9.7	6.0±0.1
Mg	53.9	148-154	53.4-55.7	69.4±1.6
Ca	2019 (1425)	870-952	1877-2001	1135±6
Sr	37.1	13.8-14.6	31.5-35.0	19.9±0.5
$Fe_{(tot)}$	0.105	0.221-0.819	0.542	0.200
Mn	0.338	0.554-0.632	0.279-0.321	0.338
Si	3.7	6.4-7.2	3.2-3.4	4.7
Al [µg/L]	136	25.1-769	4.6-701	13.3
PHREEQC calc.:				
Charge balance (%)	-1.04	-1.01	-0.54	-1.45
Ionic strength [M]	0.32	0.155	0.32	0.177

Rock samples

After transfer of the rock cores to KIT-INE all samples were directly stored under Ar atmosphere (slight overpressure) in a drum. For same preparation (cores, rock discs, crushed material of different size fractions), selected sections were transferred in to an

Argon glove box equipped with a diamond saw (see Figure 2). Most of the results presented in this S&T contribution are documented in detail in (Stage, 2012).

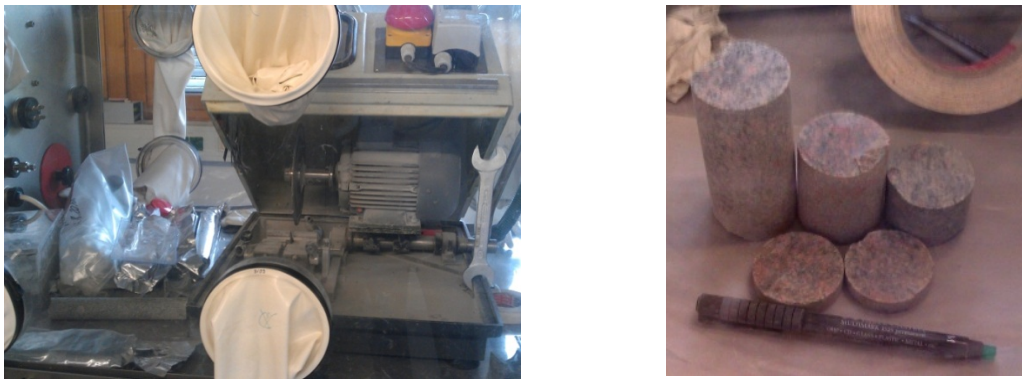

Figure 2: *(left) Ar- glovebox equipped with the circular diamond saw for preparation of cores and discs of defined length. The crushed material and sieving procedure was prepared in the same box. (right) Äspö diorite cores of 10cm, 5cm, 3cm length and two discs of 1 cm thickness.*

By this preparation procedure Äspö diorite samples (discs, crushed material and cores) for the partners CIEMAT, NRI-REZ, HZDR and KIT-INE were produced, as requested and shipped to the partners in autoclaves under Ar atmosphere. Further chemical and mineralogical characterization of the material was mainly performed on the crushed material (CM) as described below.

Surface area

A key aspect with respect to retention/sorption capacity of the rock samples is the specific surface area and the pore size distribution giving information on the pore matrix. Here, in a first step 5-point N_2- BET measurements for surface area quantification are performed. For the 1-2 mm fraction of ÄD, FGG and ÄG in addition full adsorption/desorption isotherms to retrieve the pore size distribution have been measured. The total surface area increases generally with the reduction in average size and is almost half a magnitude higher for the < 125µm fraction (0.79-1.03 m^2/g) compared to the 1-2mm fraction (0.14-0.26 m^2/g), see Table 3. Comparing the volume or surface area BJH (Barrett-Joyner-Halenda) pore size distribution (Figure 3) assuming cylindrical pore shape the three 1-2mm materials are very similar with respect to pore size distribution. A significant difference between the materials investigated appears only to the lower end (<2 nm) of the pore size distribution showing for Ävrö granite a considerable amount of pores in this size range, whereas the Äspö diorite sample seems to be limited to pores >1nm and the fine grained granite (FGG) lying in between.

Table 3: *Summary of surface area measurements by 5-points N_2-BET (samples were outgassed for 1h over N_2 stream at 300°C).*

Sample type:	<125µm [m^2/g]	125-250µm [m^2/g]	250-500µm [m^2/g]	0.5mm-1mm [m^2/g]	1-2mm [m^2/g]
Äspö diorite:	0.88	0.38	0.42	0.19	0.14
Fine grained granite (FFM):	0.79	0.94	0.55	0.29	0.23
Ävrö diorite:	1.03	0.70	0.66	0.44	0.26

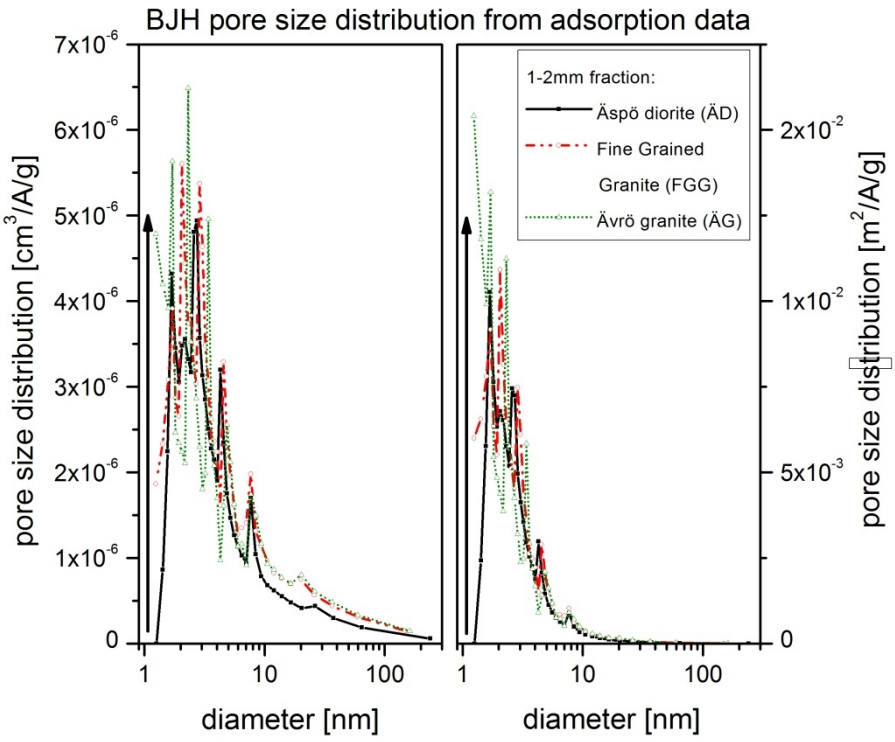

Figure 3: *BJH pore size distribution derived from N_2- adsorption data for the ÄD, FGG and ÄG. (left) volume derived distribution (right) surface derived distribution.*

Rock chemistry

Concerning bulk rock chemistry of the available new Äspö diorite material both X-Ray fluorescence analysis (XRF) and scanning electron microscopy (SEM-EDX) were applied. The data of the new material is compared to older studies (Huber et al., 2011) using an oxidized material (Table 4). Beside the typical (expected) composition of granite type material with high concentrations of SiO_2 and Al_2O_3 (quartz, feldspar) considerable differences in the iron content and especially in the ferrous iron content could be found. Taken the photometric determined ferrous iron content and the total Fe concentration measured by XRF the material in the studies of (Huber et al., 2011) clearly shows a lower Fe^{2+} content with only ~33% of the total iron pool compared to the new material with ~57% Fe^{2+}/Fe_{tot}). Furthermore, the total iron content with 4.39 wt. % is now considerably higher. Additional analysis performed by 1M $CaCl_2$ treatment (see S&T contribution Totskiy et al.) showed also a considerably higher exchangeable ferrous iron content. All this data is leading to the conclusion that the sampling and

preparation procedure applied has, at least, conserved part of the ferrous iron pool in the rock material. Measurements on FGG and ÄG have not been performed so far.

Table 4: *Comparison of XRFdata on major and trace elements for the new CP-CROCK material (Äspö diorite; ÄD, 1-2mm size fraction) compared to the data presented in (Huber et al., 2011).*

element	Äspö diorite (ÄD) concentration [wt. %]	Äspö diorite (Huber et al., 2011) concentration [wt. %]
SiO_2	62.71	66.06
Al_2O_3	17.27	16.89
Fe_2O_3	4.39	2.6
FeO	**2.51**	**0.87**
MnO	0.08	0.05
MgO	1.76	0.8
CaO	3.75	2.41
Na_2O	4.55	4.91
K_2O	3.05	4.38
TiO_2	0.66	0.35
P_2O_5	0.24	0.12
LOI	0.67	1.37
Sum	**99.1**	**98.6**
Trace element	**concentration [ppm]**	**concentration [ppm]**
Ba	1162	n.d.
Co	11	5
Cr	24	6
Cu	2	1
Ga	23	19
Nb	15	9
Ni	18	6
Pb	17	16
Sc	6	4
Sr	1052	770
Th	9.5	5.7
U	4.4	1.8
V	62	36
Y	22	16
Zn	76	43
Zr	168	139

n.d.: not detected

Comparing the trace element analyses the new material shows for all elements detected slightly higher concentration, whereas especially Ba and Sr with 1162 ppm and 1052 ppm are considerably enriched. Uranium, as one of the prioritized elements selected within CP-CROCK for sorption/migration studies is found in the new samples to be present in a concentration range of 4.4. ppm. The concentration difference found can be attributed to the heterogeneous U distribution within the Äspö diorite.
Scanning electron microscopy (SEM-EDX) analysis were performed on the different sieving fractions 0.125-0.25mm, 0.25-0.5mm, 0.5-1mm and 1-2mm for the Äspö diorite (ÄD). Due to the general heterogeneity of the material a number of points (n=6) were measured on arbitrarily chosen locations. In Table 5 the average weight percentage and the standard deviation are given. The results show for all size fractions (within the uncertainty given by the standard deviation) a good consistency and no size fraction dependent chemistry. Concerning the iron concentration however, some hot spots especially in the 0.5-1mm fraction have been observed. Overall, the Fe content tends to be higher compared to the XRF measurements.
To give an impression on the chemical heterogeneity SEM-EDX maps have been obtained and an example is given in Figure 4. The 1-2mm fraction of the Äspö diorite by SEM imaging shows considerable surface morphology/roughness A zoom-in on this sample shows beside the 1-2mm grains mineral detritus of smaller sizes associated with the surface most probably due to the mechanical treatment of the sample. Pure Fe spots due to abrasion of the tooling equipment used for preparation could not be detected.

Table 5: *EDX measurements on different size fractions of Äspö diorite (n=6), given in wt. %.*

Element	Size fraction 0.25-0.125mm	Size fraction 0.5-0.25mm	Size fraction 0.5-1mm	Size fraction 1-2mm
C	6.95 ± 0.11	5.86 ± 3.79	8.71 ± 1.81	7.22 ± 1.42
O	38.87 ± 4.74	43.75 ± 8.20	36.88 ± 9.83	38.22 ± 2.93
Na	3.35 ± 0.90	4.90 ± 3.24	1.79 ± 0.15	3.75 ± 2.00
Al	7.13 ± 1.57	7.17 ± 5.10	2.86 ± 1.63	8.53 ± 1.71
Si	24.40 ± 9.50	26.97 ± 12.40	27.35 ± 16.13	28.87 ± 15.32
Ca	6.06 ± 5.24	6.33 ± 5.03	2.95	4.79
Mg	4.31 ± 2.06	2.52 ± 2.32	2.98 ± 1.79	6.52 ± 3.89
K	5.25 ± 3.06	5.00 ± 4.37	8.30 ± 0.11	5.88 ± 3.29
Ti	1.98 ± 0.24	5.30 ± 5.01	3.59 ± 0.11	1.76 ± 0.60
Fe	11.94 ± 2.45	5.86 ± 6.16	15.06 ± 21.39	11.55 ± 4.89
Cl	n.d.	1.16 (n=1)	n.d.	0.89
Mn	n.d.	1.43 (n=1)	n.d.	1.35

n.d.: not detected

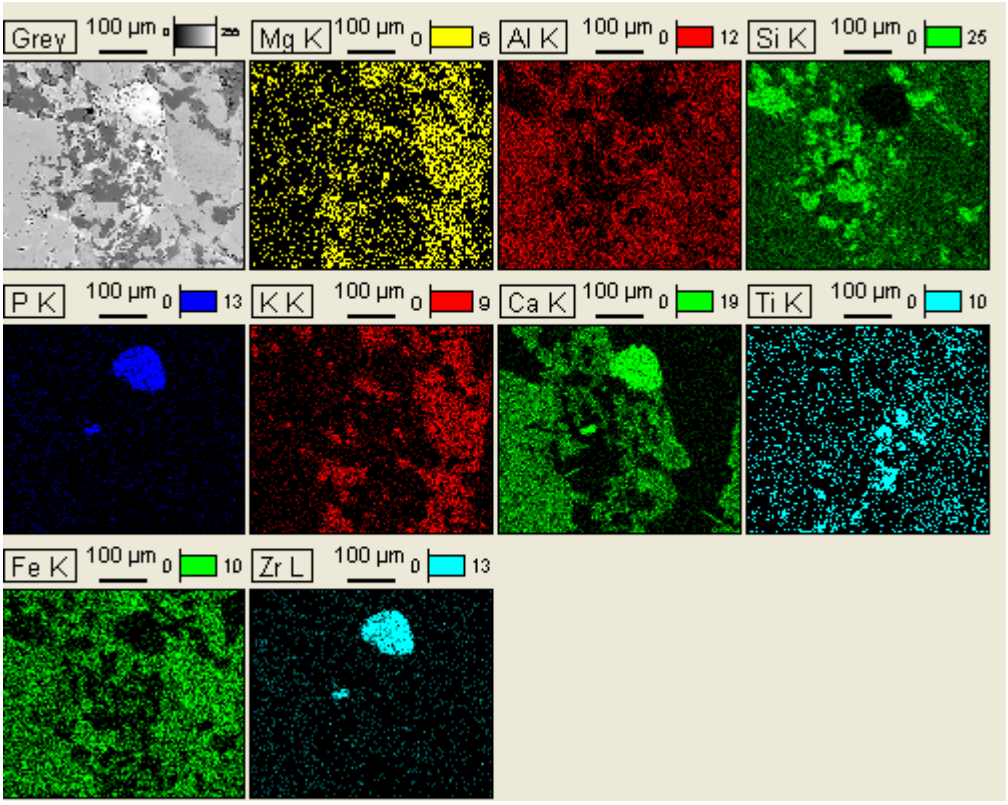

Figure 4: *SEM-EDX element maps on an Äspö diorite sample. Element distribution maps for Mg, Al, Si, P, K, Ca, Ti, Fe and Zr are given. The scale bar represents 100µm.*

Conclusions and Future work

This S&T contribution serves as a documentation of the sampling at the Äspö Hard Rock Laboratory (HRL), sample preparation and first bulk analysis of the material used by different partner, namely CIEMAT, NRI-REZ, HZDR and KIT-INE within CP-CROCK. Future analysis will be discussed within the 1st Annual meeting based on the needs of the different partners.

Acknowledgement

The research leading to these results has received funding from the European Union's European Atomic Energy Community's (EURATOM) Seventh Framework Programme FP7/2007-2011 under grant agreement n° 269658 (CROCK project)

References

Huber, F., Kunze, P., Geckeis, H., Schäfer, T. (2011). Sorption reversibility kinetics in the ternary system radionuclide–bentonite colloids/nanoparticles–granite fracture filling material. Applied Geochemistry, 26(12): 2226-2237.

Stage, E. (2012). Experimentelle Untersuchungen zur Cs, Eu und U Sorptionskinetik an Äspö-Granodiorit, Freie Universität Berlin, Berlin, 77 pp.

Stage, E., Huber, F., Heck, S., Schäfer, Th. (2012b). Soprtion/desorption of ^{137}Cs(I), ^{152}Eu(III) and ^{233}U(VI) onto new CROCK derived Äspö diorite – A batch type study - 1st CROCK Workshop (May 22-24, 2012, Stockholm, Sweden), Paper.

Totskiy Y., Geckeis H., Schäfer T. (2012). Sorption of Tc(VII) on Äspö diorite - 1st CROCK Workshop (May 22-24, 2012, Stockholm, Sweden). Paper

DECREASING UNCERTAINTY OF RADIONULCIDE MIGRATION PREDICTIONS IN SAFETY ASSESSMENT MODELLING

James Crawford[1*]

[1] Kemakta Konsult AB, Box 11265, S-112 93 Stockholm (SWE)

* Corresponding author: james@kemakta.se

Abstract

This paper summarises the work that has been performed during the first period of the CROCK FP7 project. The work involves efforts within three separate work packages with very different focus: diffusive retention processes, interpretation of batch sorption data, and deployment of process based models of sorption in safety assessment. The overall aim is to reduce uncertainty in predictions of radionuclide transport by incorporating more process-based thinking in both the interpretation of material property measurement data, and in the models of radionuclide retardation used in safety assessment.

Introduction

The work that has been done is divided into contributions to 3 separate work packages. The specific work performed in each work package is described in the following sections. Each work package is discussed separately as they consider different aspects of data interpretation and radionuclide migration modelling.

Work Package 3 Component – Diffusive retention processes

Background

One of the key features of solute transport in fractured crystalline rock is the existence of connected microporous structures in the bulk of the rock into which dissolved solutes can migrate, a process customarily referred to as matrix diffusion. Very dense igneous rocks such as granite typically contain a few tenths of a percent of water-filled porosity in the form of microfractures and grain boundary porosity and it has been known for many years (e.g. Neretnieks, 1980) that the diffusive uptake of solutes to the immobile water contained in this porosity and subsequent sorption on rock matrix microsurfaces should significantly retard the migration of radionuclides transported in flow-bearing fractures. As such, a central parameter necessary for modelling radionuclide migration in fractured rock is the effective diffusivity for solute diffusion in the rock matrix. The effective diffusivity is also often described in terms of the geometric formation factor

which is operationally defined as the ratio of the effective diffusivity of the solute in the rock matrix relative to the free solute diffusivity in water.
As part of the site investigations recently carried out by the Swedish Nuclear Fuel and Waste Management Company (SKB), the influence of microporosity on matrix diffusion processes has been studied using a number of independent laboratory-based methods as well as an in-situ method. The methods that have been used include through-diffusion experiments involving diffusion of a tracer through rock coupons between a high and low concentration chamber, out-diffusion of saline porewater from large core samples into water of low ionic strength, and electrical resistivity based methods which rely on the analogy between ionic mobility and diffusion as formalised in the Nernst-Einstein equation (e.g. Atkins and De Paula, 2009).
A recognised problem with the laboratory-based methods is the possibility that rock samples become mechanically damaged during core drilling and sample preparation and also that the grain boundary porosity can become decompacted by stress release when samples are retrieved from highly stressed rock. These effects can potentially lead to the overestimation of effective diffusivity given that mechanical damage typically leads to an increase in the intensity of microfracturing and connectivity of porous structures. In the case of through-diffusion experiments, the impact of microfracturing can potentially be exacerbated by the use of short core samples (1-3 cm) which are often necessary to obtain results in a reasonable time frame. Geometric formation factors estimated using the different measurement techniques are also not always in exact agreement owing to subtle differences in the physical processes being characterised and the different tracer moieties active in the measurement method.

Measurement of in-situ formation factors by electrical resistivity based methods

The in-situ method is based on a down-hole geophysical resistivity technique which propagates an alternating current into the rock matrix. Based on the bulk rock resistivity, $\rho_r = 1/\kappa_r$ and knowledge of the porewater electrical conductivity, κ_w (noting that electrical conductivity, κ is the reciprocal of resistivity, ρ), it is possible to infer the geometric formation factor from the relation:

$$F_f = \frac{\kappa_r}{\kappa_w} \tag{1}$$

The in-situ resistivity based method, although less prone to the same mechanical damage artefacts, is subject to other problems which impedes its use. Chief among these is uncertainty concerning the true pore water electrical conductivity which is necessary for interpretation of measurements. Another uncertainty is the enhanced conduction of current in the electrical double layer adjacent to mineral surfaces in the matrix microporosity. A precondition for the use of resistivity measurements is also that the mineral grains themselves do not conduct current. This condition is generally fulfilled in granitic rock since the constituent minerals have electrical conductivities many orders of magnitude less than that of the water saturated rock. If, however, there are non negligible amounts of electronically conductive mineral grains in the rock, resistivity measurements may not accurately reflect charge conduction in the pore spaces.
While the direct effect of uncertainty concerning the pore water electrical conductivity generally gives rise to a lognormally distributed uncertainty in the point-estimated

formation factor, the phenomenon of surface conduction gives rise to a measurement bias that results in overestimation of the true geometric formation factor. In order to produce reliable estimates of the effective rock matrix diffusivity, under as close to undisturbed in-situ conditions as possible, it is necessary to introduce corrections to account for this bias in situations where surface conduction is non-negligible.

Correction of in-situ measurement data for surface conduction bias

When using electrical resistivity measurements in the laboratory it is usual to saturate the pore system with water of known ionic strength to facilitate measurement interpretation. Since surface conductivity phenomena are most prominent at low ionic strengths, it is also usual to use a contact solution of relatively high ionic strength to minimise this effect and also the possible impact of anion exclusion (i.e. ~1 M NaCl, equivalent to an electrical conductivity of 7.8 S/m at 25°C). While it is possible to have very good control over porewater ionic strength for measurements made in the laboratory, it is generally not possible to directly measure the pore water electrical conductivity when using in-situ methods. Moreover, in many situations the porewater ionic strength will be somewhat less than that which would be desirable to minimise surface conduction bias. Methods used to estimate the in-situ porewater conductivity are discussed in the following section.
If surface conduction and conduction in the bulk of the porewater can be reasonably assumed to be analogous to parallel connected resistances in an electrical circuit, the apparent formation factor measured by the in-situ method can be shown to be equal to the true formation factor plus a contribution from surface conduction:

$$F_f^{app} = \frac{\kappa_{meas}}{\kappa_w} = \frac{\kappa_s + \kappa_r}{\kappa_w} = \frac{\kappa_s}{\kappa_w} + F_f \qquad (2)$$

As can be readily appreciated from equation (2), uncertainty concerning the porewater conductivity influences both the estimated apparent effective diffusivity, F_f^{app} (i.e. κ_{meas}/κ_w) as well as the magnitude of the contribution from surface conduction, κ_s/κ_w. Since there is currently a lack of data for site-specific rock types at Forsmark, the surface conductivity has been assessed using data obtained in previous investigations of typical Swedish intrusive igneous rocks (Löfgren, 2001; Ohlsson, 2000). In these studies, the surface conductivity was inferred by comparing the resistivity of the same rock samples diffusively equilibrated with water of high ionic strength (1M NaCl) and low ionic strength (deionised water), respectively. These data are used together with the single, currently available data point for Forsmark site-specific rock (Löfgren et al. 2009) to derive an empirical power law relation between surface conductivity and true formation factor:

$$\log_{10}\kappa_s \approx \left(-2.92 \pm 0.11\right) + 0.415 \times \log_{10}\left(F_f\right) \qquad (3)$$

Since the simultaneous equations (2) and (3) cannot be combined to give F_f explicitly, a numerical treatment is needed. Furthermore, in order to determine the uncertainty of F_f, the uncertainties of the porewater composition and prediction error of the empirical relation (3) need to propagate in the calculation in a consistent manner. In the present

work, this has been addressed by simple Monte-Carlo sampling of the underlying uncertainty distributions (10^4 realisations per rock resistivity measurement) and use of a Matlab optimisation routine to obtain estimates of the true formation factor and its uncertainty distribution. For the calculations, κ_w and κ_s are assumed to have lognormally distributed uncertainties.
Although site-specific formation factors derived from in-situ resistivity measurements (e.g. Löfgren and Neretnieks, 2003) and corrections for surface conductivity bias (Crawford and Sidborn, 2009) have been described previously, the novel aspect of the present work is the propagation of error estimates using the Monte-Carlo method where both the direct error associated with uncertain porewater conductivity and the prediction error of the empirical surface conduction relation are considered simultaneously.

Estimation of in-situ porewater electrical conductivity

Since it is generally not feasible to directly measure porewater conductivity in-situ, there are two principle means by which porewater conductivity can be estimated. The first involves use of electrical conductivity data derived from water sampled in flow bearing fractures as a proxy for matrix porewater composition. This method is problematic in that it implicitly assumes diffusive equilibrium between the rock matrix and borehole-intersected conductive fractures which may be separated by many tens of metres. This is at best an optimistic assumption and the true porewater composition more than a couple of metres distant from a fracture can be significantly more, or less saline than the sampled groundwater. The other involves indirect extraction of porewater by leaching of core samples combined with mass balance modelling for estimation of original porewater composition (Waber and Smellie, 2008).
The available data for the borehole KFM01D at Forsmark are shown in Figure 1 together with data points for two other closely located boreholes, KFM08C and KFM06A. Since the present analysis concerns estimation of in-situ formation factors for the rock matrix surrounding the KFM01D borehole, the solid regression line displays the estimated, average electrical conductivity trend for this borehole only. As the electrical conductivity profiles obtained for the other boreholes follow approximately similar trends and because there are only a limited number of data points for KFM01D, an approximate uncertainty interval for the depth trend is calculated based on the standard error of the estimate for the regression line relative to the ensemble of plotted data points for the other proximate boreholes. This gives an expanded uncertainty range over that given by consideration of the KFM01D data only. Although it could be argued that the error bounds are larger than what might be strictly representative of the rock matrix surrounding KFM01D, they are intended to be cautious in that the uncertainty is likely to be overestimated rather than underestimated.

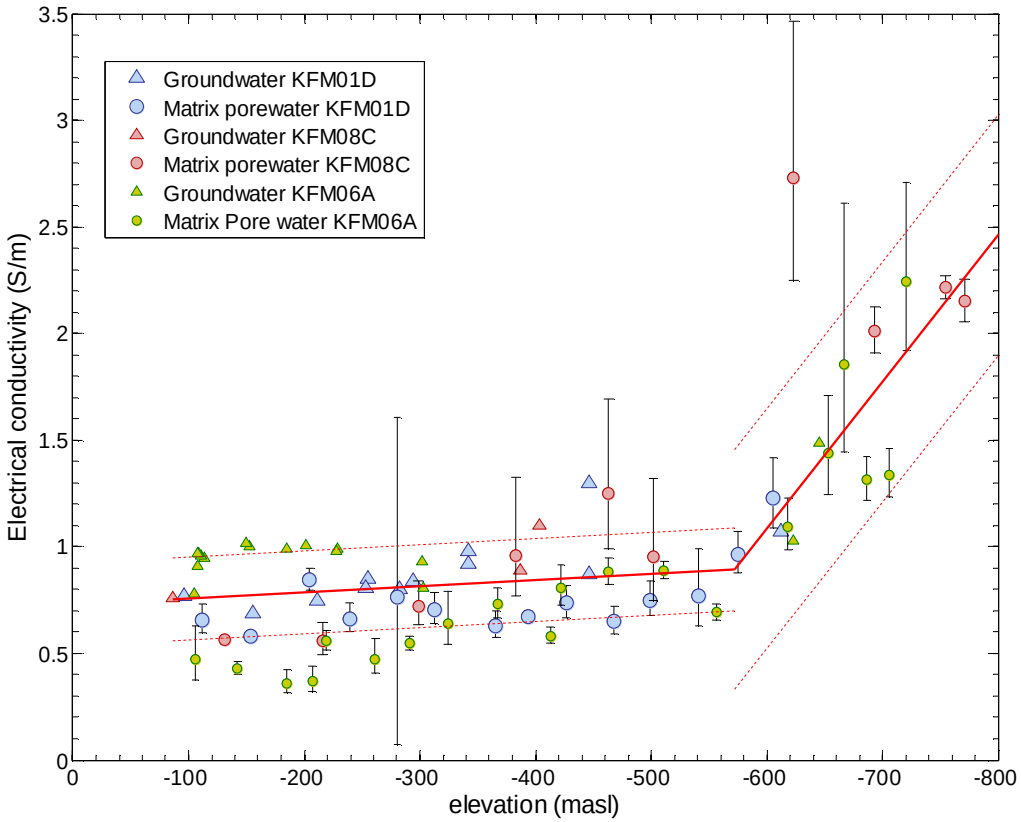

Figure 1: *Electrical conductivity of porewater and groundwater at in-situ temperature in Forsmark at drill site 1. The solid regression line is based on data for KFM01D only, while the standard error of the estimate (indicated by broken lines) also includes data from other nearby boreholes. Error bars are given for porewater conductivity estimates where available.*

As can be readily appreciated from the point samples of the estimated porewater electrical conductivity shown in Figure (and groundwater proxy measurements), the assumption of a smooth linear transition in general, does not reflect the reality of spatial variability of electrical conductivity as might be expected to arise due to diffusive disequilibrium between the rock matrix porewater and groundwater in sparsely distributed flow bearing fractures. The standard error of the estimate shown by the broken lines in the regression curve therefore attempts to capture this fundamental uncertainty in an approximate manner.

Results

Figure shows how the formation factor ($\log_{10}$ transformed data) varies with elevation around the borehole KFM01D as characterised by different methods. The grey markers (+) show the point values of the uncorrected apparent formation factor (3,636 data points). The measurements are made on a dm resolution and only values more than 0.5 m distant from mapped open fractures are included in the analysis. The black curve shows the 10m running average of the raw data values prior to correction for surface conduction bias, while the blue curve shows the 10m running average for the corrected data with a surrounding shaded region corresponding to the 1-σ error of the estimate as calculated by the Monte-Carlo marginalisation technique.

The best estimate, corrected formation factor exhibits a lognormally distributed spatial variability with mean, μ = -4.76 and standard deviation, σ = 0.14 (i.e. $\log_{10}$ units). This corresponds to an expected average in-situ formation factor of $(1.8 \pm 0.6) \times 10^{-5}$. Propagation of the underlying uncertainties in κ_w and κ_s results in a slight broadening of the tails of the distribution, giving $\sigma \approx 0.16$ when only considering the direct effect of uncertain κ_w and $\sigma \approx 0.18$ when one considers the additional uncertainty in κ_s. The largest contributor to the statistical dispersion therefore appears to be spatial variability with the direct impact of uncertain porewater conductivity playing a secondary role. The present calculations suggest that the prediction error of the surface conductivity relation (equation (3)) plays a relatively minor role for the overall uncertainty.

For comparative purposes, data based on the measurements reported in (Waber and Smellie, 2008) are shown for core samples taken from the same borehole (with 1-σ error bars). Laboratory data for the two nearby boreholes (KFM01A and KFM01B) are also shown (Selnert et al. 2008), although these were reported without error estimates. These data are based on through diffusion measurements using tritiated water (Hto) as well as laboratory based resistivity measurements.

Although the through-diffusion and lab resistivity data are for different boreholes there are some interesting features of the data sets that merit inclusion in the discussion. First is that the formation factor measured using the laboratory resistivity method shows an increasing trend with decreasing sampling elevation (i.e. increasing depth). This is what one would expect if mechanical damage of the core occurs during drilling since greater force appears to be required for drilling at increasing depth. Another feature is that the laboratory resistivity method (see data cluster at -320 m elevation) consistently predicts a formation factor roughly twice that of the through diffusion method when using the same core samples. The origin of this discrepancy is currently unclear although it appears it might be a separate phenomenon from the bias introduced by surface conduction.

The discrepancy may be related to the different tracer substances utilised by the different methods, deviations in the assumed viscosity of water in confined micropores, or possibly the impact of capacity effects in the interpretation of the through-diffusion breakthrough data (i.e. dead-end porosity that is not sampled by the electrical method). Another possibility is the existence of narrow pore throats that may partially invalidate the parallel conduction model for rock bulk resistivity. Although the role of capacitance effects was deemed to be small at the low AC frequencies used in laboratory measurements used to estimate the surface conductivity in (Löfgren, 2001; Ohlsson, 2000), the fact that the borehole data are obtained with a somewhat higher AC frequency (2 kHz) cannot be entirely neglected as a source of uncertainty when combining the different data sets in the present analysis. Further laboratory studies certainly need to be undertaken to properly clarify this and to expand the database for surface conductivity corrections. It is noted, however, that all known measurement biases and artefacts (here, taken to include capacitance effects) should result in overestimation of the in-situ formation factor when using the electrically based methods. The impact on estimates of in-situ formation factor, however, depends on whether the laboratory determined surface conductivity data over- or underestimates the magnitude of the required correction and which laboratory reference data one is comparing with.

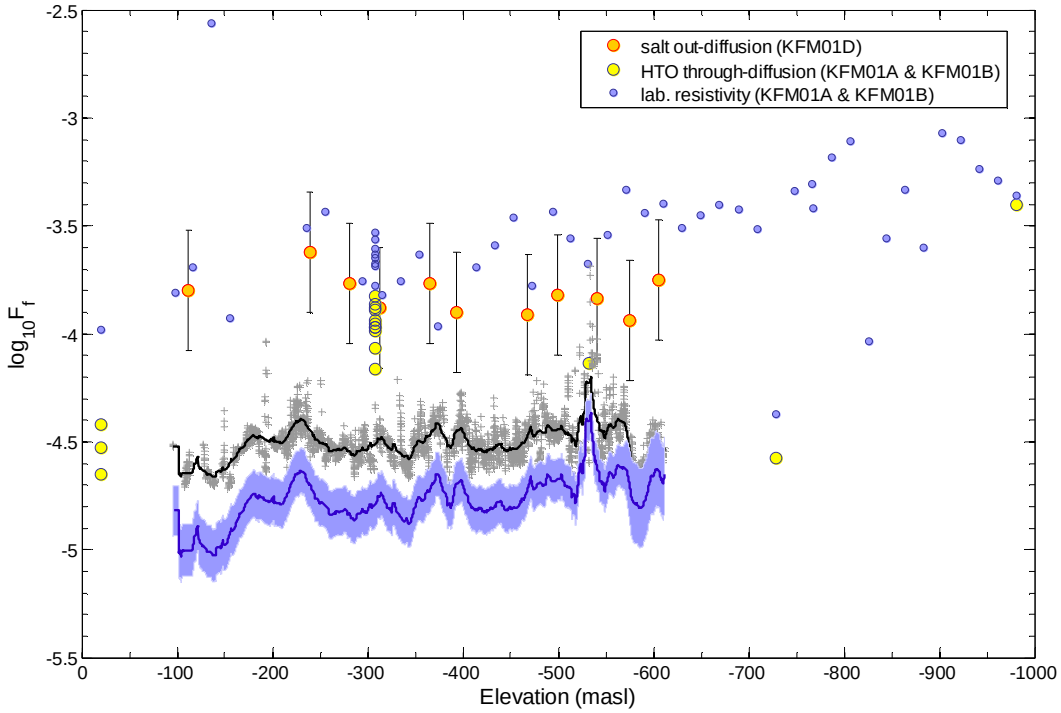

Figure 2: *Best estimate geometric formation factor (log_{10} values) as a function of borehole elevation for rock surrounding Forsmark borehole KFM01D as determined by the in-situ measurement technique shown as a 10m running average (blue curve). The shaded region represents the corresponding 1-σ error of the estimate as determined by the Monte-Carlo calculations. The black curve shows the 10m running average of the apparent formation factor which is not corrected for surface conduction bias while the grey symbols indicate associated point values. Circular markers show laboratory estimated values derived from various measurement techniques as indicated in the legend (1-σ error bars shown where available).*

There is a very small increase (< 10% over the first 500 m elevation) in the apparent in-situ formation factor with increasing depth, although this may be an artefact related to the slope of the average porewater conductivity depth trend not being fully consistent with the true depth trend. The peak at -540m elevation, on the other hand, corresponds to an observed deformation zone which is expected to deviate relative to the surrounding, sparsely fractured rock. The depth trend appears to be very faintly amplified by the correction for surface conduction, which could signify that the surface conduction bias effect is slightly overcompensated for when using the generic surface conduction correction.

Work Package 4 Component – Process based sorption modelling

Background

Migrating radionuclides are frequently in the form of aqueous ionic species and will tend to adsorb to mineral surfaces that possess a net charge of opposite sign. The most important mechanisms for this interaction are considered to be ion-exchange and surface complexation. Ion exchange involves a purely electrostatic adsorption process whereas surface complexation typically involves covalent bonding to chemically

reactive surface groups on mineral surfaces. Although the term sorption can refer to a broader range of processes including surface precipitation and solid solution formation (co-precipitation), in this work the term is used to specifically refer to ion-exchange and surface complexation processes only. Being a surface mediated process, the sorption of radionuclides on rock is sensitive to both the available surface area of the constituent minerals as well as their geochemical properties.
Typically in safety assessment studies, the sorption of radionuclides is modelled under the assumption of a linear isotherm approach whereby the sorbed concentration is deemed to be proportionally related to the dissolved concentration with the proportionality constant referred to as the K_d. In general, the definition of a K_d is a purely empirical construct that is only strictly applicable under those exact conditions under which it is measured and is not explicitly contingent upon any specific sorption mechanism or speciation considerations. The use of a conditionally constant K_d value in radionuclide migration modelling, however, implies a retention process with particular characteristics that when combined with a model of advective and diffusive mass transfer can be used to give a quantitative measure of radionuclide transport retardation. For this reason it is very important that the magnitude of the K_d value selected to represent the retardation process correctly captures the physics of the postulated retention mechanism. Other sorption processes such as precipitation and solid solution formation scale very differently in time and space to purely adsorptive processes such as ion-exchange or surface complexation and cannot be modelled using a K_d approach.

Currently available sorption data

In this Work Package, attempts will be made to construct a process-based description of radionuclide sorption based on ion-exchange and surface complexation modelling in order to provide a more robust mechanistic basis for estimating K_d values for use in safety assessment studies. Since sorption measurement data for the rock types sampled in Work Package 2 are not yet available within the CROCK project, the focus of the current work has been to re-examine sorption data obtained during the SKB site characterisation programme at Forsmark (SKB, 2008) with the aim of understanding uptake mechanisms, in particular, the nature of kinetic effects apparent in the sorption partitioning time series data. No attempt has yet been made to interpret the present data set using thermodynamic sorption models (TSMs) since the contact water compositions chosen to represent typical in-situ groundwater conditions are judged insufficient to constrain model parameters in a satisfactory fashion.
In the laboratory programme for transport properties carried out during SDM-Site (Byegård et al. 2008), sorption measurements were made on different size fractions of crushed matrix rock. Sorption time series measurements were made for the sieve size fractions 63-125 μm, 0.25-0.5 mm, and 1-2 mm. BET surface area measurements were made for the 63-125 μm size and a 2-4 mm size that was not used for sorption experiments. Partitioning coefficients (R_d values) were calculated using a radiometric mass balance and recorded on a geometric time schedule corresponding to approximately 1, 7, 30, 90, 180 days contact time and for a liquid to solid ratio of 4:1 (i.e. ml/g). Crushed rock samples were pre-equilibrated with the synthetic contact groundwater for a period of roughly 90 days (with 10 water changes during the first 36 days) prior to spiking with the radionuclide tracer. Radionuclide tracers studied were ^{85}Sr, ^{134}Cs, $^{241}Am/^{152}Eu$, ^{226}Ra, ^{63}Ni, ^{233}U, and ^{237}Np. In all experiments performed, trace concentrations of radionuclide were used in order to not perturb the composition

of the contact water. Provided the contact water composition can be reasonably assumed to be constant over time and the radionuclide concentration is sufficiently low that site saturation does not occur, the uptake of solute can then be reasonably modelled using conditionally constant partitioning coefficients.
In the following paragraphs, it should be noted that the term R_d (m^3/kg) is used to refer to apparent partitioning coefficients (i.e. as they are measured on crushed materials), whereas the term K_d (m^3/kg) is reserved for partitioning coefficients applicable to intact rock.

On the interpretation of batch sorption data

In laboratory investigations of sorption it is typically found (e.g. André et al. 2008) that the measured partitioning coefficient, R_d (or K_d) of different solutes is approximately proportional to the measured BET surface area. The relationship is usually most compelling for different samples of the same rock type as significant differences can exist between rocks of different origin featuring different mineralogy and subjected to different weathering or alteration processes. This is usually rationalised in terms of different geological surfaces having different sorptive affinities, binding site types, and site densities. The BET surface area, on the other hand, is simply a proxy estimate of the total available surface area and does not discriminate between different site types or the affinity of those sites for reactions with ionic solutes. Although this is a well known fact, the question remains as to the best means of extrapolating R_d data obtained from laboratory measurements on crushed rock samples to K_d values appropriate for in-situ conditions in relatively undisturbed (intact) rock.
When using crushed size fractions of granitic rock, it has become customary to interpret sorption data in terms of a model whereby sorption is deemed to occur on external particle surfaces as well as within the internal microporosity of the rock (e.g. Widestrand et al. 2003). This usually takes the form of a linear regression analysis where the specific sorptivity on external particle surfaces is inversely proportional to the characteristic particle dimension plus a contribution from sorption on internal microsurfaces under the assumption that the data represent an approximate equilibrium state. Similar analyses can also be made for the variation of BET surface area with particle size (e.g. Brantley and Mellott, 2000). Such analysis results in the following empirical relations for R_d and BET surface area:

$$R_d \approx K_d + \frac{6K_a}{\rho_b d_p} \tag{4}$$

$$A_{BET} \approx A_{\text{int}} + \frac{6\lambda}{\rho_b d_p} \tag{5}$$

Generally, the external particle surface area interpreted using regression analysis is somewhat greater than what would be expected for a collection of spherical particles (a sphere being the minimal surface enclosing a three dimensional volume), and therefore an empirical "surface roughness" parameter, λ is used to account for deviations from sphericity in equation (5) (ρ_b, is the bulk density of the rock). The characteristic particle size, d_p is variously defined as the volumetric mean (e.g. Byegård et al, 1998; Widestrand et al. 2003), geometric mean (Brantley and Mellott, 2000), or the representative particle size based on the assumption of a uniform particle size

distribution between bracketing sieve sizes (André et al. 2009a). It should be noted that in this approach, both the K_d and K_a fitting parameters in equation (4) and the corresponding A_{int} and λ parameters in equation (5) are assumed to be constant and independent of particle size.
An example of such a regression analysis is shown in
Figure . It is noted that data for different size fractions frequently exhibit significantly greater scatter than that apparent in the example, which may be considered a relatively "well-behaved" data set.

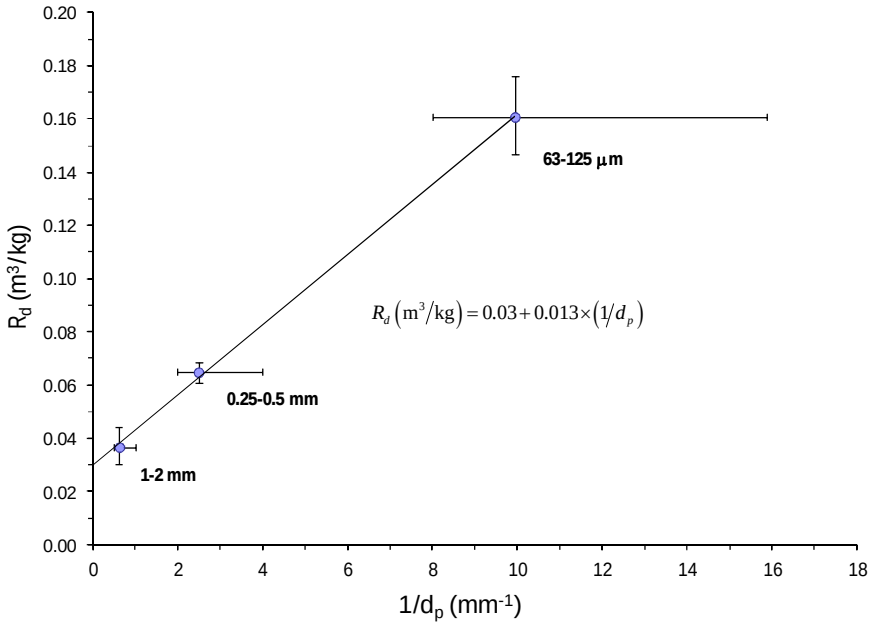

Figure 3: *An example regression analysis of R_d measurement data for Am(III) sorption correlated against inverse of particle size, $1/d_p$ (as defined by André et al, 2009a) to infer K_d for sorption on internal rock microsurfaces using equation (4). The data are based on triplicate measurements for a crushed sample of Forsmark metagranite and 180 days contact time with a non-saline, synthetic groundwater. Horizontal error bars represent the possible range of particle sizes as bounded by the bracketing sieve sizes.*

In this treatment, considerable uncertainty can arise due to the strong leverage effect of small size fractions in the regression analysis which, in some cases can imply approximately zero or even non-physically meaningful, negative sorptivities for internal surfaces. This may also be compounded by the arbitrary definition of characteristic particle size, d_p when simple regression analysis is performed without additional consideration of "error in variables" uncertainty. Furthermore, it is not always clear that that very small particle sizes are representative since fractionation of fine grained minerals such as biotite can occur amongst different sieve sizes and because freshly exposed mineral surfaces may react with the contact solution over a period of time giving rise to secondary precipitates such as hydrous ferric oxides that may be a non-negligible source of bias. Recently, André et al. (2009a, b) have found that the method encapsulated in equation (4) appears to overestimate the K_d of intact rock (for Cs^+ sorption) by as much as an order of magnitude when compared with results based on an electromigration method and intact core samples. This is likely to be due to mechanical

damage effects since comparison of BET measurement data for intact core samples with extrapolated data using equation (5) suggests a similar discrepancy for surface area.
An alternative procedure which attempts to account for this discrepancy, and avoids the "negative" K_d values sometime predicted in regression analysis, is to use BET surface area normalised data based on the R_d values measured for a reference crushed size fraction and the BET surface area of the crushed and intact rock, respectively:

$$K_d \approx R_d \cdot \left(\frac{A_{BET}^{\text{intact}}}{A_{BET}^{\text{crush}}} \right) \tag{6}$$

While this might be considered a more conservative approach for safety assessment, it is not necessarily more physically correct, neither does it inform us whether the rescaled data for crushed materials used in laboratory investigations are representative of the in-situ rock. Given that the BET surface area of crushed rock can be as much as 1-2 orders of magnitude greater than that of monolithic samples (Crawford, 2010), this is not a trivial uncertainty. In fact, the mm-size sieve fractions that are most ideal for such analysis (being most similar to intact rock) are also sufficiently large that diffusive disequilibrium effects cannot be neglected and one might just as well use monolithic materials and dispense with the added uncertainty introduced by crushing and grinding. This should not be taken to mean that more accurate results are automatically obtained by inverse estimation of parameters from transport modelling since it is generally not possible to obtain diffusion and sorption parameters that uniquely describe the solute uptake in the absence of independent corroborating information. When modelling in-diffusion experiments on intact core samples, for example, different D_e and K_d values can be shown to give identical fits to the aqueous phase time series data provided the product of D_e and K_d is constant. To reduce the number of degrees of freedom in the analysis, independent information such as post-mortem depth profiles of sorbed radionuclides is therefore desirable.
Historically, the argument against the use of monolithic materials was the fact that the sorption partitioning coefficient cannot be estimated directly and must be interpreted through a transport model which simultaneously couples diffusion and sorption (e.g. Bradbury and Baeyens, 1998). The use of finely crushed materials allows the fast equilibration of sorption sites that otherwise would require many months to equilibrate with the contact solution and thus dispenses with the necessity for transport modelling. Both approaches, however, represent compromise situations whereby different uncertainties dominate the analysis. The position taken in this paper is that the laboratory data based on either crushed or monolithic materials must be consistent with time dependent uptake predicted by coupled transport modelling if they are to be considered physically meaningful for deployment in safety assessment.

Re-analysis of sorption data using a simple diffusive transport model

The site specific data (including the data set from which
Figure was derived) were re-interpreted using a single rate model of diffusive uptake from a solution of limited volume as described by Crank (1975), although modified to account for fast equilibrium sorption on external surfaces of crushed particles. In general it is very difficult to make a convincing fit to the time series data for different

crushed size fractions, using any simple surface area and particle size scaling relation which is simultaneously consistent with either equation (4) or (6).

The time series data exhibit similar kinetic characteristics for different particle sizes and (in many cases) similar R_d ratios for different size fractions at both short (~1 day) and long (~180 day) contact times. This appears to be the case for a large proportion of the data sets obtained for Forsmark site specific materials where clearly systematic time dependency can be ascertained (some data sets for particular size fractions and groundwater compositions exhibit considerable scatter). Convergence to an apparent equilibrium only appears to occur in a very small number of cases for the smallest size fractions, although data scatter makes this uncertain. The data suggest that the specific sorptivity of internal surfaces is not constant over different size fractions and that the sorption on both internal and external surfaces scales in a similar fashion with regard to characteristic dimension, d_p. The data also appear to imply that the characteristic timescale of diffusion is very similar for different particle sizes, implying either that the apparent diffusivity scales in a very peculiar and precise way for different particle size fractions or that the particle size, d_p is not a representative parameter for the diffusive uptake kinetics.

An example of a modelling interpretation of the sorption time series data using the diffusion model is shown in Figure . The curves shown in the Figure are based on a simple visual curve fit and shouldn’t be taken to imply an optimised fit in a least squares sense. There are actually a number of different parameter combinations that can be shown to be approximately consistent with the measurement data. In principal, however, all assumptions inherent in the regression analysis presented in

Figure must be broken in order to simultaneously fit (approximately) the time series data for the different size fractions. Furthermore, the implied variation of model parameters required to fit the uptake data suggests that any simple extrapolation of data derived from measurements made using crushed materials to in-situ conditions is both fundamentally unsound and subject to excessively large conceptual and parametric uncertainties.

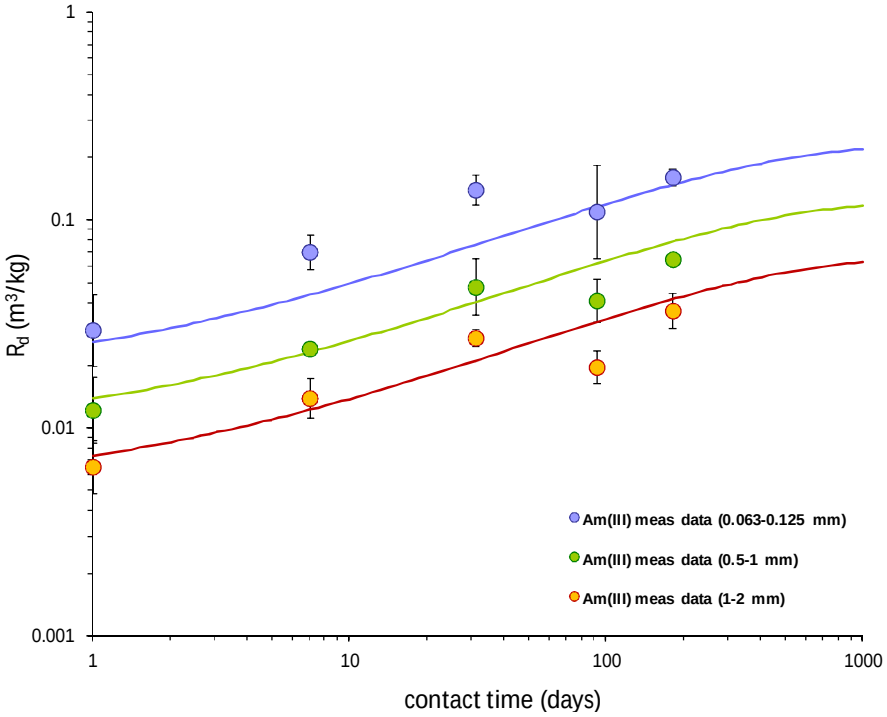

Figure 4: *An example of a transport modelling interpretation (curves) of R_d measurement data for Am(III) sorption plotted as a function of contact time. The data are based on triplicate measurements for a crushed sample of Forsmark metagranite and three different crushed particle size fractions in contact with a non-saline, synthetic groundwater. The 3 final data points at 180 days correspond to the data shown previously in Figure 3.*

In the current work it is argued that the broadly similar time dependency exhibited by each size fraction may be related to microstructural features of the internal porosity of the crushed rock. Specifically, the uptake characteristics are strongly suggestive of bi-disperse storage porosity where uptake to the secondary porosity is both rate limiting and dominates the overall sorption capacity of the rock (e.g. Ruckenstein et al. 1971; Neogi and Ruckenstein, 1980). This is suspected from the apparent non-representativity of the particle size for the observed kinetic effects. Furthermore, the timescale of diffusive disequilibrium exhibited by solutes exhibiting very different geochemical characteristics (Am, Cs, Ni) are sufficiently similar that it is speculated that this may be due to the existence of diffusive "bottlenecks" possibly in the form of hydrous ferric oxide microprecipitates residing in the pore structures immediately adjacent to the dominant sorption sites. The apparent scaling of K_d with particle size also suggests that the mechanical damage induced by crushing increases the accessible internal sorptive surface area in a fundamentally non-linear fashion.
Here, it is proposed that the main locations for Cs sorption are the frayed edge sites and internal surfaces of biotite mineral grains, while Am and other surface complexers sorb preferentially on aluminol and silanol edge sites of biotite grains and ferrol sites of associated ferric oxide phases. This also suggests that diffusion through microcrystalline ferric precipitates is the rate limiting step for the apparent timescale of diffusive disequilibrium as implied by the time series data. Although speculative and not strictly related to the main aim of this work package (i.e. to develop a thermodynamic sorption model, TSM), the data give some indications as to what might be a good candidate for a

generalised sorption model in granitic rock. This conceptual model of the rock matrix microstructure also provides a possible basis for incorporating a simultaneous description of the reducing properties of the rock matrix in a parsimonious fashion (i.e. by way of the kinetic release of Fe(II) from biotite coupled with Fe(III) oxide precipitation in the micropores).

Work Package 5 Component – Deployment of process based models in safety assessment

Background

It is generally accepted that a constant K_d modelling approach fails to reproduce certain aspects of radionuclide transport that could have significant impact on quantitative assessments of radiological risk. At the same time it is important to note that this breakdown in realism is not always strictly related to the use of a K_d formulated approach as such, but rather the assumption of a constant (i.e. temporally and spatially invariant) K_d value in transport modelling. Provided certain criteria are reasonably fulfilled and there is a direct functional correspondence between sorbed and dissolved concentrations, a model allowing for a conditionally variable (parametric) K_d can reproduce a wide variety of non-linear phenomena that would normally be considered the preserve of fully coupled thermodynamic sorption models. The requirement that there be a direct correspondence between sorbed and dissolved concentrations is generally fulfilled for true adsorption processes. This is not the case for immobilisation processes involving precipitation-dissolution where the activity of the solid phase is independent of the amount of solid phase present and it only holds under the limiting equilibrium case for solid solutions.
The other basic criterion that needs to be fulfilled in order to justify the use of a variable K_d model concerns whether the description of trace solute (radionuclide) sorption can be decoupled from the transport processes and interactions of the major groundwater species that determine the overall solution chemistry. Here, this is referred to as the decoupled major ion chemistry approximation. This is justifiable if the transported radionuclide is sufficiently dilute that it does not exert an appreciable influence on the groundwater chemistry itself. There are, of course, radionuclides and migration scenarios for which this assumption may not hold. In particular, the concentration of uranium in groundwater may be sufficiently high that it exerts a non-negligible influence on the redox state of the groundwater in certain situations. On the other hand it would seem unlikely that concentrations of, for example, Ra, Cs, or Sr would be sufficiently high to influence bulk groundwater chemistry.

Modelling strategy

For a matrix diffusion process and neglecting radioactive decay and in-growth, the differential mass balance of a single trace solute (radionuclide) undergoing adsorption is customarily represented as:

$$\frac{\partial}{\partial t}\left(\varepsilon_p + K_d \rho_b\right) C_1 = \nabla \cdot \left(D_e \cdot \nabla C_1\right) \qquad (7)$$

For a parametrically defined K_d value that varies as a function of specific groundwater composition variables (C_1,…, C_k) where C_1 is the concentration of the transported radionuclide and C_2,…, C_k are concentrations of other solution components, one can write:

$$K_d = f\left(C_1, C_2, \ldots, C_k\right) \tag{8}$$

Although a spatially variable K_d arising due to material property variation of the rock is relatively straight-forward to handle, in the case of a temporally variable K_d it is important that the parameter dependencies are correctly represented with respect to the accumulation term on the left-hand side of equation (7). If the transported radionuclide exerts no influence on the bulk groundwater composition itself there is an effectively one-way dependency on other groundwater parameters. This assumption allows the non-linear component of the mass balance to be split into an intrinsic non-linear accumulation and pseudo-reaction term:

$$\left(\varepsilon_p + K_d \rho_b \left(1 + \frac{\partial \ln K_d}{\partial \ln C_1}\right)\right)\frac{\partial C_1}{\partial t} = \nabla \cdot \left(D_e \cdot \nabla C_1\right) - C_1 \rho_b \sum_{i=2}^{k} \frac{\partial K_d}{\partial C_i} \cdot \frac{\partial C_i}{\partial t} \tag{9}$$

The intrinsic accumulation term on the left-hand side of equation (9) accounts for Langmuirian saturation of different sorption site classes (giving Freundlich isotherm-like behaviour if there are several different site classes), whereas the pseudo-reaction term on the far right-hand side of the equation accounts for non-linearities arising due to the evolving bulk groundwater chemistry.
In the recent SR-Site safety assessment (SKB, 2011), K_d values for site-specific application conditions were estimated using a transfer factor approach. For a radionuclide that sorbs by way of an ion-exchange mechanism it is postulated (Crawford, 2010) that the application specific K_d value can then be defined as:

$$K_d = K_d^0 \cdot f_m \cdot f_{cec} \cdot f_{chem} \tag{10}$$

Where K_d^0 is the partitioning coefficient for a given set of reference conditions (accessible bulk rock specific surface area, accessible cation exchange capacity, and reference contact water chemistry). The factors f_m and f_{cec} account for differences in the accessible sorptive surface area and cation exchange capacity of the geosphere rock matrix relative to the typically crushed materials used in laboratory experiments, while the f_{chem} factor accounts for deviations in groundwater chemistry relative to the contact water composition used in the experiments. Assuming approximately constant material properties along a migration path and considering only temporal variations in groundwater chemistry, one can assume in the present example $f_m \approx f_{cec} \approx 1$.

Results

For the purposes of a prototype demonstration simulation, the K_d for Ra^{2+}, Cs^{+}, and Sr^{2+} sorption has been simulated using a simplified, single-site ion-exchange model for Äspö fine-grained granite (Byegård et al. 1998) assuming geochemical analogy between Ba^{2+} and Ra^{2+}. The value of f_{chem} can then be estimated as the ratio of the simulated K_d value

for the application groundwater and that calculated for a given reference groundwater composition (here taken to be a typical saline groundwater composition encountered at repository depth at the Forsmark site):

$$f_{chem} = \frac{K_{d(sim)}^{GW}}{K_{d(sim)}^{SaF}} \tag{11}$$

Since this particular ion-exchange model assumes a single binding site, it does not predict intrinsic non-linear sorption behaviour (i.e. site saturation) in the normal concentration ranges likely to be encountered under application conditions. Variation in the major ion composition of the groundwater, on the other hand, is found to have a profound effect on the simulated sorptivity of the trace components Ra, Cs, and Sr. The variation of f_{chem} is shown in Figure for a hypothetical mixing process involving an altered meteoric water and the saline reference groundwater. As can be seen from the figure, the sorptivity of the ion exchanging solutes Ra, Cs, and Sr is strongest for meteoric conditions and weakest under saline conditions as would be expected for these ion-exchanging solutes.

For the system being modelled, equation (9) simplifies to:

$$\left(\varepsilon_p + K_d \rho_b\right)\frac{\partial C_1}{\partial t} = \nabla \cdot \left(D_e \cdot \nabla C_1\right) - C_1 \rho_b \frac{dK_d}{d\mu} \cdot \frac{d\mu}{dt} \tag{12}$$

Where μ is the ionic strength of groundwater comprised of mixed fractions, x_A of the meteoric (μ_A) and saline (μ_B) end-members:

$$\mu = x_A \mu_A + \left(1 - x_A\right)\mu_B \tag{13}$$

The term $dK_d / d\mu$ is calculated according to:

$$\frac{dK_d}{d\mu} = K_d^0 \cdot \frac{d}{d\mu}\left(f_{chem}\right) \tag{14}$$

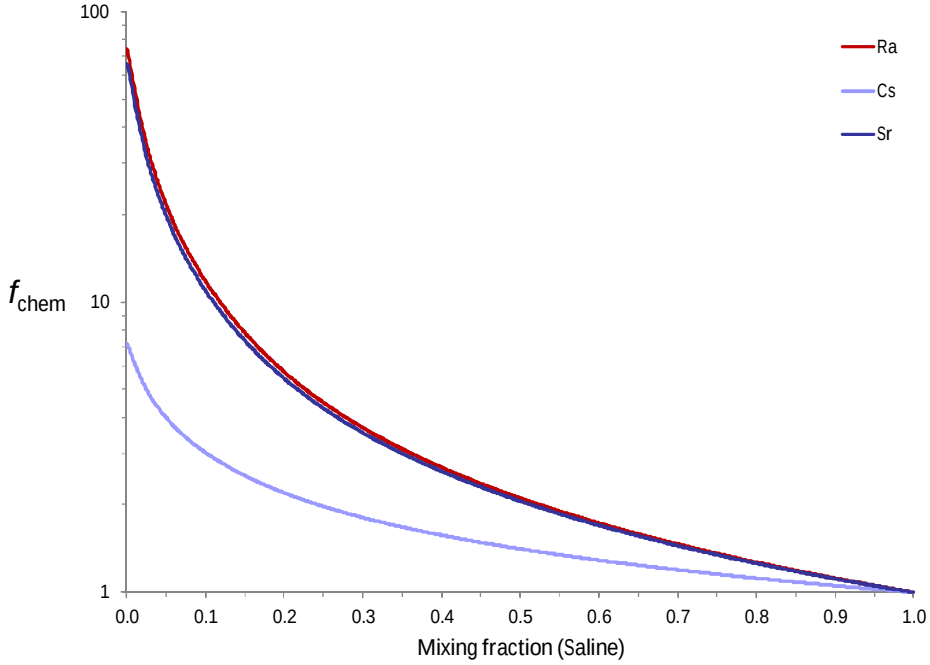

Figure 5: *groundwater chemistry transfer factor, f_{chem} plotted as a function of groundwater mixing fraction for mixing of an altered meteoric type (fresh) groundwater with a saline groundwater type typical of contemporary groundwater conditions at repository depth at Forsmark.*

To illustrate the non-linear impact of evolving groundwater composition, a simple scenario is modelled involving intrusion of meteoric groundwater into a fracture system initially equilibrated with saline groundwater. Here, a typical low-range F-factor of 10^4 y/m, advective travel time of 10 y, and typical material properties for the rock matrix at repository depth at Forsmark (ε_p = 0.001, D_e = 10^{-14} m^2/s) are assumed. In the present calculations the focus is upon provoking clearly observable non-linear phenomenon rather than safety assessment realism, so a sequence of abrupt fresh and saline groundwater pulses are simulated.

The mixing of the groundwater end-members due to matrix diffusion can be addressed by a simple transport calculation using a hypothetical conservative component as a proxy for the mixing fraction. The value of μ and $d\mu/dt$ can be readily calculated either by using an analytical model (e.g. Neretnieks, 1980) directly, or by including the proxy component in a 2-component numerical transport model. For the prototype calculations presented here, we use an analytical solution to describe the salt transport and solve the coupled advection and matrix diffusion equation system separately for the ion-exchanging component using a purpose written Matlab program (PATHTRAC). The particular value of f_{chem} and $df_{chem}/d\mu$ is then calculated in terms of the ionic strength, μ by way of a suitable interpolating function or lookup table that is accessed during run time.

A simulated breakthrough curve for Ra^{2+} migration is shown in Figure for an aquifer initially equilibrated with meteoric water and in Figure for the inverted groundwater situation of an aquifer initially equilibrated with saline groundwater. In this case, a reference K_d value of 10^{-3} m^3/kg is assumed for Ra^{2+} sorption under saline aquifer conditions. The non-linear transport of Ra^{2+} is calculated for a pulse train of alternating

fresh and saline groundwater inflows to the system (each of 2 ka duration) and for an extended pulse concentration boundary condition for Ra^{2+} (4 ka duration, no decay). The pulse release due to remobilisation of previously sorbed Ra^{2+} in response to changes in groundwater composition is clearly apparent in the breakthrough curves for both scenarios of groundwater chemical evolution.

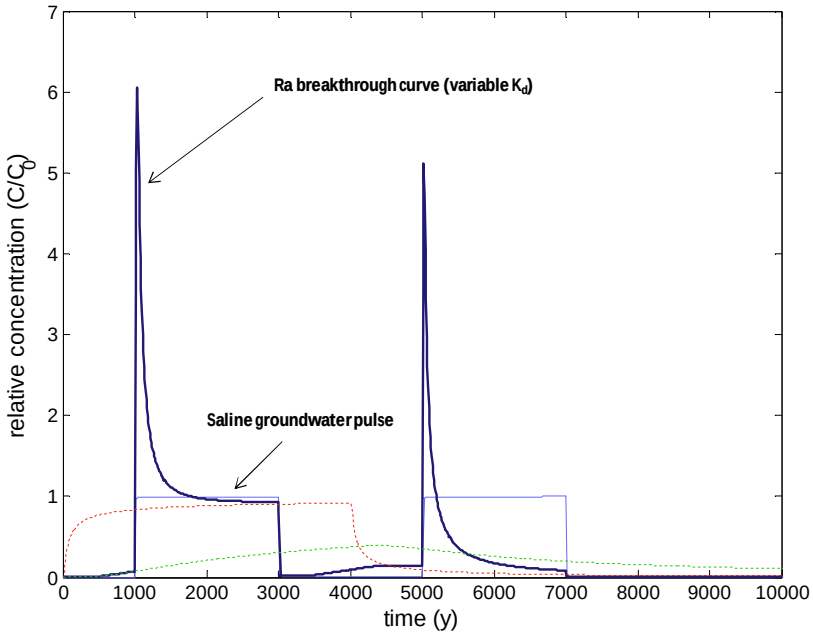

Figure 6: *Breakthrough characteristic (dark blue curve) for Ra^{2+} migration considering advective transport and matrix diffusion under the influence of alternating fresh and saline groundwater pulses (light blue curve) of 2 ka duration and non-linear sorption. The aquifer is initially equilibrated with fresh groundwater and the Ra^{2+} source boundary condition is a single extended pulse of 4 ka duration (initiating at t = 0 y). The red and green curves show the breakthrough curves obtained for the limiting constant K_d cases for saline ($K_d = 10^{-3}$ m^3/kg) and meteoric ($K_d = 7.4\times10^{-2}$ m^3/kg) groundwater, respectively.*

Although the treatment of sorption in this prototype calculation is very simple, it nevertheless reproduces the non-linear, pulse remobilisation of sorbed Ra^{2+} as might be expected for this radionuclide. Although not an exact representation of ion-exchange sorption, the main advantage of the modelling approach is that the calculations can be performed much faster than is possible using a fully coupled code. For deployment to safety assessment applications, speed of calculation is of paramount importance, particularly in cases where probabilistic simulations are used to build up a picture of radiological risk associated with different scenarios of repository evolution.

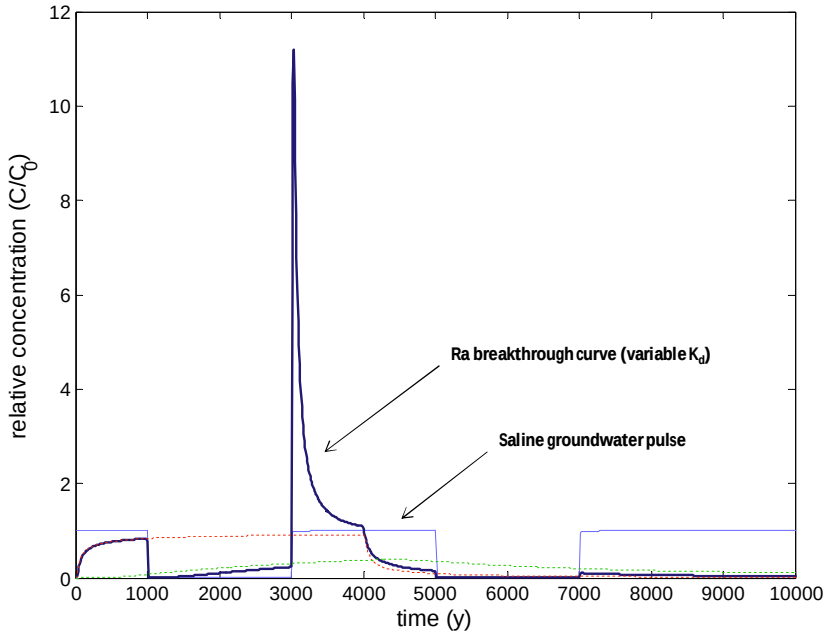

Figure 7: *Breakthrough characteristic (dark blue curve) for Ra^{2+} migration with inverted groundwater chemistry. The aquifer is initially equilibrated with saline groundwater.*

Conclusions and Future work

Work Package 3

Although in-situ formation factor data have already been used in the most recent safety assessment undertaken by SKB by appealing to arguments of conservatism (SKB, 2010), further work needs to be done to understand the physical basis for the differences between in-situ and laboratory-derived estimates as well as discrepancies between tracer and electrical resistivity based methods. The Monte-Carlo marginalisation technique developed in this Work Package also appears to be a promising technique for quantitative assessment of the uncertainty of formation factor measurements. A more detailed characterisation of the surface conductivity in site specific rock types should improve the bias correction for the in-situ data over that which can be achieved using generic data (i.e. equation (3)) as has been done in this paper.

Work Package 4

Although a thermodynamic sorption model (TSM) has yet to be created for Work Package 4, the modelling interpretation described in this paper suggests that it may be possible to describe some of the time dependent characteristics of solute uptake using a bi-disperse microstructural model of the rock matrix.
Assuming this conceptual model as a preliminary working hypothesis, a thermodynamic sorption model (TSM) will be developed that incorporates a description of surface complexation on silanol and aluminol edge sites of biotite mineral grains as well as ferrol binding sites on hydrous ferric oxides. Preliminary analysis suggests that illite might be a reasonable geochemical analogue for biotite and chlorite, at least as a first approximation. This proposal is based partly on their similar crystallographic structure

as well as comparison of some binding constants reported in the literature for Ni^{2+} surface complexation sorption. Specifically, the slope of the linear free energy relation reported by Bradbury and Baeyens (2009a) for illite, and that implied by the data reported by Zazzi et al. (2012) for chlorite, when normalised to a standard site density are very similar even though they differ slightly in absolute value. Although comparable data for sorption on biotite have not yet been examined, it is expected that the geochemical analogy with illite should also approximately hold for biotite.
As a first approximation it is proposed that a "bottom up" TSM (NEA, 2005) could be constructed by combining the 2SPNE SC/CE model (two site protolysis non-electrostatic surface complexation and cation exchange) reported by Bradbury and Baeyens (2009b) with an appropriate model for hydrous ferric oxide (e.g. Dzombak and Morel, 1990). Further work will need to be done to ascertain whether this is a workable proposition and whether the cation exchange part is approximately consistent with previously developed models described by Byegård et al. (1995, 1998). As a toy model, however, it should be a useful tool to assist in the formulation of a more accurate TSM later in the project.

Work Package 5

For Work Package 5 the immediate goal is to use a fully coupled code to attempt to reproduce the non-linear characteristics of radionuclide remobilisation as simulated using the PATHTRAC modelling approach. For this purpose, the intention is to use the CrunchFlow program (Steefel, 2009) and the same single site ion-exchange model used to calculate chemistry transfer factors in this paper. The simulation of the alternating saline-fresh groundwater regime using a fully coupled description of ion-exchange chemistry is expected to give rise to some differences due to the separation of sorption-desorption fronts of the major groundwater components. Although the major groundwater components sorb weakly by way of ion-exchange equilibria, the retardation of the components comprising the mixing fronts is expected to be very small relative to the simulated timescales and may not have a strong impact on the results for the minor radionuclide components Ra, Cs, and Sr.
When surface complexation models (SCM) become available for other radionuclides studied in work package 4, it is intended that the same approach be used to study the transport of these solutes under the influence of evolving groundwater chemistry. If multi-site TSMs become available, the additional impact of intrinsic non-linearity can also be studied. Additional work package 5 exercises could involve radionuclide migration along a hyperalkaline plume (surface complexers) or a scenario involving intrusion of an oxygenated water of glacial origin (redox sensitive solutes). It might also be possible to couple the latter with a description of redox buffering in the rock matrix due to biotite dissolution with accompanying precipitation of hydrous ferric oxide, thus providing a mechanistic link between redox buffering and sorption in the rock matrix.

Acknowledgement

The research leading to these results has received funding from the European Union's European Atomic Energy Community's (EURATOM) Seventh Framework Programme FP7/2007-2011 under grant agreement n° 269658 (CROCK project). Additional funding support from the Swedish Nuclear Fuel and Waste Management Co. (SKB) is also acknowledged.

References

André, M., Neretnieks, I., Malmström, M. (2008). Measuring sorption coefficients and BET surface areas on intact drillcore and crushed granite samples. Radiochimica Acta, 96, pp. 673-677.

André, M., Neretnieks, I., Malmström, M. (2009a). Determination of sorption properties of intact rock samples: New methods based on electromigration, Journal of Contaminant Hydrology, 103(3-4), pp. 71-81.

André, M., Neretnieks, I., Malmström, M. (2009b). Specific surface area determinations on intact drillcores and evaluation of extrapolation methods for rock matrix surfaces, Journal of Contaminant Hydrology, 110(1-2), pp. 1-8.

Atkins, P., De Paula, J. (2009). Atkins' Physical Chemistry, 9 ed. Oxford University Press, 959 pp.

Bradbury, M., Baeyens, B. (2009a). Sorption modelling on illite Part I: Titration measurements and the sorption of Ni, Co, Eu and Sn. Geochimica et Cosmochimica Acta, 73, pp. 990-1003.

Bradbury, M., Baeyens, B. (2009b). Sorption modelling on illite. Part II: Actinide sorption and linear free energy relationships. Geochimica et Cosmochimica Acta, 73, pp. 1004-1013.

Bradbury, M., Baeyens, B. (1998). N_2-BET surface area measurements on crushed and intact minerals and rocks: A proposal for estimating sorption transfer factors. Radioactive Waste Management and Disposal, 122(2), pp. 250-253.

Brantley, S., Mellott, N. (2000). Surface area and porosity of primary silicate minerals. American Mineralogist, 85(11-12), pp. 1767-1783.

Byegård, J., Selnert, E., Tullborg, E.-L. (2008). Bedrock transport properties. Data evaluation and retardation model. Site descriptive modelling SDM-Site Forsmark. SKB Report R-08-98, Swedish Nuclear Fuel and Waste Management Company, Stockholm.

Byegård, J., Johansson, H., Skålberg, M., Tullborg, E.-L. (1998). The interaction of sorbing and non-sorbing tracers with different Äspö rock types. Sorption and diffusion experiments in the laboratory scale. SKB Technical Report TR-98-18, Swedish Nuclear Fuel and Waste Management Company, Stockholm.

Byegård, J., Skarnemark, G., Skålberg, M. (1995). The use of some ion-exchange sorbing tracer cations in in-situ experiments in high saline groundwaters. In: Murakami T, Ewing R C (eds). Scientific basis for nuclear waste management XVIII: symposium held in Kyoto, Japan, 23–27 October 1994. Pittsburgh, PA: Materials Research Society. (Materials Research Society Symposium Proceedings 353), pp 1077–1084.

Crank, J. (1975). The mathematics of diffusion, 2ed., 414 pp., Oxford University Press, Oxford, UK.

Crawford, J. (2010). Bedrock K_d data and uncertainty assessment for application in SR-Site geosphere transport calculations. SKB Report R-10-48, Swedish Nuclear Fuel and Waste Management Company, Stockholm.

Crawford, J., Sidborn, M. (2009). Bedrock transport properties Laxemar. Site descriptive modelling SDM-Site Laxemar. SKB Report R-08-94, Swedish Nuclear Fuel and Waste Management Company, Stockholm.

Dzombak, D., Morel, F. (1990). Surface complexation modeling: hydrous ferric oxide. New York: Wiley, 393 pp.

Löfgren, M. (2001). Formation factor logging in igneous rock by electrical methods. Ph.D. Thesis, Department of Chemical Engineering, Royal Institute of Technology, Stockholm, Sweden.

Löfgren, M., Neretnieks, I. (2003). Formation factor logging by electrical methods: Comparison of formation factor logs obtained in situ and in the laboratory. Journal of Contaminant Hydrology, 61(1-4). pp. 107-115.

Löfgren, M., Vecernik, P., Havlova, V. (2009). Studying the influence of pore water electrical conductivity on the formation factor, as estimated based on electrical methods. SKB Report R-09-57, Swedish Nuclear Fuel and Waste Management Company, Stockholm.

NEA (2005). NEA Sorption Project, phase II: interpretation and prediction of radionuclide sorption onto substrates relevant for radioactive waste disposal using thermodynamic sorption models. Nuclear Energy Agency, Organisation for Economic Co-operation and Development (NEA-OECD),

Neogi, P., Ruckenstein, E. (1980). Transport phenomena in solids with bidispersed pores. AIChE Journal, 26(5), pp. 787-794.

Neretnieks, I. (1980). Diffusion in the rock matrix: An important factor in radionculide retardation? Journal of Geophysical Research, 85(8). pp. 4379-4397.

Ohlsson, Y. (2000). Studies of ionic diffusion in crystalline rock, Ph.D. Thesis, Department of Chemical Engineering, Royal Institute of Technology, Stockholm, Sweden.

Ruckenstein, E., Vaidyanathan, A., Youngquist, G. (1971). Sorption by solids with bidisperse pore structures. Chemical Engineering Science, 26(9), pp. 1305-1318.

Selnert, E., Byegård, J., Widestrand, H. (2008). Laboratory measurements within the site investigation programme for the transport properties of the rock. Final report. Forsmark site investigation. SKB P-07-139, Swedish Nuclear Fuel and Waste Management Company, Stockholm.

SKB (2008). Site description of Forsmark at completion of the site investigation phase. SDM-Site Forsmark. SKB Technical Report TR-08-05, Swedish Nuclear Fuel and Waste Management Company, Stockholm.

SKB (2010). Data report for the safety assessment SR-Site. SKB Technical Report TR-10-52, Swedish Nuclear Fuel and Waste Management Company, Stockholm.

SKB (2011). Long-term safety for the final repository for spent nuclear fuel at Forsmark. Main report of the SR-Site project. SKB Technical Report TR-11-01, Swedish Nuclear Fuel and Waste Management Company, Stockholm.

Steefel, C. (2009). CrunchFlow. Software for modeling multicomponent reactive flow and transport. User's manual. Berkeley, CA.: Lawrence Berkeley National Laboratory (LBNL).

Waber, H., Smellie, J. (2008). Characterisation of pore water in crystalline rocks. Applied Geochemistry, 23(7), pp. 1834-1861.

Widestrand, H., Byegård, J., Ohlsson, Y., Tullborg, E.-L. (2003). Strategy for the use of laboratory methods in the site investigations programme for the transport properties of the rock. SKB Report R-03-20, Swedish Nuclear Fuel and Waste Management Company, Stockholm.

Zazzi, Å., Jakobsson, A.-M., Wold, S. (2012). Ni(II) sorption on natural chlorite. Applied Geochemistry, 27(6), pp. 1189-1193.

SORPTION OF TC(VII) ON ÄSPÖ DIORITE (ÄD)

Yury Totskiy[1*], Horst Geckeis[1], Thorsten Schäfer[1,2]

[1] Institut für Nukleare Entsorgung (INE), Karlsruher Institut für Technologie (KIT) (DE)
[2] Institute of Geological Sciences, Department of Earth Sciences, Freie Universität Berlin, Berlin (DE)

* Corresponding author: yuri.totskiy@kit.edu

Abstract

Technetium-99 is one of the long-lived fission products in spent nuclear fuel with a half-life of $2.1 \cdot 10^5$ years that can be expected to be mobile under certain relevant repository conditions (Grambow, 2008). However, mobility and migration studies in natural host rock formations are scarce. The significance of Tc redox reactions with dissolved or solid species and the reactions mechanisms in different deep geological formations are still questions to be resolved. This work deals with sorption of Tc(VII) on crystalline rock materials from Äspö Hard Rock Laboratory (Sweden) to estimate potential mobility under natural conditions. It was found, that low concentrations of Tc(VII) added are almost completely retarded by un-oxidized granite after 1 month contact time, whereas considerably lower retention in the case of elevated concentration (10^{-5} M) or oxidized diorite material was found. Desorption was almost negligible and independent of contact time.

Introduction

The Äspö Hard Rock Laboratory (HRL) is an underground research laboratory in Sweden for *inter alia* in-situ studies of processes in crystalline formations concerning future deep geological disposal of spent nuclear fuel. Natural crystalline host rocks contain fractures, which are potential migration pathways once radionuclides have been escaped from the repository near-field. Transport processes of radionuclides strongly depend on the flow and geochemical conditions (pH, Eh, ionic strength) established. Furthermore, depending on the fracture structure (fracture filling material, fault gauge, hydrothermal alteration) fracture surfaces likely vary in mineralogical composition compared to the rock matrix and, besides advective transport, matrix diffusion may contribute significantly to radionuclide retention. Technetium mobility in natural systems strongly depends on the redox state. Both batch type sorption and column experiments on Hanford sediments (Um and Serne, 2005; Zachara et al., 2007b) have revealed that ^{99}Tc is highly mobile and shows virtually no retardation under fully oxidizing conditions and consequently can be used to trace tank waste migration through the vadose zone.

Early work by (Bondietti and Francis, 1979) on a variety of natural samples showed considerable retention (reduction of TcO_4^-) in accordance with Eh/pH conditions, which could be described by E_0= 0.738 – 0.0788pH + 0.0197 taken thermodynamic data for TcO_4^-/TcO_2.
Based on the variability in natural systems distribution coefficients and apparent diffusion coefficients found in the literature for natural systems vary by orders of magnitude, and are rarely documented together with the Eh/pH conditions studied. Furthermore, Tc redox kinetics strongly depend on the availability of reactive Fe(II) in host rock (surface complexed, precipitated, ion exchangeable) (Fredrickson et al., 2009; Heald et al., 2007; Jaisi et al., 2009; Peretyazhko et al., 2008a; Peretyazhko et al., 2008b; Zachara et al., 2007a).
In the case of Tc(VII), Äspö in-situ and laboratory migration studies (CHEMLAB-2) done prior to the CP-CROCK project (Kienzler et al., 2003; Kienzler et al., 2009) using Äspö derived natural groundwater revealed ~ 1% Tc recovery (after 254 days) of the injected quantity. In parallel, batch type studies derived K_a values of ~$2.1 \cdot 10^{-3}$ M for ^{99}Tc ($t_{contact}$= 14d) were found, whereas altered material showed significantly lower values. The data mentioned above show contact time/residence time dependent retardation and/or reduction kinetics. The present study is a first contribution to Tc(VII) sorption behaviour on natural unoxidized Äspö diorite (ÄD) in comparison to artificially oxidized samples before the accomplishment of column migration studies on samples of the same bore core.

Materials and methods

Äspö diorite

Crystalline rock material was delivered from CROCK drilling site of Äspö HRL (Sweden). Details of the sampling procedure and material characterization are presented in the S&T contribution of (Schäfer et al., 2012). The bore cores (#1.32 and #1.33) of Äspö diorite were chosen for investigations. They were transferred into the Ar glovebox, equipped with a circular saw, and cut into small discs (0.5 – 1 mm in width). The discs obtained were crushed by hammer and separated by sieves into several size fractions. For the sorption experiments documented here the 1-2 mm size fraction was chosen. Part of crushed diorite material was exposed to air for 1 week for surface oxidation to investigate the influence of sample preservation and preparation. Un-oxidized material was stored permanently under Ar atmosphere in the glovebox.

Synthetic groundwater simulant

For batch-type sorption experiments synthetic groundwater simulant (GWS) was prepared in accordance with the CP-CROCK drilling site outflow groundwater composition (sample CROCK-2) (see (Schäfer et al., 2012)). GWS has comparable composition to the groundwater KA3600-F-2 sampled in a 50L barrel at the CP-CROCK site (Heck and Schäfer, 2011). Batch-type sorption experiments were carried out in 20 mL liquid scintillation counter (LSC) vials (HDPE). For each condition two samples were prepared. Solid-liquid ratio was 2 g of diorite and 8 mL of GWS. For measurement of ^{99}Tc concentration in solutions 100µL aliquot was taken and analysed by LSC. To differentiate between colloidal phases and true solution species a phase

separation by ultracentrifugation (90,000 rpm for 1h) was performed. All sorption experiments are conducted at pH equal to 8.
In order to determine the cation exchangeable Fe(II) amount, a method proposed by (Heron et al., 1994) was applied using 10 mL 1M $CaCl_2$ (pH = 7) in contact with 2 g of granite for 24h. Afterwards, an aliquot was taken for Fe(II) quantification by the ferrozine technique (Violler et al., 2000). Redox potential was measured in the Ar glovebox using a Metrohm (Ag/AgCl, KCl (3M)) electrode and recording values every hour; the Eh values presented in this work are corrected for the standard hydrogen potential (SHE). Samples from sorption experiments were taken for desorption experiments after three month contact time. The supernatant was removed and new 8mL of liquid phase were added. Here, either Äspö groundwater or Grimsel groundwater (representing glacial melt water composition) were used.

Table 3: *Overview of the chemical compositions of the synthetic Äspö groundwater simulant (GWS), Äspö groundwater and Grimsel groundwater, respectively.*

	synth. Äspö GWS	**Synth. Äspö GWS after 122h contact time**	**Äspö GW (KA-3600-F-2)**	**Grimsel GW (MI-shear zone)**
pH	8.0		7.8	9.67
$[Mg^{2+}]$	103.64 ± 0.84 mg/L	104.6 mg/L	69.4 mg/L	12.6 µg/L
$[Ca^{2+}]$	1109.36 ± 94.46 mg/L	1134 mg/L	1135 mg/L	5.3 µg/L
$[K^{+}]$	19.346 ± 3.855 mg/L	21.56 mg/L	10.5 mg/L	
$[Li^{+}]$	2.526 ± 0.04 mg/L	2.50 mg/L	6.0 mg/L	
$[Fe^{2+,3+}]$	n.m.	n.m.	0.2 mg/L	< D.L.
$[Mn^{-}]$	2.32 ± 3.02µg/L	23.8 µg/L	0.338 mg/L	< D.L.
$[Sr^{2+}]$	19.678 ± 0.294 mg/L	20.14 mg/L	19.9 mg/L	182 µg/L
$[Cs^{+}]$	<D.L	< D.L		0.79 µg/L
$[La^{3+}]$	n.m.	n.m.		< D.L.
[U]	0.05 ± 0.01 µg/L	1.70 µg/L	0.105 µg/L	0.028 µg/L
[Th]	0.024 ± 0.005 µg/L	0.07 µg/L	0.001 µg/L	0.00136 µg/L
$[Al^{3+}]$	182.75 ± 56.29 µg/L	439.6 µg/L	13.3 µg/L	42.9 µg/L
$[Na^{+}]$	1929.25 ± 28.58 mg/L	1905 mg/L	1894 mg/L	14.7 mg/L
$[Cl^{-}]$	4749.408 ± 145.046 mg/L	4895.10 mg/L	4999 mg/L	6.7 mg/L
[Si]	n.m.	n.m.	4.7 mg/L	5.6 mg/L
$[SO_4^{2-}]$	408.682 ± 4.967 mg/L	411.88 mg/L	394.4 mg/L	5.8 mg/L
$[F^{-}]$	1.974 ± 0.093 mg/L	1.98 mg/L	1.41 mg/L	6.3 mg/L
$[Br^{-}]$	21.17 ± 0.37 mg/L	20.96 mg/L	23.2 mg/L	
$[NO_3^{-}]$	n.m.	n.m.	n.m.	< D.L.
$[HCO_3]$	n.m.	n.m.	n.m.	3.0 mg/L
[B]	306.54 ± 212.54 µg/L	146.1 µg/L	885 µg/L	

Figure 1: *Photos of the Äspö diorite (ÄD) cores #1.32 (left) and #1.33 (right) directly taken after drilling subsequently used for preparation of crushed material.*

Results and discussions

Eh measurements

Redox measurements were carried out after about 2 weeks and 1 month contact time in the sorption experiments. Every sample was measured over a period of one day in an open vial in the Ar glovebox (< 1ppm O_2) to obtain the Eh evolution. A typical time dependent Eh evolution is shown in Figure 2. The initial drop of the Eh is interpreted as the influence/readout of the sample, whereas the continuous increase in the later period is explained to be a result of oxidation due to traces of oxygen in the Ar glovebox (< 1ppm O_2) that seems to be enough to compensate the redox capacity of the sample over 24 hours.

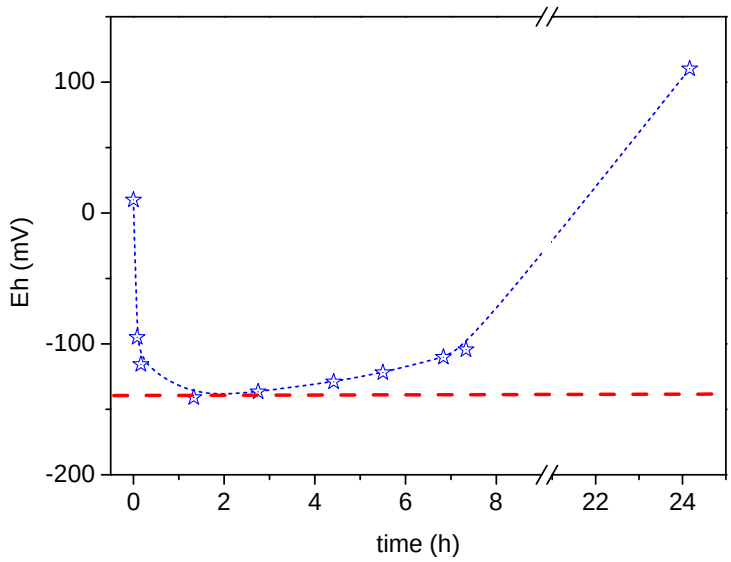

Figure 2: *Typical Eh evolution for synthetic Äspö groundwater simulant with un-oxidized diorite [Tc] = 10^{-10} mol/L.*

Figure 3 shows the Eh measurements for synthetic groundwater in contact with different ^{99}Tc concentrations equilibrated with oxidized and un-oxidized ÄD. For oxidized ÄD material the redox potential as a function of Tc concentration does not change significantly and is within the range of +250 to +300 mV. However, for un-oxidized ÄD

material two trends can be observed: (a) for low Tc concentration (up to 10^{-8} M) the Eh value decreases with time from 14 days to one month and (b) for the highest Tc concentration used (10^{-5} M) the Eh value reaches after one month the Eh range of oxidized ÄD material. Our current explanation for the Eh trend observed at 10^{-5}M is that this Tc concentration is already sufficient to exceed the redox capacity of the contacted diorite material with the solid to liquid ratio 2g/8mL used. Furthermore, the established Eh values for the lower Tc concentrations makes Tc(VII) reduction thermodynamically feasible.

Sorption

Sorption kinetics of different Tc concentrations on oxidized and un-oxidized ÄD are given in Figure 4. Here the term "sorption" implies total amount of Tc associated with the solid phase (crushed fraction of ÄD with diameter of particles 1-2 mm) after ultracentrifugation. It can be sorption/surface complexation itself, but also a precipitation of $TcO_2 \cdot xH_2O$ due to Tc(VII) reduction by e.g. Fe(II) species is a potential process. Especially in case of the highest Tc concentration this process might be feasible, as the Tc(IV) solubility is significantly exceeded.
The formation of colloidal Tc phases (eigencolloids) by comparison of ultracentrifuged to non-centrifuged samples was not detectable within the uncertainty limits (± 5-10%). Either these colloidal phases are formed or are not stable under the Äspö GWS conditions chosen (ionic strength ~0.2 M, pH 8).

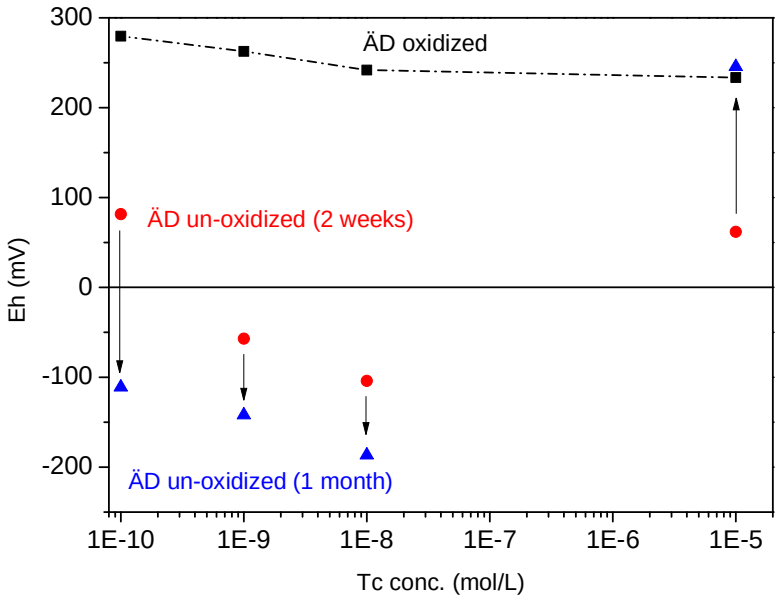

Figure 3: *Eh values for un-oxidized and oxidized ÄD material with synthetic groundwater as a function of Tc concentration and as a function of contact time (2 weeks and one month).*

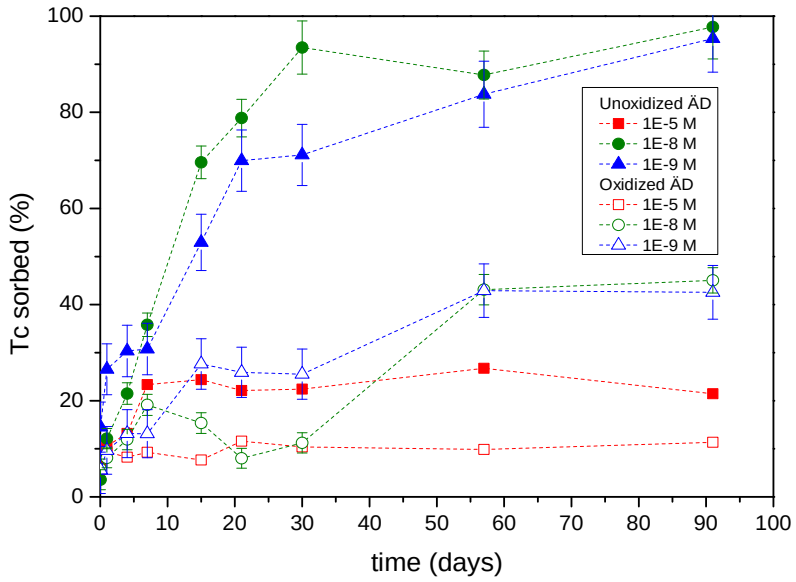

Figure 4: *Tc sorption kinetics of different concentrations on oxidized and un-oxidized ÄD.*

From the Tc sorption kinetic experiments it is evident, that sorption on un-oxidized material is much higher compared to the artificially oxidized samples. For the 10^{-8}M and 10^{-9}M Tc on un-oxidized material plateau values close to 100% sorption are obtained (after 90 days), whereas during the same observation period on oxidized ÄD only approx. ~40% are sorbed, showing the tendency to reach equilibrium within this range. Based on the Eh/pH conditions established Tc(VII) reduction on the un-oxidized ÄD crushed material or in solution seems to be feasible from a thermodynamic point of view.

In order to estimate the amount of the ferrous iron buffer available in the oxidized and un-oxidized ÄD material we used here the quantification of the ion exchangeable Fe(II) fraction. Furthermore, data on oxidized and non-oxidized ÄD material by XRF are given in the S&T by (Schäfer et al., 2012), showing that the overall Fe(II) redox buffer is drastically reduced for the oxidized samples. The ion-exchangeable Fe(II) fraction (Heron et al., 1994) for the oxidized ÄD was quantified with approx. 1-3 µg/g, whereas for the un-oxidized samples higher values around 4-6 µg/g are obtained. The rather high uncertainty in the measurements is attributed to the natural heterogeneity of the ÄD material. It has to be mentioned here, that ultracentrifugation (90,000 rpm) of the supernatant after 1M $CaCl_2$ extraction before UV/VIS measurement for Fe(II) quantification using the ferrozine method leads to values around the detection limit (0.1-0.5 µg/g) for both types of diorite samples. This can be explained by an initial exchange of Fe(II) from the ÄD surface with calcium cations and subsequent Fe(II) oxidation in the solution to form colloidal ferric iron oxyhydroxides, that was separated by centrifugation. However, the non-centrifugated results are reasonable and further studies are required to understand the oxidation step.

Again, the samples with Tc concentrations of 10^{-5} mol/L are outlying this trend and show a sorption plateau already reached after seven days around 20-25% for the un-oxidized samples and ~10% for the oxidized sample.

Taking the quantified ion-exchangeable ferrous iron buffer in the sorption samples to be from $3.6 \cdot 10^{-8}$ mol/vial (oxidized ÄD) to $2.1 \cdot 10^{-7}$ mol/vial (un-oxidized ÄD) with respect to the total amount of Tc contacted, $8 \cdot 10^{-7}$ mol/vial (10^{-5} mol/L Tc), $8 \cdot 10^{-11}$ mol/vial (10^{-8} mol/L Tc) and $8 \cdot 10^{-12}$ mol/vial (10^{-9} mol/L Tc), the sorption kinetics observed can be expected and underpin the need of well preserved un-oxidized rock material for sorption studies on redox sensitive radionuclides to estimate reliably the in-situ retention.

Desorption

First Tc desorption experiments, which covered one month of equilibration time on initially three months contacted sorption samples, show insignificant desorption in all studied cases. Both Äspö and Grimsel groundwater could desorb up to 6% of total Tc, regardless of oxidized or un-oxidized material used.

Conclusions and Future work

It was found that during the equilibration process of Tc(VII) spiked synthetic groundwater simulant with un-oxidized Äspö diorite the Eh is decreasing with time. This means the establishment of conditions favouring the Tc(VII) reduction and potential Tc(IV) precipitation in form of $TcO_2 \cdot xH_2O$. Apparently, the Tc(VII) concentration is directly influencing the sorbed Tc amount on un-oxidized and oxidized material, which can be correlated with the ion-exchangeable Fe(II) buffer available. The amount of ion-exchangeable Fe(II) on the Äspö diorite surface depends on sample preservation, and for un-oxidized samples it was found to be about 4-6 µg/g (1-2mm fraction). Future studies for more precise measurements on the use of ^{59}Fe traces to investigate Fe(II) isotopic exchange are currently started. Future studies will also focus on surface analytics (e.g. XPS) to improve our process understanding. After 1 month sorption of Tc(VII) traces on un-oxidized ÄD is close to 100%. Desorption of Tc from diorite is insignificant for all investigated cases (oxidized and un-oxidized diorite in contact with Äspö or Grimsel groundwater).
Activities within the next project year will focus also on Tc(VII) column migration studies and on sorption experiments with Tc(IV).
These data will be compared with Tc sorption data on reference materials (magnetite) and granites from Nizhnekansk granitoid massif – prospective Russian disposal site for nuclear waste.

Acknowledgement

The research leading to these results has received funding from the European Union's European Atomic Energy Community's (EURATOM) Seventh Framework Programme FP7/2007-2011 under grant agreement n° 269658 (CROCK project) and the Federal Ministry of Economics and Technology (BMWi) collaborative project VESPA (Behaviour of long-lived fission and activation products in the near field of a repository and possible retention mechanisms) under contract n° 02 E 10800.

References

Bondietti, E.A., Francis, C.W. (1979). Geologic Migration Potentials of Technetium^{99} and Neptunium^{237}. Science, 203(4387): 1337-1340.

Fredrickson, J.K., Zachara, J.M., Plymale, A.E., Heald, S.M., McKinley, J.P., Kennedy, D.W., Liu, C., Nachimuthu, P. (2009). Oxidative dissolution potential of biogenic and ablogenic TcO2 in subsurface sediments. Geochimica Et Cosmochimica Acta, 73(8): 2299-2313.

Grambow, B. (2008). Mobile fission and activation products in nuclear waste disposal. Journal of Contaminant Hydrology, 102(3-4): 180-186.

Heald, S.M., Zachara, J.M., Byong-Hung, J., McKinley, J.P., Ravi, K., Dean, M. (2007). XAFS study of the chemical and structural states of technetium in Fe(III) oxide Co-precipitates. X-Ray Absorption Fine Structure-XAFS13, 882: 173-175.

Heck, S., Schäfer, T. (2011). Short Note: CP CROCK groundwater sample characterization

Heron, G., Crouzet, C., Bourg, A.C.M., Christensen, T.H. (1994). Speciation of Fe(II) and Fe(III) in contaminated aquifer sediments using chemical extraction techniques. Environ. Sci. Technol., 28: 1698-1705.

Jaisi, D.P., Dong, H., Plymale, A.E., Fredrickson, J.K., Zachara, J.M., Heald, S., Liu, C. (2009). Reduction and long-term immobilization of technetium by Fe(II) associated with clay mineral nontronite. Chemical Geology, 264(1-4): 127-138.

Kienzler, B., Vejmelka, P., Römer, J., Fanghänel, E., Jansson, M., Eriksen, T.E., Wikberg, P. (2003). Swedish-German actinide migration experiment at ASPO hard rock laboratory. Journal of Contaminant Hydrology, 61(1-4): 219-233.

Kienzler, B., Vejmelka, P., Romer, J., Schild, D., Jansson, M. (2009). Actinide Migration in Fractures of Granite Host Rock: Laboratory and in Situ Investigations. Nuclear Technology, 165(2): 223-240.

Peretyazhko, T., Zachara, J.M., Heald, S.M., Jeon, B.H., Kukkadapu, R.K., Liu, C., Moore, D., Resch, C.T. (2008a). Heterogeneous reduction of Tc(VII) by Fe(II) at the solid-water interface. Geochimica Et Cosmochimica Acta, 72(6): 1521-1539.

Peretyazhko, T., Zachara, J.M., Heald, S.M., Kukkadapu, R.K., Liu, C., Plymale, A.E., Resch, C.T. (2008b). Reduction of Tc(VII) by Fe(II) sorbed on Al (hydr)oxides. Environmental Science & Technology, 42(15): 5499-5506.

Schäfer, T., Stage, E., Büchner, S., Huber, F., Drake, H. (2012). Characterization of new crystalline material for investigations within CP CROCK 7th EC FP - CROCK CP. 1st Workshop Proceedings.

Um, W., Serne, R.J. (2005). Sorption and transport behavior of radionuclides in the proposed low-level radioactive waste disposal facility at the Hanford site, Washington. Radiochimica Acta, 93(1): 57-63.

Violler, E., Inglett, P.W., Hunter, K., Roychoudhury, A.N., Cappellen, P.V. (2000). The ferrozine method revisited: Fe(II)/Fe(III) determination in natural waters. Applied Geochem., 15: 785-790.

Zachara, J.M., Heald, S.M., Jeon, B.H., Kukkadapu, R.K., Liu, C., McKinley, J.P:, Dohnalkova, A.C., Moore, D.A. (2007a). Reduction of pertechnetate [Tc(VII)] by aqueous Fe(II) and the nature of solid phase redox products. Geochimica Et Cosmochimica Acta, 71(9): 2137-2157.

Zachara, J.M., Serne, J., Freshley, M., Mann, F., Anderson, F., Wood, M., Jones, T., Myers, D. (2007b). Geochemical processes controlling migration of tank wastes in Hanford's vadose zone. Vadose Zone Journal, 6(4): 985-1003.

RADIONUCLIDE RETENTION IN FRACTURED MEDIA: COPING WITH UNCERTAINTY IN PA STUDIES

Paolo Trinchero[1*], Luis Manuel de Vries[1], Àngels Piqué[1], Lara Duro[1], Jorge Molinero[1],

[1] Amphos 21, Passeig Garcia i Fària 49-51, 08019 Barcelona (ES)

* Corresponding author: paolo.trinchero@amphos21.com

Abstract

The evaluation of radionuclide retention processes in fractured media requires a proper characterisation of the hydro-geochemical processes occurring in complex geological systems. This characterisation is often infeasible in real applications where the size of the medium and the high heterogeneity of its textural structure make a detailed characterisation of its geochemical and hydraulic properties impossible. Given this intrinsic uncertainty, we present a numerical framework where the main parameters controlling radionuclide retention (e.g. the amount of clay minerals, the presence of iron oxides, etc.) are treated as random variables. Based on expert judgment combined with input from field data, a probability density function (PDF) can be associated to each parameter and sampled using a Monte Carlo approach. The numerical tool has been used to simulate a generic fracture system where the main retention process is radionuclide sorption onto Illite. The analysis of the ensemble of values of repository derived thorium concentration show a high variability stemming from the uncertainty in the mineralogical characterization. A key point of the methodology lies in its capability of treating results in a probabilistic fashion. This allows for dealing with threshold values (e.g. $P[C_{radio}<C^*_{radio}]$) quantitatively.

Introduction

Predictions of hydro-geochemical processes are usually characterised by a high degree of uncertainty. The sources of uncertainty are fundamentally epistemic and can be attributed to the incomplete knowledge of the phenomena being modelled (e.g. incomplete knowledge of the hydraulic properties distribution, the actual mineralogical composition of the fractures, etc.). This uncertainty is particularly evident in "typical" fractured systems tailored to host deep geological repositories. The accurate characterization of these complex geological media is physically impossible.
There are a number of methods that aim at quantifying the uncertainty of model predictions using stochastic techniques. Among these techniques, the Monte Carlo simulation is certainly the most used. A key point of these approaches lies in the capability to integrate data and expert judgment while explicitly acknowledging uncertainty.

Automatic Uncertainty Assessment in the Treatment of sorption

Great efforts have been devoted in the last two decades to characterize sorption processes and to simulate related reactive transport problems of radionuclide migration through fractured systems.
Most of these models rely on a "classical" deterministic description of the problem while the analysis of the uncertainty is left to few sensitivity runs with minimum, maximum and average values for specific parameters. In other works, the uncertainty analysis is carried out using more robust approaches (e.g. Monte Carlo simulations) but chemistry is usually solved in a simplified fashion (e.g. using Kd based simulations).
Here, we propose an alternative approach where a complex chemical system is solved explicitly and uncertainty is evaluated through Monte Carlo simulations. This is done using a numerical tool, denoted as MCPhreeqc (MCPhreeqc, 2011), which provides a way to perform Monte-Carlo simulations using the well-known geochemical simulator Phreeqc (Parkhurst and Appelo, 1999). First, the geochemical model has to be set using the standard Phreeqc input file. This model can include a wide number of processes such as aqueous speciation reactions, redox reactions and surface complexation and can mimic either a zero-dimensional system or a 1D transport problem (the application presented here refers to a zero-dimensional system). Second, those parameters that have to be treated as random variables must be marked in the input file and based on available data or on expert judgment, a probability distribution is chosen for each of them. The setup for the stochastic analysis is entered through a user-friendly graphical interface. Combinations of random values are generated according to these distributions. Then, the framework takes care of running the geochemical speciation code Phreeqc many times for each combination of parameters in parallel and generating informative parameter plots. The combined output of these runs provides information about uncertainty for specific output variables resulting from the uncertainty of the input parameters.

Application to a generic case study

Sorption onto mineral phases can be a main retention process for some radionuclides, such as uranium, thorium, caesium and nickel, especially if the concentration in solution is not high enough to precipitate pure phases. Some elements have more affinity for oxi-hydroxides, while others are more retained onto clay minerals. Clays can be present in bedrock fractures, however, depending on the available data, it can be difficult to determine a representative amount of clays (and for instance of sorption sites). Since the amount of available sorption sites will be a major parameter controlling the amount of some radionuclides in solution, Monte Carlo simulations can help to constrain the range of dissolved concentration of radionuclides of interest, by introducing a probability function of the amount of clay in the system.
As an example, a uniform distribution was used to simulate the amount of illite (from 1 to 35 wt%) in the medium, and the mineral surface was equilibrated with a deep groundwater to simulate bedrock fracture conditions, then an influx of repository-derived radionuclides was simulated.
Ten thousand Monte-Carlo Simulations were carried out to assess the influence of the mineralogical uncertainty on the aqueous radionuclide concentration. The resulting pdf of the repository derived thorium concentration is shown in Figure 1 (concentration in mol/L). From the Figure one can see that using stochastic tools provides the modeller

with more information about the behaviour of the model. For instance, the uncertainty in the amount of illite, results in a large range of thorium concentrations (between $4.4 \cdot 10^{-14}$ and $1.5 \cdot 10^{-12}$ mol/L). Nevertheless; the probability distribution function (PDF) demonstrates that the probability of a thorium concentration higher than $2 \cdot 10^{-13}$ mol/l is very low.

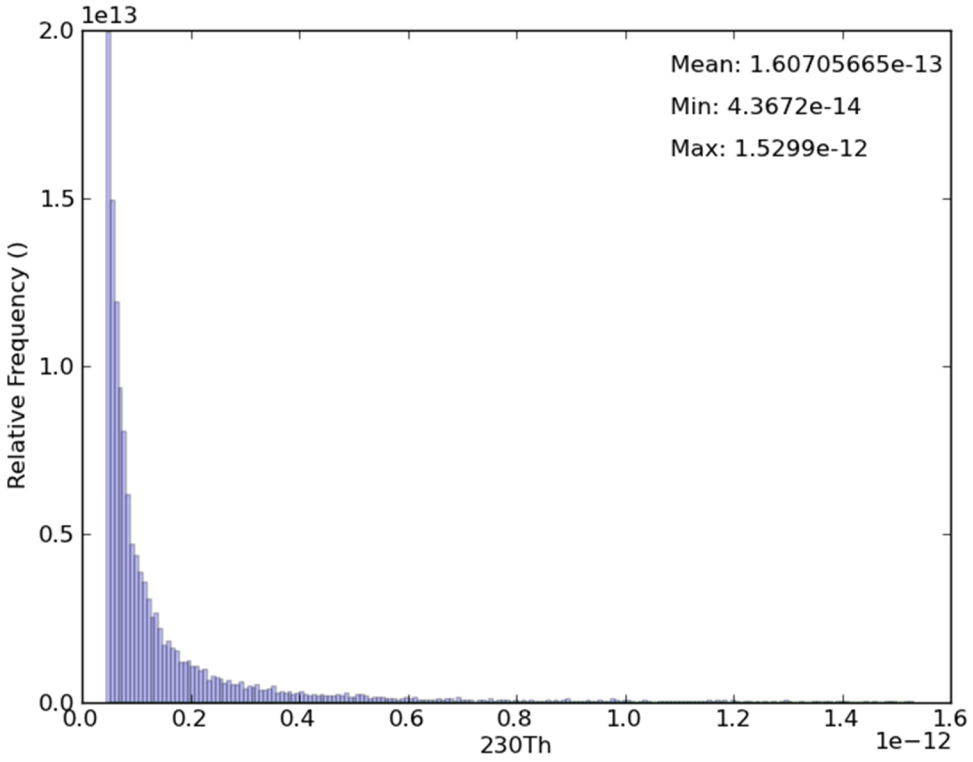

Figure 1: *Probability density function of the dissolved thorium concentration (in mol/L).*

Conclusions and Future work

Quantifying uncertainty in the prediction of radionuclide retention processes appears mandatory in PA applications since these mechanisms are highly dependent on some poorly known or unknown parameters, which moreover can describe an extended range of values. This is the case, for example, of the amount of illite present in the fracture coating. Consequently, we focused our work on the assessment of the effects of uncertainty relative to the amount of illite in a synthetic geological medium by running several Monte Carlo simulations. The geochemical model implemented in the Monte Carlo simulations reproduces the influx of repository-derived radionuclides.
The results show that the classical "deterministic" approach, which relies on parameter sensitivity analysis, is without doubt an important instrument in the understanding of geochemical models. In this article, we argue that adding a stochastic perspective will provide modellers and decision makers with important, detailed information regarding the properties of the uncertainty in the model. The approach is suitable for different types of models and, when automated, takes little effort to implement.

Acknowledgement

The research leading to these results has received funding from the European Union's European Atomic Energy Community's (EURATOM) Seventh Framework Programme FP7/2007-2011 under grant agreement N° 269658 (CROCK project)

References

MCPhreeqc (2011). A tool for PHREEQC Monte-Carlo simulations. Amphos 21. http://www.Amphos21.com/software

Parkhurst, D.L, Appelo, C.A.J. (1999). User’s guide to PHREEQC (version 2) - A computer program for speciation, batch-reaction, one-dimensional transport and inverse geochemical calculations. U.S. Geological Survey Water Resources investigations report 99-4259.

ANALYSIS OF THE CESIUM SORPTION BEHAVIOUR ON BIOTITES OF DIFFERENT ORIGIN

Tiziana Missana[1*], Miguel García-Gutiérrez[1]

[1]CIEMAT, Departamento de Medioambiente, Av. da Complutense 40, 28040 MADRID (ES)

* Corresponding author: tiziana.missana@ciemat.es

Abstract

An experimental and modelling analysis of the sorption of caesium onto biotites from different sources was carried out. Sorption behaviour of caesium was similar in all the solids analysed and it could be satisfactorily modelled according to a three-site ionic exchange simplified model.

Introduction

Crystalline hard rocks present suitable properties to host a Deep Geological Repository (DGR) of high-level radioactive waste. Crystalline hard rock is composed of a variety of different minerals (mainly quartz, feldspars and micas and other accessory minerals), which contribute in different ways to radionuclide retention. The understanding of the sorption behaviour of radionuclides on the main minerals composing the rock can be very useful for the mechanistic understanding of retention processes in such a heterogeneous system. Therefore, within the frame of the CROCK project, CIEMAT is analysing in detail the sorption of caesium on different minerals (biotite, muscovite, K-feldspar, quartz).
Micas, and in particular biotite, are especially effective sorbents for caesium and they play an important role on the overall retention of this radionuclide in granite. Thus, it is important to analyse caesium sorption behaviour on this mineral and try to interpret the data using simple sorption models. This is a first step for the description of caesium retention in the rock.
The main objective of this paper is to describe the caesium sorption behaviour onto different biotites and the preliminary modelling of sorption data.

Experimental

Materials

All the reagents were of analytical grade and they were used without further purification.. The radionuclide used in this study was ^{137}Cs (as CsCl in 0.1 HCl). The half-life of ^{137}Cs is 30.2 years. The activity of caesium in solution was measured by γ-counting with a NaI detector (Packard Autogamma COBRA 2).

Five different biotites were used for the experiments. The first one was the Geostandard biotite (*Bio_GEO*), obtained from "*Centre National de la Recherche Scientifique"* CNRS (France). Three biotites were obtained from the spanish "ElBerrocal" granite (*Bio_2C, Bio_3H and Bio_3F*); the last biotite comes from the spanish "Ratones" granite (*Bio_Rat*). The size fraction and the BET surface area of these materials are summarised in Table 1. More details on the solids, their characterisation and chemical composition can be found in Missana and García-Gutiérrez (2012).

Table 1: *Size fraction and BET area of the biotites used in the experiments*

Sample	Size fraction	BET (m^2/g)
Bio_Geo	<63 μm	Not determined
Bio_2C	63μm<x<125μm	4.81 m^2/g
Bio_3H	63μm<x<125μm	3.26 m^2/g
Bio_3F	<63 μm	5.55 m^2/g
Bio_Rat	<1 mm	1.15 m^2/g

Table 2: *Chemical composition of the aqueous solutions used in the experiments*

Element	LSW INIT.	LSW after 1 month contact with BIO-: GEO	3H	3F	2C	RAT	HSW INIT
Na^+ (mg/L)	8.3	9.1	8.8	8.8	8.8	9.0	1800
Ca^{2+} (mg/L)	7.0	6.0	8.4	7.0	9.0	6.0	1000
Mg^{2+} (mg/L)	<0.03	1.5	1.7	2.5	2.2	2.0	0.1
K^+ (mg/L)	<0.03	14.0	5.7	3.5	3.5	3.3	<0.1
Cl^- (mg/L)	28.0	30.0	30.0	30.0	30.0	29.0	4600
SO_4^{2-} (mg/L)	<0.1	0.4	1.4	1.6	1.6	1.8	0.4
F^- (mg/L)	<0.1	1.5	1.9	2.2	2.2	<0.1	<0.1
Al (mg/L)	<0.03	0.12	0.06	0.07	0.05	<0.03	<0.03
Fe (mg/L)	<0.03	<0.03	<0.03	<0.03	<0.03	<0.03	<0.03
Cs (mg/L)	<0.02	<0.02	<0.02	<0.02	<0.02	<0.02	<0.02
Si (mg/L)	0.7	4.5	4.1	2.7	2.6	1.9	<0.3
Alk (meq/L)	<0.05	0.30	0.28	0.22	0.27	0.15	<0.1

In the experiments, two different simplified aqueous phases were used, simulating two different granitic groundwaters: a *low* and a *high* saline water (LSW and HSW, respectively). The main compositions of these waters are summarised in Table 2. In

order to evaluate the solid-rock interactions, the LSW's chemical composition after 1 month of contact with the solids was analysed. The chemical composition obtained are also indicated in Table 2.

Before the addition of the radionuclide, the solid and the water were equilibrated at least 1 day.

Sorption Experiment

Sorption experiments were carried out under aerobic conditions and at room temperature. First of all, kinetic experiments were carried out at two different caesium concentrations ([Cs]=5.4E-09 M and [Cs]=9.9E-06 M); then the dependence on pH was evaluated, carrying out sorption edges changing the pH from approximately pH 6 to 10, at the lowest Cs concentration. Finally, sorption isotherms at pH 7 were carried out. The contact time for sorption edges and isotherms was 14 days.
Ten mL of the initial aqueous solution were introduced in polyethylene centrifuge tubes and 0.1 g of biotite was added. After the water/solid equilibration, the tracer was added and the pH adjusted, if necessary. The tubes were maintained under continuous stirring during the selected contact time. They were later centrifuged (26362 x g, 30 min). After the solid separation, three aliquots of the supernatant from each tube were extracted for the analysis of the final activity. The rest of the solution was used to check the pH.
The distribution coefficients were calculated using the formula:

$$K_d = \frac{Cs_{ADS}}{Cs_{FIN}} \cdot \frac{V}{m} \quad (1)$$

where Cs_{ADS} is the adsorbed cesium, C_{FIN} the final concentration of Cs in the liquid phase, V the volume of the liquid and m the mass of the solid.

Modelling

Caesium sorption onto micas is expected to occur mainly by ionic exchange reactions: The ionic exchange reactions between a cation B, with charge zB, which exists in the aqueous phase, and a cation A, with charge zA, at the clay surface (≡X) is defined by:

$$z_B A \equiv X + z_A B \Leftrightarrow z_A B \equiv X + z_B A \quad (2)$$

This reaction can be described in terms of selectivity coefficients (Gaines and Thomas, 1953).
For sake of simplicity, the first modelling was carried out considering the biotite as a simple exchanger in which monovalent exchange with caesium occurs:

$$M \equiv X + Cs \Leftrightarrow Cs \equiv X + M^+ \quad (3)$$

The modelling calculations were done with the CHESS v 2.4 code (van der Lee and De Windt, 1999), and the fits of the experimental curves were obtained with a trial and error procedure.

More details on the sorption experiments and the modelling approach can be found in Missana and García-Gutiérrez (2012).

Results and discussion

Kinetic experiments were carried out at two different caesium concentrations (high and low) during time of 30 days at initial pH values of 7-8. Figure 1 shows the results of these kinetic experiments for each analysed biotite at high and low concentrations.First of all, it is clear that sorption equilibrium is reached quite rapidly: in a few hours in the case of the highest cesium concentration and in a few days in the case of the lowest caesium concentration. Furthermore the results showed that caesium sorption is not linear, with the existence of a low and high affinity sites.

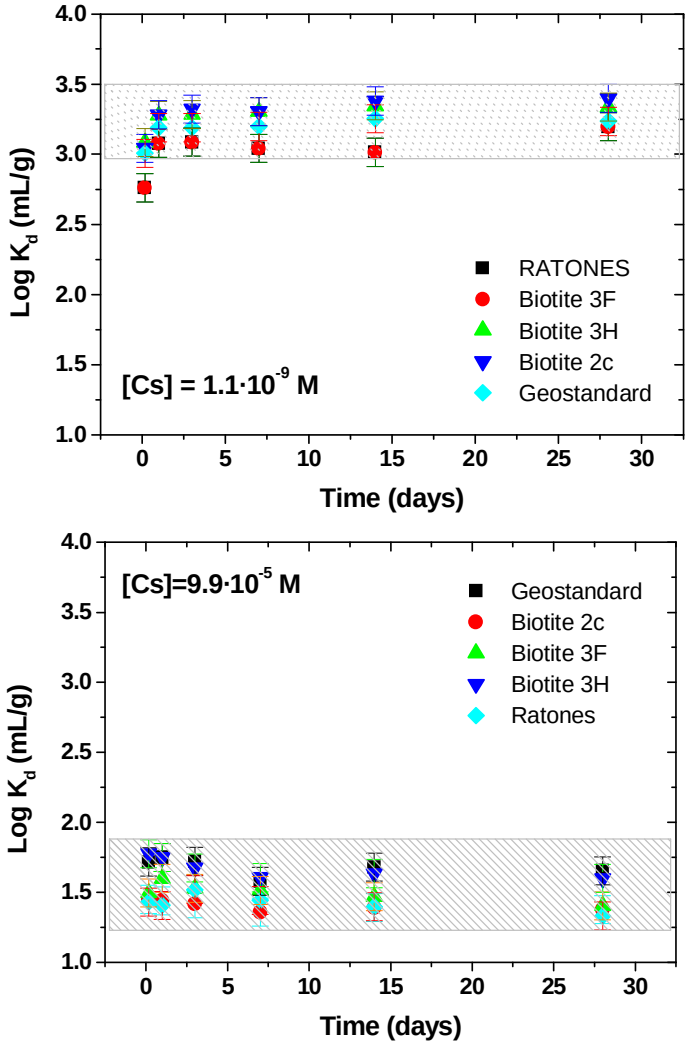

Figure 1: *Sorption kinetics of cesium for the analysed biotites in low saline waters (LSW) at two different caesium concentrations. Up: [Cs] = 1E-09 M and down [Cs] = 1E-06 M*

All the biotites shows relatively similar Kd values at both concentrations: the variability of sorption coefficient can be constrained to the range of logKd 3.0 - 3.5 at the "low" cesium concentration and logKd 1.2-1.8 at the "high" cesium concentration.
Figure 2 shows the sorption edge carried out in two different biotites (*Bio_RAT* and *Bio_3F*) at the lowest Cs concentration.

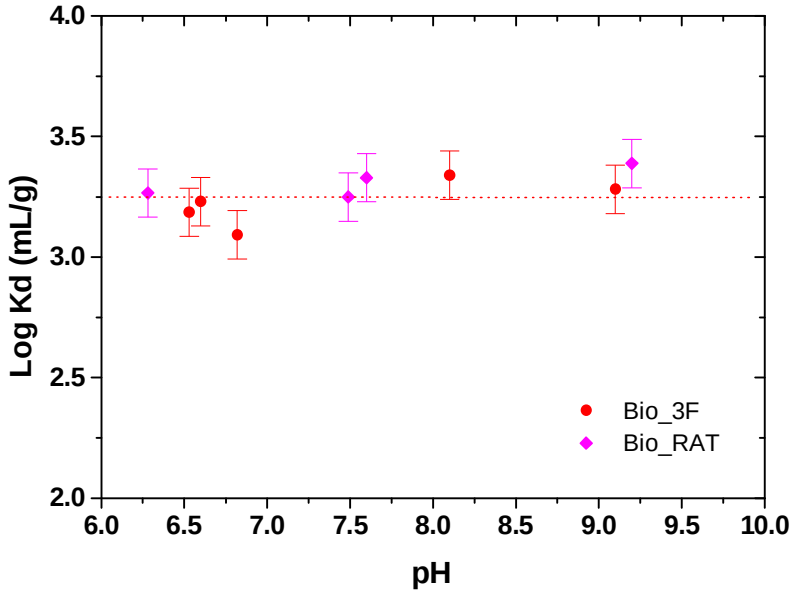

Figure 2: *Sorption edges of cesium for two biotites in LSW. [Cs] = 1E-09 M.*

A significant dependence on pH, as expected when ionic exchange mechanism is predominant in retention, was not observed.
To understand better the non-linear behaviour observed in Figure 1, sorption isotherms were also carried out, at pH of 7, with a range of caesium concentrations from approximately 1E-09 to 1E-02 M.
Figure 3 shows the results of the sorption isotherms. Figure 3 (top) shows the data represented as the logarithm of the distribution coefficient (LogKd) as a function of the caesium in solution at the equilibrium and Figure 3 (bottom) shows the same data expressed as the logarithm of cesium adsorbed versus the cesium concentration in solution at the equilibrium.
The behaviour observed is very similar in all the analysed biotites, both qualitatively and quantitatively. In all the cases, caesium sorption showed a non-linear behaviour in agreement with the existence of more than one sorption site for caesium in biotite.
At very low concentration, the slope of the isotherm is 1 (Figure 3, bottom), indicating the existence of a low capacity but high affinity sorption site. Then sorption isotherms show a region with a slope lower than 1 that is in agreement with the possibility of the existence of two additional sorption sites. Thus, a three-site ionic exchange model was used for modelling the experimental data (in some cases, however, the use of a two-site model could be also quite satisfactory in a wide range of caesium concentrations). A preliminary data analysis showed that the quantity of potassium present in the aqueous solution at the equilibrium (Table 2) could significantly affect results. Therefore, the competitive effect of potassium in caesium adsorption was explicitely taken into account, considering the reaction defined in (3) and the concentration of potassium in

the solutions at the equilibrium experimentally measured (Missana and García-Gutiérrez, 2012).

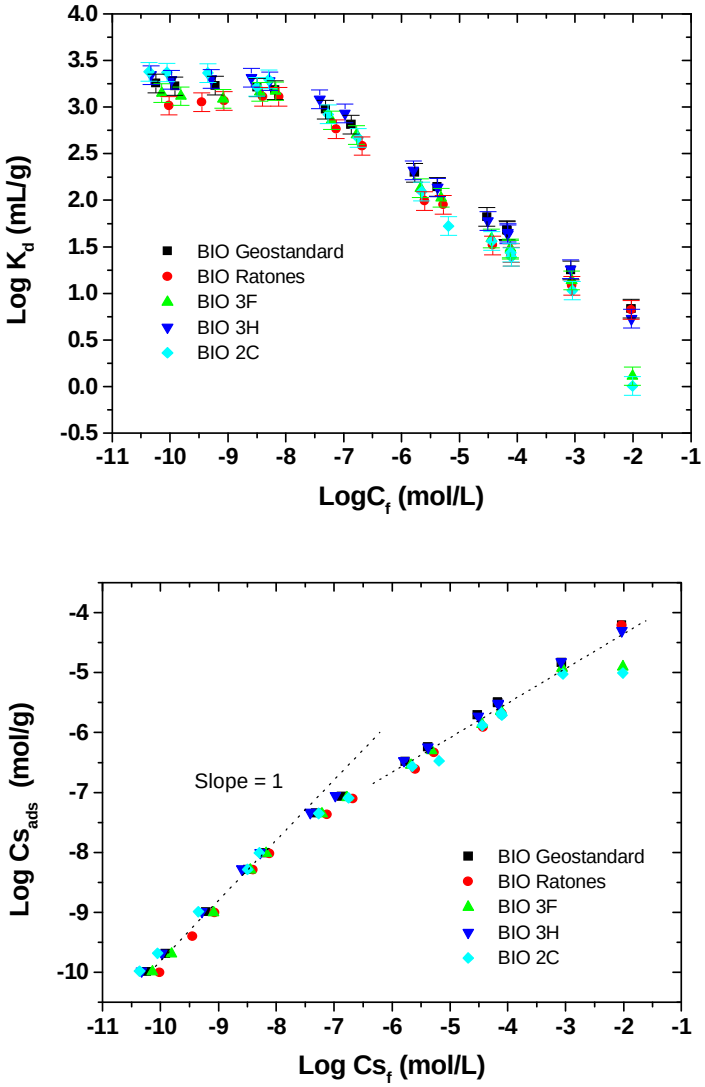

Figure 3: *Sorption isotherms of cesium for the analysed biotites in LSW. pH =7.*

Figure 4 shows an example of result of the modelling of sorption data obtained from the *Bio_3F* biotite. In the top diagram of Figure 4, the contribution to sorption of the three different sorption sites is indicated. Table 3 includes the values of parameters used in the modelling, (density of sorption sites and the selectivity coefficients for Cs and K) with respect to a monovalent ion M^+ (Na), as expressed in equation (3) for each sorption site.

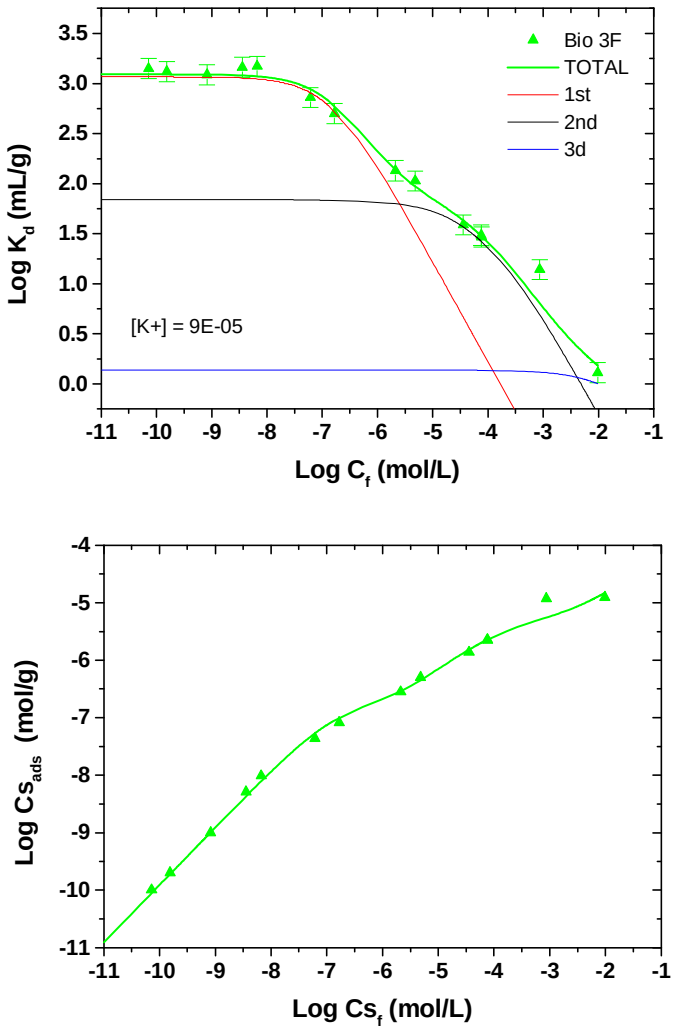

Figure 4: *Example of the modelling carried out. Sorption isotherm obtained for the BIO_3F biotite in LSW.*

Table 3: *Parameters used in the modelling of the sorption isotherms*

	Density (μeq/m^2)	LogK (Cs^+)	LogK (K^+)
Site 1	0.03	11.4	9
Site 2	0.90	4.7	5
Site 3	60	-2.9	-2.2

In order to verify the validity of the assumptions made for the modelling, another sorption isotherm was carried out in a different aqueous solution (high saline water, HSW, Table 2).

Summary of results are plotted in Figure 5, where the isotherms obtained with the *Bio_3F* biotite in the two different waters are compared. The modelling of the second

isotherm, with the parameters in Table 3 (exactly the same than those used for the LSW), was also very good, as can be observed in Figure 5.

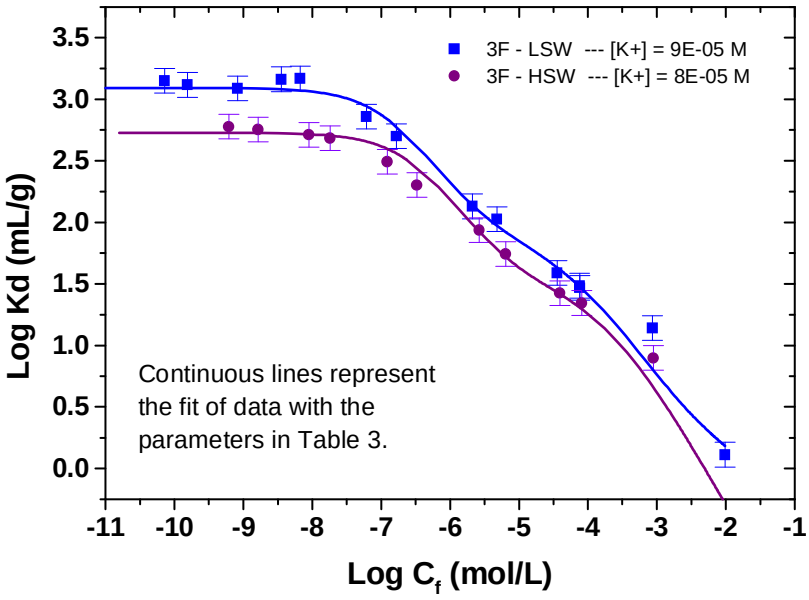

Figure 5: *Isotherms of Cesium for the BIO_3F biotite in low saline (LSW) and high saline (HSW) waters.*

Furthermore, all the data plotted in Figure 3 could be satisfactorily modelled with the simple model proposed.

Conclusions and Future work

The sorption of caesium onto five different biotite samples was analysed. Sorption was very similar in all samples both qualitatively and quantitatively. In similar chemical conditions, the differences in Kd measured from one biotite to another was within one order of magnitude or less. Caesium sorption in biotite showed a non-linear behaviour in agreement with the existence of more than one sorption site.
In order to fit the sorption data, a simplified model was proposed which was quite effective in reproducing all the sorption isotherms and in particular, the sorption as a function of caesium concentration, and the content of sodium and potassium as competing ions.
A similar work is being carried out with other minerals composing granite (muscovite, K-feldspar, quartz) to establish the basis for attempting a bottom-up modelling approach for the modelling of radionuclide sorption in the granitic rock.

Acknowledgement

The research leading tothese results has received funding from the European Union's European Atomic Energy Community's (EURATOM) Seventh Framework Programme FP7/2007-2011 under grant agreement N° 269658 (CROCK project)

References

Gaines G.I. and Thomas H.C. (1953). Adsorption studies on clay minerals II. A formulation of the thermodynamic of exchange adsorption, J. Chem Phys., 21, 714-718

Missana T. and Garcia-Gutierrez M. (2012). Summary of the experiments for the EC-CROCK Project. Part 2. Caesium adsorption onto biotite. Technical Report CIEMAT/CROCK/2/2012

van der Lee J. and De Windt L. (1999). CHESS tutorial and cookbook, Technical Report LHM/RD/99/05.

COMPARISON OF THE CESIUM ADSORPTION ON DIFFERENT CRYSTALLINE ROCKS

Tiziana Missana[1*], Miguel García-Gutiérrez[1]

[1]CIEMAT, Departamento de Medioambiente, Av. da Complutense 40, 28040 MADRID (ES)

* Corresponding author: tiziana.missana@ciemat.es

Abstract

Sorption of cesium onto granites of different origin has been experimentally studied. The analysis of the experimental data included a preliminary modelling which final aim is to evidence the possible causes of the differences in the sorption behaviour between the different rocks (mineral content, BET area, etc,).
Data obtained in this work will be also compared to other literature data obtained in the same rocks, in order to evaluate the possible sources of uncertainties on the determination of retention parameters.

Introduction

^{137}Cs (half-life, ~30 years) is an important fission product from the irradiation of uranium-based fuels. Radioactive cesium is particularly relevant from an environmental point of view, as it exists predominantly as the monovalent cation Cs^+, which presents very high solubility. Adsorption is recognized to be one of the most important retention mechanisms of radionuclides in the far –field of a Deep Geological Repository (DGR) of nuclear wastes, thus the understanding and quantification of sorption is fundamental for assessing the long term behavior of a DGR.
Crystalline rocks are considered as possible hosts rock for a DGR in different countries and for this reason, sorption onto these rocks has been widely studied in the past. However, several uncertainties on the determination of retention parameters to be used in Performance Assessment (PA) of DGRs still exist. In PA, sorption is handled using the "Kd approach" and the distribution coefficients (Kd values) are experimentally derived, generally from static *batch* experiments with the crushed material under site-specific conditions. To provide a better insight on retention processes, to estimate their uncertainties in a sound way and to support a defendable choice of Kds, is a need for radioactive waste repositories PA.
Mechanistic models are sometimes used to provide support to expert judgment for Kd selection, but their application is still very limited and a convincing picture of modeling retention processes in crystalline rocks is still missing. Thus, consequently, one of the main problems is the extrapolation of Kd values from laboratory batch experiment to field conditions.

The objective of this work is to study the adsorption of cesium in granites of different origin, under as similar as possible experimental conditions to reduce the experimental uncertainties, and to analyze the experimental data with the aim of evidencing the possible differences in the sorption behavior amongst the different rocks (mineral content, BET area, competitive ions in solution, etc.), with the help of simple thermodynamic models.
Crystalline rocks are characterized by mineralogical heterogeneity and retention processes may comprise ionic exchange (with constant-charge minerals like micas and clay minerals) and/or surface complexation (with minerals exhibiting pH-dependent surface charge). However, the extent of Cs adsorption onto rocks mainly depends on their cation exchange capacity and their content in mica-like minerals, which offer sorption sites with high selectivity for alkali cations (Sawhney, 1972). Thus, caesium sorption in micas is being also analysed in parallel (Missana and Garcia Gutiérrez, 2012 a,b,c); this will allow evaluating the advantage and disadvantages of different modeling approaches (top-down and bottom-up).

Experimental

All the reagents were of analytical grade and they were used without further purification. The radionuclide used in this study was ^{137}Cs (as CsCl in 0.1 HCl). The half-life of ^{137}Cs is 30.2 years. The activity of caesium in solution was measured by γ-counting with a NaI detector (Packard Autogamma COBRA 2).
Four different granites were used for the experiments reported here. The first two comes from the Grimsel Test Site (GTS, Switzerland): one comes from the FEBEX tunnel (from here to hereafter referred to as Grimsel FEBEX granite (GFEB) which corresponds to the central Aare type granite. Of the GFEB granite the fraction <0.5 mm was used (F1). The other, GTS's granite comes from the MIGRATION tunnel, which corresponds to a granodiorite type and will be referred to hereafter to as Grimsel MIGRATION granite (GMIG). The third granite comes from Los Ratones mine (Spain), *Rat* granite, and the fourth one comes from the Äspö Hard Rock Laboratory (Sweden), provided in two different fractions (fine and gross) by KIT-INE for the CROCK project (*Äsf* and *Äsg*, respectively), in October 2011.
The size fraction and the BET surface area of these materials are summarized in Table 1. Table 2 shows the main mineralogical composition of these solids taken from the literature. More details on the solids, their characterization and chemical composition can be found in Missana and García-Gutiérrez (2012a).

Table 1: *Size fraction and BET area of the granites used in the experiments*

Sample	Size fraction	BET (m^2/g)
GFEB (F1)	< 0.5 mm	0.089
GMIG	64 μm	2.87
Rat	< 1 mm	0.49
Äsf	1<mm<2	0.094
Äsg	2<mm<4	0.072

Table 2: *Main mineralogical composition of the granites used in the experiments.*

MINERAL (%)	GFEB	GMIG	*Rat*	Äspo
Quartz	30-36	25-31	33-35	14
Plagioglase /Albite	19-23	26-32	29-32	45
K-Feldspar	31-37	22-26	26-28	15
Biotite	6-8	10-12	2-3	15
Chlorite				--
Muscovite	1-2	3-4	5-6	--

In the experiments, a synthetic aqueous solution was used, simulating either granitic waters with "low" and "high" salinity (LSW and HSW, respectively) or a synthetic water representative of the rock volume in Äspö where the solid samples were obtained (Synthetic ÄSPÖ).
The main composition of these waters is summarized in Table 3. In order to evaluate the solid-rock interactions, the composition of waters after 1 month of contact with the solids was analysed (Missana and García-Gutiérrez, 2012a). The most important variation in the waters might be related to the potassium content, which generally increases after the interaction with the solid phases. Before the addition of the radionuclide, the solid and the water were equilibrated at least 1 day.

Table 3: *Chemical composition of the aqueous solutions used in the experiments. Nd=not determined. INIT=initial composition.*

Element	LSW	HSW	Aspö
(mg/L)	**INIT.**	**INIT**	**INIT**
Na^+	8.3	1800	1700
Ca^{2+}	7	1000	1200
Mg^{2+}	<0.03	0.09	105
K^+	<0.03	<0.1	0.42
Li	Nd	nd	13
Cl^-	28	4600	4700
SO_4^{2-}	<0.1	0.42	400
Br-	Nd	nd	17
F^-	<0.1	<0.1	1.2
Al	<0.03	<0.03	< 0.03
Fe	<0.03	<0.03	< 0.03
Cs	<0.02	<0.02	< 0.03
Si	Nd	<0.3	nd
Alk (meq/L)	<0.05	<0.1	0.24

Sorption experiments with Äspö diorite were carried out in a glove box under N_2+CO_2 atmosphere, while the others were carried out under aerobic conditions. Preliminary kinetic tests were carried out to determine the contact time. In general, cesium sorption kinetic was fast for the finest sample used (<0.5 mm) whereas increased for the largest ones. Therefore, all the experiments were carried out with a contact time of 14 days. The dependence on pH was evaluated, carrying out sorption edges changing the pH from approximately pH 6 to 10. No pH-buffers were used in the experiments with Cs. Finally, sorption isotherms at pH 7 were carried out.
Ten mL of the initial aqueous solution were introduced in polyethylene centrifuge tubes and 0.1g of the rock was added. After the water/solid equilibration, the tracer was added and the pH adjusted if necessary. The tubes were maintained under continuous stirring and then were centrifuged (26362 g, 30 min). After the solid separation, three aliquots of the supernatant from each tube were extracted for the analysis of the final activity. The rest of the solution was used to check the pH.

The distribution coefficients were calculated using the formula:

$$K_d = \frac{Cs_{ADS}}{Cs_{FIN}} \cdot \frac{V}{m} \quad (1)$$

where Cs_{ADS} is the adsorbed cesium, C_{FIN} the final concentration of Cs in the liquid phase, V the volume of the liquid and m the mass of the solid.

Results and discussion

Low saline water

Sorption edges showed a negligible dependence of cesium sorption on pH in all the granites investigated. An example of the results is shown in Table 4, which summarises the data obtained with the GMIG granite. This is the first indication that cesium retention is mainly controlled by ionic exchange.

Table 4: *Sorption values at a function of pH in the GMIG granite.*

pH	Kd	Log Kd
3.52	148	2.171
6.13	176	2.245
7	160	2.190
7.9	160	2.205
9.3	137	2.137
Mean	**155 ± 14**	**2.19 ± 0.04**

Figure 1 shows the sorption isotherms of cesium onto three different granites in the low saline water. Data are expressed as the logarithm of the distribution coefficient, Kd, as a function of the logarithm of the cesium in the aqueous phase at the equilibrium.

Sorption of cesium is clearly not linear in all the solids investigated. As cesium exists in the aqueous phase only in the form of monovalent Cs^+, the non linearity in sorption can be attributed to the existence of different sorption sites with different density and affinities. From the shape of the isotherms, it is clear that a site of high affinity and low density exist (with a very similar density for all the granites investigated) dominating the sorption behavior at low cesium concentrations. At higher concentration sorption must be controlled by, at least, an additional sorption site.

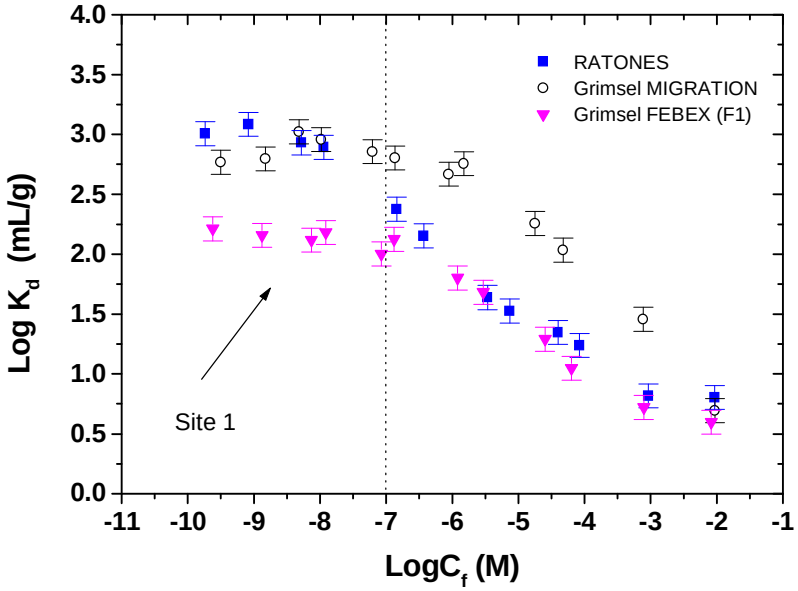

Figure 1: *Sorption isotherms of cesium in the analysed granites and LSW. pH =7.*

High saline waters (HSW and Synthetic Äspö)

Also in the case of the experiments with high saline waters, sorption edges indicated a very small dependence of cesium sorption on pH (Missana and García-Gutierrez, 2012a).

Figure 2 shows the sorption isotherms of cesium onto three different granites in high saline waters. Sorption isotherms present the same characteristics observed in the experiments with LSW. In the case of the GFEB and GMIG, and especially at the low cesium concentrations, sorption is lower than that observed in the low saline waters. This is true in the case of retention by ionic exchange; however the experimental dependence observed with the ionic strength is not completely in agreement with the theoretical one and this would be an indication that competing ions are affecting sorption.

A preliminary modeling analysis indicated that potassium, as expected, is the ion which most can affect cesium retention. Furthermore, the effect of monovalent ions is in general higher than that of divalent ones. Potassium values were measured in the aqueous phases after the contact with the solid.

Therefore, the first modeling approach consisted in considering the granite as a simple exchanger in which monovalent exchange with cesium (and potassium) occurs.

$$M \equiv X + Cs \Leftrightarrow Cs \equiv X + M^+ \qquad (2)$$

As the main monovalent ion in solution is sodium, M^+ corresponds to Na^+.

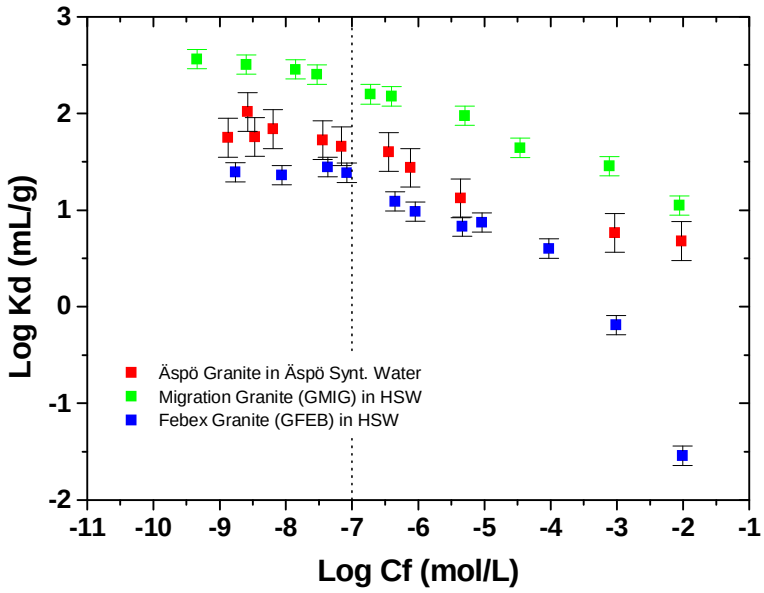

Figure 2: *Sorption isotherms of cesium in the analysed granites and high saline waters (HSW and Äspö). pH =7.*

Three sorption sites were considered and their density was a fixed parameter for all the granites (site 1= 0.9 μeq/m^2; site 2 =5 μeq/m^2 and site 3 = 110 μeq/m^2). The modelling calculations were done with the CHESS v 2.4 code (van der Lee and De Windt, 1999), and the fits of the experimental curves were obtained with a trial and error procedure. More detail on the modeling approach can be found in Missana and García Gutiérrez (2012a).
Figure 3 shows an example of the modeling of the sorption data performed in the GFEB granite in both low and high saline waters and Figure 4 shows the modeling of the isotherms obtained with the Äspo granite in Äspo synthetic water. The contribution to sorption of all the sorption sites is included in the graph, as well as the quantity of potassium present in solution. Table 5 includes the values of the parameters used in the modeling (selectivity coefficients, logK, of cesium and potassium with respect with the main monovalent ion Na).

In the case of the two granites (GFEB and Äspö) for which the modeling is shown in Figure 3 and Figure 4, the values of the selectivity constants at the sites dominating sorption in the widest range of concentrations are quite similar. In both cases, the predominant mica is the biotite.

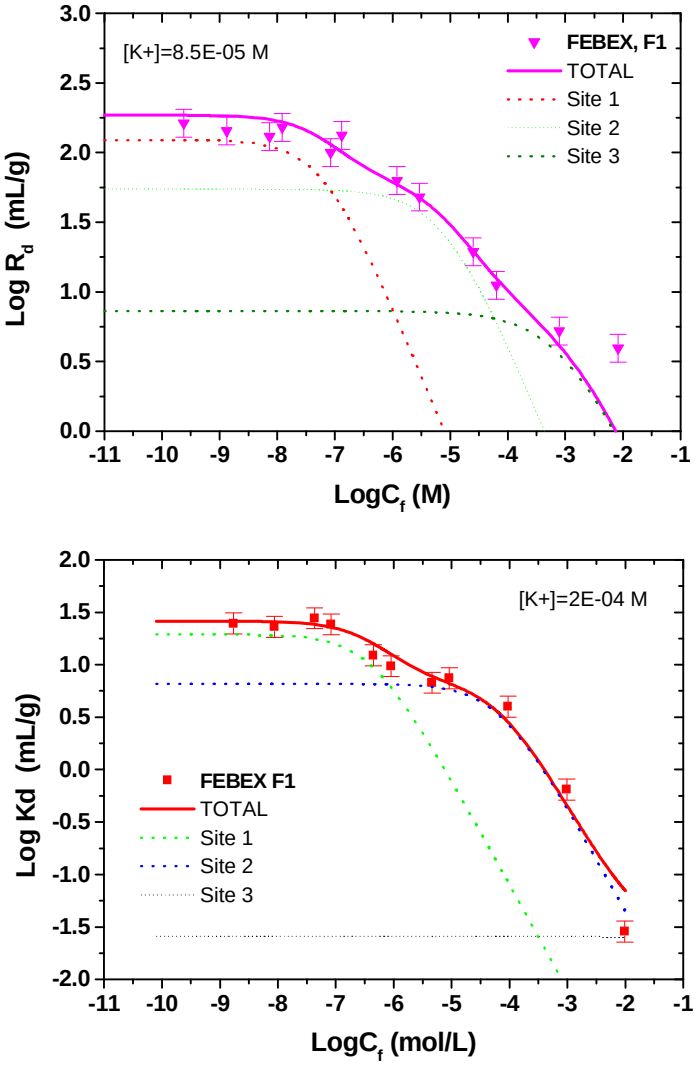

Figure 3: *Modelling of the sorption isotherms obtained in GFEB in low (left) and high (right) saline waters.*

Table 5: *Parameters used in the modelling of the sorption isotherms plotted in Figure 3 and Figure 4. LogK is the logarithm of the exchange reaction (2) where M is Na^+ exchanged with either Cs^+ or K^+.*

Sample	Site 1	Site 2	Site 3	Site 1	Site 2	Site 3
	LogK (Cs)	LogK (Cs)	LogK (Cs)	LogK (K)	LogK (K)	LogK (K)
GFEB (LSW)	8.35	4.75	-0.65	5.50	4.00	-0.65
GFEB (HSW)	8.20	4.50	-0.65	5.50	4.00	-0.65
Äspö Gross (Syn Wat)	8.50	5.00	1.80	5.50	3.80	1.00

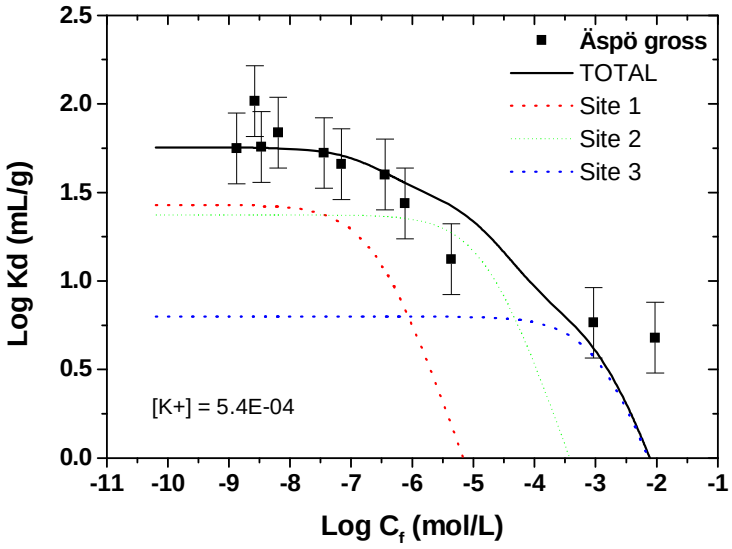

Figure 4: *Modelling of the sorption isotherms obtained in Äspo granite (gross) in Äspo synthetic water.*

Conclusions and Future work

The sorption of cesium onto four different crystalline rocks was experimentally studied using both low and high saline waters. In all the granites cesium sorption showed a non-linear behavior, small dependence on the pH and dependence with the ionic strength. This seems indicating that the main mechanism of cesium retention in these rocks is ionic exchange. In order to reproduce the sorption data a top-down modeling approach was followed. In particular, a three-site exchange model was used accounting for the presence of potassium in the system. In the analyzed cases, the modeling has been quite successful.
In the next future, all the data will be modeled and the selectivity coefficients obtained in all the granites will be related to the main mineralogical properties of the rock.

Acknowledgement

The research leading to these results has received funding from the European Union's European Atomic Energy Community's (EURATOM) Seventh Framework Programme FP7/2007-2011 under grant agreement N° 269658 (CROCK project)

References

Missana T. and García-Gutiérrez M. (2012a). Summary of the exeriments for the EC-CROCK Project. Part 1: Cesium adsorption onto granite. Technical Report CIEMAT/CROCK/1/2012.

Missana T. and García-Gutiérrez M. (2012b). Summary of the exeriments for the EC-CROCK Project. Part 2: Cesium adsorption onto biotite. Technical Report CIEMAT/CROCK/2/2012.

Missana T. and García-Gutiérrez M. (2012c). Summary of the exeriments for the EC-CROCK Project. Part 3: Cesium adsorption onto moscovite. Technical Report CIEMAT/CROCK/3/2012.

Sawhney B.L. (1972). Selective sorption and fixation of cations by clay minerals: a review, Clays and Clay Minerals, 20, 93-100.

van der Lee J. and De Windt L. (1999). CHESS tutorial and cookbook, Technical Report LHM/RD/99/05.

STATUS OF WORK PACKAGE 6 – STATE-OF-THE-ART OF RETENTION PROCESSES

Andres Idiart[1*], Marek Pekala [1], Mireia Grivé [1]

[1] Amphos 21 Consulting (Barcelona, Spain)

* Corresponding author: andres.idiart@amphos21.com

Abstract

Within Work Package 6 (WP-6) of the CROCK European collaborative project, the physical, chemical and biological processes thought to govern the behaviour of radionuclides in crystalline rocks are being reviewed. In particular, the project focus on those processes which exert a major influence on the transport and retention of radionuclides in the far-field, as well as on the main conceptual models describing these processes available in the scientific literature. The project also includes an analysis of how these retention processes are taken into account and modelled in the different Performance Assessments (PAs) currently being carried out by European radioactive waste management organisations to evaluate the long-term safety of deep geological disposal facilities for radioactive waste in crystalline rocks. This document is a succinct summary of the work being carried out within the project. It will subsequently be updated with the advances made during the course of the project.

Introduction

There have been two previous projects within the EURATOM Program specifically addressed to the transport and retention of radionuclides in the far-field of nuclear waste repositories, namely the RETROCK project (2001-2004) and the FUNMIG project (2005-2008). The RETROCK project was specifically concerned with crystalline rock environments. Therefore, the on-going work in WP-6 of the CROCK project intends to include an update of the scientific and PA knowledge previously compiled and generated within the RETROCK project, and published in RETROCK (2004), RETROCK (2005), and the FUNMIG project, see e.g. Bruno and Montoya (2012), Schwyn et al. (2012), Lützenkirchen (2012), Reiller et al. (2012). It should also be mentioned that sorption processes in clay host rocks are being investigated within a separate European collaborative project (CATCLAY, 2010-2014), which is conducted in parallel to CROCK, and from which useful information for the CROCK project will also be obtained.

The objective of WP-6 of the CROCK project is to compile and document the state-of-the-art on retention processes in crystalline rock, in a form that serves the purpose of regular updating of the advances achieved within the project. In addition, one further objective of the WP-6 is to process all the information and scientific results generated

within the CROCK project with the aim of suggesting possible ways of application in Performance Assessments.

Questionnaires

Two questionnaires were generated and distributed to all the beneficiaries to collect information on:
1) The scientific activities carried out by the different WP participants of the project
2) How the most recent PAs from different countries consider the retention processes affecting the mobility of RN,
with the aim of:
• Gathering and merging information to elaborate a precise picture of what are the main fields of research in the project and who is involved.
• Collecting information on how the different participants envisage that their research may have an impact on future PA exercises.
• Acquiring information on the level of understanding and on the treatment of retention processes in the most recently published safety cases.
• Identifying the existing gaps of knowledge in the present PA exercises and the challenges to be addressed in the future.
The collected information is being processed and will be reported accordingly to give a general view of the scope of the project and a picture of the present status of different PA exercises. In addition, a number of external contributors have also agreed to participate in the questionnaire regarding the Performance Assessment and how retention processes are being taken into account.

Overview of transport and retention processes in crystalline host rocks

In the following, a brief description is given of how different processes affecting transport and retention of radionuclides in the geosphere are considered in recent PAs. Particular attention is paid to the work done by the Finnish and Swedish radioactive waste management organisations (Posiva and SKB, respectively). SKB has recently submitted a PA to the Swedish authorities for the Forsmark site, SKB (2011). Posiva is also about to submit a PA for the Olkiluoto site, which is planned for end 2012, Posiva (2010), Nykyri et al. (2008).
Groundwater flow field, rock matrix diffusion, and sorption on mineral surfaces have been previously recognized as the processes which exert a major influence on the behaviour of radionuclides in fractured rocks, see RETROCK (2005). Other processes which may also affect this behaviour include gas phase transport, microbial activity, the presence of colloids in groundwater (which may facilitate radionuclide transport), and the overall hydrochemical and mineralogical composition of the system. These different processes are briefly described below, and some insight is given on how these processes have been taken into account in recent PAs, Posiva (2010), SKB (2011).

Groundwater flow

In the recent PA of SKB (2011), advective-dispersive transport from individual canisters to the biosphere has been considered through a methodology based on a mixture of Discrete Fracture Network (DFN) and Continuum Porous Media (CPM) flow concepts, SKB (2010a), from which advective travel times (from individual canisters to

the biosphere) and the flow-related transport resistance along flow paths have been obtained. Those results have been used as input for the analysis of radionuclide transport in the aqueous phase, which has been idealized as one-dimensional pathlines with advective-dispersive flow and a dual porosity to account for both matrix diffusion and changes in the flow magnitude. In this PA, matrix diffusion in the host rock and sorption on mineral surfaces are the only retardation processes considered. Other processes such as co-precipitation, and retention by colloid filtration have not been considered.
The approach followed by Posiva (2010) considers both an Equivalent Porous Medium (EPM) and a DFN model as complementary methods. The results serve as input for the radionuclide transport in the fractures, which has also been considered through a 1D dual porosity description. Also in this case, rock matrix diffusion and linear sorption are the only retardation processes considered. Purely advective flow has been assumed in the 1D model since it was previously determined in a previous PA, i.e. TILA-99, Vieno and Nordman (1999), that longitudinal dispersion was of minor importance, Posiva (2010).

Matrix diffusion

In the PA of SKB (2011), the advective transport of radionuclides is subject to a dual-porosity rock matrix diffusion process. Matrix diffusion is assumed to be reversible and linear, implying a Fickian behaviour characterised by an effective diffusivity that can vary spatially along the flowpath to account for the local microstructural properties of the rock. It has further been assumed that diffusion into the rock matrix is one-dimensional and perpendicular to the advective flowpath along which the radionuclide is transported. Matrix diffusion has been considered for the case of an unaltered host rock, i.e. the presence of fracture-filling minerals such as clays has been neglected. Finally, a finite penetration depth for radionuclides based on fracture half-spacing has been considered in the model. Whether this assumption is equivalent to an infinite penetration depth or not depends on the timescale analysed and the diffusion coefficient of the rock matrix.
Matrix diffusion in the Finnish PA, Posiva (2010), has been considered in a similar way as in the Swedish PA, SKB (2011), i.e. the process is described by Fick's law and the diffusion is limited to a small penetration depth within the rock. However, in the Finnish PA the limited penetration depth is conceptualized as connected rock matrix porosity within a few centimetres of fracture surface. Also, diffusion into stagnant water pools in the fractures has not been taken into account (conservatively omitted). Anion exclusion in the rock matrix has been considered for some radionuclides, affecting their diffusion coefficients and the effective porosity that they encounter.

Sorption on mineral surfaces

In the PA SKB Performance Assessment, SKB (2011), linear equilibrium sorption (Kd concept) has been considered both for sorption processes occurring in the stagnant water within the rock matrix and in the flowing phase zone (i.e. sorption on fracture walls). Similarly, the PA of Posiva (2010) considers sorption of radionuclides within the rock matrix assuming a Kd approach. Sorption within the rock matrix has been considered to be entirely represented by ion-exchange and surface complexation, SKB (2010b). Sorptive properties of the rock were assumed to follow constant linear partitioning

coefficient which can also vary spatially along a flowpath depending on the local mineralogy of the rock and porewater chemistry. The Kd values have been carefully chosen so that retention of radionuclides is treated in a conservative manner, Crawford (2010). Radionuclide retention by sorption on fracture walls and by formation of solid solutions with naturally occurring minerals has been considered only in scoping calculations, SKB (2010b), with special attention to its implications in the context of remobilisation scenarios. Although difficult to incorporate in PA exercises at the present time for numerical reasons, consideration of thermodynamic sorption models should result in significant improvements in the description of retention processes.

Generation of gases

Gas components can be generated in nuclear waste repositories through metal corrosion (generation of H_2), water radiolysis (generation of H_2 and O_2), and bacterial degradation of organic wastes (generation of CO_2). The generated gas may be transported as a solute in the groundwater moving through a saturated fracture network. If the amount of gas generated exceeds its aqueous solubility, a gas phase may form. Besides the fact that a gas phase may transport some radionuclides (mostly ^{14}C and ^{222}Rn) much more rapidly towards the outside than aqueous solutions, gas components are involved in many microbiological reactions which may also affect the environmental fate of radionuclides. Some details are given on how gas generation from canisters is taken into account in the PA of SKB (2011) and Posiva (2010).

Microbial activity

Microbial activity results in the production of organic chelates which may affect the mobility of radionuclides. In addition, microbes may consume O_2 in case of an oxygen intrusion in the repositories. Notwithstanding the growing recognition of the importance of microbes in geochemical processes, their influence is presently not taken into account in PA exercises due to difficulties inherent to the modelling of bacterially-mediated reactions. However, significant progress has been made over the last few years which makes it possible to incorporate the influence of bacterial activity in geochemical models through the evaluation of metabolic energies.

Colloid-facilitated transport

Bentonite colloids are expected to form in the groundwater near deposition holes due to buffer/backfill erosion. These colloids may potentially increase the transport of radionuclides with a strong sorption affinity for bentonite. In the PA of SKB (2011), rapid reversible sorption of radionuclides on colloids has been considered by the use of partition coefficients. Potential mitigating processes for the colloid-facilitated transport of radionuclides (by filtration or straining of colloids, etc.) have been ignored, and colloid exclusion from rock matrix diffusion has been assumed in order to place an upper limit on the possible effect of colloids on radionuclide transport. As a limiting case, irreversible sorption onto colloids has also been studied in recent scoping calculations, SKB (2010b), considering a finite number of sorption sites on the colloids as the only mitigating process. Although colloid-facilitated transport of radionuclides is not currently taken into account in the PA of Posiva (2010), there are plans to include this process in their future PA.

Geochemistry

No thermodynamic model is currently incorporated in PA exercises for the aqueous speciation of radionuclides, and each solute is considered as a unique species. However, there exist detailed models for radionuclide speciation which can be used to validate the simplifications made in the PA exercises. Similarly, the description of the co-precipitation of radionuclides during the formation of secondary phases (e.g. calcite) is lumped in the sorption description using Kd coefficients (see above).

Conclusions and Future work

The physical, chemical and biological processes thought to govern the behaviour of radionuclides in crystalline rocks are being reviewed. In particular, the project focus on those processes which exert a major influence on the transport and retention of radionuclides in the far-field, as well as on the main conceptual models describing these processes available in the scientific literature and recent Performance Assessments (PAs). The review of the scientific literature and the approaches followed in recent PAs will be focused mainly in the work published after the end of the RETROCK project (i.e. from 2005), with the exception of the information generated in the FUNMIG project, which is summarized elsewhere. Two questionnaires were generated and distributed among the different beneficiaries and also among external contributors to collect information on how retention processes are considered in recent PAs. The results of the survey and a discussion will be published by the end of the project.

Acknowledgement

The work presented here has received funding from the European Union's European Atomic Energy Community's (EURATOM) Seventh Framework Programme FP7/2007-2011 under grant agreement n° 269658 (CROCK project).We are also grateful with all the beneficiaries of the CROCK project for their participation in this Work Package and for filling the questionnaires.

References

Bruno, J., Montoya, V. (2012). From aqueous solution to solid solutions: A process oriented review of the work performed within the FUNMIG project. Applied Geochemistry, 27(2), 444-452.

Crawford, J. (2010). Bedrock Kd data and uncertainty assessment for application in SR-Site geosphere transport calculations, SKB R-10-48, Svensk Kärnbränslehantering AB.

Lützenkirchen, J. (2012). Summary of studies on (ad)sorption as a "well-established" process within FUNMIG activities. Applied Geochemistry, 27(2), 427-443.

Nykyri, M., Nordman, H., Löfman, J., Poteri, A., Marcos, N. and Hautojärvi, A. (2008). Radionuclide release and transport (RNT-2008), POSIVA 2008-06. Posiva Oy, Eurajoki, Finland.

Posiva (2010). Interim Summary Report of the Safety Case 2009, POSIVA 2010-02. Posiva Oy, Eurajoki, Finland.

Reiller, P.E., Vercouter, T., Duro, L., Ekberg, C. (2012). Thermodynamic data provided through the FUNMIG project: Analyses and prospective. Applied Geochemistry, 27(2), 414-426.

RETROCK (2004). RETROCK Project. Treatment of geosphere retention phenomena in safety assessments. Scientific basis of retention processes and their implementation in safety assessment models (WP2). SKB R-04-48, Svensk Kärnbränslehantering AB.

RETROCK (2005). Treatment of radionuclide transport in geosphere within safety assessments. Final report of the RETROCK Concerted Action. EUR 21230, European Commission.

Schwyn, B., Wersin, P., Rüedi, J., Schneider, J., Altmann, S., Missana, T., Noseck, U. (2012). FUNMIG Integrated Project results and conclusions from a safety case perspective. Applied Geochemistry, 27(2), 501-515.

SKB (2010a). Geosphere process report for the safety assessment SR-Site, SKB TR-10-48, Svensk Kärnbränslehantering AB.

SKB (2010b). Radionuclide transport report for the safety assessment SR-Site, SKB TR-10-50, Svensk Kärnbränslehantering AB.

SKB (2011). Long-term safety for the final repository for spent nuclear fuel at Forsmark Main report of the SR-Site project, Vols. I-III, SKB TR-11-01, Svensk Kärnbränslehantering AB.

Vieno, T., Nordman, H. (1999). Safety assessment of spent fuel disposal in Hästholmen, Kivetty, Olkiluoto and Romuvaara TILA-99. Posiva Report POSIVA 99-07. Posiva Oy, Helsinki, Finland.

DETERMINATION OF ROCK MIGRATION PARAMETERS (F_f, D_e): APPLICATION OF ELECTROMIGRATION METHOD ON SAMPLES OF DIFFERENT LENGTH

Petr Vecernik[1], Vaclava Havlova [1*], Martin Löfgren[2]

[1] Nuclear Research Institute Rez plc., Husinec-Rez 130, 250 68, Rez (CZ)
[2] Niressa AB, Stockholm (Swe)

* Corresponding author: hvl@ujv.cz

Abstract

Through-Electromigration Method (TEM) is an efficient method enabling successfully determination of migration parameters (formation factor F_f and effective diffusion coefficient D_e). The method was successfully tested for Äspö diorite with rather low water accessible porosity 0.21 %. Migration parameters (F_f, D_e), gained by both resistivity and through-electromigration methods, revealed a good consistency for 3 samples with different lengths. Effective diffusion coefficient D_e for I^-, used as a tracer, varied in the range of 2.7 - 4.6x10^{-13} $m^2.s^{-1}$. Formation factor F_f(TEM) reached values in the range 1.3 - 2.3 x10^{-4}. The difference between the apparent formation factor F_f^a and F_f(TEM) decreased with increasing formation factor presumably due to decreasing impact of surface diffusion. Such an observation was in clear consistency with previous measurements on samples from Forsmark and Oskarshamn.

Introduction

Diffusion of radionuclides from fractures into adjacent altered or fresh rock is considered to be one of the important retardation processes for safety assessment of radioactive waste in a deep geological repository. Diffusion within crystalline rocks with low porosity (< 1%) is a slow process that results in the need to use samples of limited length in the laboratory in order to receive results in reasonable time scales. The usage of short samples brings some contradictions: even though the experiments can deliver the results within a month, samples in fact do not represent real rock conditions, namely due to possible interconnections of pores that would not be connected in real rock massive. This causes increased pore connectivity and possible overestimation of laboratory diffusion results.
Moreover, it is known from the literature that the disturbed zone on the sample surface, produced by sawing and drilling, can extent up to 15 mm from the edge (Möri, 2009; results of LTD experiment in Grimsel Test Site), giving rise or increased tracer diffusivity through the sample. It was reported in the literature, that formation factor F_f decreases with increasing sample length (Valkiainen et al., 1996) as non-realistic connectivity vanishes with less disturbed samples. Electromigration methods (Löfgren, 2004; Löfgren and Neretnieks, 2006; Löfgren et al., 2009) enables speeding up

laboratory diffusion experiments, gaining rock migration parameters (F_f, D_e) in relatively short times (hours). The aim of the study presented was to test the use of the apparatus, previously tested, for longer samples in order to obtain migration data for less disturbed rock and to study the dependence of migration parameters on sample length.

Theory

The theory of electromigration experiments has been based on through-electromigration (TEM) method, described in Löfgren (2004), Löfgren and Neretnieks (2006) and in Löfgren et al. (2009) where the methodology was applied in NRI Rez labs.
The methodology is based on the Einstein relation, describing the interrelation between the diffusivity and ionic mobility of ionic solutes:

$$D = \frac{\mu R T}{z F} \tag{1}$$

where D ($m^2.s^{-1}$) is the diffusivity, μ ($m^2.V^{-1}.s^{-1}$) is the ionic mobility, z (-) is the charge number of the migrating ionic solute, and R ($J.mol^{-1}.K^{-1}$), T (K), and F ($C.mol^{-1}$) are the gas constant, temperature, and Faraday constant, respectively. In an inert porous medium the diffusivity and ionic mobility in equation 1 can be substituted by the effective diffusivity D_e ($m^2.s^{-1}$) and effective ionic mobility μ_e ($m^2.V^{-1}.s^{-1}$), respectively:

$$D_e = \frac{\mu_e R T}{z F} \tag{2}$$

If an electric field is applied over a saturated rock sample holding an ionic tracer, the electromigratory tracer flux N_μ ($mol.m^2.s^{-1}$) through the sample is:

$$N_\mu = -\mu_e C_p \frac{dU}{dx} \tag{3}$$

where C_p ($mol.m^{-3}$) is the tracer concentration in the pore water and dU/dx ($V.m^{-1}$) is the electrical potential gradient over the sample.

Simplifying and assuming that the sample is homogenous, a constant electrical potential gradient can be calculated from the quotient of the potential drop over the sample and the sample length. If combing equations 2 and 3, and using the formation factor F_f (-) and the diffusivity in unconfined pore water D_w ($m^2.s^{-1}$) instead of D_e, the electromigratory tracer flux through the rock sample is described by:

$$N_\mu = -\frac{F z D_e}{RT} C_p \frac{dU}{dx} = -Ff \cdot \frac{F z D_w}{RT} C_p \frac{dU}{dx} \tag{4}$$

With the TEM method, the electromigratory tracer flux N_μ can be directly obtained. This is achieved by applying an electrical potential gradient over a saturated rock sample and by allowing an ionic tracer to migrate through the sample. By recording and

analysing a breakthrough curve, as in a traditional Through-Diffusion (TD) experiment, N_μ can be obtained.

When resistivity ρ_r is constant in time, the apparent formation factor F_f^a can be calculated according to equation 5 (Löfgren et al., 2009)

$$F_f{}^a = \frac{\rho_w}{\rho_r} = \frac{\kappa_r}{\kappa_w} \tag{5}$$

where F_f^a is apparent formation factor (from electrical measurement, -), ρ_w is pore water (electrolyte) resistivity (Ω.m), ρ_r is saturated rock resistivity (Ω.m), κ_r is electrical conductivity of saturated sample ($S.m^{-1}$) and κ_w is electrical conductivity of the electrolyte ($S.m^{-1}$). Electrical conductivity of electrolyte is measured directly by conductivity electrode and conductometer. Electrical conductivity of saturated sample is calculated from potential drop over sample and electric current passing through the sample, corrected to the conductivity of electrolyte column between the potential electrodes and sample surface.
Determination of apparent diffusion coefficient F_f^a using resistivity measurements enables laboratory support to resistivity measurements in-situ.

Samples and experimental methodology description

Rock samples obtained and characterisation

For details of processing the samples from Äspö Hard Rock laboratory see Deliverable 1.1.
Two discs (~45 mm diameter) of approx. 10 mm thickness and one sample of identical diameter and 30 mm thickness were used for electromigration experiments. For sample identification see Table 1.
Samples from borehole KA2368A (AD-1, AD-3) were received as O_2 disturbed samples, i.e. samples that were not held under anaerobic atmosphere. Sample AD-31 (30 mm thick) was originally received in an autoclave, being held under Ar atmosphere altogether with other core samples. Those were transfered into an anaerobic box where they have been held until now. As transfer and operation of the electromigration cell into a glove box Ar controlled atmosphere is not possible, all the analyses and electromigration measurements were performed under oxic conditions.

Table 1: *Sample origin, identification and size.*

Sample	Borehole	Log No.	Borehole length (m)	Diameter (mm)	Length (mm)
AD-1	KA2368A-01	# 1.27	10.65-11.12	45.22	12.40
AD-3	KA2368A-01	# 1.27	10.65-11.12	45.25	11.45
AD-31	KA2370A-01	# 2.30	11.63-12.13	45.29	33.11

Samples from both boreholes are Äspö diorite. Sample photos are presented on Figures 1, 2 and 3a,b.

Figure 1: *Sample AD1 for electromigration measurement.*

Figure 2: *Sample AD3 for electromigration measurements.*

Figure 3a: *Sample AD31 for electromigration measurement.*

Figure 3b: *Sample AD31 for elecktromigration measurement.*

Sample saturation and porosity measurements

Rock samples were saturated using a vacuum saturation method, presented by Melnyk and Skeet (1986) or in Ohlsson (2000). The methodology used in NRI lab is described in detail in Löfgren et al. (2009). The porosity was determined by using the so called water immersion methodology, presented in the same publication Melnyk and Skeet (1986). The method determines the amount of connected pores that are available for water molecules.

Electromigration measurements

In NRI laboratories, the TEM method was further developed in cooperation with the author (Löfgren et al., 2009). The NRI electromigration cell concept is carefully described in Löfgren et al. (2009).
In this arrangement the TEM cell consists of four compartments, as presented in Figures 4 and 5. The rock sample (usually 10 mm long) is placed in a special rubber seal and mounted between two compartments (200 ml). The seal tightness was tested as reported in Löfgren et al. (2009). In this case, the apparatus was also tested for the longer samples (30 mm).
The first inlet compartment (V = 200 ml) was filled with 0.05 M NaCl electrolyte. 10 ml of electrolyte was replaced by 0.1 M NaI in order to obtain 0,005 M concentration of I- in the inlet compartment (see Figure 1). The outlet compartment (V = 200 ml) was filled with 0.05 M NaCl. The potential gradient over the sample is gained by placing an

electrode in each electrolyte and connecting the electrodes to a direct current power supply. To avoid the electrolysis at the anode and cathode, the electrodes are placed in separated compartments. Furthermore, the high and low pH electrolytes formed in the anode and cathode compartments are used to neutralise each other, by drop wise intermixing them. The electrolyte concentration used here (0.05 M NaCl) were used in previous experiments and hereby is considered as a reference one, even though the ionic strength (I) of Äspö groundwater is higher (0.18 M).

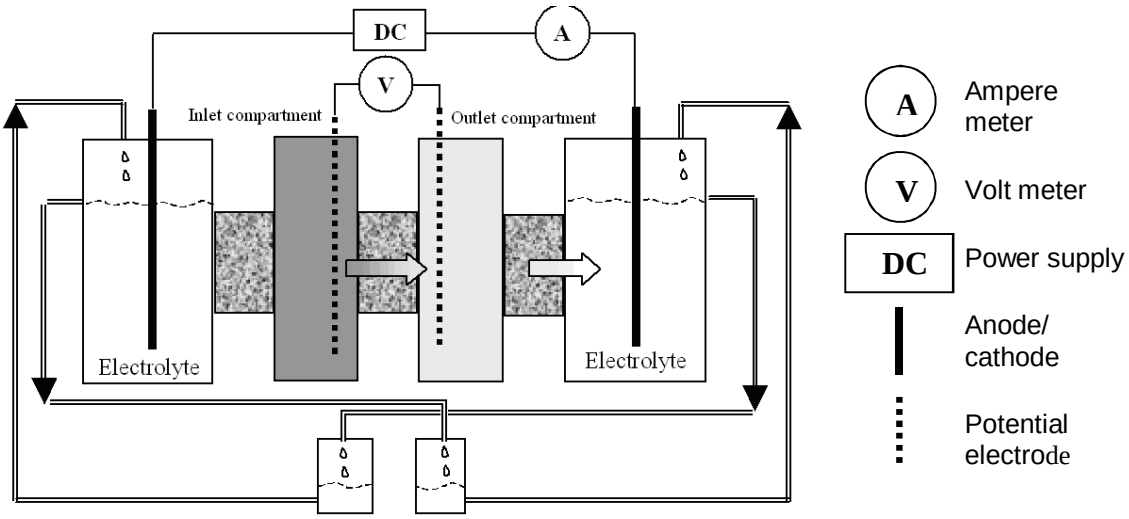

Figure 4: *The scheme of through-electromigration cell. Reproduced from (Löfgren et al., 2009).*

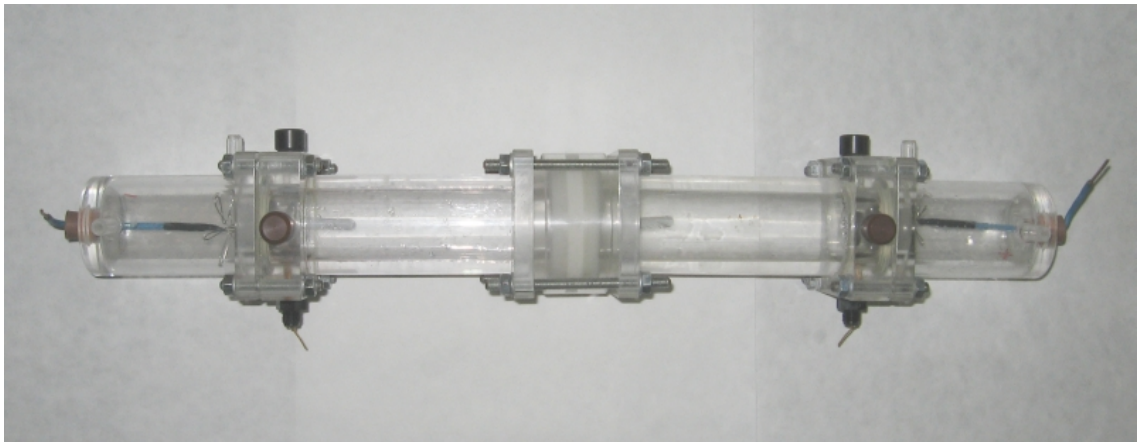

Figure 5: *The photo of inlet compartment, outlet compartment and sample mounted between as a part of the through-electromigration apparatus (NRI Rez concept; reproduced from Löfgren et al., 2009).*

Current and voltage values are then collected, enabling calculation of resistivity value for saturated sample ρ_r. When resistivity ρ_r is constant in time, the apparent formation factor F_f^a can be calculated according to equation 5.

After the direct current (DC) measurement is terminated, the electrodes are connected with slight modification to alternating current (AC) circuit and F_f^a is calculated, following the same approach as reported above. The electrolytes are sampled afterwards from all compartments. Their pH and conductivity are measured.
Through-electromigration experiment with a tracer is possible to accomplish after system equilibration and resistivity stabilization. In this case I^- was used in the NaI form. Iodide corresponding to the concentration 0.005 M is inserted into high concentration reservoir (t = 0). The current and voltage measurements are performed in the same manner as presented above. In addition, the tracer concentration is measured in low concentration cell (see Figure 4).
Using non-active I^-, an ion selective electrode (Theta 90, CZ) is used for concentration measurement (measurement range 10^{-6}–10^{-1} M; calibration from 10^{-6}–10^{-4} M). The concentration increase is recorded with time. Assuming that tracer concentration increase is linear at steady state, the effective diffusion coefficient can be calculated. Afterwards, the formation factor F_f can be calculated, using equation 6 and knowing tracer diffusion coefficient in free water D_w (e.g. Miller, 1983).

$$F_f = \frac{D_e}{D_w} \tag{6}$$

where F_f is TEM formation factor (-), D_e is effective diffusion coefficient ($m^2.s^{-1}$), D_w is diffusion coefficient in free water ($m^2.s^{-1}$).

As indicated above, the formation factor is not only estimated from the tracer breakthrough curve. It is also estimated by measuring the rock resistivity and electrolyte resistivity (see equation 5). However, the rock resistivity is affected by so called surface conduction, which can be described as ionic conduction by cations in the electrical double layer at the pore walls. Such surface bound migration is not normally included in the concept of formation factor. Accordingly "formation factors" derived in this manner is called the apparent formation factor. By subtracting the contribution from surface conduction, the formation factor F_f can be estimated (Crawford and Sidborn, 2008).

$$F_f = F_f^{\,a} - \frac{\kappa_s}{\kappa_w} \tag{7}$$

where κ_s is surface conductivity ($S.m^{-1}$).

Results

Porosity measurements

Porosity was calculated on the basis of measurements and methodology of Melnyk and Skeet (1986). The method also enables one to calculate sample density ($kg.m^{-3}$).

Table 2: *Porosity and density measurements for Äspö rock samples.*

Sample	Porosity value (%)	Density (kg.m^{-3})
AD-1	0.22±0.01	2 650±60
AD-3	0.21±0.01	2 660±60
AD-31	0.29±0.01	2 741±62

Electromigration measurements

In Figure 6, 7 and 8 iodide breakthrough curves for the samples are presented, emphasizing the part at steady state condition for further F_f (TEM) and D_e (TEM) calculations. D_e was calculated from steady state part of the curve, using the procedure from Löfgren et al. (2009). F_f was calculated according to equation 6, using $D_w = 2\times10^{-9}$ $m^2.s^{-1}$ from Miller (1983). F_f^a was calculated from equation 5. In Table 3 all formation factors are listed.

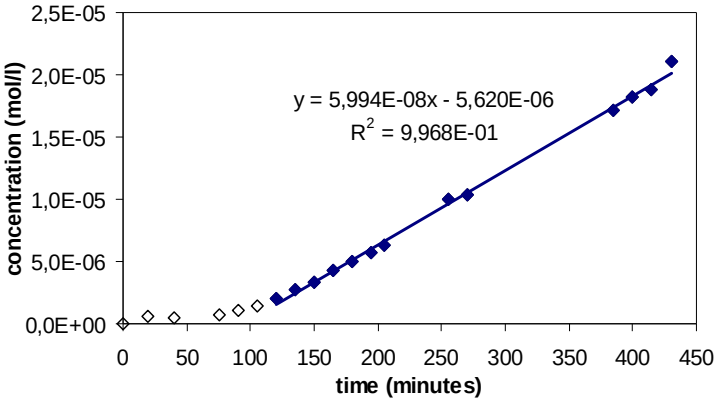

Figure 6*: TEM experiment: Iodide breakthrough curve for sample AD-1 (10 mm length). Full diamonds represent steady state conditions.*

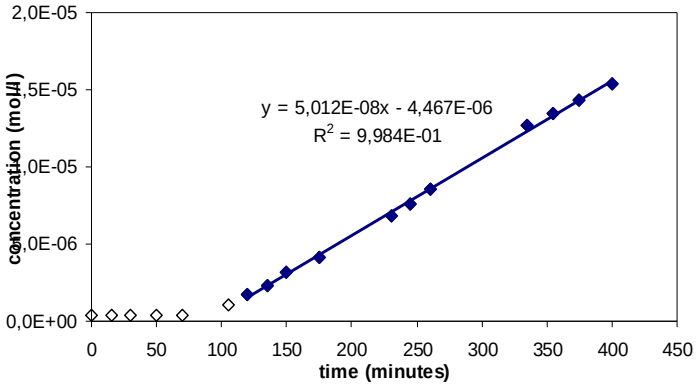

Figure 7: *TEM experiment: Iodide breakthrough curve for sample AD-3 (10 mm length). Full diamonds represent steady state conditions*

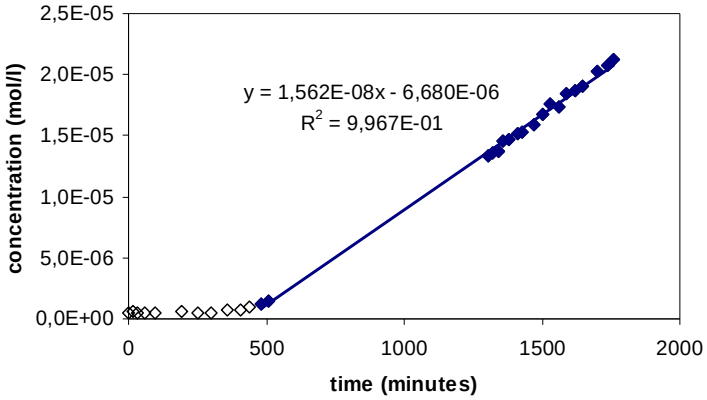

Figure 8: *TEM experiment: Iodide breakthrough for sample AD-31 (30 mm length). Full diamonds represent steady state conditions.*

Table 3: *TEM Formation factor F_f and apparent formation factor F_f^a for samples from Äspo hard rock laboratory measured by electromigration methods.*

Sample	AD-1	AD-3	AD-31
D_e ($m^2.s^{-1}$)	4.64×10^{-13}	3.90×10^{-13}	2.70×10^{-13}
F_f (TEM)	2.3×10^{-4}	1.8×10^{-4}	1.3×10^{-4}
F_f^a (DC)	6.1×10^{-4}	5.70×10^{-4}	6.5×10^{-4}
F_f^a(AC 10 Hz)	7.7×10^{-4}	7.4×10^{-4}	7.4×10^{-4}
F_f^a (AC 100 Hz)	7.9×10^{-4}	7.5×10^{-4}	7.5×10^{-4}
F_f^a (AC 1 kHz)	8.2×10^{-4}	7.8×10^{-4}	7.7×10^{-4}
F_f^a (AC 2 kHz)	8.2×10^{-4}	7.8×10^{-4}	7.8×10^{-4}

Discussion

Porosity measurements revealed that the Äspö diorite samples are of rather low porosity (0.21%). It has to be taken into account that the Melnyk and Skeet (1986) methodology measures namely the connected porosity, accessible for water molecules, i.e. pores smaller than 0.3 nm cannot be included into the calculation. However, if the main presumed transport within undisturbed rock matrix is supposed to be by diffusion within pore water, the <0.3 mm pore size fraction seems to be out of relevance for radionuclide migration assessment.

Migration parameters (F_f, D_e), gained by both resistivity and through-electromigration methods, revealed a good consistency for 3 samples with different lengths (see Table 3). Effective diffusion coefficient D_e for anionic I^- varies in close values within one order of magnitude ($2.7–4.64\times10^{-13}$ $m^2.s^{-1}$). Even though the lower value was measured for the longest sample (AD31), it cannot be assumed that D_e decreases with the length of the sample as the value variation is not significant. This presumption, delegated in the very first paragraph, should be studied using a wider range of long samples. On the other hand, the results showed that Äspö diorite reveals similar properties even for samples from different boreholes (KA2368A-01, KA2370A-01).

Furthermore, rather consistent data range was gained for formation factor determination. F_f (TEM) is calculated from D_e. F_f^a were calculated, using DC and AC electrical circuits. Previous publications (Löfgren, 2004; Löfgren et al., 2009) reported overestimation of F_f by DC and AC measurements in comparison with TEM measurement. The similar trend is visible within the results for Äspö diorite in Table 4. It is in part due to surface condition but may in part also be due to anion exclusion. In the tracer test, only anionic tracers have been used. However, when estimating the diffusion properties from direct and alternating current measurements, the charge is carried by both cations and anions, and the impact of anion exclusion is thus reduced.
Once more, the ratios of F_f(TEM)/F_f^a revealed a picture in consistency with measurement of Löfgren et al. (2009) on samples from Forsmark and Oskarshamn, even measured in situ: the overestimation of F_f^a(DC) values is always lower than for AC frequencies. F_f^a values increase slightly with increasing AC frequencies. Moreover, it is clearly visible that the difference between the apparent formation factor F_f^a and F_f(TEM) decreases with increasing formation factor, most probably due to a smaller relative impact of surface conduction. However, the difference is not significant.
Using the electromigration method and anionic species, the influence of anion exclusion can be also studies, by using either ^{3}H through-diffusion experiments for comparison or by correcting F_f^a values. However, as F_f^a values, obtained by electrical methods, to some extent also are affected by anion exclusion, this latter approach may be difficult. The experiments using ^{3}H are planned for the next period.

Table 4: *Ratio of F_f^a/Ff(TEM) under different measurement conditions.*

Sample	AD-1	AD-1	AD-31
DC	2.6	3.2	4.9
AC 10 Hz	3.3	4.1	5.5
AC 100 Hz	3.4	4.2	5.6
AC 1 kHz	3.5	4.3	5.7
AC 2 kHz	3.6	4.3	5.8

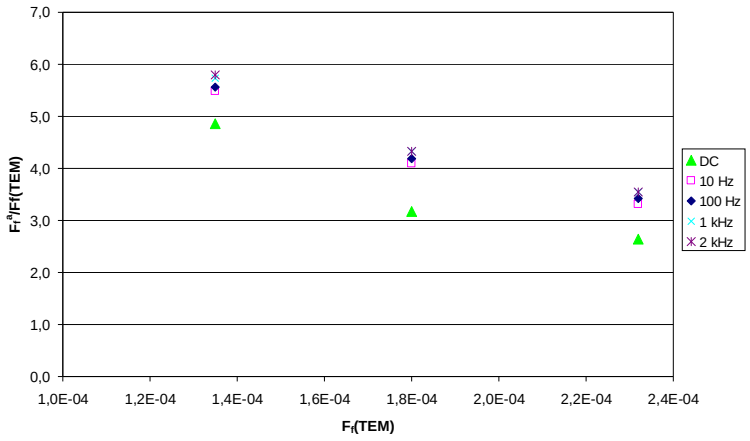

Figure 9: *Ratio of apparent formation factor F_f^a to TEM formation factor F_f with increasing F_f(TEM).*

Conclusions and future work

A modified electromigration apparatus was successfully tested for samples with different length under reference conditions. The experiments enable one to measure migration parameters (geometric formation factor F_f, apparent formation factor F_f^a and effective diffusion coefficient D_e for iodine), for Äspö diorite, even using samples with different length (10 mm, 30 mm). The results showed a rather consistent range of data, not revealing any important result on dependency of migration parameters on sample length. One has to take into account that only a limited number of disc samples were available and therefore the data set is very small.
Formation factor F_f(TEM), determined by through-electromigration method with anion (I^-) tracer is important for performance modellers namely in comparison with F_f gained using conservative tracer (^3H), comparing the extent of anionic exclusion. Formation factor F_f^a gained by resistivity measurement is important namely for laboratory verification of in-situ resistivity measurement in boreholes.
Further TEM cell extension for longer samples (50 mm, 100 mm) is under way and will be tested within the next period. It should be noted that increasing the sample length would decrease the importance of interconnections of pores that would not be connected in real rock massive, as well as the impact mechanical damage due to sawing. However, it will not tackle the artefacts of stress release and impact of mechanical damage due to drilling.
If one is concerned about the fact that the electrolyte used did not represent the real ionic strength of Äspö groundwater (0.18 M), F_f and D_e measurements should be repeated in 0.18 M electrolyte. Those are important especially if we want to compare TEM and AC/DC results with through-diffusion experiments (TD) with ^3H. TD experiments will be performed with Äspö groundwater as a solution. The comparison can bring additional information, enabling evaluation of the possible effect of anion exclusion on I^- migration. ^{36}Cl will be added to the solution as an additional anionic and conservative tracer.

Acknowledgement

The research leading to these results has received funding from the European Union's European Atomic Energy Community's (EURATOM) Seventh Framework Programme FP7/2007-2011 under grant agreement n° 269658 (CROCK project) and from the Czech Ministry of Trade and Industry under the contract FR-TI1/36.

References

Crawford J., Sidborn M. (2008). Bedrock transport properties Laxemar. Site descriptive modelling SDM-Site Forsmark. SKB R-08-48, Svensk Kärnbränslehantering AB, Stockholm, Sweden.

Löfgren M. (2004). Diffusive properties of granitic rock as measured by in-situ electrical methods, Doctoral thesis, Royal Institute of Technology Stockholm.

Löfgren M., Neretnieks I. (2006). Through electromigration: A new method of obtaining formation factors and investigating connectivity. J. of Contam. Hydrol., 87, 237-252.

Löfgren M., Večerník P., Havlová V. (2009). Studying the influence of pore water electrical conductivity on the formation factor, as estimated based on electrical methods. SKB R-09-57, Svensk Kärnbränslehantering AB, Stockholm, Sweden

Melnyk T.W., Skeet A.M.M. (1986). An improved technique for the determination of rock porosity. Can. J. Earth Sc., 23, 1068-1074.

Miller D.G. (1982). Estimation of diffusion coefficients of ions in aqueous solution. LLNL Report UCRL-533319. Lawrence Livermore National Laboratory, Livermore, California, USA.

Möri A. (2009). In situ matrix diffusion in crystalline rocks – An experimental approach. PhD thesis. University Bern.

Ohlsson Y. (2000). Studies of Ionic Diffusion in Crystalline Rock. Doctoral thesis at the Royal Institute of Technology, Stockholm, Sweden. ISBN 91-7283-025-5.

Valkiainen M., Alto H., Lehikonen H., Uusheimo K. (1996). The effect of thickness in through-diffusion experiments. Final Report. VTT Research Notes 1788, VTT Vuorimiehentie 5, Finland.

SPECIATION OF SELENIUM IN ÄSPÖ SYNTHETIC GROUNDWATER

Kateřina Videnská[1, 2*], Václava Havlová [1], Jani Vejsadů[1]

[1]Nuclear Research Institute Řež plc., Husinec-Řež 130, 250 68, Řež (CZ)
[2]Institute of Chemical Technology and Engineering Prague (CZ)

* Corresponding author: hvl@ujv.cz

Abstract

Speciation modelling was performed for selenium in Äspö synthetic goundwater. The results revealed that both oxidic and anaerobic conditions considered for batch sorption experiments can lead to formation Se(0) solid phases. The area of the solid stability field increases with increasing selenium concentration. Ca^{2+} content seems also to play a role in solid phase formation, namely in higher Se concentrations.

Introduction

Selenium belongs between elements with high relevance to safety assessment of radioactive waste disposal. ^{79}Se belongs among long-lived ($T_{1/2}$ = 3.56×10^5 yrs) and highly radiotoxic radionuclides, found in spent nuclear fuel. The element can significantly contribute to the risk due to its complicated chemistry, long life-time, high mobility and prevailing anionic character. Therefore, knowledge of selenium migration behaviour under different conditions can significantly help to improve the input into performance and safety assessment models.
Selenium is a redox-sensitive element that can occur in various oxidation states (-II, 0, +IV, +VI) depending on environment redox conditions. Specie occurrence and solubility depend on redox conditions of the environment.
The aim of the study presented was to assess potential selenium forms in Äspö groundwater if considering different total element concentrations. Tracer form, i.e. its speciation in the solution, is important for prediction of potential reactions that can appear in the batch sorption experiments in the system of tracer–solution–solid. The batch experiments with different concentration of Se(IV) and Se(VI) and crushed Äspö granodiorite under oxic and anaerobic conditions are ongoing.

Synthetic groundwater preparation and characterisation

The composition of groundwater from Äspö hard rock laboratory was provided by Heck and Schäfer (2011). As it was unrealistic to perform experiments with the real groundwater from Äspö hard rock laboratory in NRI laboratories, synthetic Äspö ground water (AGW) was prepared on the basis of KIT-INE report (Heck and Schäfer, 2011).

Synthetic groundwater was prepared adding corresponding salt amounts into distilled water. The composition was check afterwards (see Table 1). For anaerobic experiments the AGW was prepared in anaerobic box under Ar atmosphere leaving the solution to equilibrate under anaerobic conditions. Eh and pH were measured until constant values have been reached. That was reached basically after 30 days.

Table 1: *Äspö groundwater composition and synthetic groundwater (SGW) composition, prepared in NRI including comparison of calculated concentrations of chemical species with analytical results of two different batches of SGW. All values are in mg.l^{-1} N.A. means Not Analyzed.*

Species	**In-situ measured groundwater composition (mg.l^{-1}, Heck and Schäfer, 2011)**	**SGW composition (NRI, 2011), calculation**	**SGW composition, 2 different batches (mg.l^{-1}, ICP-AES, ion chromatography)**	
pH	7.8	-	7.2/8.87*	7.3
Eh (mV)	31	-	390/ 28.9*	N.A.
I (M)	0.18	0.18	0.18	0.19
Na^+	1889.9	1889.9	2000	2100
K^+	10.5	10.6	24.7	25.1
Mg^{2+}	69.4	99.7	89.3	90.5
Ca^{2+}	1135	1122.2	1210	1230
Sr^{2+}	19.9	20.2	21.3	22.5
Cl^-	4999	4909	4880	4920
F^-	1.4	1.41	1.43	1.42
Br^-	23.2	21.6	N.A.	N.A.
SO_4^{2-}	394.4	393.7	395.4	396.9
HCO_3^-	11.68	11.6	N.A.	N.A.

**Eh and pH values were measured in the anaerobic box after 30 days of GW equilibration*

Speciation modelling

Speciation modelling for selenium species in Äspö synthetic groundwater was modelled using The Geochemist's Workbench®, Professional 8.0, module Act2. Three total selenium concentrations as planned for the batch sorption experiments, were considered:
$c(Se)_{tot} = 2\times10^{-3}$ mol.l^{-1}, $c(Se)_{tot} = 2\times10^{-4}$ mol.l^{-1}, $c(Se)_{tot} = 2\times10^{-5}$ mol.l^{-1}. The conditions considered were 25 ºC and atmospheric pressure.

Results

Stability diagrams for selenium total concentrations were generated (Figure 1-3), taking into account Äspö synthetic groundwater composition (Table 1).
Under acidic conditions (pH<4) selenium is predicted to be as a solid elemental Se(0) and its field increases with increasing total selenium concentration. It is clear that experimental conditions for batch sorption experiments with Äspö groundwater (pH around 8, Eh 290 mV under oxic and 29 mV under anaerobic conditions respectively) can be favour to selenium precipitation and formation of solid phases. Moreover, the stability field of calcium selenate $CaSeO_3.2H_2O$ for $Se_{tot} = 2\times10^{-3}$ mol.l^{-1} increases the extent of solid phases under conditions considered. Eh conditions do not seem to play such a role in this case.

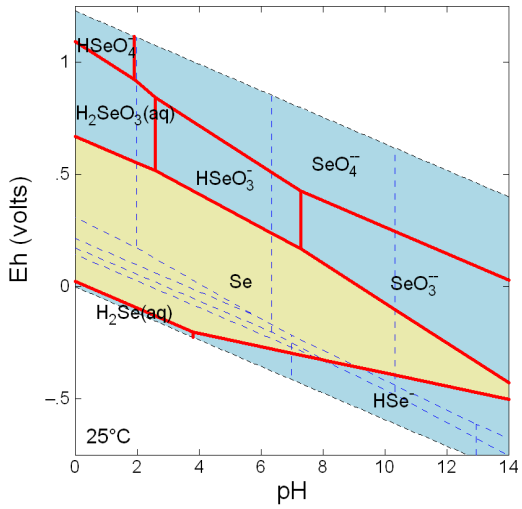

Figure 1: *Speciation of Se in Äspö synthetic groundwater. c(Se) = 2×10^{-5} mol.l^{-1}.*

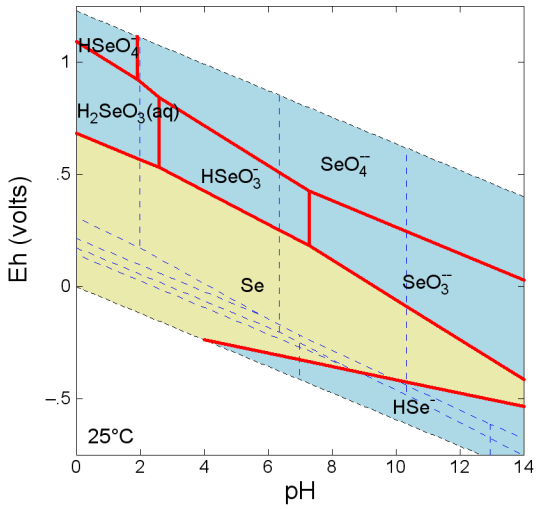

Figure 2: *Speciation of Se in Äspö synthetic groundwater. c(Se) = 2×10^{-4} mol.l^{-1}.*

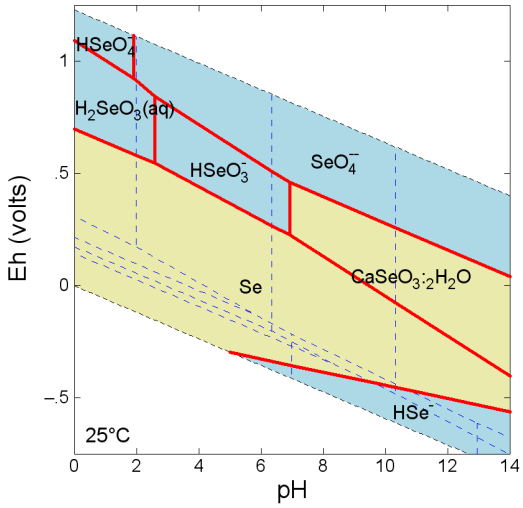

Figure 3: *Speciation of Se in Äspö synthetic groundwater. c(Se) = 2×10^{-3} mol.l^{-1}.*

On the other hand, the Se(-II) fields (as HSe^- and even dissolved H_2Se at Se(tot) = 10^{-5} mol.l^{-1}) increases with decreasing selenium total concentration.
Selenium anionic species prevail in the solution under oxidising conditions (see Figure 1-3). Oxidation state (from Se(IV) towards Se(VI)) increases with increasing Eh and pH.

Discussion

If one considers potential selenium interaction reaction, after short search in the literature it is clear that selenium sorption is still not fully understood. Some of the publications presume that selenium main sorption mechanism is a reduction and precipitation as the solid phase, either as Se(0) or Se(-II), caused namely by presence of phases containing iron (Jan et al., 2007; Hayes et al., 1987, 1988; Peak, 2006; Zhang and Sparks, 1990; Yllera del Llano et al., 1996 etc.). On the other hand, some of them refer to binding on the surface due to formation surface complexes (Jordan et al., 2011).
Jan et al. (2007) studied migration of selenium in granitic rock environment. They presented that selenium sorption is dependent of iron oxide presence where Se(IV) can be reduced to Se(0) and even Se(-II). On the other hand, Chuan-Pin (2007) claimed that reduction of selenium on elemental Se(0) was very slow. Pointeau (Pointeau et al., 2008) and Bonhoure (Bonhoure et al., 2006) reported that the most important element for selenium retention is presence of Ca^{2+} and formation of calcium complexes. That result is in consistency with formation of $CaSeO_3$ stability field at increasing Se(tot) (Figure 3). Finally, Jordan et al. (2011) reported that Se(VI) does not get reduce, being sorbed due to formation of selenium outer sphere complexes on TiO_2 surface on the whole range of pH.
The reference contradictions clearly reflect gaps that still exist in the assessment of safety relevant radionuclides. Some of those gaps, namely for crystalline rocks, were intended to be filled with series of batch sorption experiments.
Batch sorption experiments with crushed Äspö granite represent further step in the effort to study selenium retention mechanisms in crystalline rocks. The experiments will include both Se(IV) and Se(VI) oxidation states, crushed granite and Äspö synthetic groundwater. As rock samples are available also un-oxidised, a part of batch experiments will be held under anaerobic atmosphere.
According to the literature and the speciation results it can be expected that Se(VI) will not be reduced and sorbed on granitic surface during short-term experiments (days) in contradiction with Se(IV). However, as the time scale of batch experiments rises up to 6 months, some results of long-term processes, namely for Se(VI) can appear.
According to speciation modelling, it also seems that Eh conditions need not necessarily play such an important role in the case of the experiments planned. Even though Eh difference between AGW under aerobic conditions (Eh=390 mV, pH 7.2) and AGW under anaerobic conditions (Eh=28,9 mV, pH 8.87) is eminent, both experimental conditions fall into the Se(0) stability field (see Figure 1-3). However, how fast and intensive would be Se(VI) reduction and sorption is questionable. Moreover, the difference in Se(IV) reduction intensity under different conditions will be more clear after Se batch experiments under both type of environment.

Conclusions

Selenium speciation modelling gives an overview which element forms will be present in the defined solution under certain pH and Eh conditions. Hereby, the selenium speciation calculation presumes that Äspö groundwater conditions are favour for Se precipitation for all element concentrations considered (from 2×10^{-5} mol.l^{-1} to 2×10^{-3} mol.l^{-1}). However, according to the literature, it is not clear if Se(VI) reduction take place under Äspö groundwater conditions and what sorption mechanism one can presume. Speciation modelling results indicated also that difference in Eh conditions for oxic and anaerobic experiments might not play as important role as expected as for both Se(0) formation is presumed. However, namely the extent of Se(VI) reduction and sorption has to be confirmed.

Acknowledgement

The research leading to these results has received funding from the European Union's European Atomic Energy Community's (EURATOM) Seventh Framework Programme FP7/2007-2011 under grant agreement n° 269658 (CROCK project) and from the Czech Ministry of Trade and Industry under the contract FR-TI1/36.

References

Bonhoure, I., Baur, I, Wieland, E, Johnson, C. A., Scheidegger, A. M. (2006). Uptake of Se(IV/VI) oxyanions by hardened cement paste and cement minerals: An X-ray absorption spectroscopy study, Cement and Concrete Research, 36, 91-98.

Chuan-Pin, L., Yi-Lin, J., Pei-Lun, L., Yuan-Yaw, W., Shi-Ping, T., Chun-Nan, H. (2007). Anaerobic and aerobic sorption of cesium and selenium on mudrock. Journal of Radioanalytical and Nuclear Chemistry, 274, 145-151.

Hayes, K.F., Papelis, C., Leckie, J.O. (1988). Modeling ionic-strength effect on anionic adsorption at hydrous oxide solution interfaces. J. Colloid Interface Sci., 125, 717-726.

Hayes, K.F., Roe, A.L., Brown, G.E., Hodgson, K.O., Leckie, J.O., Parks, G.A. (1987). In situ X-ray absorption study of surface complexes: selenium oxyanions in a-FeOOH. Science, 238, 783-786.

Heck, S. and Schäfer, Th. (2011). Provision of new fracture bearing drill core samples obtained, handled, transported and stored under anoxic conditions, including first documentation. Deliverable 1.1. CROCK Project EC Seventh Framework Programme FP7/2007-2011 under grant agreement n° 269658 (CROCK project).

Jan, Y.L., Wang, T.H., Li, M.H., Tsai, S.Ch., Wei, Y.Y., Hsu, C.N., Teng, S.P. (2007). Evaluating adsorption ability of granite to radioselenium by chemical sequential extraction. Journal of Radioanalytical and Nuclear Chemistry, 273, 299-306.

Jordan, N., Foerstendorf, H., Weis, S., Heim, K., Schild, D., Brendler, V. (2011). Sorption of Se(VI) onto anatas: Macroscopic and microscopic characterisation. Geochimica et Cosmochimica Acta, 75, 1519-1530.

Peak, D. (2006). Adsorption mechanisms of selenium oxyanions at aluminum oxide/water interface. J. Colloid Sci., 303, 337-345.

Pointeau, I., Coreau, N., Reiller, P. E. (2008). Uptake of anionic radionuclides onto degraded cement pastes and competing effect of organic ligands. Radiochim. Acta, 96, 367–374.

Yllera de Llano, A., Bidoglio, G., Avogadro, A., Gibson, P.N., Rivas Romero, P. (1996). Redox reactions and transport of selenium through. J. Contaminant Hydrol., 21, 129-139.

Zhang, P.C. and Sparks, D.L. (1990). Kinetics of selenate and selenite desorption at the goethite water interface. Environ. Sci. Technol., 24, 1848-1856.

RADIONUCLIDE TRANPORT MODELLING BY MOLECULAR CHEMISTRY, SURFACE COMPLEXATION AND REACTIVE TRANSPORT MODELLING

Markus Olin[1*], Eini Puhakka[1], Aku Itälä[1], Merja Tanhua-Tyrkkö[1], Veli-Matti Pulkkanen[1], Henrik Nordman[1], Karita Kajanto[1], Esa Puukko[2], Lasse Koskinen[3]

[1] VTT Technical Research Centre of Finland (FI)
[2] University of Helsinki, Laboratory of Radiochemistry (FI)
[3] Posiva Oy (FI)

* Corresponding author: markus.olin@vtt.fi

Abstract

Radionuclide transport calculations, usually done for set of radionuclides, in large systems, over long periods and variations of conditions, form an essential part of any safety study of final disposal of spent nuclear fuel. Therefore, simplified models are applied in these Performance Analysis (PA) calculations. However, in order to verify and validate the simplified models and data applied by PA models, some deeper scientific analysis is needed. Accordingly, we approach the PA models from the scientific basis through three different spatial levels: molecular level, surface complexation and single fracture transport modelling.

Introduction

A final repository for spent nuclear fuel has a major demand to restrict the release and transport of radionuclides below the limits specifically given to different barriers and time scales by authorities. It is the duty of waste producer to design the repository in a way these limits and other possible demands are fulfilled in all time scales. Radionuclide transport calculations, usually done for set of radionuclides, in large systems, over long periods and variations of conditions, form an essential part of these studies. Therefore, simplified models are applied in these Performance Analysis (PA) calculations. In the KBS-3 concept, the buffer material, bentonite, can be modelled as homogeneous system, but the bedrock in Finland is fractured, and therefore, radionuclides migrate via the fracture network consisting of fractures of varying apertures and other properties. Two major retarding mechanisms in these fractures are sorption on surfaces and matrix diffusion into intact rock. In a simple model a fracture of constant aperture is modelled by Darcy's law for flow, K_d approach for sorption and Fickian diffusion into intact rock. However, in order to verify and validate the simplified models and data applied by PA models, some deeper scientific analysis based either on experimental work or modelling is needed. In our work we are applying basically three different spatial levels (Figure 1): molecular level (less than 100 atoms), surface complexation (0-dimensional, laboratory scale) and fracture transport modelling

locally in a single fracture (3D, scale: meters). Extending this approach to a long heterogeneous transport pathway would require analysing each rock type in the pathway according the approach but that is not in the scope of our work.

Usually PA studies are based on experimentally defined K_d values, selection of which may be supported by Surface Complexation Modelling (SCM). In principle, SCM can be applied in extrapolation of K_d values outside measured conditions, but the modelling must then be supported for example by molecular level modelling, which is not directly applying any macroscopic experimental data. In addition to producing experimental K_d *values* for PA purposes, the SCM can be applied to produce mechanistic sorption *models* to be applied in Reactive Transport Modelling (RTM). All these approaches together can be used in evaluation of uncertainties and applied conceptual thinking (Figure 1).

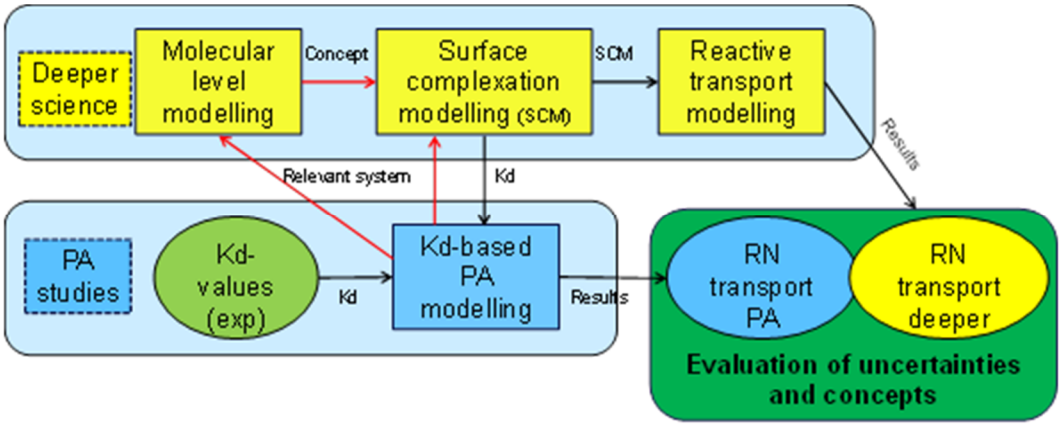

Figure 1: *Overall concept of our approach.*

Methods

Molecular level modelling

Density functional calculations are performed with the CASTEP (CAmbridge Serial Total Energy Package) code implemented into Materials Studio versions 6.0 (Accelrys, 2011). The exchange-correlation is described with Perdew, Burke and Ernzerhof version of Generalized Gradient Approximation function (GGA-PBE), and the ultrasoft pseudopotentials are used for each element. In the potential of iron, the semicore states are treated as a part of the core. The kinetic cut-off energy for a plane wave expansion of the wave function is 310 eV.

Surface complexation modelling

Surface Complexation Modelling (SCM) is done by re-fitting our earlier experimental results (Olin et al., 2008), but new work includes the extension of the modelling to 2-pK models and fitting of K_d values directly. First, both the titration curves of Luumäki biotite surface and the observed sorption percentages of Ni and Eu on Luumäki biotite are re-fitted by FITEQL 4.0 software by combination of cation exchange and 1-pK models. Second, the model fitting will be done also with a combination of Matlab scripts and COMSOL Multiphysics solvers, which is more flexible than FITEQL and

also K_d values may be fitted. Third, the both modelling approaches are compared and applied to predict K_d values for Olkiluoto biotite and rock samples, and the SCM to be applied in reactive transport modelling will be chosen after that.

Reactive Transport Modelling (RTM) and PA calculations

In PA related radionuclide transport calculations, flow field is obtained from Darcy's law in simplified fracture geometry and sorption is usually modelled by linear K_d approach. In order to test the validity of these approximations, we are applying the Navier-Stokes equations to solve the flow field in a fracture of spatially varying aperture (data from experiments) and surface complexation modelling is applied for sorption. In the PA level transport equations of radionuclides an additional diffusive term is added for dispersion, while dispersion follows from applying Navier-Stokes equations in spatially varying fracture geometry in the reactive (radionuclide) transport calculations. It is possible to mix PA and RTM options (flow, geometry and sorption) in any combination starting from pure PA modelling to full RTM modelling. We will implement RTM models into COMSOL Multiphysics, while PA calculations are done by Goldsim, REPCOM or COMSOL Multiphysics.

Results

Molecular level modelling

Biotite, which ideal chemical formula can be expressed as $K(Mg,Fe)_3AlSi_3O_{10}(OH,F)_2$, has a sheet-like structure, where the sheets are connected to each other by potassium cation layer (Accelrys, 2011). According to the density functional calculations, the optimized lattice parameters of the energetically stable biotite structure are a = 528.4 pm, b = 916.2 pm, c = 2 077.3 pm and c/a = 3.931 (Figure 2a). Construction of surface models to molecular modelling studies revealed that the smallest meaningful models are very atomic-rich, which causes long calculation times. In order to simplify model structures, it is possible to use end-members of biotite: annite and phlogopite. In annite all magnesium ions are substituted by iron ions, and on the contrary, in phlogopite iron is substituted by magnesium (Accelrys, 2011). The unit cell of annite and phlogopite is about half of that of biotite. The optimized lattice parameters of annite are a = 513.1 pm, b = 893.3 pm, c = 1 037.3 pm, and c/a = 2.022 (Figure 2b), and those of phlogopite are a = 520.2 pm, b = 905,1 pm, c = 1 036.4 pm, and c/a = 1.992 (Figure 2c). In these structures, the Si:Al ratio is 3:1, but in order to do additional simplification and receive the higher symmetry, the structures were modified so that the unit cell includes only silicon or aluminium atoms. It was concentrated on annite structures $K_2Fe(II)_6Si_8O_{20}(OH)_4$ and $K_2Fe(III)_6Al_8O_{20}(OH)_4$) and their terminal and basal surfaces.

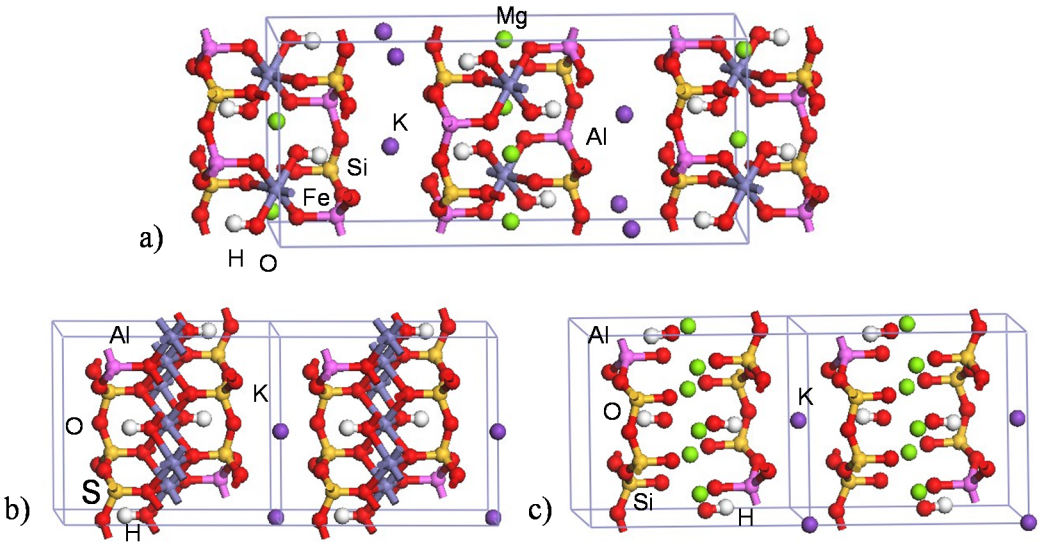

Figure 2: *Optimized unit cells for a) biotite, b) annite, and c)phlogopite.*

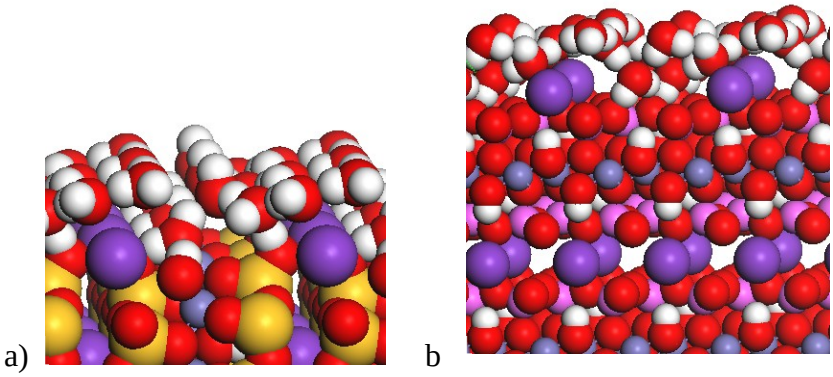

Figure 3: *The first water molecular layer on the annite surfaces: a) (110) and b) (001).*

Adsorption and dissociation of water were considered on both the terminal (110) and basal (001) surfaces. On the (110) surface, there are no empty vacancies in the coordination sphere of aluminium and/or silicon atoms. However, this site can be very reactive with water forming hydroxylated surface structure. Also, the formation of iron hydroxyls are presumable on this surface. On the (001) surface, the reactivity of the surface depends on the existence of potassium ions on the surface. Otherwise, the surface structure is rather stable. In the water adsorption studies, water molecules were adsorbed onto the surface one by one, and water molecules were allowed to find their energetically favourable positions on the surface. The target was to define the formation of the first water molecular layer.

On the ideal terminal (110) surface of annite, there are 2.2 x 10^{18} hydroxyl groups / m^2. Based on the calculations, every fifth water molecule dissociates forming surface hydroxyl groups in the adsorption of water onto the surface. On the first water molecular layer, there are 6.6 x 10^{18} surface hydroxyl groups / m^2 and 8.8 x 10^{18} water molecules / m^2 (Figure 3a).

On the ideal basal (001) surface, there are no hydroxyl groups, and water dissociation does not happen on this surface. On the first water molecular layer, there are 1.9 x 10^{18} potassium ions / m^2 and 1.3 x 10^{19} water molecules / m^2.

Surface complexation modelling

During FUNMIG project we produced experimental data for biotite surface properties and sorption of Ni and Eu on the biotite surface (Figure 4), and made only 1-pK modelling by FITEQL. Our new results by 2-pK models and COMSOL Multiphysics are not yet completed.

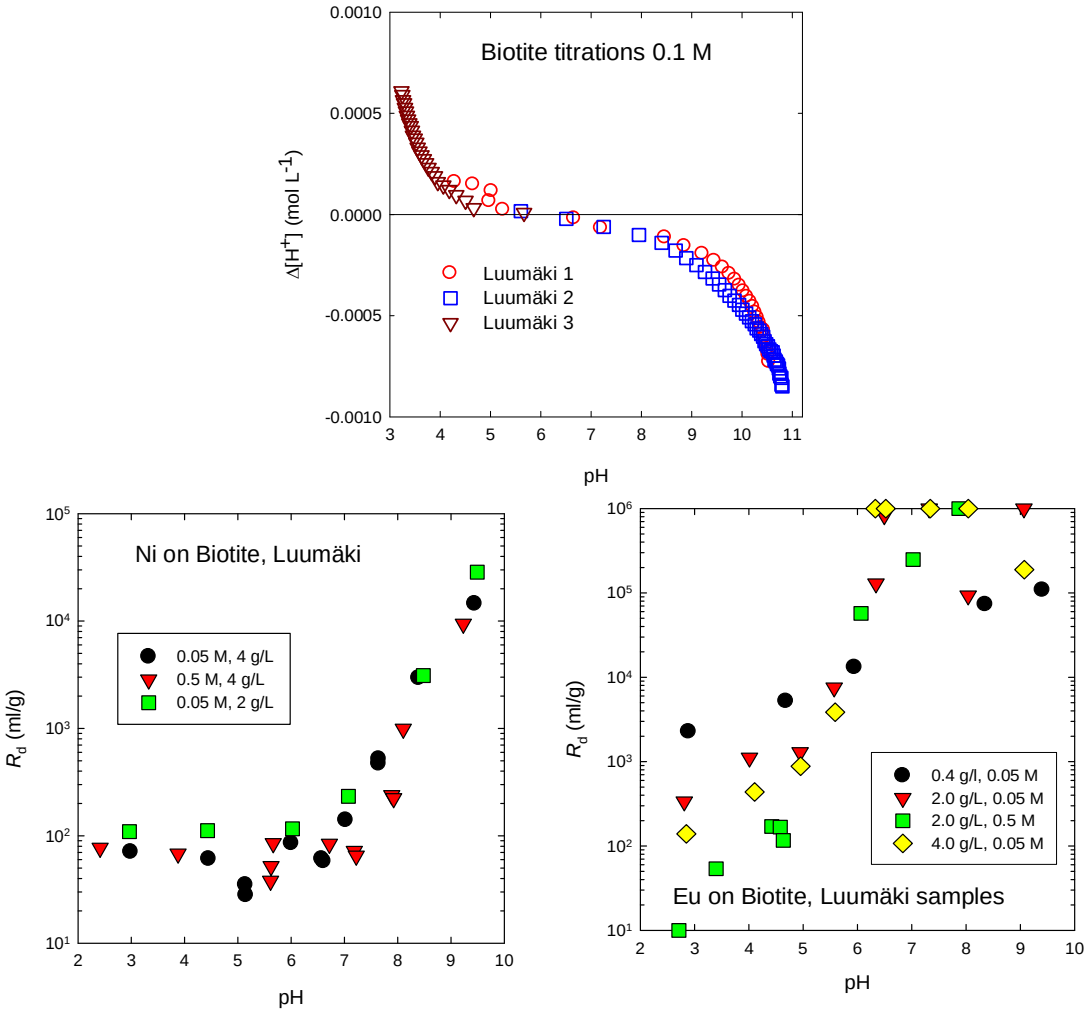

Figure 4: *Experimental data of Luumäki biotite to be applied in model fitting to Olkiluoto biotite and rock: titration (up), sorption of nickel (bottom left) and sorption of europium (bottom right) (Olin et al., 2008).*

Reactive transport modelling and PA calculations

We have modelled this far the migration of a pulse of radionuclides through a randomly generated, varying aperture fracture with Navier-Stokes flow. Different aperture distributions are examined (Figure 5).

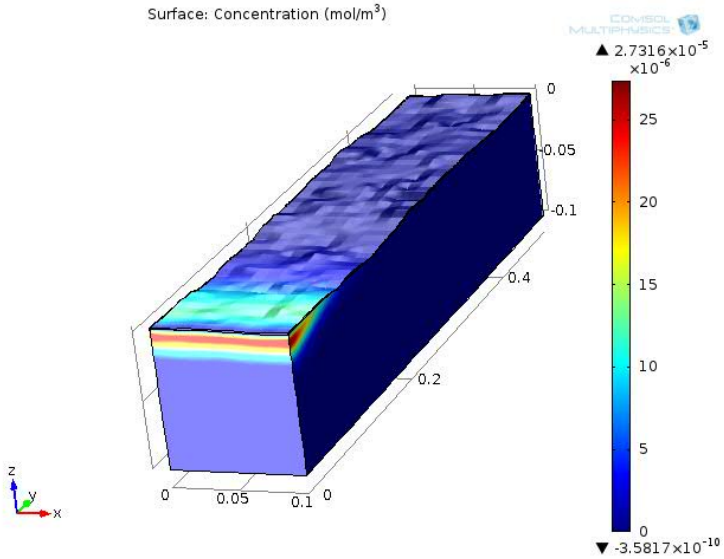

Figure 5: *An example case of radionuclide transport through a fracture, and diffusion of the nuclides into surrounding bedrock. K_d value is 10^{-3} m^3/kg and elapsed time of the pulse of radionuclides in the 1mm fracture is 10^7 s*

Conclusions and Future work

The chosen multiscale approach to extrapolate K_d values for conditions without measured data and evaluation of uncertainties in PA studies appears promising, but very tedious and time consuming work. We have results from molecular level modelling; we are developing surface complexation modelling and reactive transport modelling. After having all these ready, we can start extrapolation of K_d values and evaluation of uncertainties.

Acknowledgement

The research leading to these results has received funding from the European Union's European Atomic Energy Community's (EURATOM) Seventh Framework Programme FP7/2007-2011 under grant agreement n° 269658 (CROCK project) and the Finnish Research Programme on Nuclear Waste Management (KYT) 2011-2014 (LS-TUPER project).

References

Accelrys (2011). *MS Modeling*, Release 6.0. San Diego: Accelrys Software Inc.

Olin, M., Puukko, E., Puhakka, E., Hakanen, M., Lindberg, A. and Lehikoinen, J. (2008). Sorption on biotite. Final Annual Workshop Proceedings- 6th EC FP-FUNMIG IP, Forschungszentrum KarlsruheReport. Forschungszentrum Karlsruhe GmbH, pp. 335-343. http://bibliothek.fzk.de/zb/berichte/FZKA7461.pdf

SNAPSHOTS OF IMPORTANCE OF GEOSPHERE PARAMETERS

Henrik Nordman[1*]

[1] VTT Technical Research Centre of Finland (FI)

* Corresponding author: henrik.nodrman@vtt.fi

Abstract

Radionuclide migration calculations are an essential part of Performance Analysis (PA) of the final disposal of spent nuclear fuel. In these calculations, the migration of a large number of radionuclides is often solved simultaneously due to the chemical and the radioactive decay couplings. The number of calculated scenarios and cases is also usually large. Therefore, the PA level radionuclide transport models include a set of simplifications. One such a simplification is often done for the matrix diffusion and the radionuclide sorption into the bedrock: the geometry of a bedrock fracture is assumed plain, the diffusion is considered only in the direction perpendicular to the fracture, the water flow profile in the fracture is kept constant and the sorption is assumed linear. In this work, an analytical solution for such a system is given and a number of cases with different parameters are calculated. These results give an idea which parameters are important and serve as a basis for comparison of the PA models and the more detailed models ranging from molecular level modelling via surface complexation modelling to reactive transport models.

Geosphere conceptual model

The radionuclide transport model considers advection along fractures. Matrix diffusion is the only phenomenon assumed to lead to dispersion and retardation. After entering the rock matrix, the radionuclides also are affected by sorption (Figure 1).

Diffusion and sorption in the rock matrix are modelled according to the porous medium and linear equilibrium sorption approaches. The essential characteristics of a transport route can thus be presented by means of a single parameter (u) taking into account the distribution of groundwater flow in the fracture system and the effects of matrix diffusion. For the case where a constant water phase concentration C_0 of a stable species is prevailing at the inlet of the fracture beginning from t = 0, the water phase concentration at the distance of L in the fracture is (Vieno and Nordman, 1999):

$$C_f(L,t) = C_0 \operatorname{erfc}\left[\frac{u}{\sqrt{t}}\right], \quad (1)$$

where u is a parameter describing the transport properties of the migration route for the given species in equation 2:

$$u = \left[\varepsilon_p D_e R_p\right]^{1/2} \cdot \frac{W L}{Q} \quad (2)$$

where
ε_p is the porosity of the rock matrix (-),
D_e is the effective diffusion coefficient from the fracture into the rock matrix (m^2/s),
R_p is the retardation factor of the species in the rock matrix (-),
W is the width of the flow channel i.e. the width, over which the flow is measured (m),
L is the transport distance (m),
Q is the flow rate in the channel or over the given width (m^3/a),
t is the time (a).

N.B. In above equations the depth of matrix diffusion is considered to be unlimited, but in this work the results from FTRANS code assume limited depth of rock matrix. If the depth is deep enough in FTRANS model, the above equations are valid.

The first factor ($\varepsilon_p D_e R_p$) of the u-parameter is related to diffusion and sorption into the unlimited rock matrix and the second (WL/Q) to flow properties of the fracture. The retardation factor R_p depends on the rock properties and the volume-based distribution coefficient, K_d (m^3/kg) in the following way:

$$R_p = 1 + \frac{(1-\varepsilon_p)}{\varepsilon_p} K_d \rho_s \quad , \quad (3)$$

where ρ_s is the density of the rock (2 700 kg/m^3).

In the case of a delta pulse input of a stable species, the peak output (m_{max}) and its occurrence time (t_{max}) are:

$$t_{max} = t_w + \frac{2u^2}{3}$$
$$m_{max} \approx \frac{0.23}{u^2} \quad (4)$$

where t_w is the groundwater transit time (a).

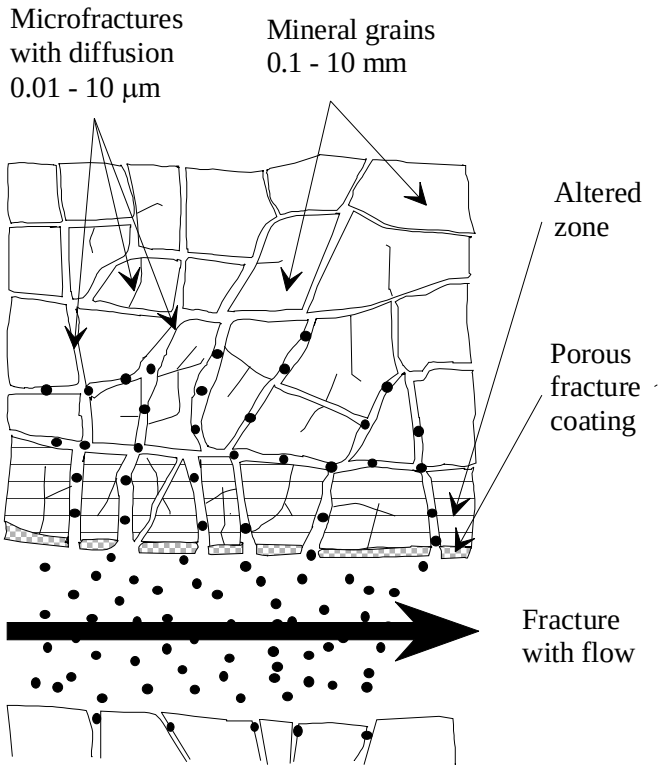

Figure 1: *Matrix diffusion concept.*

Effect of *u* parameter on certain important nuclides

In these cases the release pulses from near-field are similar to those of the high flow and large defect case Lh Q of RNT-2008 report (Nykyri et al., 2008). The finite element method FTRANS code has been used (Vieno and Nordman 1999). The code has limited depth of matrix diffusion, but equation 1 is valid if the depth is deep enough.

The selection of two nuclides and the cases are based on experience of the importance of phenomenon.

Case A: C-14, half life $5.7 \cdot 10^3$ a

C-14 is typically considered to be as a non sorbing neutral (organic) or slightly sorbing anion (carbonate) species, meaning that its retardation in geosphere is typically regarded negligible. Thus the following phenomena will be studied.

- Effect of WL/Q
- Effect of distribution coefficient K_d
- Effect of available matrix depth

The maximum release from geosphere occurs typically just after 1 000 years when the metal parts containing 33 % of C-14 inventory have corroded. Table 1 presents the results obtained by using following data for rock matrix: D_e is 10^{-14} m^2/s and porosity 0.1% corresponding to a neutral species.

From Table 1 it can be seen that for C-14 a small K_d value is sufficient to effectively decrease the peak value of the near field pulse within the geosphere. The increased allowed matrix diffusion depth has a minor effect when K_d zero (Cases C2, C3 and C4) and no effect when K_d is 0.001 (cases C6 and C7). N.B. The near field pulse is quite flat as it's a result from evenly corroding metal parts.

Table 1: *Release rate maximum of C-14 and time of maximum from geosphere with different matrix diffusion depths and flow rates. Maximum release rate from near-field was 1.31E+07 Bq/a.*

Case	Allowed depth (m)	*WL/Q* (a/m)	K_d (m^3/kg)	t_{max} (a)	max. from geosphere (Bq/a)
C1	0.1	5 000	0	1.06E+3	1.28E+7
C2	1	5 000	0	1.06E+3	1.28E+7
C3	1	50 000	0	1.06E+3	1.22E+7
C4	1	500 000	0	1.52E+3	6.90E+6
C5	0.1	50 000	0.0001	1.27E+3	5.43E+6
C6	0.1	50 000	0.001	3.16E+3	1.24E+6
C7	1	50 000	0.001	3.16E+3	1.24E+6
C8	0.1	500 000	0.001	4.32E+4	2.22E+1

Case B: Ra-226, half-life $1.6 \cdot 10^3$ a

The following phenomena will be studied

- Effect of *WL*/*Q*
- Effect of D_e and K_d values of rock matrix
- Ra-226 migration alone without its parents in U-238 chain.

The results are given in Table 2.

In case Ra2 where data is changed so that the rock matrix has a 10 times lower D_e value, the effect to release rate is dramatic. Ra-226 release rate increases from 9.14E+1 in Case Ra1 to 2.59E+3 Bq/a in Case Ra2. The importance of the u parameter can be noticed. The t_{max} from Equation 4 explains very well the decrease of release rate as Ra-226 has a short half-life of 1600 years. The increased allowed matrix diffusion depth has no effect (Cases Ra3 and Ra4).

In cases Ra1 and Ra5 the u parameter for Ra-226 is same. As WL/Q is increased in Case Ra5 the release rate of its parent nuclide Th-230 is also so the release rate of Ra-226 is slightly decreased compared to the Ra1 case. In Ra6 case where parent nuclides are not included, the release rate decreases slightly compared to case Ra5.

Table 2: *Release rate maximum of Ra-226 and time of maximum from geosphere with different flow rates. Maximum release rate from near-field was 4.13E+05 Bq/a. In the last two rows the parent nuclides are not included.*

Case	Allowed depth (m)	*WL/Q* (a/m)	K_d (m^3/kg)	D_e (m^2/s)	*u* (a½)	t_{max} *for delta pulse* (4)	t_{max} (a)	max. from geosphere (Bq/a)
Ra1	0.1	50 00	0.2	10^{-13}	206	2.8E+4	2.94E+5	9.14E+1
Ra2	0.1	5 000	0.2	10^{-14}	65	2.8E+3	2.90E+5	2.59E+4
Ra3	0.1	5 000	0.02	10^{-14}	20.6	2.8E+2	2.90E+5	1.70E+5
Ra4	1.0	5 000	0.02	10^{-14}	20.6	2.8E+2	2.90E+5	1.70E+5
Ra5	0.1	50 000	0.02	10^{-14}	206	2.8E+4	9.74E+5	8.32E+1
Ra6	0.1	50 000	0.02	10^{-14}	206	2.8E+4	2.94E+5	6.91E+1 (1
Ra7	0.1	50 000	0.2	10^{-14}	650	2.8E+5	3.14E+5	3.20E-7 (1

(1 Parent nuclides in U-238 decay chain are not included.

Conclusions and Future work

The comparison calculations, in which the sensitivity of radionuclide transport to different parameters is investigated, form an essential part of the estimation of uncertainties and sensitivities of the chosen modelling approaches. The calculations also provide a basis for comparison of the PA models and the more detailed models. Moreover, they give information about the important variables, on which phenomena the studies with the more detailed techniques, such as molecular level chemistry and reactive transport modelling, should be focused. This information is valuable since the more detailed studies are often somewhat laborious.

It can be seen from above snapshot results, that C-14 is not very sensitive to flow rate in fracture, if it is non-sorbing. This is of course the situation with more long lived non sorbing nuclides like I-129 and Cl-36 which are often important in a safety case. The Ra-226 is a bit different case. Especially in some disturbance situations with high flow e.g. post glacial rock shear case, the properties of rock matrix may be very important.

Acknowledgements

The research leading to these results has received funding from the European Union's European Atomic Energy Community's (EURATOM) Seventh Framework Programme FP7/2007-2011 under grant agreement n° 269658 (CROCK project), Posiva Oy and the Finnish Research Programme on Nuclear Waste Management (KYT) 2011-2014 (LS-TUPER project) and VTT Technical Research Centre of Finland. We thank Veli-Matti Pulkkanen for his valuable comments during finalising this article.

References

Nykyri, M., Nordman, H., Marcos, N., Löfman, J., Poteri, A., Hautojärvi, A. (2008). Radionuclide release and transport RNT-2008. Posiva Report 2008-06 Posiva Oy, Olkiluoto, Finland.

Vieno, T. and Nordman, H. (1999). Safety assessment of spent fuel disposal in Hästholmen, Kivetty, Olkiluoto and Romuvaara, TILA-99. Posiva Oy, Helsinki, Finland. Report POSIVA 99-07.

SORPTION OF U(VI) AND Np(V) ONTO DIORITE FROM ÄSPÖ HRL

Katja Schmeide*, Sylvia Gürtler, Katharina Müller, Robin Steudtner, Claudia Joseph, Frank Bok, Vinzenz Brendler

[1] Helmholtz-Zentrum Dresden-Rossendorf, Institute of Resource Ecology, P.O. Box 51 01 19, 01314 Dresden, Germany

* Corresponding author: k.schmeide@hzdr.de

Abstract

Sorption of the redox-sensitive actinides U and Np onto diorite obtained from Äspö Hard Rock Laboratory (HRL, Sweden) was studied by batch sorption experiments. The influence of various parameters, such as solid-to-liquid ratio (2 to 200 g/L), grain size (0.063 – 0.2 mm, 0.5 – 1 mm, 1 – 2 mm) and temperature (25 and 10°C), on the actinide sorption was studied under anoxic conditions (N_2) applying a synthetic Äspö groundwater (pH 7.8, I = 0.178 M). The influence of grain size on actinide sorption was also investigated under aerobic conditions ($pCO_2 = 10^{-3.5}$ atm). Applying $NaClO_4$ as background electrolyte, the actinide sorption onto diorite was studied as a function of ionic strength (I = 0.1 to 1 M, pH 7.8). Distribution coefficients, K_d values, were determined. Radionuclide speciation in solution was verified by time-resolved laser-induced fluorescence spectroscopy (TRLFS). Furthermore, the sorption of U and Np onto diorite was also studied by in situ time-resolved attenuated total reflection Fourier-transform infrared (ATR FT-IR) spectroscopy to characterize the sorbed species.

Introduction

Granitic subsurface environments are considered as potential host rock formations for the deep underground disposal of radioactive waste (Bäckblom, 1991). Sorption on mineral surfaces of the host rock is one important retardation process for radionuclides to be considered in long-term safety assessments for radioactive waste repositories. For this study, crystalline rock material from Äspö HRL was chosen. This kind of rocks has already been used for various sorption and migration studies (e.g., Kienzler et al., 2009; Park et al., 2012).
Objective of this work is to determine retention behavior of crystalline rock represented by diorite toward the redox-sensitive actinides U and Np and to identify speciation of radionuclides in solution as well as sorbed onto the rock matrix.

Results and Discussion

Characterization of the materials applied in the study

Diorite (Äspö HRL, Sweden), sampled and transported under as anoxic conditions as possible by KIT-INE, was obtained in the grain size fractions 1 – 2 mm and 0.5 – 1 mm. The material was transferred immediately into an inert gas box (N_2). There, part of the fraction 1 – 2 mm was further crushed with a swing mill (MM 2000, Retsch) and subsequently sieved with stainless steel sieves. Thereby, the fractions 0.063 – 0.2 mm and < 0.063 mm were obtained. All fractions (except < 0.063 mm) were washed with degassed Milli-Q water to remove any dust or fine material and then, dried. The Kr-BET surface areas of the various grain size fractions, determined by using a surface area and pore size analyzer (mod. Coulter SA 3100, Beckman Coulter, Fullerton, USA), are given in Table 1.

Table 1: *Specific surface areas of various grain size fractions of diorite.*

Grain size fraction (mm)	Specific surface area (m^2/g)
1 – 2	0.065 ± 0.004
0.5 – 1	0.079 ± 0.003
0.063 – 0.2	0.249 ± 0.014
< 0.063	1.583 ± 0.031

A synthetic Äspö groundwater was prepared based on the composition of the natural Äspö groundwater KA3600-F-2 (Heck and Schäfer, 2011). Its composition is given in Table 2.

Table 2: *Composition of the synthetic Äspö groundwater applied in this work.*

Element/Ion	Concentration (mol/L)
Li	7.4×10^{-5}
Na	8.2×10^{-2}
K	2.7×10^{-4}
Mg	4.1×10^{-3}
Ca	2.8×10^{-2}
Sr	2.3×10^{-4}
B	4.0×10^{-5}
F^-	7.4×10^{-5}
Cl^-	1.4×10^{-1}
Br^-	2.7×10^{-4}
SO_4^{2-}	4.1×10^{-3}
CO_3^{2-}/HCO_3^-	1.9×10^{-4}
I	0.178
pH	7.8

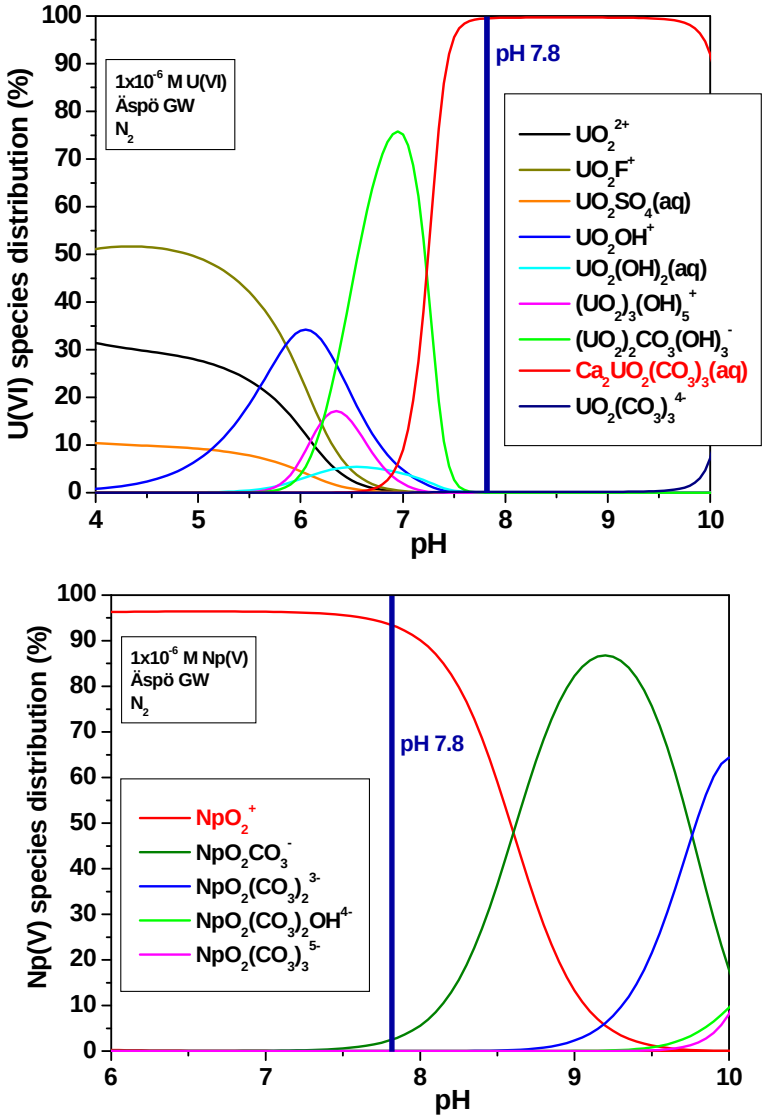

Figure 1: *U(VI) and Np(V) speciation in Äspö groundwater. Species below 5% are not plotted.*

The actinide speciation in solution was calculated with the speciation code EQ3/6 (Wolery, 1992) applying U(VI) and Np(V) thermodynamic data compiled in the OECD/NEA Thermodynamic Database (Guillaumont et al., 2003) with addition of thermodynamic data of the $Ca_2UO_2(CO_3)_3(aq)$ complex ($\log \beta°_{213} = 30.45 \pm 0.35$ (Bernhard et al., 2001)).
Figure 1 shows that the U(VI) and Np(V) speciation in the synthetic Äspö groundwater at pH 7.8 is dominated by $Ca_2UO_2(CO_3)_3(aq)$ or by NpO_2^+, respectively.
To verify the calculated U(VI) species in Äspö groundwater, Time-Resolved Laser-induced Fluorescence Spectroscopy (TRLFS) was applied. For this, luminescence spectra of the following solutions were recorded: First, of 1×10^{-5} M U(VI) equilibrated with Äspö groundwater at pH 7.8 and second, of a reference solution prepared comparable to (Bernhard et al., 2001) (1×10^{-5} M U(VI), 0.01 M $Ca(ClO_4)_2$, 0.003 M $NaHCO_3$, 0.145 M $NaClO_4$) and equilibrated at pH 7.8. Laser pulses at 266 nm with an average pulse energy of 300 µJ (Nd-YAG Laser-System (Minilite, Continuum))

were used for excitation of the U(VI) luminescence (room temp.). Figure 2 shows that the main luminescence emission bands of the U(VI) species present in Äspö groundwater correspond to the bands of the $Ca_2UO_2(CO_3)_3$(aq) species in the reference solution. The luminescence lifetime of the complexes in Äspö groundwater and in the reference solution was determined with 39.5 ns and 32.3 ns, respectively (36 ± 10 ns (Bernhard et al., 2001)). This indicates that the same U(VI) species is present in these solutions. Thus, formation of $Ca_2UO_2(CO_3)_3$(aq) in Äspö groundwater could be verified by TRLFS.

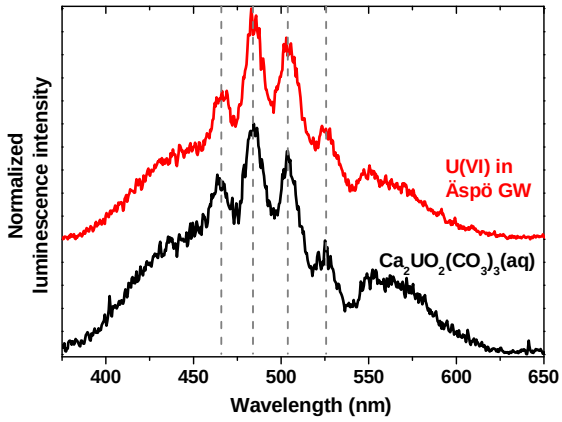

Figure 2: *U(VI) luminescence spectra of U(VI) equilibrated in Äspö groundwater ([U(VI)] = 1×10^{-5}M) and of $Ca_2UO_2(CO_3)_3$(aq).*

Batch sorption experiments

With the exception of the experiments performed under aerobic (pCO_2 = $10^{-3.5}$ atm) conditions, all other sorption and desorption experiments were performed in a glove box under anoxic conditions (N_2 atmosphere). ^{233}U(VI) and ^{237}Np(V), with an initial concentration of 1×10^{-6} M, were applied for the batch sorption experiments. Suspensions of diorite and background electrolyte were pre-equilibrated for 10 d. To start the sorption experiment, an aliquot of the respective actinide was added. Kinetic experiments, performed within the present study, have shown that a sorption time of 10 d is sufficient. The solid and liquid phases were separated by centrifugation at 4000 rpm (2880 g) for 15 min (Sigma 3K18, Sigma, Germany) and subsequent filtration of the supernatants (450 nm; polyethersulfone). Prior to filtering, the filters were rinsed with 1 mL of the sample solutions. Regular tests showed that actinide concentration in associated supernatants and filtrates was identical. The actinide concentration in solution was determined by liquid scintillation counting (LSC, Winspectral α/β, Wallac 1414, Perkin Elmer). Conventional distribution coefficients (K_d values) were determined by using the following equation:

$$K_d\,(\mathrm{L/kg}) = \frac{C_0 - C_{eq}}{C_{eq}} \frac{V}{m} \qquad (1)$$

where C_0 and C_{eq} (mol/L) are the initial and equilibrium actinide concentration in solution, V (L) represents the solution volume and m (kg) the mass of solid. The

sorption experiments were performed in triplicate, mean values with standard deviations are given in Figs. 3 to 5.

In Figure 3a, the actinide sorption in dependence on solid-to-liquid (S/L) ratio is shown for two background electrolytes. In Äspö groundwater, the K_d value for the U(VI) sorption decreases slightly between 2 and 100 g diorite/L. The K_d value for the Np(V) sorption decreases between 10 and 50 g diorite/L. Above 100 and 50 g/L, the K_d values of the U(VI) and Np(V) sorption, respectively, are nearly independent of S/L ratio. In contrast, in 0.1 M $NaClO_4$ the U(VI) sorption decreases strongly between 10 and 100 g/L. The reason for this strong decrease becomes clear considering the U(VI) species distribution in 0.1 M $NaClO_4$ as a function of the S/L ratio which is shown in Figure 3b. It was calculated for $NaClO_4$ solutions equilibrated with diorite, i.e. the concentration of ions leached out of diorite (cf. Table 3) was included. Figure 3 shows that the U(VI) speciation changes strongly from mainly $(UO_2)_3(OH)_5^+$ (at 10 g/L) to predominantly $(UO_2)_2CO_3(OH)_3^-$ (at 50 g/L) and finally to $Ca_2UO_2(CO_3)_3(aq)$ and $UO_2(CO_3)_3^{4-}$ (at 100 g/L). The U(VI) carbonates, formed in solution at higher S/L ratios, cause the reduced U(VI) sorption onto diorite. This shows that the speciation and the sorption behavior of uranium clearly depend on the chemistry of the background electrolyte, in particular on the calcium and carbonate content.

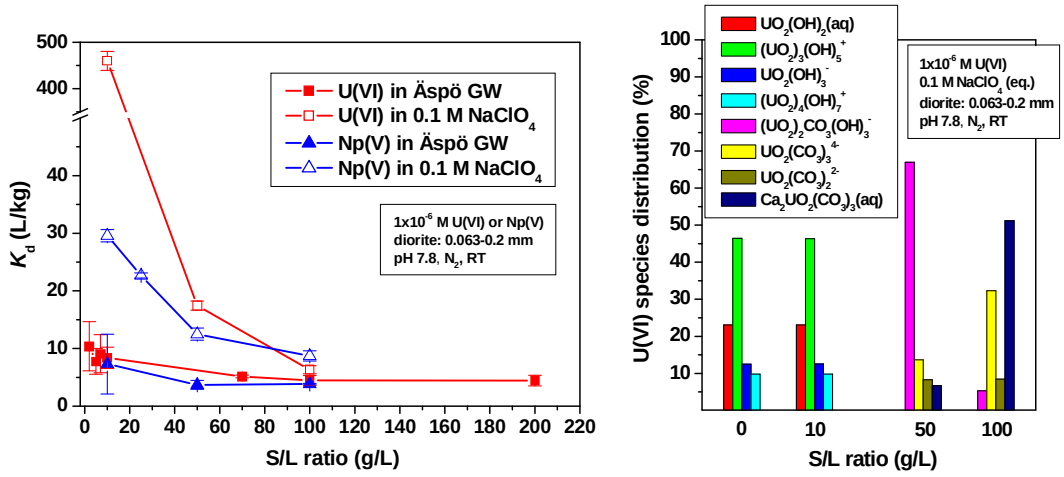

Figure 3: a) *U(VI) and Np(V) sorption onto diorite in Äspö groundwater and 0.1 M $NaClO_4$ in dependence on S/L ratio and* ***b)*** *U(VI) speciation in 0.1 M $NaClO_4$ equilibrated with various amounts of diorite (S/L: 10-100 g/L). Species below 5% are not plotted.*

In contrast to U(VI), Np(V) shows a much weaker dependence of sorption on the S/L ratio in 0.1 M $NaClO_4$. This can be attributed to the Np(V) speciation which was found to be much more stable in the equilibrated $NaClO_4$ solutions (not shown). Between 10 and 100 g diorite/L the amount of NpO_2^+ slightly decreases from 99% to 87.6%. Maximal 7.5% $NpO_2CO_3^-$ is formed at 100 g diorite/L.

U(VI) and Np(V) sorption onto diorite in dependence on grain size is shown in Figure 4. As expected, the U(VI) sorption decreases with increasing grain size which is connected with decreasing BET surface areas. Compared to U(VI) sorption under anaerobic conditions, the U(VI) sorption is lower under aerobic conditions.

Np(V) shows a different dependence of the sorption on the grain size. With increasing grain size, Np sorption remains constant or increases slightly. That means the K_d values

for Np sorption do not correlate with the surface areas of the various grain size fractions. This could mean that the surface of the grains was changed during crushing or sieving of the material. A partial oxidation of rock components during these processes effects the sorption behavior of the redox-sensitive Np, but not that of U which occurs as $Ca_2UO_2(CO_3)_3(aq)$ under the conditions of these experiments and thus, is stabilized against reduction (see below). The amount of Np that was desorbed from diorite within 2 d decreased from 88% (0.063 – 0.2 mm fraction) to 59% (1 – 2 mm fraction). This is an indication for a stronger binding of Np on the larger grains.

Table 3: *Composition of the background electrolyte (0.1 M $NaClO_4$) equilibrated with various amounts of diorite (S/L: 10-100 g/L) during 20 d contact time.*

Element/Ion	10 g/L	50 g/L	100 g/L
	Concentration (mol/L)		
Li	3.5×10^{-7}	6.5×10^{-7}	8.6×10^{-7}
Na	1.0×10^{-1}	1.1×10^{-1}	1.0×10^{-1}
K	5.2×10^{-3}	4.2×10^{-3}	3.8×10^{-3}
Mg	1.4×10^{-5}	3.9×10^{-5}	6.0×10^{-5}
Ca	1.1×10^{-4}	5.1×10^{-4}	9.0×10^{-4}
Sr	5.6×10^{-7}	2.1×10^{-6}	3.8×10^{-6}
Ba	1.8×10^{-6}	7.4×10^{-6}	1.2×10^{-5}
Al	8.6×10^{-6}	1.0×10^{-5}	7.9×10^{-6}
Mn	5.1×10^{-7}	1.0×10^{-6}	1.1×10^{-6}
Fe	1.1×10^{-6}	1.8×10^{-6}	2.0×10^{-6}
Si	3.3×10^{-5}	7.2×10^{-5}	8.0×10^{-5}
F^-	7.4×10^{-6}	1.7×10^{-5}	1.8×10^{-5}
Cl^-	5.8×10^{-3}	4.6×10^{-3}	4.1×10^{-3}
SO_4^{2-}	4.8×10^{-6}	1.7×10^{-5}	3.3×10^{-5}
CO_3^{2-}/HCO_3^-	b.d.	2.0×10^{-4}	4.6×10^{-4}

b.d. – below detection limit.

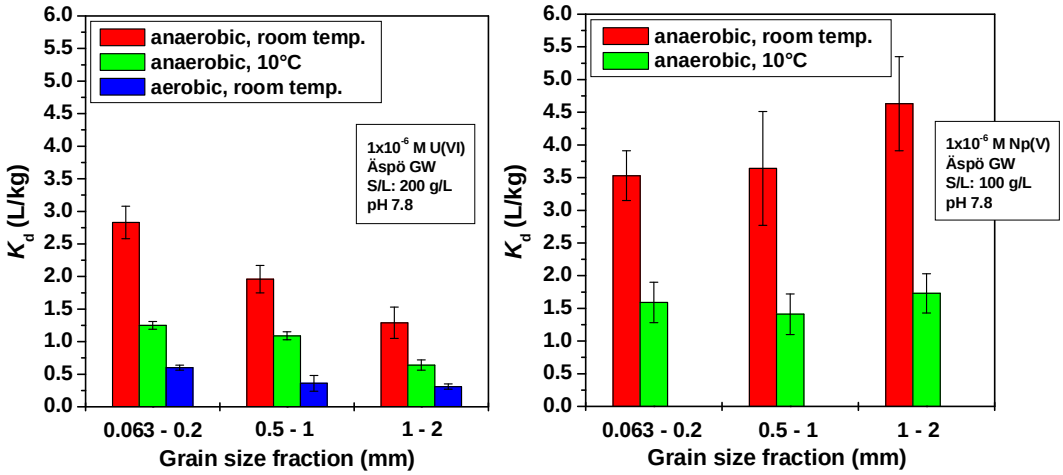

Figure 4: *U(VI) and Np(V) sorption onto diorite in Äspö groundwater in dependence on grain size, atmosphere and temperature.*

As expected, the actinide sorption determined at 10°C is lower than that at room temperature. However, the general trend in dependence on grain size, decreasing K_d for U and constant or slightly increasing K_d for Np, is visible at both temperatures.
For determination of the redox state of the sorbed U and Np, the actinides were desorbed by contacting the rock material with 1 M HCl. The redox state of actinides, sorbed onto diorite or in the supernatant solutions, was checked by means of solvent extraction using 0.5 M 2-ThenoylTrifluoroAcetone (TTA; puriss. p.a., Fluka, Taufkirchen, Germany) in xylene (puriss. p.a., Fluka) (Bertrand and Choppin, 1982). The amount of U and Np, that was not sorbed onto diorite but remained in solution, still occurred as U(VI) and Np(V). The amount of U, desorbed from diorite by 1 M HCl also occurred predominantly as U(VI). U(IV) was detected only in trace amounts. In the fraction of desorbed Np, Np(IV) was clearly detected. The data show that the amount of Np desorbed from diorite and its fraction of Np(IV) depends on desorption time.

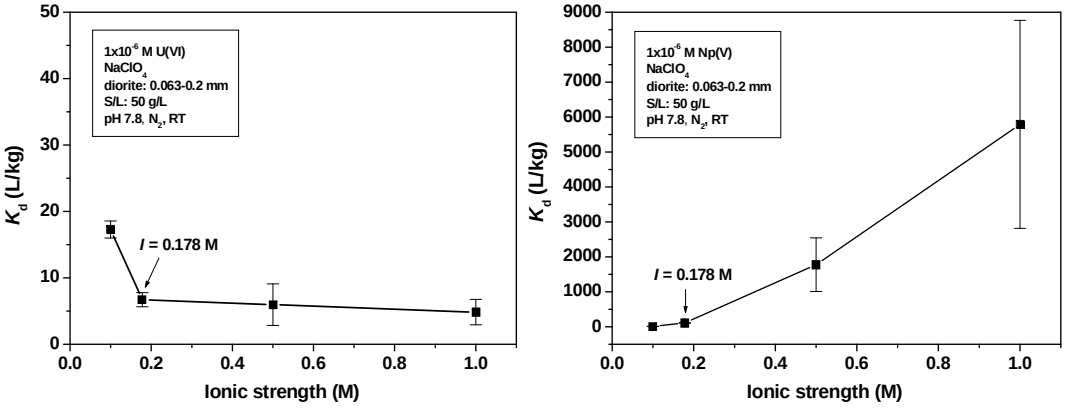

Figure 5: *U(VI) and Np(V) sorption onto diorite in $NaClO_4$ in dependence on ionic strength.*

Figure 5 shows a decreasing U(VI) sorption onto diorite in dependence on ionic strength (0.1 to 1 M $NaClO_4$). The decrease of the U(VI) sorption can again be explained by a change of the U(VI) speciation from predominantly $(UO_2)_2CO_3(OH)_3^-$ at 0.1 M $NaClO_4$

to predominantly $UO_2(CO_3)_3^{4-}$ at increased ionic strength. In contrast to U(VI), the Np(V) sorption increases strongly with ionic strength although the Np(V) speciation detected in solution is independent of ionic strength. However, desorption experiments have shown that with increasing ionic strength desorption of Np is increasingly hindered (73% → 58%, desorption time: 5 min) whereby simultaneously the Np(IV) content in the desorbed Np fractions increases.

ATR FT-IR spectroscopy

The ATR FT-IR spectroscopic study of the actinide sorption onto diorite was performed under ambient atmosphere in the case of U and in a glove box under N_2 atmosphere in the case of Np. At first, a suspension of the diorite in blank solution was prepared (2.5 g/L, < 63 µm). For the determination of U sorption, Äspö groundwater was used as blank solution and 20 µM U(VI) in Äspö groundwater as sample solution. For the determination of the Np sorption, 0.178 M NaCl in D_2O was used as blank solution and 50 µM Np(V) and 0.178 M NaCl in D_2O as sample solution. The pH value of these solutions was adjusted to 7.8 with diluted HCl and NaOH solutions (U sorption study) and diluted DCl and NaOD solutions (Np sorption study).
The performance of the in situ ATR FT-IR experiments requires a thin diorite film prepared directly on the surface of the ATR diamond crystal as a stationary phase. This is accomplished by pipetting aliquots of 5 µL of the diorite suspension (2.5 g/L) on the crystal and subsequent drying with a gentle stream of nitrogen until an average mass density of 0.2 mg/cm² was obtained. The diorite film was conditioned by flushing with the blank solution for 60 min in a flow cell (V = 200 µL) at a flow rate of 200 µL/min. The sorption reactions were induced by rinsing the stationary phase with the respective sample solution for 90 min. Subsequently, the mineral phase was flushed with a blank solution in order to verify the reversibility of the sorbed species.

U(VI) sorption

The spectrum of the conditioning shows no significant bands indicating a sufficient stable stationary phase which is indispensable for the detection of sorbed species during the following sorption process. During U(VI) sorption, increasing bands at 1525 cm^{-1}, 1356 cm^{-1}, 1020 cm^{-1} and 891 cm^{-1} are observed with sorption time (Figure 6).
Since no shift of the absorption bands occurs and the absorption bands at 891 cm^{-1} as well as at 1525 and 1356 cm^{-1} are also observed in the spectra of aqueous U(VI) solution in Äspö groundwater (Figure 7), it can be assumed that the aqueous complexes present in solution are accumulated at the mineral's surface. The band at 891 cm^{-1} represents the antisymmetric U–O stretching vibration of the uranyl ion. The bands at 1525 and 1356 cm^{-1} can be assigned to the antisymmetric and symmetric stretching vibration of the carbonate ion. Consequently, the sorption spectra indicate the accumulation of the $UO_2(CO_3)_3^{4-}$ complex at the mineral's surface. This seems to be confirmed by the band at 1020 cm^{-1} which can be most likely assigned to Si–OH surface modes which undergo significant alterations during the sorption reactions. The comparison with further minerals (SiO_2, illite) shows that similar uranium surface complexes are formed irrespective of the adsorbent. During the flushing of the diorite film with blank solution, negative bands are observed. It can be suggested that the U(VI) surface species is only weakly bound to the surfaces and can be easily released as a $UO_2(CO_3)_3^{4-}$ complex.

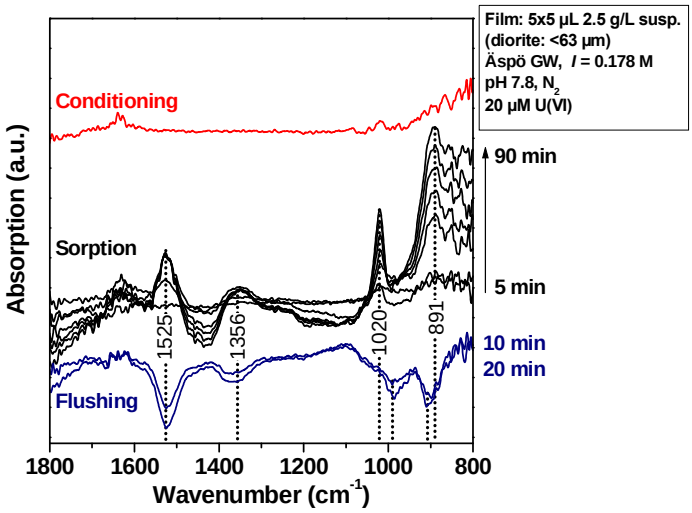

Figure 6: *In situ time-resolved ATR FT-IR spectra of U(VI) sorption onto diorite.*

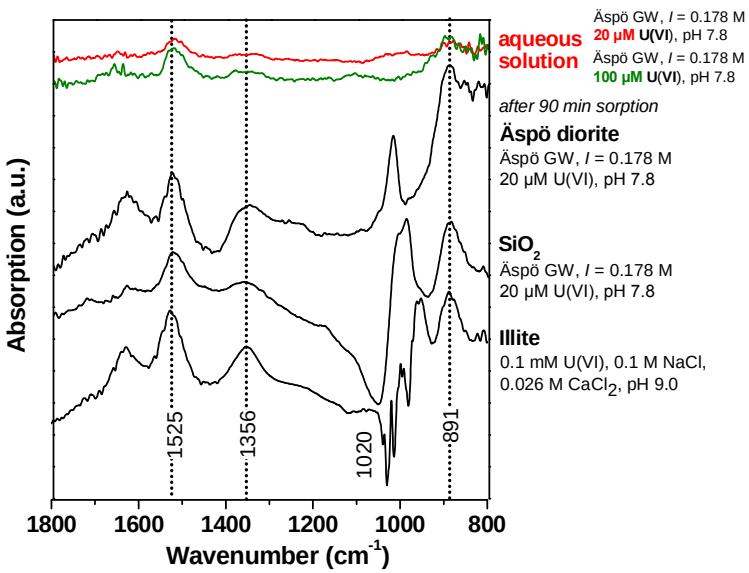

Figure 7: *ATR FT-IR spectra of U(VI) in aqueous solution and of U(VI) sorbed onto different solids.*

Np(V) sorption

In solution at pH 6, Np(V) shows an absorption band at 818 cm^{-1} representing the antisymmetric stretching vibration of NpO_2^+ (Müller et al., 2009). The increasing absorption band at 789 cm^{-1}, observed during sorption of Np(V) on diorite (Figure 8), can be attributed to NpO_2^+. A reduction of Np(V) to Np(IV) on the diorite surface to a significant extent can be excluded, since such a reduction would imply the disappearance of the neptunyl band in the IR spectrum. The absorption band at 789 cm^{-1} was also observed with increased intensities during Np sorption onto TiO_2 and SiO_2 (Figure 9). Therefore, the formation of similar surface species is suggested.

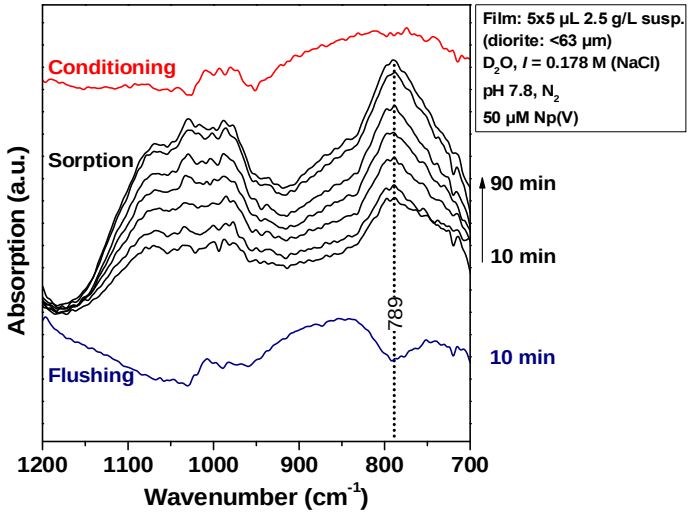

Figure 8: *In situ time-resolved ATR FT-IR spectra of Np(V) sorption onto diorite.*

Whether the sorption takes place as inner-sphere or outer-sphere sorption can not unequivocally decided yet. The negative absorption band at 789 cm^{-1} observed during the flushing step indicates the formation of weakly bound surface species. However, the weak amplitude of this spectrum might reflect a minor release of Np(V) surface species. In homology to the U(VI) sorption, an increase of the Si-O band at 1020 cm^{-1} can be observed.

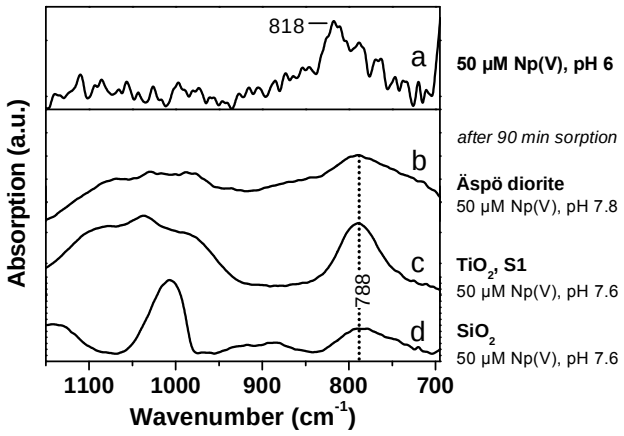

Figure 9: *ATR FT-IR spectra of Np(V) in aqueous solution and of Np(V) sorbed onto different solids.*

Conclusions

The speciation of U(VI) in solution and thus, its sorption onto diorite is strongly influenced by the groundwater composition. From the ions leached out of diorite, calcium and carbonate ions have the strongest influence. In the case of Np(V), the effect of the groundwater composition on speciation and sorption behavior is much weaker. In Äspö groundwater, sorption of U and Np onto diorite is comparable. Actinide sorption decreases with decreasing temperature.
By in situ time-resolved ATR FT-IR spectroscopy, the surface species on diorite were identified as $UO_2(CO_3)_3^{4-}$ and NpO_2^+ for the U and Np sorption, respectively.

Acknowledgement

The research leading to these results has received funding from the European Union's European Atomic Energy Community's (EURATOM) Seventh Framework Programme FP7/2007-2011 under grant agreement n° 269658 (CROCK project). We also thank KIT-INE for providing the diorite, Ch. Müller for the help in performing sorption experiments, U. Schaefer, A. Ritter and C. Eckardt for cation and anion analyses and BET determinations.

References

Bäckblom, G. (1991). The Äspö hard rock laboratory – a step towards the Swedish final repository for high-level radioactive waste. Tunn. Undergr. Space Technol., 4, 463.

Bernhard, G., Geipel, G., Reich, T., Brendler, V., Amayri, S., Nitsche, H. (2001). Uranyl(VI) carbonate complex formation: Validation of the $Ca_2UO_2(CO_3)_3$(aq.) species. Radiochim. Acta, 89, 511-518.

Bertrand, P.A., Choppin, G.R. (1982). Separation of actinides in different oxidation states by solvent extraction. Radiochim. Acta, 31, 135-137.

Guillaumont, R., Fanghänel, Th., Fuger, J., Grenthe, I., Neck, V., Palmer, D.A., Rand, M.H. (2003). Update on the chemical thermodynamics of uranium, neptunium, plutonium, americium and technetium. Chemical Thermodynamics, vol. 5. (OECD Nuclear Energy Agency, ed.) Elsevier, Amsterdam.

Heck, St., Schäfer, Th. (2011). Short Note: CP CROCK groundwater sample characterization, KIT-INE.

Kienzler, B., Vejmelka, P., Römer, J., Schild, D., Jansson, M. (2009). Actinide migration in fractures of granite host rock: Laboratory and in situ investigations. Nucl. Technol., 165, 223-240.

Müller, K., Foerstendorf, H., Brendler, V., Bernhard, G. (2009). Sorption of Np(V) onto TiO_2, SiO_2, and ZnO: An in situ ATR FT-IR spectroscopic study. Environ. Sci. Technol., 43, 7665-7670.

Park, C.K., Kienzler, B., Vejmelka, P., Jeong, J.T. (2012). Modeling and analysis of the migration of HTO and ^{237}Np in a fractured granite core at the Äspö hard rock laboratory. Radiochim. Acta, 100, 197-205.

Wolery, T.J. (1992). EQ3/6. A software package for the geochemical modeling of aqueous systems. Lawrence Livermore National Laboratory Report UCRL-MA-110662, Part 1, Livermore, USA.

REAL SYSTEM ANALYSIS

John Smellie[1*]

[1] CONTERRA (SE)

* Corresponding author: john.smellie@conterra.se

Objective.

The objective of this work is to supply all relevant background sources of the analytical and field porewater data, together with interpretations, from the Swedish site characterisation programme with a focus on matrix diffusion.

Background.

Two areas in Sweden have been studied to identify a suitable site for deep geological disposal of nuclear spent fuel waste. Both sites, Forsmark and Laxemar, are located close to the Baltic Sea coast and the hydrogeochemistry is documented in Laaksoharju et al. (2008, 2009) and Smellie et al. (2008). Several groundwater types which are now present in the bedrock can be associated with past climatic events in the late Pleistocene, including interglaciations, glaciations, deglaciations, and associated shore level displacements in connection with marine/non-marine transgressions and regressions. Among these, the last glaciation and postglacial period is the most important for the groundwater development in the Fennoscandian Shield. Generally, to varying degrees, both sites have been subjected to the same palaeoclimatic conditions following the last glaciation, i.e. since the last deglaciation (18,000-8000 BC). The climatic changes and resulting different groundwater types introduced into the bedrock since the last deglaciation stage to present conditions are well documented. In chronological order the most important are dilute glacial meltwaters, brackish waters (Littorina/Baltic Sea) and recent fresh waters. These successive water intrusions have interacted to a various extent with the resident porewaters which can be considered an archive of the past hydrogeological (and therefore hydrogeochemical) history at the Forsmark and Laxemar sites.

The quantitative interpretation of the porewater-fracture groundwater interaction as a function of time is complex and depends on many factors such as the transport properties in the rock matrix, the distance to the nearest water conducting fracture, and the time period of fracture groundwater circulation with constant chemical and isotopic conditions (Waber et al., 2008, 2009; Waber and Smellie, 2009, and publications therein). Most demanding in such an interpretation is the case if a transient state (i.e. a difference in the chemical and isotopic composition between porewater and fracture groundwater) is established because of unknown conditions at the start of the interaction

(initial conditions). In the situation of a steady state, on the other hand, at least a minimum and maximum time of interaction can be deduced more easily. In both cases, however, changes in the boundary conditions (i.e. the fracture groundwater composition) may become masked and superimposed in the course of the interaction. Furthermore, changes in the boundary conditions might not be equally present for all components. For example, the Cl^- concentration in fracture groundwater might grossly change with time while the water stable isotope composition remains similar as, for example, in the case of Littorina and Baltic Sea water, or the Cl^- concentration might remain similar whereas the water isotope composition changes dramatically as, for example, in the case of present day meteoric and past glacial meltwater infiltration.

The calculation of the concentration of chloride (or any other chemically conservative element) in the porewater (from out-diffusion concentrations) is inversely proportional to the water content in the rock sample in question. The uncertainty of the indirectly derived porewater concentrations thus strongly depends on the accuracy of the water content determination and the degree to which the measured values represent *in-situ* conditions. The reliability of this method is addressed in Waber and Smellie (2008) and Waber et al. (2008, 2009, 2011).

The Forsmark Site.

The Forsmark site (Figure 1) hydrogeologically can be subdivided into the 'footwall' (apart from the upper 150 m the footwall is basically characterised by low transmissivity and a low frequency of single discrete water conducting fractures) and the 'hanging wall' (characterised by a highly transmissive dynamic flow system to about 500 m depth and a high frequency of water conducting fractures including large subvertical deformation zones). The separation of the footwall and hanging wall in Figure 1 is denoted by the major deformation zones A2, F1 and NE65; these two hydraulic regimes reflect a contrasting palaeohydrogeological evolution in the Forsmark site.

Generally at Forsmark, depending on the distance to the nearest water conducting fracture and the depth of the rock sample, the porewater preserves signatures of exchange with fracture groundwaters during Holocene, Pleistocene and pre-Pleistocene times (Waber et al., 2008). Furthermore, solute transport in the intact rock matrix appears to be dominated by diffusion, and matrix diffusion was identified to occur at least over several decametres into the rock matrix. Experimentally derived average pore diffusion coefficients of Cl^- for the major rock types at a temperature of 25 °C are: metagranite to granodiorite = 1.2×10^{-10} $m^2/s \pm 0.40 \times 10^{-10}$ m^2/s (n = 21), granodiorite to tonalite = 8.1×10^{-11} m^2/s (n = 1), aplitic granite = 9.4×10^{-11} $m^2/s \pm 4.2 \times 10^{-12}$ m^2/s (n = 5) and fine-grained granite = 1.1×10^{-10} $m^2/s \pm 0.38 \times 10^{-10}$ m^2/s (n = 3).

The footwall.

With respect to the porewater, the following characteristics can be noted:

- In the porewaters occurring locally in the shallowest levels down to about 200 m depth, only a weak influence of Holocene time fracture groundwater is

developed that can be associated to the exchange with brackish marine Littorina type fracture groundwater.

- At intermediate depths below 200 m, porewater is dilute to moderately brackish in composition with stable isotope signatures depleted in the heavy isotopes down to about 640 m depth. A transient state with respect to higher mineralised fracture groundwater is established. These porewaters have evolved from pre-Pleistocene meteoric to brackish fracture groundwater of warm climate origin and support the very long average residence times derived for some groundwaters from this area.
- At the greatest depths sampled (>700 m), the origin of the saline Ca-Na-Cl type porewater cannot be related to any fracture groundwater because of the absence of such data. Their origin is, however, even older than that of the brackish type porewaters at intermediate depths.
- In conclusion, the porewater composition of the footwall bedrock suggests an evolution with a well developed component of rock-water interaction in a weakly active hydraulic system (mainly limited to the shallow zone) at least during Holocene and Pleistocene times.

The hanging wall.

- Down to about 700 m, the porewater is generally dilute and has characteristic signatures of interaction with glacial and brackish marine type fracture groundwaters. Compositional changes are related to the fracture frequency (mainly deformation zones F1 and A2; Figure 1) and do not show a regular distribution with depth.
- The porewater composition indicates that the system became essentially saturated with dilute glacial type water after the last glaciation (Weichselian) and such cold climate glacial water was circulating for a considerable time period in the fractures down to more than 500 m depth. Since the last deglaciation, this cold climate porewater signature has become overprinted with a brackish marine Littorina type signature as indicated by Cl^-, Mg^{2+} and $\delta^{18}O$ in porewaters sampled closer to the conducting fracture.
- In the shallow zone of the hanging wall bedrock, the brackish marine Littorina and/or Baltic Sea signature is now becoming overprinted by the circulation of present day meteoric groundwaters.
- In conclusion, the porewater is dominated by rapid exchange with fracture groundwater within a few thousands of years in a hydraulically very active system.

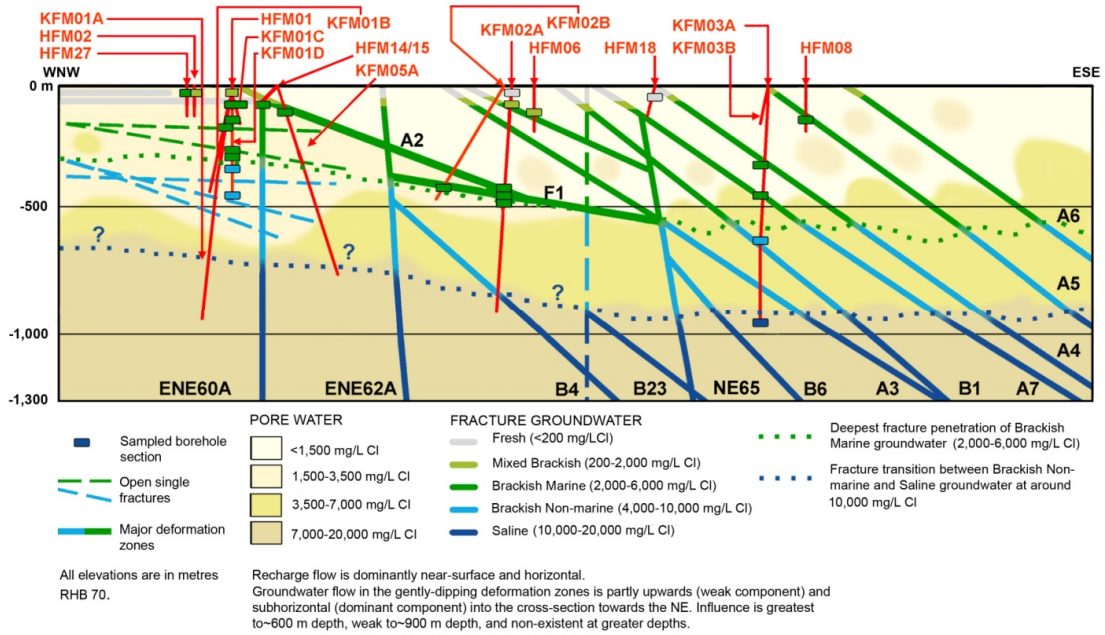

Figure 1: *Forsmark site visualisation of the hydrochemical data along cross-section WNW-ESE (Smellie et al., 2008). Shown are: a) the location of the boreholes and the sections which have undergone hydrochemical sampling, b) the main colour coded fracture groundwater types which characterise the site, c) the chloride distribution with depth along the major deformation zones and minor single open fractures, and d) the chloride subdivisions of the rock matrix porewater. The groundwater flow directions are explained in the legend. The dotted lines in different colours crossing the section represent the approximate penetration depths of (or extrapolation of) the various groundwater types along hydraulically-active deformation zones. (Cross-section length = 6,790 metres).*

The Laxemar site.

The regional groundwater flow in the Laxemar subarea, in contrast with Forsmark, is strongly driven by topography with a general gradient from the high elevated areas in the west to the Baltic Sea in the east. The flow pattern is largely governed by the mutual connections of the deformation zones which characterise the region. The topography also results in localised areas of recharge/discharge which represent groundwater circulation cells of varying depth and extent, and therefore of varying ages. The maximum effect of groundwater circulation is considered to be down to depths of around 1,000 m (Figure 2).

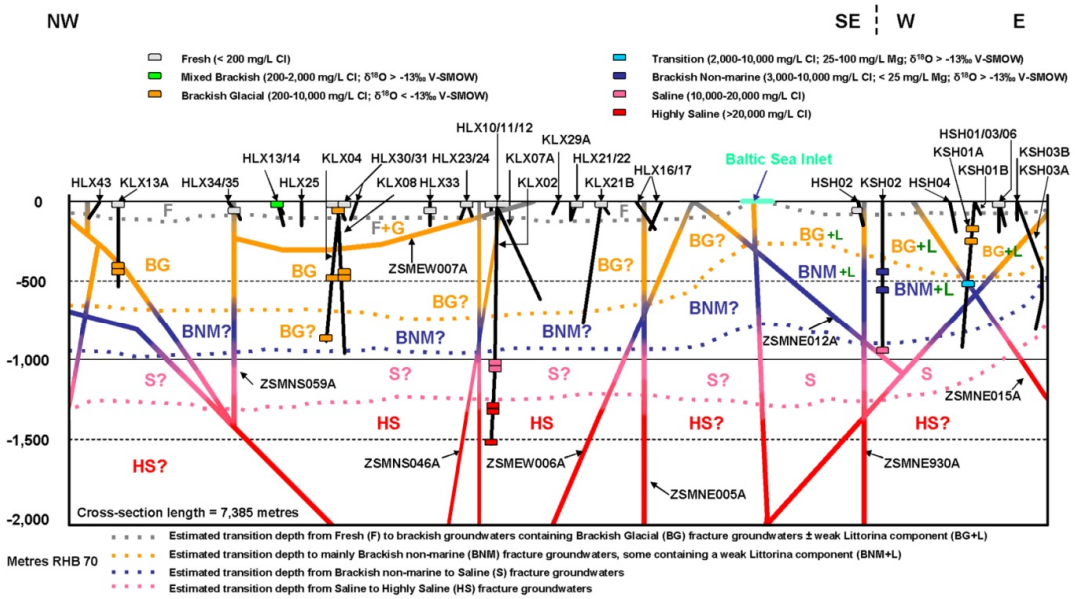

Figure 2: *Approximately NW-SE/W-E cross-section through the Laxemar-Simpevarp area (Laaksoharju et al., 2009). Shown are: a) the location of the boreholes and the sections which have undergone hydrochemical sampling, b) the main fracture groundwater types (colour coded) which characterise the site, and c) the chloride distribution with depth along the major deformation zones. The dotted lines in different colours represent the approximate depths of penetration of the various fracture groundwater types along hydraulically active deformation zones. The main regional groundwater flow direction is from the west (recharge) to the east (discharge), approximately parallel to the section. (Cross-section length = 7,385 metres).*

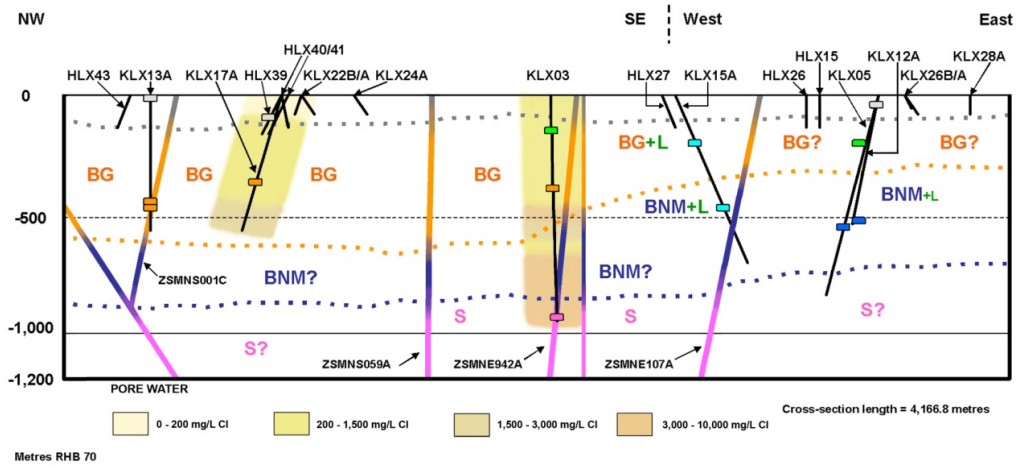

Figure 3: *Different orientated section (Laaksoharju et al., 2009) to illustrate the limited porewater data and their relationship to the main fracture groundwater types (cf. Figure 2 text for description).*

In common with Forsmark, depending on the distance to the nearest water conducting fracture and the depth of the rock sample, the porewater at the Laxemar site preserves signatures of exchange with fracture groundwaters during Holocene, Pleistocene and pre-Pleistocene times (Waber et al., 2009). However, the Littorina Sea signatures are much weaker because of greater topography and hydraulic gradients resulting in a diluted Littorina end-member water which was limited in the extent of infiltrating into the bedrock. Furthermore, last deglaciation meltwaters and present meteoric groundwaters extend to much greater depths than at Forsmark because the bedrock is more fractured and hydraulically transmissive.

Experimentally derived average pore diffusion coefficients of Cl^- for the major rock types at a temperature of 25 °C are: Ävrö granite = 6.3×10^{-11} $m^2/s \pm 2.9 \times 10^{-11}$ m^2/s (n = 9), quartz monzodiorite = 8.4×10^{-11} $m^2/s \pm 5.5 \times 10^{-11}$ m^2/s (n = 3), diorite = 3.8×10^{-11} $m^2/s \pm 4.1 \times 10^{-12}$ m^2/s (n = 2).

With respect to the porewater, the following characteristics can be noted:

- Matrix diffusion was identified to occur at least over several decametres into the rock matrix.
- There is some evidence of warmer climate meteoric influences from temperature maximums during the Pleistocene prior to the last glaciation.
- Down to depths of about 400 m, the porewater is of a dilute Na-HCO_3 type and present-day meteoric influence dominates in porewaters.
- Cold climate influence from the last glaciation occurs in the still dilute Na-HCO_3 type porewaters between about 135-350 m depth and sometimes down to about 500 m depth.
- A distinct change in chemical and isotopic composition to a highly mineralised Na-Ca-SO_4 and Ca-Na-SO_4 type porewater is observed between about 430-550 m depth and sometimes to 600-750 m depth. One possibility is that these signatures may have evolved from fracture groundwaters influenced by permafrost-related freeze-out processes.
- Modelling of a porewater profile extending from a conducting fracture into the intact rock matrix (Waber et al., 2008, 2009, 2012) indicated that changes in fracture groundwater composition during Holocene time left their (superimposed) signatures a few metres into the rock matrix. Further into the rock matrix, older (i.e. prior to the last glaciation), warm climate signatures are still preserved, lending additional support to the hydrogeochemical conceptual model.

Acknowledgement

The research leading to these results has received funding from the European Union's European Atomic Energy Community's (EURATOM) Seventh Framework Programme FP7/2007-2011 under grant agreement n° 269658 (CROCK project).

References

Laaksoharju, M., Smellie, J., Tullborg, E-L., Gimeno, M., Hallbek, L., Molinero, J. and Waber, N. (2008). Bedrock hydrogeochemistry Forsmark. Site descriptive modelling SDM-Site Forsmark. SKB R-Report (R-08-47), SKB, Stockholm, Sweden.

Laaksoharju, M., Smellie, J., Tullborg, E-L., Wallin, B., Drake, H., Gascoyne, M., Gimeno, M., Gurban, I., Hallbeck, L., Molinero, J., Nilsson, A-C. and Waber, N. (2009). Bedrock hydrogeochemistry Laxemar, Site descriptive model, SDM-Site Laxemar. SKB R-Report (R-08-93) SKB, Stockholm, Sweden.

Smellie, J., Tullborg, E-L., Nilsson, A-C., Gimeno, M., Sandström, B. Waber, N. and Gascoyne, M. (2008). Hydrogeochemical evaluation. Forsmark area (version 2.2/2.3). SKB R-Report (R-08-84), SKB, Stockholm, Sweden.

Waber, H.N., Gimmi, T. and Smellie, J.A.T. (2008). Porewater in the rock matrix. Site descriptive modelling, SDM-site Forsmark. SKB R-Report (R-08-105), SKB, Stockholm, Sweden.

Waber, H.N., Gimmi, T. and Smellie, J.A.T. (2011). Effects of drilling and stress release on transport properties and porewater chemistry of crystalline rocks. Journal of Hydrology, 405, 316-332.

Waber, H.N., Gimmi T. and Smellie, J.A.T. (2012). Reconstruction of palaeoinfiltration during the Holocene using porewater data (Laxemar, Sweden). Geochimica et Cosmochimica Acta. (In Press)

Waber, H.N., Gimmi, T., Smellie, J.A.T. and deHaller, A. (2009). Porewater in the rock matrix. Site descriptive modelling. SDM-Site Laxemar. SKB R-Report (R-08-112), SKB, Stockholm, Sweden.

Waber, H.N. and Smellie, J.A.T. (2008). Characterisation of porewater in crystalline rocks. Applied Geochemistry, 23, 1834-1861.

Waber, H.N. and Smellie, J.A.T. (2009). Forsmark site investigation. Borehole KFM02B. Part I: Diffusion experiments and porewater data. SKB P-Report (P-09-14), SKB, Stockholm, Sweden.

URANIUM RETENTION UNDER ANOXIC CONDITIONS ON ÄSPÖ DIORITE: FIRST MICRO-SCALE ANALYSES

Ursula Alonso[1*], Tiziana Missana[2], Alessandro Patelli[2], Valentino Rigato[3], Daniele Ceccato[3]

[1] CIEMAT (ES)
[2] CIVEN (I)
[3] INFN-LNL (I)

* Corresponding author: ursula.alonso@ciemat.es

Abstract

This study presents first results on uranium retention on diorite samples from the Äspö underground research laboratory, handled, transported and stored under anoxic conditions. Experiments were carried out by micro-Particle induced X-ray Emission analyses that allow visualizing and quantifying radionuclide surface distribution, at a mineral scale, in a heterogeneous rock surface.

Introduction

Performance assessment studies of deep geological repositories for high-level radioactive waste are very sensitive to the selection of radionuclide retention parameters within the repository barriers. Retention is generally described by a single distribution coefficient (Kd) obtained on powder material, under certain experimental conditions, that may not be fully representative, especially in high heterogeneous materials as crystalline rocks. It is therefore required to develop methodologies for decreasing the uncertainties related to the selection of retention data on crystalline rock.
To provide sound sorption values, distribution coefficients measured on powder (Kd) must be related to coefficients on intact rocks (Ka), but very few radionuclide retention data measured on intact rock surface are available.
To perform the experiments under anoxic conditions, from the granite extraction to the sorption studies, is also considered particularly relevant, because retention mechanisms highly depend on RN speciation, and the same element under different oxidation states can be mobile or immobile.
This study presents the first micro-scale analyses carried out, by ion beam technique micro-Particle Induced X-Ray Emission (μPIXE), on rock samples from the Äspö underground research laboratory (Sweden) extracted, handled and transported to CIEMAT (Spain) under anoxic conditions (KIT-INE, 2011). μPIXE is a very sensitive technique that allows quantifying elemental composition on rock surface and therefore adequate to characterize a heterogeneous material as granitoids. Moreover, previous experiments demonstrated that μPIXE is a powerful technique to visualize and quantify the retention of contaminants on heterogeneous rock surface, at mineral scale (Alonso et al., 2004).

Preliminary rock characterization and first analyses on uranium surface retention are presented. Special emphasis was put on preserving reducing conditions during sorption experiments and transportation to the nuclear microprobe facility of the Laboratori Nazionali di Legnaro (LNL-INFN, Italy), where μPIXE measurements were carried out. The ultimate goal of this type of study is to relate the distribution coefficients measured on the rock surface (Ka) with bulk distribution coefficients (Kd) measured in the same solid samples.

Experimental set-up

Drill cores were sampled at the Äspö underground research laboratory, handled, transported and stored under anoxic conditions (KIT-INE, 2011). For μPIXE analyses, rock sheets (cm^2 area and a 6.60 mm thick) were cut, inside a glove box, from the rock discs provided from Core #2-3, that corresponds to fresh unaltered diorite (KIT-INE, 2011). Figure 1a shows a picture of the typical diorite sample used for retention experiments by micro-scale analyses.

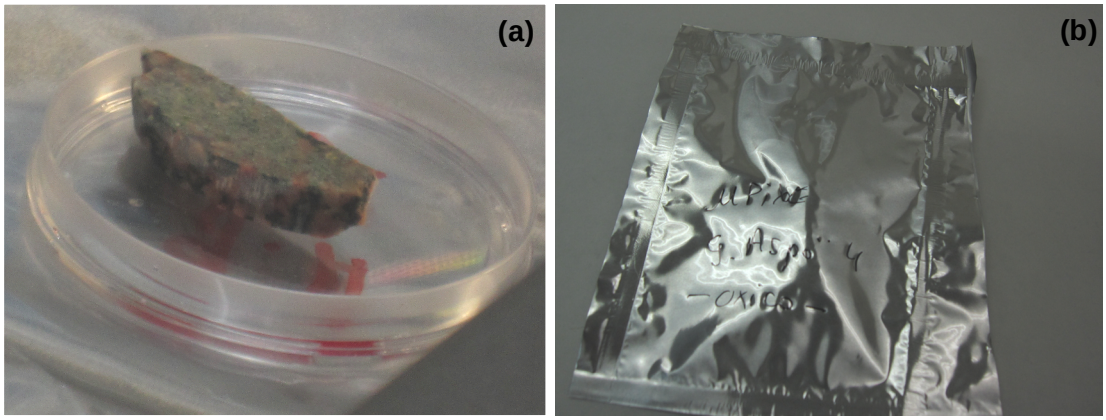

***Figure 1: (a)** Äspö sample for μPIXE experiments within the glove box. **(b)** Sample packing prepared under vacuum, inside the glove box.*

Prior to sorption experiments, rock samples were immersed during one day in 10 mL of Aspö synthetic water (pH 6.51, conductivity 14.40 mS/cm) prepared following the groundwater composition described in (Heck and Schäfer, 2011). Some samples were left, without tracer, for rock characterisation.
Sorption experiments were carried out under anoxic conditions inside a glove box (N_2+CO_2 atmosphere). Uranium solution ($UO_2(NO_3)_6$) was added to a final concentration of 10^{-3} M. This rather high concentration was used to improve tracer detection by μPIXE analyses. Upon uranium addition, pH is acidified and final pH were around 6.2 ± 0.3. Sorption experiments lasted 10 days. Experiments were done in triplicate and the average distribution coefficient (Kd) was determined measuring the activity remaining in solution. The average distribution coefficient measured was Kd = 4.4 ± 0.6 mL/g.
Before μPIXE measurements, samples were cleaned with deionised water and later with ethanol, dried and packed inside the glove box under vacuum, as can be seen in Figure 1b.
In each rock sample, several areas (2 mm x 2 mm) were analyzed by the nuclear ion beam technique micro-Particle Induced X- Ray Emission (μPIXE) (Johansson et al.,

1995) at the LNL-INFN laboratories (Italy). Samples were irradiated with 2 MeV protons with a beam size of around 4 μm^2, at perpendicular incidence. The typical beam currents ranged between 700 pA and 1 nA. A Ge detector ORTEC IGLET-X with a 170 eV maximum nominal resolution was used for the X-ray detection. To enhance the sensibility to heavy elements, measurements were carried out with an Al filter 113 μm thick with a hole in the centre that allows passing no more than 0.6 % of the total signal. The collected charge for each measurement was about 5-6 μC. The spatial resolution was 2 μm.
The μPIXE technique allows mapping of a studied area to obtain elemental distribution maps, so that main minerals and tracers distribution can be visualised. For quantitative analyses, the maps are processed with the Mappix code (Ceccato, 2009) to obtain the individual PIXE spectra on selected regions (0.2 - 0.01 mm^2 areas). The area (in m^2) of any of the selected regions in each image was recorded.
Quantitative analyses were carried out with the windows version of GUPIX (Maxwell et al., 1995) that fits the characteristic X- Ray peak intensities, recorded in each PIXE spectrum, to convert them to relative elemental concentrations (Johansson et al., 1995). Both the mineral composition and the retained uranium concentration can be obtained. The average distribution coefficients (Ka) on selected regions are calculated as described in (Alonso et al., 2009).

Results

μPIXE analyses carried out on Äspö diorite samples, without any tracer, showed areas with major presence of plagioclase, biotite, titanite and quartz. Minerals identified as hornblende type, apatite or zircon were as well detected. Precise mineral composition of the studied samples is not yet available but the present analyses are in agreement to the typical mineralogy reported for Äspo diorites (Johansson et al., 1998; Sundberg, 2002). The average natural presence of uranium measured on the studied samples was lower than 10 ppm, and in most regions undetectable.
Figure 2 shows the elemental distribution maps of Si, K, Fe, Ti, Ca and U obtained on an Äspö diorite area after immersion in uranium solution, under anoxic conditions, during 10 days.
In the maps, different colors indicate different concentration and the red squares refer to the zones that were selected to obtain the individual PIXE spectra for quantitative analyses with the Mappix code. In this area, the main minerals identified (marked in red in Figure 2) were: (1) plagioclase, (2) biotite, (3) K-feldspar, (4) hornblende, (5) titanite, (6) hornblende and (7) epidote. It can be appreciated that uranium is distributed all over the surface, but presents higher concentration onto specific minerals, generally with Fe content, and lower uranium is detected on K-feldspar areas.

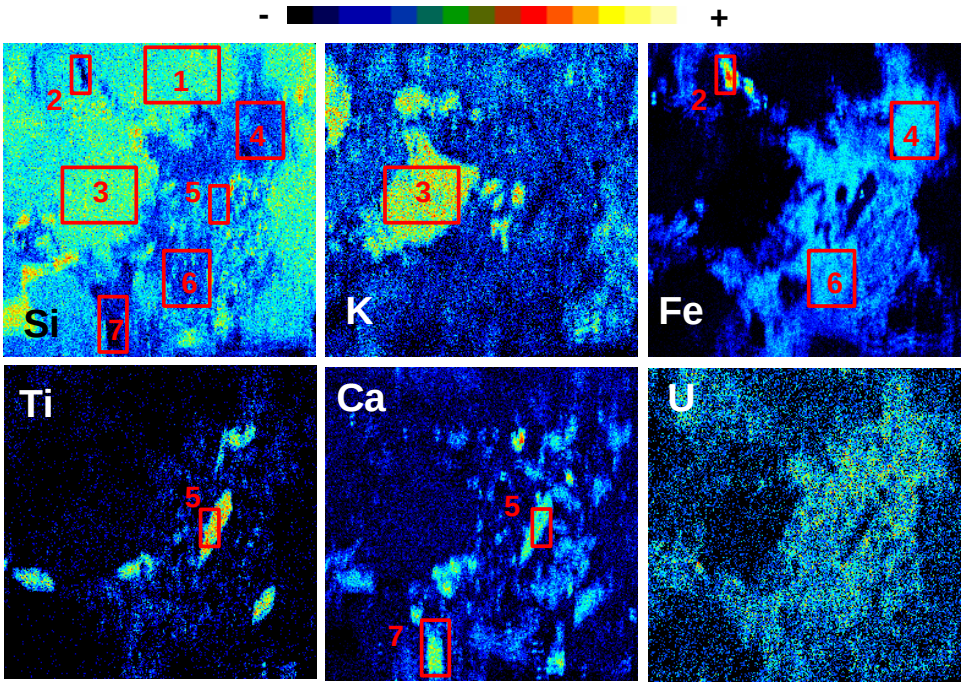

Figure 2: *Elemental distribution maps obtained by μPIXE on a 2 mm×2 mm Äspö diorite area after immersion in uranium solution under anoxic conditions. Red squares indicate regions selected to obtain the individual PIXE spectra for quantitative analyses.*

The surface was cleaned before μPIXE analyses but, considering the high uranium concentration used, precipitation cannot be discarded. But also, it has to be noted that the elemental maps are obtained during the spectra acquisition and give an idea of the elements distribution, but can also include signals from other origin. In the maps, only the main characteristic X-Ray line (K_α or L_α) is recorded and the intensity is not corrected. The signals many times include other contributions, mainly coming from superposition of characteristics X- ray lines of other elements or mainly from background noise.

Therefore, to ensure that an element is really present in a certain area, the individual PIXE spectra have to be analyzed. In the spectrum, the presence of any element must be supported by all corresponding lines (K_α, K_β, L_α, L_β, L_γ,...) with a certain downward trend of intensity ratio (Jaksic et al., 1995; Johansson et al., 1995).

Figure 3 shows the PIXE spectra and the simulation obtained on the regions marked in Figure 2 as feldspar (Figure 3a) and hornblende (Figure 3b).In the spectra, peaks attributable to Al, Si, K, Ti, Fe or Sr, can be perfectly identified. The uranium X-Ray characteristic lines are also clearly visible. From the analyses, the uranium retained concentration is obtained and surface distribution coefficients were calculated as described in (Alonso et al., 2009).

The average surface distribution coefficient measured for uranium was Ka = $(4.4 \cdot \pm 0.1) \cdot 10^{-4}$ m, with higher values on Fe minerals (Ka = $8 \cdot 10^{-4}$ m). These values are higher than those measured for U on granite under oxic conditions. However, further studies on Äspö diorites are still required. To perform the experiments at longer times would be also of interest, since sorption kinetic can not be discarded.

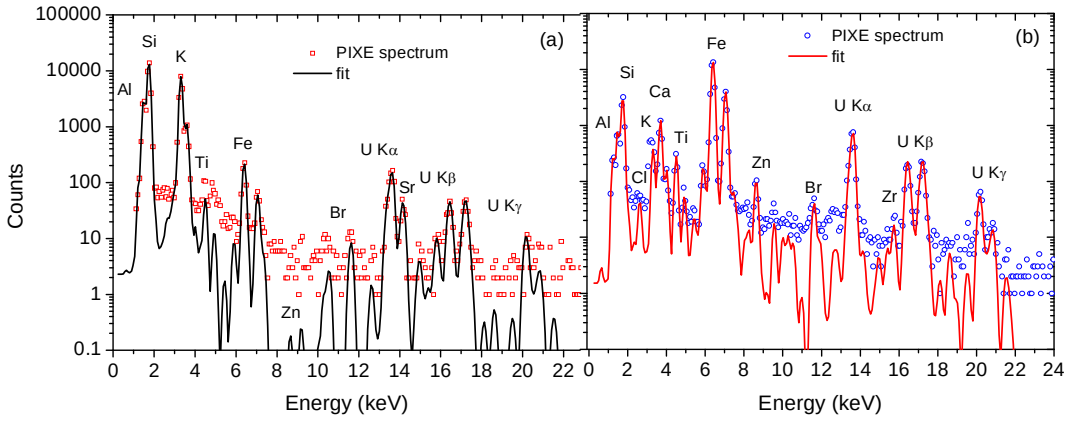

Figure 3: *PIXE spectra and the simulation obtained on the Äspö diorite regions after immersion in uranium solution under anoxic conditions: (a) K-Feldspar (area (3) in Figure 2) and (b) hornblende (region (6) in Figure 2).*

Conclusions and Future work

First micro-scale analyses on uranium retention on Äspö diorite samples are presented. Experiments were carried out maintaining anoxic conditions from the rock core extraction to the micro-scale analyses. Uranium distribution and sample elemental concentration was analysed by the ion beam technique μPIXE.
Results showed that uranium retention on Äspö diorite surface was heterogeneous. Quantitative distribution coefficients (Ka) on selected minerals were obtained by PIXE spectra analyses. Higher sorption values were generally observed on Fe-bearing minerals.
For future experiments, to perform sorption experiments under longer times would be particularly interesting, since sorption kinetics cannot be ruled out. To analyse more diorite regions to have more statistics on uranium retention values on minor minerals is still required. To complete the experiments under oxic conditions is considered also of interest, to compare the uranium retention under both redox conditions. Final aim of these studies is to relate the Ka distribution values measured on specific minerals on the granite surface to the bulk distribution coefficients determined by batch experiments.

Acknowledgments

The research leading to these results has received funding from EU Seventh Framework Programme (FP7/2007-2011) under the grant agreements Nº 269658 (CROCK, Crystalline Rock Retention Processes and Nº 2620109 (ENSAR, European Nuclear Science and Applications Research.

References

Alonso U., Missana T., García-Gutiérrez M., Patelli A., Ravagnan J. Rigato V. (2004). Study of the uranium heterogeneous diffusion through crystalline rocks and effects of the "clay-mediated" transport. Scientific Basis for Nuclear Waste Management XXVII. V.M. Oversby & L.O. Werme Eds. Materials Research Society Symp. Proc. 807, Warrandale PA, 621-626.

Alonso U., Missana T., Patelli A., Ceccato D., Albarran N., García-Gutiérrez M., Lopez-Torrubia T., Rigato V. (2009). Quantification of Au nanoparticles retention on a heterogeneous rock surface. Colloids & Surfaces A: Physicochemical and Engineering Aspects, 347, 230-238.

Ceccato D. (2009). MAPPIX: A software package for off-line micro-pixe single particle aerosol analysis. Nuclear Instruments and Methods in Physics Research B, 267 (12-13), 2077-2079.

Heck, S. and Schäfer, T., (2011). Short Note: CP CROCK groundwater sample characterization. KIT-INE, Karlsruhe, Germany.

Jaksic M., Bogdanovic I., Fazinic S. (1995). Limits of detection for PIXE analysis using proton microbeam. Nuclear Instruments and Methods in Physics Research B, 104: 152-156.

Johansson S.A.E., Campbell J.L., Malmqvist, K.G.E. (1995). Particle Induced X-Ray Emission Espectrometry (PIXE) Chemical Analysis, a series of monographs on analytical chemistry and its applications 13. John Wiley& Sons, Ltd.

Johansson, H., Siitari-Kauppi, M., Skalberg, M., Tullborg, E.L., (1998). Diffusion pathways in crystalline rock-examples from Aspo-diorite and fine-grained granite. Journal of Contaminant Hydrology, 35, 41-58.

KIT-INE (2011). Provision of new fracture bearing drill core samples obtained, handled, transported and stored under anoxic conditions, including first documentation. CROCK Project Deliverable (D-N°:1.1).

Maxwell J.A., Teesdale, W., Campbell J.L. (1995). The GUPIX PIXE software package II. Nuclear Instruments and Methods in Physics Research B, 95: 407.

Sundberg, J. (2002). Determination of thermal properties at Äspö HRL. Comparison and evaluation of methods and methodologies for borehole KA 2599 G01. SKB Report R-02-27, Sweden.

ISSN 1869-9669
ISBN 978-3-86644-925-1

ISBN 978-3-86644-925-1